

Edited by
Volodymyr Korzhyk

SURFACE MODIFICATION OF METAL PRODUCTS BY ELECTROLYTE PLASMA

Monograph

UDC 621.785.5

BBK 34.65

K75

Published in 2021
by PC TECHNOLOGY CENTER
Shatylova dacha str., 4, Kharkiv, Ukraine, 61165

Approved by the Academic Council of E. O. Paton Electric Welding Institute of the National Academy of Sciences of Ukraine, Protocol No. 2 of 25.10.2021

Reviewers:

Valerii Lykoshva, Doctor of Technical Sciences, Professor, Head of Department of Concentrated Energy Impacts, Physico-technological Institute of Metals and Alloys of National Academy of Sciences of Ukraine;

Yurii Kunitskii, Doctor of Physical and Mathematical Sciences, Professor, Researcher Consultant, Limited Liability Company «Foreign Economic Representation of Chinese-Ukrainian E. O. Paton Welding Institute».

K75

Authors:

Edited by **Volodymyr Korzhyk**

Volodymyr Korzhyk, Yuriy Tyurin, Oleg Kolisnichenko

Surface modification of metal products by electrolyte plasma: monograph / V. Korzhyk, Yu. Tyurin, O. Kolisnichenko. – Kharkiv: PC TECHNOLOGY CENTER, 2021. – 180 p.

The monograph presents the results of theoretical and experimental studies of non-stationary processes of modification of metal surfaces by electric current, by switching it with a liquid-electrolyte electrode. On the basis of the research carried out, complex hardening technologies and equipment have been created. Technologies allow oxidizing, alloying and changing the structure of local areas of the surface of products, which greatly increases their physical and mechanical properties without changing the structural state of the entire product. Along with theoretical material, the monograph provides extensive information on the application and efficiency of the developed technologies in industry.

The monograph is intended for engineering and technical workers of machine-building enterprises and institutes that specialize in the field of hardening processing of products.

Figures 147, Tables 12, References 109 items.

All rights reserved. No part of this book may be reprinted or reproduced or utilised in any form or by any electronic, mechanical, or other means, now known or hereafter invented, including photocopying and recording, or in any information storage or retrieval system, without permission in writing from the authors. This book contains information obtained from authentic and highly regarded sources. Reasonable efforts have been made to publish reliable data and information, but the author and publisher cannot assume responsibility for the validity of all materials or the consequences of their use. The authors and publishers have attempted to trace the copyright holders of all material reproduced in this publication and apologize to copyright holders if permission to publish in this form has not been obtained. If any copyright material has not been acknowledged please write and let us know so we may rectify in any future reprint.

The publisher, the authors and the editors are safe to assume that the advice and information in this book are believed to be true and accurate at the date of publication. Neither the publisher nor the authors or the editors give a warranty, express or implied, with respect to the material contained herein or for any errors or omissions that may have been made.

Trademark Notice: Product or corporate names may be trademarks or registered trademarks, and are used only for identification and explanation without intent to infringe.

DOI: 10.15587/978-617-7319-47-3

ISBN 978-617-7319-47-3 (on-line)

ISBN 978-617-7319-48-0 (print)



9 786177 319473

Copyright © 2021 V. Korzhyk, Yu. Tyurin, O. Kolisnichenko
This is an open access paper under the Creative Commons CC BY license

AUTHORS

VOLODYMYR KORZHYK

Corresponding Member of National Academy of Sciences of Ukraine,
Doctor of Technical Sciences, Professor, Head of Department
Department of Electrothermal Processes of Materials Processing
E. O. Paton Electric Welding Institute of the National Academy of Sciences of Ukraine
 ORCID ID: <https://orcid.org/0000-0001-9106-8593>

YURIY TYURIN

Doctor of Technical Sciences, Senior Researcher
Department of New Physical and Chemical Ways of Welding
E. O. Paton Electric Welding Institute of the National Academy of Sciences of Ukraine
 ORCID ID: <https://orcid.org/0000-0002-7901-7395>

OLEG KOLISNICHENKO

PhD, Senior Researcher
Department of New Physical and Chemical Ways of Welding
E. O. Paton Electric Welding Institute of the National Academy of Sciences of Ukraine
 ORCID ID: <https://orcid.org/0000-0003-4507-9050>

ABSTRACT

The monograph presents the results of theoretical and experimental studies of non-stationary processes of modification of metal surfaces by electric current, by switching it with a liquid-electrolyte electrode. This process is called plasma electrolyte treatment (PET). On the basis of the research carried out, complex hardening technologies and equipment have been created. Technologies allow oxidizing, alloying and changing the structure of local areas of the surface of products, which greatly increases their physical and mechanical properties without changing the structural state of the entire product.

The complex of developed technologies multiplies: strength, wear resistance, fatigue strength of products under cyclic loads under conditions of friction and wear. Along with theoretical material, the monograph provides extensive information on the application and efficiency of the developed technologies in industry.

The monograph is intended for engineering and technical workers of machine-building enterprises and institutes that specialize in the field of hardening processing of products.

KEYWORDS

Electrolytic dissociation, electrical breakdown, plasma, heat treatment, surface modification, oxidation, industrial application.

CONTENTS

List of Tables	vii
List of Figures	viii
Circle of readers and scope of application	xvi
Introduction	1
1 Theoretical principles of electrolytic-plasma processing	3
1.1 Principles of electrolytic-plasma heating	5
1.2 Thermal cyclic hardening	11
1.3 Research of electrolytic-plasma cells	18
1.4 Study of heat flows	23
2 Electrolytic-plasma thermal cyclic treatment (EPTCT) of engineering products	26
2.1 Features of heating technology	26
2.2 Principal diagrams of units and description of technology	28
2.3 Hardening of drill pipes and drilling rig connectors	35
2.4 Saw tooth hardening	40
2.5 Modification of the heavy crankshaft trunnion surface	45
2.5.1 Theory and experiment to optimize the relief on the trunnion surface	45
2.5.2 Technology of forming a relief on the trunnion surface	48
2.6 Thermal cyclic treatment of internal cylinder surfaces	52
2.6.1 Problem statement	52
2.6.2 Electrolytic-plasma thermal cycling treatment (EPTCT)	53
2.6.3 Principle of chemical-thermal treatment of the cylinder surface	54
2.6.4 Equipment	55
2.7 Surface study	59
2.7.1 Properties of the hardened layer	59
2.7.2 Fundamental capabilities of EPT technology	60
2.8 Device for hardening the tool holders (cams) of the cutting units of the roadheaders and shearers	62
2.9 Hardening of sheet steel parts	68
2.9.1 Method of hardening sheet products	68
2.9.2 Sheet steel parts (pan bottom, mesh)	69
2.9.3 Units for electrolytic-plasma hardening of products from sheet material	71

2.10 Heater constructions and their application	74
2.10.1 Electrolytic-plasma heaters	74
2.10.2 Tools for agricultural machinery and processing industry	84
3 Cleaning and heating of rolled metal	91
3.1 About devices for cleaning and heating sheets	91
3.2 Efficiency of electrolytic-plasma cleaning	95
3.3 Device for cleaning and heating rolled products	98
Conclusions	105
4 Electrolytic-plasma chemical-thermal treatment	106
4.1 Introduction	106
4.2 Examples of equipment for surface CTT	107
4.3 CTT using soluble net anodes	113
4.4 CTT using micropowders in electrolyte solution	116
4.5 CTT in electrolytes based on aqueous nitrogen fertilizer	120
Conclusions	125
5 Electrolytic plasma oxidation (EPO)	126
5.1 Equipment and technology	126
5.1.1 Technology features	126
5.1.2 Design of the MAO unit	127
5.2 Constructions of reaction chambers for MAO of surface of products	129
5.3 Examples of MAO of parts with different configuration of working surfaces	138
5.4 Electrolyte composition	140
5.5 Composition and structure of coating	141
5.5.1 MAO of aluminum-magnesium alloys in direct current	141
5.5.2 MAO of aluminum-magnesium alloys in alternating current	148
5.6 Oxide coating characteristics and application	154
References	156

LIST OF TABLES

2.1	Technological parameters of the electrolytic-plasma unit	34
2.2	Modes of electrolytic-plasma hardening of the sample surface	43
2.3	Comparative analysis of the efficiency of shaft hardening by electrolytic-plasma technology and nitriding	52
2.4	Characteristics of the hardened layer depending on the material of the product and technological processing parameters	59
3.1	Modes of electrolytic-plasma technology for cleaning and heating rolled products	104
4.1	Content of Cr and Si after electrolytic-plasma heating of the surface in different modes	115
4.2	Content of chemical elements of a sample doped from an electrolyte containing copper oxide powder	116
4.3	Content of chemical elements on the sample surface (heating temperature is 900 °C) doped from an electrolyte containing powders of titanium oxide, aluminum oxide and carbon	118
4.4	Content of chemical elements on the sample surface (heating temperature 1100 °C), doped from an electrolyte containing powders of titanium oxide, aluminum oxide and carbon	118
5.1	Technical data of the reaction chamber	130
5.2	Phase composition of the ceramic layer	147
5.3	Modes and some characteristics of oxide films [106–109]	153

LIST OF FIGURES

1.1	Diagram of an electrolytic-plasma heater	5
1.2	Change in the strength of the electric field between the surface of the product, the cathode and the anode	9
1.3	View of the gap between the metal cathode-1 and the liquid electrode anode-2 at electric potential voltages: $a - U_1=60-120$ V; $b - U_2=80-160$ V; $c - U_3=120-200$ V; $d - U_4=180-260$ V; $e - U_5=240-320$ V	9
1.4	Layout of thermoelectric junctions in the surface layer of the sample when measuring temperature in the process of electrolyte-plasma heating	11
1.5	Temperatures of the surface of the product depending on the heating time (1; 2; 3) and cooling time (4; 5; 6; 7) with periodic connection of the electric potential, which has the following intensity: 1 - $U_1=320$ V; 2 - $U_2=200$ V, $U_1=320$ V, $U_{cool}=30$ V; 3 - $U=220$ V and during cooling: 4 - $U_{cool}=60$ V; 5 - $U_{cool}=40$ V; 6 - $U_{cool}=20$ V; 7 - $U_{cool}=0$ V	13
1.6	The hardness of the hardened layer on the surface of the iron-carbon alloy (0.50 % C) depending on the time - t of heating and the voltage of the electric potential - $U_p=320$ V, $U_n=200$ V: 1 - $t=5$ s; 2 - $t=15$ s; 3 - $t=30$ s; 4 - $t=40$ s; 5 - $t=50$ s; 6 - $t=60$ s; 7 - $t=70$ s	14
1.7	Diagram of the frequency of connecting the electric potential during thermal cyclic heating: 1 - $U_1=320$ V, $U_2=200$ V, $U_{cool}=36$ V; 2 - $U_1=320$ V, $U_2=200$ V, $U_{cool}=0$ V	15
1.8	Change in the hardness of the surface layer of the alloy sample (0.50 % C) after thermal cycling. Cooling time between cycles is t_p . Electric potential during cooling - U_{cool} : 1 - $t_p=10$ s, $cool=0$; 2 - $t_p=6$ s, $cool=0$; 3 - $t_p=4$ s, $cool=0$; 4 - $t_p=2$ s, $U_{cool}=0$; 5 - $t_p=10$ s, $cool=36$ V	16
1.9	Layout of hardened sections on the surface of the product: a - sections in the form of ellipses, placed in a checkerboard pattern; b - sections located along a helical line; c , d - stripes of the hardened surface at different angles to the generatrix of the product	17
1.10	Graph of changes in the hardness of the surface hardened by local areas of the product	18
1.11	Schemes of electrolyte-plasma cells for heat treatment of products: 1 - end heating; 2 - hardening of the disk periphery; 3 - hardening of the axle surface; 4 - heating with a sprayer; 5 - heating by immersion; 6 - axle heating; 7 - heating under a layer of electrolyte	19

LIST OF FIGURES

1.12	Change in temperature in the surface layer of the product from the time of heating and cooling: <i>a</i> – on the surface ($U_1=300$ V, $U_2=180$ V, $\Sigma\tau=20$ s); <i>b</i> – at a depth of 2; 4; 6 mm ($U_1=300$ V, $U_2=180$ V, $U_3=0$, $\Sigma\tau=20$ s)	19
1.13	Change in the heating temperature and current strength from time to time at various technological modes: <i>a</i> – at a voltage on the cell of 240 V (1), 220 V (2), 180 V (3) and at 300/180 V (4); <i>b</i> – graph of voltage changes 300/180 V	21
1.14	Change in the rate of heating and cooling of the product: <i>a</i> – on the surface ($U_1=300$ V, $U_2=180$ V, $\Sigma\tau=20$ s); <i>b</i> – at a depth of 2 mm (1 – 50 V, 2 – 40 V, 3 – 30 V, 4 – 20 V, 5 – 0 V). Voltage for electrolyte cells – 300/180 V, heating time – 10–20 s	22
1.15	Dependence of the product temperature at a depth of 6 mm on time during heating and cooling	22
1.16	Change in the power density of the heat flux along the depth of the layer at different voltages to the electrolyte cells: 1 – 280 V; 2 – 270 V; 3 – 260 V; 4 – 250 V; 5 – 240 V; 6 – 230 V	24
1.17	Change in temperature in the product at different voltages for electrolyte cells: 1 – 280 V; 2 – 270 V; 3 – 260 V; 4 – 250 V; 5 – 240 V; 6 – 230 V	24
2.1	Diagrams of technological devices intended for electrolytic-plasma hardening of products: <i>a</i> , <i>b</i> , <i>c</i> – flat surface; <i>d</i> – end face of the part; <i>e</i> – periphery of the saw blade; <i>f</i> – surfaces inside the cylinder	27
2.2	View of unit for electrolytic-plasma treatment of the surface of the rolls: <i>a</i> – unit diagram; <i>b</i> – view from the side of the tailstock of the unit; <i>c</i> – view of the heater and shaft rotation drive	29
2.3	Heater for electrolyte-plasma heating: <i>a</i> – heater circuit; <i>b</i> – heater for rollers; <i>c</i> – heater for drill pipes	30
2.4	Universal unit for electrolytic-plasma treatment: <i>a</i> – general view; <i>b</i> – view of the manipulator	31
2.5	Typical layout of a specialized area for electrolyte-plasma hardening	32
2.6	Unit for electrolytic-plasma hardening of cylindrical parts: <i>a</i> – general view; <i>b</i> – view of the part processed by plasma	32
2.7	Exterior view of reinforced locations on the drill pipe	36
2.8	Structure of the hardened layer	37
2.9	Unit for electrolytic-plasma hardening of drill rods-pipes	37
2.10	View of the unit in the place of attachment of electrolyte heaters	38
2.11	Type of unit for EPTCH drill rod adapters	39
2.12	Appearance of hardened adapters, various options	39
2.13	Saw tooth hardening diagram	40
2.14	Diagram of immersing a saw tooth into the electrolyte cell of the heater	41

2.15	Scheme of saw tooth processing with an indenter (ceramic/carbide)	41
2.16	Scheme of interaction of the saw with electrolyte cells	42
2.17	View of the saw tooth electrolyte heater	43
2.18	Hardening device for EPC saw tooth tops	43
2.19	Scheme for modeling and calculating the hydrodynamic lubrication of a sliding friction pair with a special relief on the trunnion surface	46
2.20	Thickness of the lubricating layer between rubbing surfaces with a relief having parameters: 1 – $R_z=0.6 \mu\text{m}$; 2 – $R_z=4 \mu\text{m}$; 3 – $R_z=8 \mu\text{m}$; 4 – $R_z=12 \mu\text{m}$; 5 – $R_z=16 \mu\text{m}$	47
2.21	Change in friction coefficients depending on the relief and sliding speed	48
2.22	Volumetric graph of the change in hardness on the surface of the crankshaft trunnion	48
2.23	Microsection with a graph for measuring the hardness of the hardened layer of the shaft trunnion	49
2.24	Electrolyte-plasma heater for the formation of solid areas on the surface of the crankshaft trunnion: <i>a</i> – diagram; <i>b</i> – type of working heater	49
2.25	Unit for hardening the main trunnions of the crankshafts: <i>a</i> – unit diagram; <i>b</i> – type of operating unit	51
2.26	View of the hardened surface of the crankshaft trunnion: <i>a</i> – view of the shaft; <i>b</i> – view of solid rectangular areas	51
2.27	Variants of hardening the inner surface of the cylinders: <i>a</i> – hardening of the entire surface; <i>b</i> – hardening with stripes, width 10–35 mm, which are perpendicular to the generatrix; <i>c</i> – variant of the distribution of solid inclusions on the inner surface of the cylinder; <i>d</i> – hardening with stripes 10–35 mm wide, which are performed at an acute angle to the generating surface	53
2.28	Sketch of a device for electrolytic-plasma treatment of the inner surface of pipes	56
2.29	Unit diagram for electrolytic-plasma treatment of the inner surface of pipes/cylinders	56
2.30	View of the cylinder heater: <i>a</i> – the moment the heater is inserted into the cylinder; <i>b</i> – the moment of heating-switching on the operating voltage	57
2.31	View of the slurry pump cylinders: <i>a</i> – external view of the cylinder; <i>b</i> – view of the hardened surface	58
2.32	View of an electrolytic-plasma heater for hardening the inner surface of cylinders	58
2.33	Microstructure of medium carbon steel 45 after EPT	60
2.34	Diagram of devices for electrolytic-plasma hardening: <i>a, b, c</i> – devices for hardening sheet products; <i>d, e, f</i> – devices for hardening by dipping; <i>g, h, i</i> – devices for hardening surfaces of complex shapes. Internal, cylindrical, flat products – 1; electrolyte cell body – 2; telescopic device – 3; heated surface – 4; anode – 5	61

LIST OF FIGURES

2.35	View of the cam of the GPK-type roadheader (1 hardened layer, 10–15 mm thick)	63
2.36	Schematic view of a unit for electrolytic-plasma hardening of cams	64
2.37	Schematic representation of the bath for the implementation of electrolyte-plasma heating and cooling of the cam	64
2.38	Diagram of the system for electrolyte regeneration and its distribution into the heating cells of the unit	65
2.39	Electrical circuit of power supply of electrolyte cells	66
2.40	Device for electrolyte-plasma heating in the mode of automatic control of the electrolyte temperature by means of a pneumo-hydraulic valve	67
2.41	Resistance to bending of steel 35 sheet after hardening by local areas, 20 % of the nominal surface	69
2.42	Sketch of a reinforced welded structure of a scraper conveyor pan [72, 73]: 1 – hardened sections; 2 – bottom; 3 – sidewalls; 4 – welded seam	70
2.43	Hardening of a sheet with a thickness of 6 mm, local spots with a diameter of 30 mm: <i>a</i> – surface type; <i>b</i> – cross-sectional view of the spot with hardening to a depth of 3 mm	70
2.44	View of a sieve of a coal preparation machine after electrolytic-plasma hardening	71
2.45	Schematic view of unit for electrolytic-plasma hardening of sheet products	72
2.46	Schematic view of a technological block for strengthening sheets	72
2.47	Diagram of a device with a hydrostatic rise of electrolyte-plasma heaters	73
2.48	View of the unit for hardening the surface of sheets	73
2.49	Electrolyte heater with activation of heating by a magnetic field, according to USSR Patent 1375659 A1	74
2.50	Electrolytic device for heating and cleaning local surface areas according to USSR Patent SU 1331074 A	75
2.51	Heater for cylindrical products according to USSR Patent SU 1537695 A1	77
2.52	Heating control device according to the USSR Patent SU 1481260 A1	79
2.53	Device for cleaning the chain according to USSR Patent SU 1611625 A1	81
2.54	Coating device according to USSR Patent SU 1277646 A	83
2.55	Universal electrolytic-plasma unit of low power (up to 5 kW) for local hardening of wear surfaces of products	85
2.56	Type of unit in the adjustment and hardening mode: <i>a</i> – adjustment mode; <i>b</i> – hardening of the seeder disks; <i>c</i> – harrow disk hardening	86
2.57	Type of hardened agricultural machine tool: <i>a</i> – feed grinder hammer; <i>b</i> – knife for crushing feed; <i>c</i> – workpiece of a carbide saw; <i>d</i> – beet harvester disc	86
2.58	Reinforced tool for agricultural machines: <i>a</i> – plow blade; <i>b</i> – forage drum lining	87
2.59	Long cylindrical parts, after hardening of the inner surface, cast iron compressor cylinder	87

2.60	Sketches of parts that wear locally along flat and cylindrical surfaces: <i>a, b</i> – shackle of a heavy chain conveyor; <i>c</i> – gantry crane wheel	88
2.61	Wheel of a heavy gantry crane: <i>a</i> – view after hardening; <i>b</i> – view of strengthened local places	88
2.62	Gear wheel: <i>a</i> – wheel segment; <i>b</i> – view of the hardened layer at the tooth apex	88
2.63	Lining of a heavy ball mill after hardening: <i>a</i> – top view; <i>b</i> – view from the lining end	89
2.64	Steel parts after hardening with local inclusions of 60 mm diameter, used in the repair of railway transport; <i>a, b</i> – parts fixed by electric arc welding; <i>c</i> – parts fixed with bolts	89
2.65	Type of hardened tool: <i>a</i> – knives for sheet bending; <i>b</i> – knives for cutting rolled products	89
2.66	Ball joint	90
3.1	Diagram of an ANDRITZ electrolyte sheet peeler	93
3.2	Electrolyte cleaning scheme adopted at NLMP	93
3.3	Diagram of a device for electrolytic-plasma cleaning of a sheet, heating and heating control	94
3.4	Iron hydroxides of various thicknesses and lengths on the surface of the sheet: <i>a</i> – local layers of corrosion; <i>b</i> – scale	95
3.5	Layers of corrosion, scale and loose contamination of various thicknesses and lengths on the sheet surface	96
3.6	Scheme of processing (cleaning) samples in laboratory conditions	96
3.7	View of the sheet surface after one pass of the heater: <i>a</i> – steel Q30/CRS; <i>b</i> – steel Full Hard/Q27	97
3.8	View of the surface of a Full Hard/Q27 steel sheet after electrolytic-plasma cleaning	98
3.9	Chambers for cleaning and heating rolled products	99
3.10	Details of the chamber for cleaning and heating rolled products: <i>a</i> – dielectric body; <i>b</i> – anode	99
3.11	Schematic view of a device for heating rolled products	100
3.12	View of a device for heating rolled products, section through the heater	101
3.13	View of the bath with cameras fixed in it	102
3.14	General view of the device for cleaning and heating rolled products	102
3.15	Type of unit with 8 chambers for cleaning and heating rolled products	104
4.1	Unit diagram for cylinders CTT	108
4.2	Unit of chemical-thermal surface treatment of cylindrical surfaces	108
4.3	A set of equipment for the control of electrolyte-plasma heating: <i>a</i> – a heater with a temperature measurement sensor; <i>b</i> – type of measuring complex and electrolytic-plasma equipment	109

LIST OF FIGURES

4.4	Diagram of a heater for a CTT of the inner surface of a cylinder	111
4.5	View of the unit in the process of chemical-thermal treatment of cylinders	112
4.6	Electrolyte-plasma heater: <i>a</i> – parts; <i>b</i> – assembled	113
4.7	Surface morphology after chemical-thermal treatment: <i>a</i> – local areas – diameter 30 mm; <i>b</i> – in stripes – width 30 mm, length 200 mm	114
4.8	Surface morphology with a coating obtained in a mode with heating up to 1000 °C	114
4.9	Surface morphology with a coating obtained in a mode with heating up to 800 °C	115
4.10	Surface morphology of a sample doped from an electrolyte containing copper oxide powder. The numbers indicate the local surface where the elemental analysis was carried out	117
4.11	Surface morphology of a sample doped from an electrolyte containing powders of titanium oxide, aluminum oxide and carbon (graphite). Surface temperature is 900 °C	117
4.12	Titanium concentration in the surface layer of the sample	119
4.13	Surface morphology of a sample doped from an electrolyte containing powders of titanium oxide, aluminum oxide and carbon (graphite). Surface temperature is 1100 °C	119
4.14	View of the surface layer of a VTO-1 titanium specimen after CTT in nitrogen-containing plasma: <i>a</i> – etched in a solution of hydrofluoric acid, 20 sec; <i>b</i> – without etching	123
4.15	Results of hardness measurements in the surface layer of a VTO-1 titanium specimen after HTT in nitrogen-containing plasma	123
4.16	View of the surface layer of a VTO-1 titanium specimen (0.3 % C) after chemotherapy in nitrogen-containing plasma. Etched in hydrofluoric acid solution – 1 min	124
4.17	View of the surface layer of a steel specimen (0.3 % C) after CTT in nitrogen-containing plasma	125
4.18	Results of hardness measurements in the surface layer of a steel specimen (0.3 % C) after CTT in nitrogen-containing plasma	125
5.1	Universal unit for micro-arc oxidation of samples and products	128
5.2	Type of universal units for MAO samples and products: <i>a</i> – unit for large-sized parts; <i>b</i> – laboratory (bench-top) unit for MAO surface of samples and small parts	129
5.3	Reaction chamber for micro-arc oxidation of products by immersion with an electrolyte flow sensor: <i>a</i> – diagram; <i>b</i> – general view	130
5.4	Distribution of electrolyte flows in the reaction chamber of a typical micro-arc oxidation plant	131
5.5	Diagram of a device for coating the walls of the combustion chamber of a piston of an internal combustion engine	132

5.6	Diagram of the device for MAO of the inner surface of the cylinders	133
5.7	Technological equipment for oxidation of the end surface of the part	133
5.8	Formation of a protective layer on the inner surface of a cylindrical part: <i>a</i> – diagram of the part and the hardened surface; <i>b</i> – technological scheme of MAO	135
5.9	Creation of a protective layer on the outer surface of a cylindrical part: <i>a</i> – part diagram; <i>b</i> – technological scheme of MAO	135
5.10	MDO of the end surface of the part: <i>a</i> – sketch of the part; <i>b</i> – technological scheme of hardening treatment	136
5.11	Formation of a protective layer in a cylindrical hole of a large-sized product: <i>a</i> – sketch of a hole in the product body; <i>b</i> – diagram of the hole walls MAO	136
5.12	MAO on alternating voltage of a surface of complex geometric shape on two parts	137
5.13	Formation of a protective layer on the surface of an extended product (pipe)	137
5.14	Type of heat-protective coating on the bottom of the pistons: <i>a</i> – diesel engine; <i>b</i> – ICE	138
5.15	Wear-resistant coatings: <i>a</i> – on the surface of the end bearing; <i>b</i> – on the rotor of the feed crusher	138
5.16	Instrument covers	139
5.17	Enclosures of geodetic instruments with electrical insulating and wear-resistant coating	139
5.18	Parts of die tooling with ceramic coating	139
5.19	Chemical analysis of coating on samples of aluminum alloy 7075 (Al-Zn-Cu-Mg) after MAO	142
5.20	Chemical analysis of the coating on samples of the aluminum alloy A6062 (Al-Mg-Si) after MAO	143
5.21	Oxide layer obtained on a sample of AlMg after micro-arc oxidation	144
5.22	Mass spectrum of secondary ions obtained by bombarding an aluminum alloy with an argon ion beam after micro-arc oxidation	145
5.23	Results of X-ray phase analysis of the coating	146
5.24	View of the sample surface after MAO in an alkaline electrolyte with the addition of Cr ₂ O ₃ micropowder	146
5.25	View of the surface of sample A5052 after MAO at direct current: <i>a</i> – at the anodic mode with a periodic increase in voltage; <i>b</i> – periodic switching to the cathodic mode	148
5.26	View of the surface of sample A5052 after MAO on alternating current with a smooth increase in electric potential from 150 to 400 V	149
5.27	View of the surface of the sample A5052 after MAO on alternating current with a pulsed voltage of 500 V and a smooth increase in the main electric potential up to 400 V	149

LIST OF FIGURES

5.28	View of a cross-sectional section of an aluminum sample after MAO with an alternating electric potential connected with a smooth increase in voltage from 150 to 400 V	150
5.29	View of a thin section of a coating with imprints obtained by measuring hardness	151
5.30	View of a cross-sectional section of aluminum samples A6061 (<i>a</i>) and A5252 (<i>b</i>) after MAO on alternating current with a pulsed connection of a voltage of 500 V and a smooth increase in the main electric potential from 150 to 400	152
5.31	Results of X-ray phase analysis of the coating obtained by MAO with the connection of two samples to an alternating current electric circuit with a pulsed voltage of 500 V and a gradual increase in the main electric potential from 150 to 400	153



CIRCLE OF READERS AND SCOPE OF APPLICATION

The monograph is intended for engineering and technical workers of machine-building enterprises and institutes that specialize in the field of hardening processing of products.

INTRODUCTION

In industry, a class of machines and mechanisms is widespread, where large-sized metal products operate under conditions of increased contact loads and abrasive wear. These are, for example, rolling rolls, saws, ball mill linings, tool holders, drill pipes, gears, hydraulic jacks, knives, crankshafts, cylinder-piston group and many other products used in mechanical engineering, metallurgy and other industries. The wear and tear of these products, as a rule, begins from local areas of the surface.

The monograph contains original technologies and equipment that ensure high efficiency of modification of local areas of the wearing surface. The technology is based on the heating of surface layers by electric discharges to the temperature of phase transformations and cooling with an electrolyte – an aqueous solution of an alkaline salt. This ensures the formation of a system of hard areas that have a thickness of 1...10 mm and a hardness of 55...68 HRC.

High-speed heating of the surface layer and martensitic transformations generate elastic-deformation processes that propagate deep into the product and form compressive stresses. The system of hard inclusions on the wearing surface prevents its wear, and the soft parts of the surface serve for stress relaxation. Compressive stresses in the surface layer increase the fatigue strength and rigidity of the product.

In plain bearings under fluid friction conditions, for example, when soft areas are worn, a relief is formed on the surface with hydrodynamic wedges, which provide a separating lubricant layer in the bearing and reduce wear. The formation of a system of solid inclusions in the inner layer of the sliding surface of a long cylinder increases its rigidity and provides a liquid friction mode, which significantly reduces piston wear.

Of interest are developments in the field of thermal cycling cleaning the surface of rolled products from contamination and scale. This development can be used at metallurgical enterprises in the preparation of the surface of rolled products before coating. The combination of heating of rolled products and cleaning provides high adhesion and density of the coating and economically justifies the cost of electrical energy.

The results of a search in the field of thermal diffusion surface alloying and micro-arc oxidation using alternating voltage and electrolyte-plasma heating show that such a technology can be effective for complex alloying of local areas of the product surface and the formation of dense oxide coatings on the surface of valve-type metal products.

The advantage of the electrolyte-plasma thermal cyclic technology for modifying local areas of the surface of large-sized products includes: the absence of heating of the entire product and, accordingly, its deformation, a multiple reduction in energy consumption during heat treatment, environmental friendliness. An electrolyte based on aqueous solutions of alkali metal salts is used many times and is easily disposed of. Only water vapor is released.

The examples of the use of thermal cyclic electrolyte-plasma modification of local areas on the surface of metal products given in the monograph show the high efficiency of the technology in hardening existing structures.

The use of the modification technologies outlined in the monograph makes it possible to replace alloys and significantly reduce the material consumption of machines and mechanisms during their design.

ABSTRACT

A brief description of the process and an explanation of the physical phenomena occurring in the implementation of the technology of electrolytic-plasma surface treatment are given. The data on the modes and schemes of processing, the study of temperature fields, etc.

KEYWORDS

Electrolyte-plasma process, heater, heat flux, hardening, hardness of surface layers.

In mechanical engineering, complex requirements are imposed on products: for example, it is necessary to provide resistance to abrasive surface wear and destruction under alternating dynamic loads. These requirements made it necessary to develop a technology for local electrolytic-plasma treatment (EPT), which ensures the formation of solid inclusions on the wearing surfaces of the article. Hard inclusions, up to 10 mm thick, on the surface of the part prevent abrasive wear, while soft (not hardened) ones serve for stress relaxation. Experimental work carried out on flat workpieces (steel 45) showed that the system of solid inclusions increases the permissible load on the sheet (with the same deflections) by 30–40 %. This is due to an increase in the volume of hardened areas and the creation of compressive stresses in the product.

Additional alloying of the surface, along with an increase in strength properties, will provide an increase in corrosion resistance. The paper presents the results of analyzes carried out on samples of steel treated with electrolytic plasma in three different modes (with Cu; Cr electrodes). As a result, of processing, the surface layer is alloyed with elements from an electrode and an electrolyte. The surface relief is a highly developed surface. An uneven hardening along the depth is found, associated primarily with a different number of pulses and an uneven distribution of different phases: FeO, Fe₃O₄, Cr, FeCr, Fe₂O₃.

The monograph provides an overview of the processes of electrolytic-plasma treatment of the surface of metal products. Prospects for their use for modifying local areas of surfaces without heating the product are shown. Despite some differences in the materials of the processed products and technological parameters of electrolytic-plasma treatment (EPT), these technologies are considered as a special group of surface treatment methods. In each of these methods, there are two characteristic phenomena: electrolysis of a liquid medium by electric current using the difference in electrical potentials between the surfaces of the product and the electrodes; heating of materials, plasma-chemical synthesis, carried out in the plasma of electrical discharges that are generated in the plasma layer on the surface of the product.

The phenomenon of electric discharge in water-based electrolytes was discovered by Sluginov [1]. This process was studied in the 1930s. Gunterschultze and Betz [2]. The practical use of an electric discharge in an electrolyte was carried out for the deposition of cadmium niobate on a cadmium anode in an electrolyte containing Nb in the 1960s by McNiell and Gross [3, 4]. In the 1970s, the formation of an oxide layer on an aluminum anode was carried out under the conditions of an electric arc discharge by Markov and colleagues [5, 6]. Later, this technology was improved and received the name «micro-arc oxidation» [7]. In the 1980s, the possibility of using surface discharges for the deposition of oxides on various metals was studied in great detail in Russia – Snezhko et al. [8–13], Markov et al. [14–16], Fedorov [17], Gordienko et al. [18–20] and in Germany Kurze et al. [21–24]. At this stage, the first attempts at industrial application appeared [25–27]. Scientists from the United States and China have also been involved in research in this area [28–30]. Different authors have used different names for the same technology: «microplasma oxidation», «anodic spark electrolysis», «plasma electrolytic anodic treatment», «anodic oxidation by spark discharge». These are typical examples of definitions for the general concept of plasma electrolyte oxidation (PEO).

The theory of the processes of electrolysis of electrolytes, the passage of electric current, oxidation and heating of the surface layer of metal products are quite fully described in a number of reviews and monographs [31–38].

At present, heating by radiation from a technological laser, electron guns, or high-frequency currents is used for hardening heat treatment of the surface of tools and machine parts. The electrolyte-plasma technology of product surface heating and hardening has been known for 50 years [33]. This technology is unique in its ability to change the surface properties of products. In the electrolyte-plasma technology, the transfer of electrical energy to the product-cathode is carried out from the metal anode through the electrolyte and plasma layer. The plasma layer is formed from the electrolyte material in the gap between the liquid electrode and the electrically conductive surface of the product [33–38]. A water-based electrolyte is used as a liquid electrode. An appropriate choice of the electrolyte composition and electrical modes provides a wide variety of processing technologies [37]. The main reason for the limitation when used in technology is the low reliability and stability of the heating technology. This is primarily due to the instability of the formation of an electrically conductive (plasma) layer between the liquid electrode and the surface of the product.

In the electrolytic-plasma technology, the transfer of electrical energy to the product is carried out from the metal anode through the electrolyte and plasma layer. The plasma layer is formed from the electrolyte material in the gap between the liquid electrode and the electrically conductive surface of the product [1–5]. A water-based electrolyte is used as a liquid electrode. An appropriate choice of the electrolyte composition and electrical modes provides a wide variety of processing technologies [2]. The main reason for the limitation when used in technology is the low reliability of heating. This is primarily due to the instability of the formation of an electrically conductive (plasma) layer between the liquid electrode and the surface of the product. This review presents materials on the technology of heat treatment of local areas of the surface of products. The use of special heaters

made it possible to increase the conductivity of the electrolyte jet, which, in turn, ensured the release of energy on the heated surface, comparable in power density with the energy of the laser plasma.

1.1 PRINCIPLES OF ELECTROLYTIC-PLASMA HEATING

The combination of processes simultaneously occurring in the electrode, in practice, these are electrochemical systems, as well as the uniformity of the electric field and electrolysis parameters, contribute to the wide variety of discharge characteristics observed during plasma electrolysis. Due to this, some scientists associate the phenomena observed in plasma with the difference in the types of discharges, such as «glow», «corona», «spark» or «plasma-arc» [38]. Estimates of the discharge temperature also vary greatly from 800–3000 K to 3000–6000 K and even 10000–20000 K. These differences can be attributed to the complex structure of the discharge channel, in which a hot core (6800–9500 K) and a «cold» peripheral region (1600–2000 K), as shown by special studies. The diameter of the discharge channel and the thickness of the zone exposed to heat were estimated as 1–10 μm and 5–50 μm , respectively, [30, 37–47].

The distribution of electrical energy and the formation of a plasma layer can be traced on the heater circuit (**Fig. 1.1**), which contains a metal anode with a characteristic size D_a and through holes. An electrolyte flows through these holes, which at a distance H is compressed by dielectric walls to the diameter of the outlet nozzle D_k and is directed to the surface of the product. The electrolyte speed increases in proportion to the ratio of the total area of the holes in the anode and the area of the nozzle.

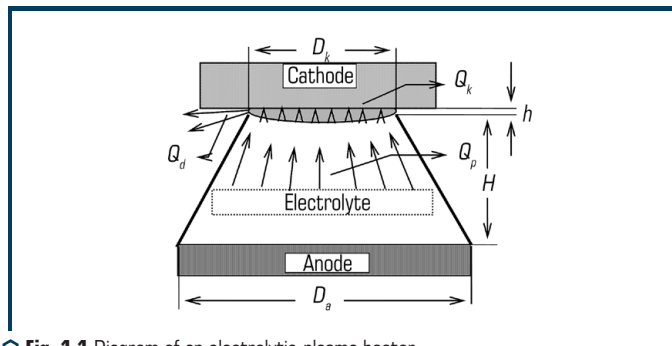


Fig. 1.1 Diagram of an electrolytic-plasma heater

The interaction of electric and hydrodynamic fields in such devices is described in the works of G. Ostroumov [31].

In the volume of the electrolyte, between the electrodes, cross effects take place. On the one hand, the electric field creates volumetric forces of a mechanical nature in the fluid – «ponderomotive forces». These forces in the equations of hydrodynamics are added to the forces of inertial,

gravitational, baric and viscous nature. On the other hand, the hydrodynamic flows of a medium charged with electricity with a density ρ carry out electric convection currents.

The interaction of electrical and hydrodynamic roles is carried out by cross-over effects. On the one hand, electric fields of a certain configuration can create volumetric forces of a mechanical nature in a fluid – «ponderomotive forces». These forces in the equations of hydrodynamics are added to the forces of inertial, gravitational, baric and viscous nature. On the other hand, the hydrodynamic flows of a medium charged with electricity with a density ρ carry electric currents of convection. These currents are added to the conduction and displacement currents, as well as to the osmotic concentration currents of certain types of ions, which can also be in the form of free space charges [31].

In its simplest form, the system of equations of electrohydrodynamics reflects, within the continuum concepts of classical physics, the mathematical relationship between electric j , E , φ , ρ and hydrodynamic v , p functions of coordinates (12 unknown functions in total), limited to certain approximations [31]:

$$j = \sigma E + \rho v, \tag{1.1}$$

$$\operatorname{div} j = 0, \tag{1.2}$$

$$E = -\operatorname{grad} \varphi, \tag{1.3}$$

$$4\pi\rho = \operatorname{div}(\varepsilon E), \tag{1.4}$$

$$\gamma(v\nabla)v = -\operatorname{grad} p + \mu\Delta v + \rho E, \tag{1.5}$$

$$\operatorname{div} v = 0. \tag{1.6}$$

The functions of the equations of electrodynamics satisfy Maxwell's equations for conducting media. For the case of stationary media, they were represented in the required approximation by the formulas [48]: $j = \partial j / \partial t = 0$, $\operatorname{div} j = 0$, $E = -\operatorname{grad} \varphi$, $\operatorname{rot} E = 0$, $D = \varepsilon E$, $-W = (jE)$, $j = \sigma E$, $\sigma = \sigma(r)$, $\varepsilon = \varepsilon(r)$.

The hydromechanical functions are determined by the laws of mechanics of continuous isotropic weightless inert viscous fluids [49, 50].

Equations (1.1)–(1.6) are independent of each other and constitute a closed system. Therefore, the system is in principle solvable, and the functions participating in the equations provide, within the specified approximations, exhaustive mathematical information about the phenomena underlying them.

Equation (1.1) reflects Ohm's differential law for any nature or mechanism of electrical conductivity and a significant addition of the convection current ρv caused by the entrainment of electric charges ρ by the flow of a medium moving with mass speed v to relativistic. Equation (1.2) marks the approximation of stationarity of the process – «direct current». Equation (1.3) reflects the «weakly conducting medium» approximation. Equation (1.4) reproduces the Ostrogradsky-Gauss

relation. Equation (1.5), which is a modification of the Navier-Stokes equation for a stationary flow, reflects the law of conservation of momentum per unit volume of the medium under the action of a force of non-mechanical origin ρE . Equation (1.6) reflects the approximation of non-compressibility of the medium.

The coefficients in equation (1.5) are considered constant: $\gamma = \gamma_0$, $\mu = \mu_0$. The coefficients in equations (1.1)–(1.4) represent the known functions of the coordinates $\sigma = \sigma(r)$, $\varepsilon = \varepsilon(r)$. When these coefficients, moreover, also depend on the heating caused by the electric current, i.e. from the inhomogeneous temperature distribution in the medium, then the Fourier-Kirchhoff heat equation with its coefficients must be added to the indicated system of six equations (1.1)–(1.6). If they also depend on the local strength of the electric field, then it is necessary to add also the ratio of the conductivity of the medium to the strength.

A simpler mathematical description of the passage of an electric current through a moving electrolyte is based on the simple hypothesis that the total current density in the electrolyte is the sum of the densities of only three independent currents. This is primarily a conduction current or «migration current» – ions move relative to the enclosing liquid along or against the electric field under the action of forces of an electrostatic nature, regardless of their own concentration or the movement of the entire liquid. Then the diffusion current – ions of the same type diffuse under the action of osmotic pressure relative to the surrounding liquid as electrically neutral molecules against the gradient of their own concentration, regardless of the strength of the electric field or the movement of the liquid. And, finally, convective current – ions move by the flowing solution, as if they were «frozen» into a neutral liquid, regardless of the field strength or their concentration gradient.

A linear combination of three current densities in the total dissociation approximation is written for each type of ions by the Nernst-Planck relation [32],

$$J_i = u_i p_i E_i - \frac{\varphi_0 U_i}{z_i \text{grad } p_i} + v p_i, \quad (1.7)$$

here u_i , z_i – characteristic parameters of ions number $i=1, 2, 3, \dots$ – their mobility and valence; $p_i = n_i z_i$, n_i , j_i – the local bulk density of the distribution of electric charges, the concentration of ions and the current density due to ions of only type i ; E , v – electric field strength and mechanical fluid flow rate; $\varphi_0 = kT/e$ – specific osmotic potential, equal for aqueous solutions at room temperature $T=300$ K, approximately 25.9 mV; k , e – Boltzmann constant and electron charge modulus.

The linear relationship (1.7) has been tested many times and has found excellent accuracy. It is the only determination of the current density in the electrolyte in electrochemistry. There can be many types of ions, their interactions with each other, with electrodes and with the insulating walls of experimental vessels can be complex, the densities of the three component currents can have different values and directions – this is reflected in the boundary conditions – but equation (1.7) retains its unique significance.

The total current density in the electrolyte is the sum of the densities of three independent currents. This is, first of all, the conduction current or «migration current» – the ions move relative

to the enclosing liquid under the action of forces of an electrostatic nature, regardless of their own concentration or the movement of the entire liquid. Then the diffusion current – ions of the same type diffuse under the action of osmotic pressure relative to the surrounding liquid as electrically neutral molecules against the gradient of their own concentration, regardless of the strength of the electric field or the movement of the liquid. And, finally, convective current – ions move by the flowing solution, as if they were «frozen» into a neutral liquid, regardless of the field strength or their concentration gradient.

In an aqueous solution of Na_2CO_3 , ions Na^+ , CO_3^- , OH^- , H^+ are formed, ions with a negative charge give off excess electrons when passing through the anode holes, cations are carried away by the hydrodynamic flow of the electrolyte, and recombine at the cathode – the surface of the product.

There are many types of ions, their interactions with each other, with the electrodes and with the insulating walls of the heater are quite complex, but with a large volume charge and a high flow rate of the electrolyte, the convective current is much higher than the diffusion and migration current, which makes it possible to ignore them in the calculation. It is only due to the hydrodynamic component that it is possible to ensure sufficient conductivity of the electrolyte and significantly, up to $3 \cdot 10^3 \text{ W/cm}^2$, increase the power density of surface heating.

Conversion of electrical energy into heat occurs mainly in the plasma layer on the heated surface of the product-cathode. The distribution of energy in the heater can be represented as (**Fig. 1.1**),

$$Q_k = U_{ak} J_{ak} - Q_p - Q_d, \quad (1.8)$$

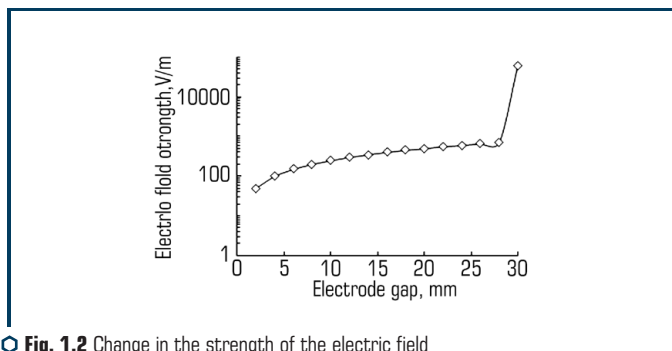
where: Q_k – energy spent on heating the plasma layer and cathode; Q_p – energy spent on evaporation of the plasma-forming electrolyte; Q_d – radiation energy of the plasma layer; J_{ak} – electric current passing through the plasma layer; U_{ak} – voltage of the electric potential in the plasma layer.

Since the thickness of the plasma layer is small ($h=2-3 \text{ mm}$) with respect to the length of the layer perimeter (D_k 30–50 mm), the energy dissipation in the form of radiation (Q_d) can be neglected. Heating of the electrolyte is a consequence of the diffusion and migration current. A predominantly convective conduction mechanism takes place in the heater, which explains the low losses for electrolyte heating.

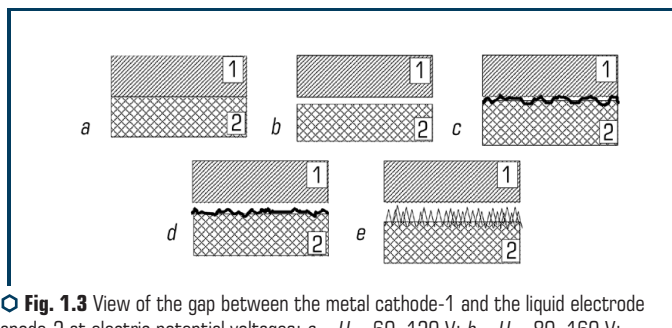
Experiments show that they amount to 5–10 % of the total power consumption. The main energy costs are spent on the formation of the plasma layer and heating the surface of the product. In the plasma layer, energy is transferred to the product in the form of a specific form of non-equilibrium electrical discharges. The discharges are in the form of a film with a low gas temperature and a high electron temperature. They have a diffusion binding and are located near the surface of the liquid anode electrode.

Under the influence of changing pressure at the place of discharge binding, the surface of the liquid electrode acquires an oscillatory motion. As a result, the size of the gap between the liquid electrode and the cathode surface changes periodically. The electric field strength in the electrolyte itself is low (up to 10 V/cm), but in the plasma layer the intensity is variable and can reach 1000–100000 V/cm (**Fig. 1.2**).

Depending on the strength of the electric field and the temperature of the electrolyte and the metal cathode, five characteristic regions of interaction between the surfaces of the liquid electrode and the product – the cathode can be traced (**Fig. 1.3**).



○ **Fig. 1.2** Change in the strength of the electric field between the surface of the product, the cathode and the anode



○ **Fig. 1.3** View of the gap between the metal cathode-1 and the liquid electrode anode-2 at electric potential voltages: $a - U_1 = 60-120$ V; $b - U_2 = 80-160$ V; $c - U_3 = 120-200$ V; $d - U_4 = 180-260$ V; $e - U_5 = 240-320$ V

The first area of dependence of the electric field voltage between the anode and cathode is $U = 60-120$ V. The electrolyte (liquid electrode) washes the surface of the cold cathode (**Fig. 1.3, a**). The electrolyte temperatures on the cathode surface are lower than the boiling points of the electrolyte.

The second area, $U = 80-160$ V, is characterized by an increase in the cathode surface temperature above the boiling point of the electrolyte. A thin vapor-gas layer appears on the cathode (**Fig. 1.3, b**), which reduces the current value with increasing voltage.

The surface of the cathode is not heated. Analysis of the current-voltage characteristics of electrolyte-plasma heating when using an aqueous solution of sodium carbonate (Na_2CO_3) shows [3] that with an increase in voltage after $80-160$ V, the current decreases.

The third area is $U=120\text{--}200$ V. Sharp current fluctuations are observed, which indicates the boiling of the electrolyte and the passage of electric discharges at different points of the interelectrode region.

Oscillation of the electrolyte surface ensures that it touches the cathode surface, which ensures the existence of simultaneous local heating and cooling (**Fig. 1.3, c**). The fourth region is $U=180\text{--}260$ V. A stable gas layer is formed between the surfaces of the cathode and electrolyte (**Fig. 1.3, d**). A stable glow is observed in the cathode region, which indicates the stabilization of the discharges and a decrease in the current. In this case, a stable vapor-gas layer reduces the electric field strength [4]. Due to the heating of the cathode, thermionic emission $J_t=60\text{--}700$ A/(cm K)² occurs [8], which compensates for the decrease in the conductivity of the vapor-gas layer. A further increase in voltage (up to 240–320 V) increases the electric field strength in the plasma layer (**Fig. 1.3**), which causes autothermoelectronic emission of electrons and the formation of electric discharges. The layer in the interelectrode space has a stable glow (**Fig. 1.3, e**). The electric field strength in the plasma layer is 2–4 orders of magnitude higher than in the electrolyte (**Fig. 1.3**).

Electrolyte plasma treatment (EPT) is carried out by heating parts of the product surface with electric discharges through the plasma layer. The plasma layer is formed from a water-based electrolyte material in the gap between the liquid (electrolyte) electrode and the surface of the article. An appropriate choice of the composition of the electrolyte and modes of electrical discharges provides a wide variety of processing technologies.

Special heaters for electrolytic-plasma treatment, (**Fig. 1.1**), provided control of the power density on the heated surface in the range of $10^2\text{--}10^4$ W/cm², which expands the field of application of the technology from cleaning from contamination to thermal cycling. When performing EPO, electrical discharges in the plasma layer create local zones of high pressure and temperature on the metal surface, in which the processes of brittle destruction of non-metallic and organic films and exfoliation of loose contaminants take place. This makes it possible to combine the processes of cleaning the surface of the product and heating it to the required temperature. Experimental work shows that when the EPO is heated, up to 80 % of the consumed electrical energy is introduced into the product in the form of heat, and the cost of equipment for the EPO is lower than, for example, for HFC at 5–10 with the same processing performance. In addition, EPO provides a wide range of control over the heating rate, which allows heating and hardening thick layers of the product surface (up to 10 mm). The principal features of the heater for EPO are shown in the diagram, **Fig. 1.1**. The heater contains a metal anode with a characteristic size D_a and through holes for electrolyte flow. The electrolyte in the heater is compressed by dielectric walls at a distance H to the diameter of the outlet nozzle D_n . The electrolyte speed increases in proportion to the ratio of the area of the holes in the anode and the area of the nozzle. In the volume of the electrolyte, between the electrodes, cross effects take place. On the one hand, an electric field acts on the medium. On the other hand, the hydrodynamic flows of a medium charged with electricity with a density ρ carry electric currents of convection.

Heating of the electrolyte is a consequence of the action of the current, as well as radiation. The main energy costs are spent on evaporation and heating of the electrolyte (formation of a plasma layer) and heating the surface of the product with electric discharges. The discharges have the form of micro-arc discharges evenly distributed over the processing area.

1.2 THERMAL CYCLIC HARDENING

Experimental work was carried out to determine the temperature on the sample surface. The sample was made from an iron-based alloy with a carbon content of 0.3 %. The temperature was measured with thermocouples, which were made by the method of natural thermal junction in two layers of the sample product at a depth of 1.0 and 2.0 mm from the heated surface. The location of the junctions is shown in **Fig. 1.4**.

The thermal junction was obtained by the method of pulsed electric welding of the end of the wire made of almel to the surface of the bottom of the hole in the sample. The thermocouples were calibrated by heating in a muffle furnace and simultaneously measuring the temperature with reference thermometers.

When determining the surface temperature of the sample, it was assumed that the entire heat flux goes from the surface to the depth of the product.

It was believed that the cross section of the heated layer is tens of times smaller than the heated area on the surface of the product and the heat flux dissipation was neglected.

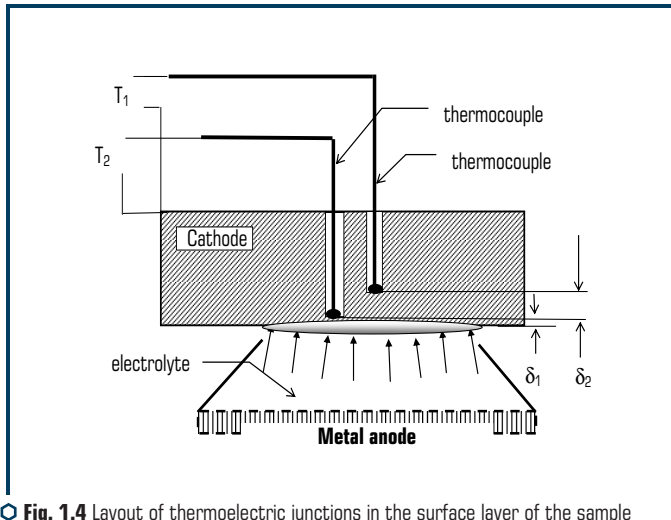


Fig. 1.4 Layout of thermoelectric junctions in the surface layer of the sample when measuring temperature in the process of electrolyte-plasma heating

This assumption makes it possible to calculate the temperature on the surface of the article-cathode based on the results of experimental temperature measurements in two layers of the sample. The results of measuring the temperature made it possible to calculate the value of the heat flux according to the formula:

$$Q = qF = \frac{\lambda}{\delta}(T_1 - T_2)F, \quad (1.9)$$

or specific heat flux:

$$q = \frac{\lambda}{\delta}(T_1 - T_2),$$

here Q – magnitude of the heat flux; q – specific heat flux; F – heated area of the sample; λ – thermal conductivity of the heated material; δ – distance between thermal junctions; T_1 and T_2 – temperatures of the first and second layers in the product, respectively.

Then the temperature T_0 of the sample surface was calculated by the formula:

$$T_0 = T_1 + q(\delta_1/\lambda_1). \quad (1.10)$$

The above formula was obtained under the assumption that the thickness of the material layer from the surface to the first layer is δ_1 .

Here λ_1 – thermal conductivity of the material at temperature T_1 ; q is taken according to the results of an experiment with measurements of temperatures T_1 and T_2 .

The experimental results are presented in the form of a graph of the surface temperature change versus heating time (**Fig. 1.5**). Heating and cooling of the sample was carried out at different values of the electric potential.

Studies have shown that when a 320 V electric potential heater is connected to the electric circuit, the sample surface is heated. The power density of the energy at the cathode is so high that almost 5–10 sec later the melting of the surface layer begins. The heating rate on the surface of the product reaches 500 °C/s (**Fig. 1.5**, curve 1).

With periodic switching on of high voltage electric potential (320 V) and low (200 V), a periodic increase and decrease in the heating rate is observed, which makes it possible to increase the time and obtain a thicker heated layer (**Fig 1.5**, curve 2). Connecting a 200 V voltage heater to the electric circuit is characterized by the fact that the surface practically did not heat up for 8–12 seconds (**Fig. 1.5**, curve 3). This is due to the fact that at the initial moment of time of the electric circuit current jumps occur from 0 to 50–60 A/cm², which corresponds to periodic transitions between the first, second and third regions of interaction of the liquid anode electrode and the surface of the product (**Fig. 1.5, a–c**). The duration of this process is up to 12 s. Then, after the formation of a vapor-gas layer (**Fig. 1.5, d**) with a relatively low electrical conductivity $\sigma = 0.5–0.7 \text{ Ohm}^{-1} \cdot \text{m}^{-1}$, the current density drops to the nominal value: $J = 5–8 \text{ A/cm}^2$.

Experiments have shown that the time until the formation of a stable plasma layer depends on the magnitude of the electric potential. At voltages up to 200 V, the surface of the product may not heat up for tens of seconds (**Fig. 1.5**, curve 3). This is the 1st, 2nd and 3rd area of interaction between the surfaces of the liquid electrode and the product-cathode (**Fig. 1.5, a-c**). A periodic increase and decrease in the voltage of the electric potential is accompanied by a periodic transition from the fifth to the fourth or even the third interaction region. This makes it possible to alternate a high density of surface heating power with a low one and, as a result, obtain an average heating rate of the surface layer of the article of 30–60 °C/s (**Fig. 1.5**, curve 2). The connection of the electric potential at the moment of cooling the surface of the product allows to reduce the cooling rate (**Fig. 1.5**, curves 4–7), and creates the possibility of hardening products made of an alloy with a high carbon content. The decrease in the cooling rate is explained by the fact that the connection of an additional electric potential increases the lifetime of the plasma layer, providing a smooth transition from the fifth to the fourth, then to the third and second regions of interaction between the surfaces of the liquid electrode and the product-cathode.

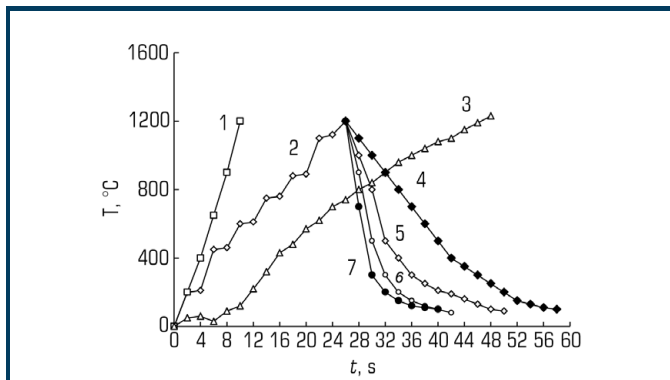
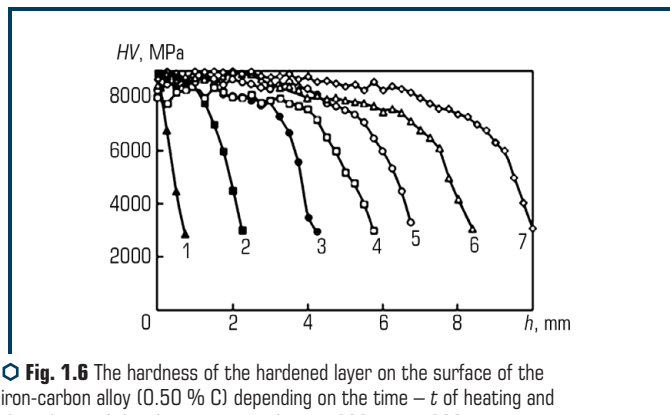


Fig. 1.5 Temperatures of the surface of the product depending on the heating time (1; 2; 3) and cooling time (4; 5; 6; 7) with periodic connection of the electric potential, which has the following intensity: 1 – $U_1=320$ V; 2 – $U_2=200$ V, $U_1=320$ V, $U_{cool}=30$ V; 3 – $U=220$ V and during cooling: 4 – $U_{cool}=60$ V; 5 – $U_{cool}=40$ V; 6 – $U_{cool}=20$ V; 7 – $U_{cool}=0$ V

By periodically changing the density of the heating power, it is possible to obtain hardened layers with a thickness of 0.5 mm, 1.5 mm, 4 mm, 6 mm, 7 mm, 8 mm and 9 mm (**Fig. 1.6**). In this case, heating was carried out with periodic switching on of high voltage $U_1=320$ V for 2 seconds and low voltage $U_2=200$ V for 4 seconds. With a total heating time of 30 seconds, the hardened layer thickness is 4 mm.

Total heating for 70 seconds provides a hardened layer thickness of 9 mm. The experiment was carried out on a flat sample 50 mm thick and containing 0.5 % carbon. Heating and cooling

was carried out with a heater having an outlet nozzle diameter of 35 mm. A 13 % aqueous sodium carbonate solution was used as the electrolyte. The hardness of the hardened layer was measured with a hardness tester.



○ Fig. 1.6 The hardness of the hardened layer on the surface of the iron-carbon alloy (0.50 % C) depending on the time – t of heating and the voltage of the electric potential – $U_1=320$ V, $U_2=200$ V: 1 – $t=5$ s; 2 – $t=15$ s; 3 – $t=30$ s; 4 – $t=40$ s; 5 – $t=50$ s; 6 – $t=60$ s; 7 – $t=70$ s

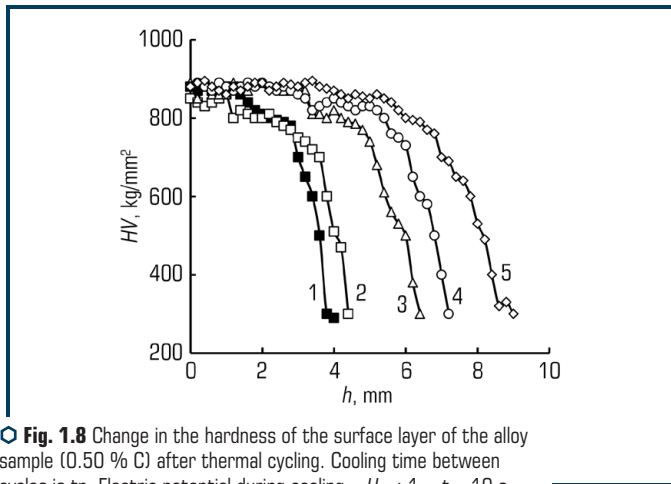
Analysis of the results of the experiment (**Fig. 1.6**) shows that the alternation of switching on the electric potential at a voltage of $U_1=320$ V and $U_2=200$ V provides heating of the product surface to a depth of 10 mm. In this case, the maximum hardness of the surface layer (900 kg/mm²) practically does not depend on the thickness of the hardened layer. The hardness of the hardened layer of the product gradually decreases from the maximum (900 kg/mm²) to the hardness of the base (250–300 kg/mm²) and, as a rule, does not depend on the heating time.

A periodic change in the electric field strength between the surfaces of the liquid electrode and the product changes the power density of the surface heating, which ensures the control of the electrolyte-plasma heating and the creation of the necessary thermal conditions for the formation of hardening structures.

The heating power density was calculated from the experimentally measured values of current, voltage, and heating area. The heater had an outlet nozzle diameter of 30 mm. When the voltage of the electric current was changed from 200 to 300 V, the current value varied in the range of 30–45 A. Accordingly, the heating power density varied from $1 \cdot 10^3$ to $3 \cdot 10^3$ W/cm². In addition, the ability to control the power density of electrical discharges will ensure the use of electrolytic-plasma treatment in cleaning, melting and soldering technologies.

It is known that obtaining a microcrystalline structure of an alloy with higher values (20–30 % higher) of strength characteristics, including fatigue strength, is obtained by «pendulum» thermal cycling treatment (TCT) [41].

lead to supercooling of the surface layer. The layer thickness reaches 9 mm in three heating and cooling cycles.



○ Fig. 1.8 Change in the hardness of the surface layer of the alloy sample (0.50 % C) after thermal cycling. Cooling time between cycles is t_p . Electric potential during cooling – U_{cool} : 1 – $t_p=10$ s, $cool=0$; 2 – $t_p=6$ s, $cool=0$; 3 – $t_p=4$ s, $cool=0$; 4 – $t_p=2$ s, $U_{cool}=0$; 5 – $t_p=10$ s, $cool=36$ V

Periodic increase and decrease in the voltage of the electric potential allows alternating high power density of surface heating with a low one and, as a result, to obtain an average heating rate of the surface layer of the product in the range of 25–150 °C/s. Connecting a low electrical potential at the time of cooling the surface of the product allows to reduce the cooling rate, and makes it possible to harden products that are made of an alloy with a high carbon content.

By periodically changing the power density of heating by electric current, it is possible to obtain hardened layers with a thickness of 0.5 mm, 1.5 mm, 4 mm, 6 mm, 7 mm, 8 mm and 9 mm (Fig. 1.6).

In this case, heating was carried out with periodic switching on of high voltage $U_v=320$ V for 2 seconds and low voltage $U_n=200$ V for 4 seconds. With a total heating time of 30 seconds, the hardened layer thickness is 4 mm. Total heating for 70 seconds provides a hardened layer thickness of 9 mm.

The experiment was carried out on a flat sample 50 mm thick and containing 0.5 % carbon. Heating and cooling was carried out with a heater having an outlet nozzle diameter of 35 mm. A 13 % aqueous sodium carbonate solution was used as the electrolyte. The hardness of the layer was measured with a PMT hardness tester.

Analysis of the results of the experiment (Fig. 1.8) shows that the alternation of switching on the electric potential at a voltage of $U_v=320$ V and $U_n=200$ V provides heating of the surface of the product to a depth of 10 mm. In this case, the maximum hardness of the surface layer (900 kg/mm²) practically does not depend on the thickness of the hardened layer.

The hardness of the hardened layer of the product gradually decreases from the maximum (900 kg/mm²) to the hardness of the base (250–300 kg/mm²) and, as a rule, does not depend on the heating time.

The periodic change in the voltage of the electric field between the surface to be treated and the liquid electrode provides control of the electrolyte-plasma heating and the creation of the necessary heating and cooling modes for the formation of hardening structures.

Experimental work has shown that, depending on the technological conditions, it is possible to obtain hardened layers on the surface of the product, which have a thickness of 0.3 to 10 mm and a hardness of up to 68 HRC. The placement of thermally treated layers on the surface of the product depends on the speed, the trajectory of movement of the electrolyte heaters relative to the surface to be hardened and the design features of the heaters themselves (**Fig. 1.9**).

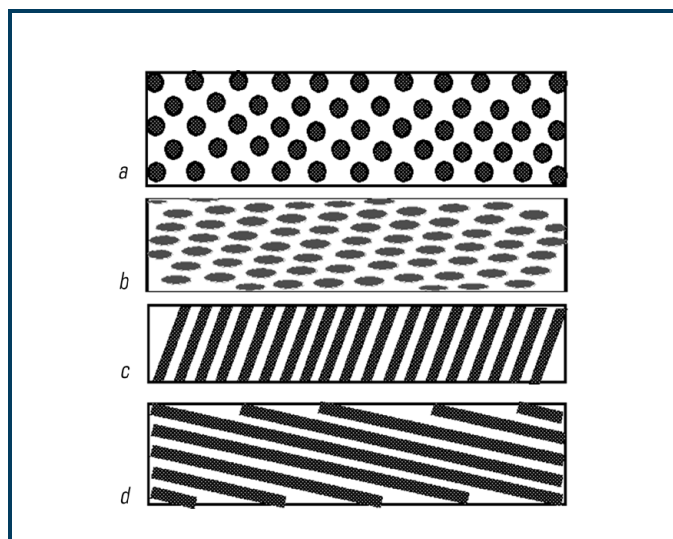


Fig. 1.9 Layout of hardened sections on the surface of the product: *a* – sections in the form of ellipses, placed in a checkerboard pattern; *b* – sections located along a helical line; *c*, *d* – stripes of the hardened surface at different angles to the generatrix of the product

It is of interest to harden the surface of the product by local areas. In **Fig. 1.10** shows a three-dimensional graph of changes in the hardness of the surface layer, up to 10 mm thick. The thickness of the hardened layers is 5–10 mm. A smooth transition from a hard layer to a soft layer and the presence of evenly distributed hard areas provides a combination of high wear resistance with strength and the ability to work under high alternating loads.

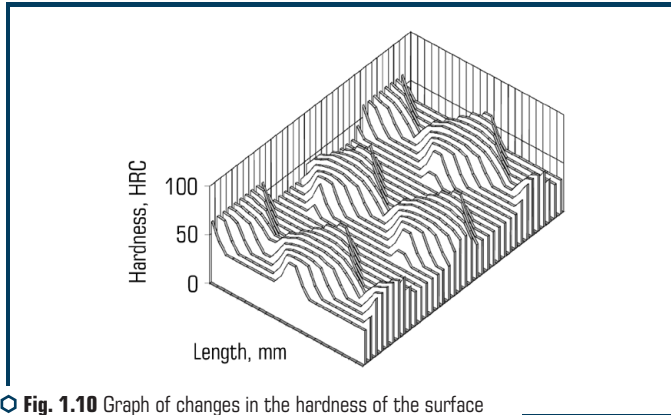


Fig. 1.10 Graph of changes in the hardness of the surface hardened by local areas of the product

This technology makes it possible to bend the product in the hardened state, weld the product in non-hardened areas and save energy by hardening only the wearable areas of the surface. In the volumes of metal, between the hardened areas, areas of positive stresses are formed, which increase the rigidity of the product and the ability to resist bending, which is in great demand, for example, for such products as crankshafts, drill pipes, hydraulic ram rod, parts of the scraper conveyor, and other products.

1.3 RESEARCH OF ELECTROLYTIC-PLASMA CELLS

Heating the surface of a product is possible when it is connected both to an electric circuit as a cathode (cathode process) and in reverse polarity (anodic process). Cathodic heating allows to heat the surface to higher temperatures, up to reflow, and use, at the same time, one-component electrolytes, chemically resistant and not aggressive.

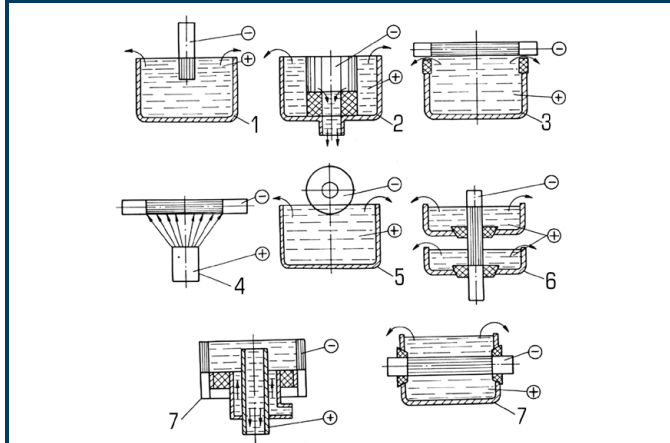
The anodic process is used in chemical-thermal treatment (nitriding, nitro-carburizing, sulfonitriding, etc.). With this scheme, it is possible to maintain a constant temperature of the heated layer for a long time.

Plasma electrolyte plants usually consist of a tank (0.5–1.0 m³), a pump, a process current source, a product manipulator, and an electrolytic plasma cell, typical diagrams of which are shown in **Fig. 1.11**.

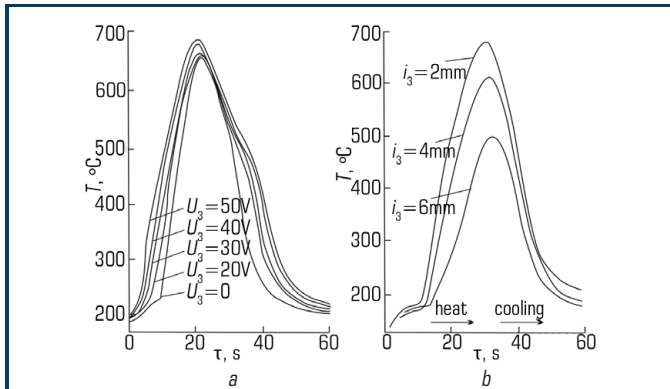
The method of electrolyte-plasma heating includes an alternating change in the electric field strength and a short-term connection of a low potential before the start of heating between the product and an electrode immersed in a water-based electrolyte. The use of appropriate cells is dictated by the product configuration and the requirements of the hardening technology.

A low voltage in the electrolyte cells is necessary in order for a vapor-gas layer of increased ohmic resistance to form on the heated surface. This allows immediately after switching on the operating voltage to start heating this layer.

Surface heating studies have shown that without preliminary formation of a vapor-gas layer, the surface heating delay, regardless of the layer depth, can reach 10–15 seconds (Fig. 1.12).



○ Fig. 1.11 Schemes of electrolyte-plasma cells for heat treatment of products: 1 – end heating; 2 – hardening of the disk periphery; 3 – heating with a sprayer; 4 – heating by immersion; 6 – axle heating; 7 – heating under a layer of electrolyte



○ Fig. 1.12 Change in temperature in the surface layer of the product from the time of heating and cooling: a – on the surface ($U_1=300\text{ V}$, $U_2=180\text{ V}$, $\Sigma\tau=20\text{ s}$); b – at a depth of 2; 4; 6 mm ($U_1=300\text{ V}$, $U_2=180\text{ V}$, $U_3=0$, $\Sigma\tau=20\text{ s}$)

This makes it difficult to obtain a stable heating technology and to ensure high quality hardening. In addition, after heating the surface of the product, it is important to ensure the required rate of its cooling, which is also ensured by connecting an additional low potential to the electrolyte cell and during cooling. With an increase in the voltage of the electric potential, upon cooling, the rate of temperature decrease will greatly decrease. Research has shown that it is possible to use the same potentials, both when preparing a product for heating and when cooling (**Fig. 1.12, b**). The mechanism of the potential influence during cooling, in fact, as well as during preparation, consists in the creation and maintenance of a vapor-gas layer, which has good thermal insulation properties.

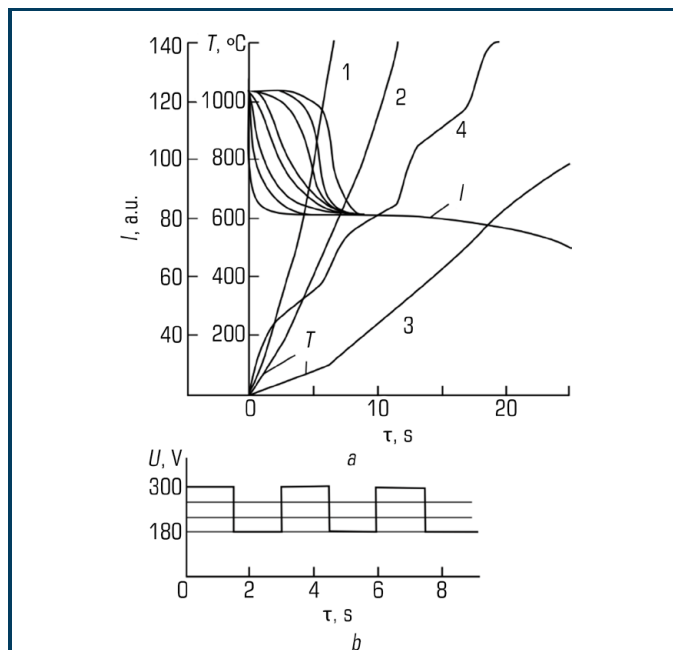
Experimental verification was carried out on an electrolyte heater in the form of a metal bath measuring 250–250–100 mm. The electrolyte (an aqueous solution of soda ash 12–15 %) was supplied through a sprayer fixed in the bottom of the bath. The product was immersed from above to a depth of 5.0 mm. Thermocouples with XK graduation were built into the product to various depths, which were connected to a secondary device of the KSP type.

A welding rectifier with a voltage of 20–50 V, adjustable rectifiers 150–220 V, and a thermistor switching system were used as a source of technological current. To ensure high-quality heating, a fundamentally new method was developed, which consisted of periodically connecting under-voltage and overvoltage. The hardening technology was controlled by setting the time of periodic switching on of low and high voltage. **Fig. 1.13** shows, as an example, a graph of the control of the process voltage with a switching frequency of 2 s.

Simultaneous measurements of the current strength and surface temperature at different electrical potentials showed that at a high voltage (240 V) the heating rate is so high that almost 8 s later the surface melting began, a voltage drop to 220 V had little effect on the heating rate, but at a voltage of 180 the heating process is no longer stable, it is characterized by sharp fluctuations in the technological current and it is practically impossible to heat the surface until it melts. At the initial moment of supplying the process current, due to the instability of the process, the current fluctuates within 40 A (**Fig. 1.13**).

Studies of heating the product when connecting periodically varying voltages of 300 V and 180 V (switching period 2 s) showed that the heating current, almost instantly, dropped to 80 A and further, as the temperature rises, the current gradually decreases. Thus, periodic connection provides an almost linear change in the heating rate and high technology stability.

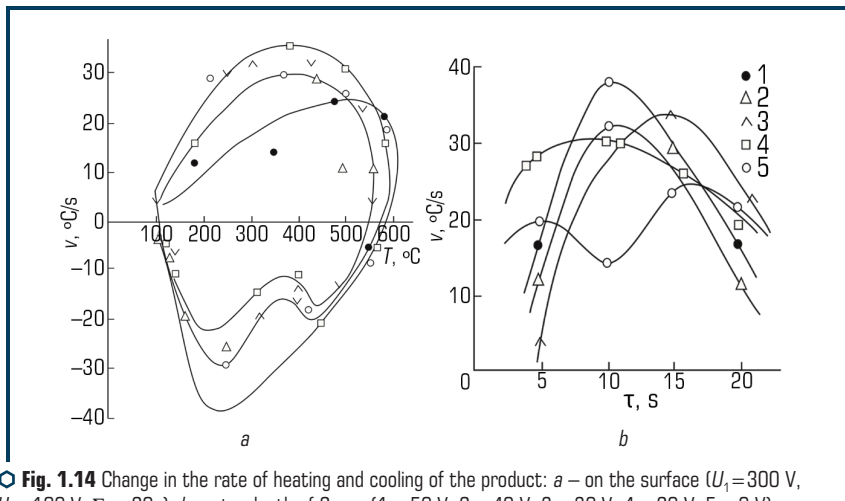
The results of measurements of the temperature of the heated surface of the product in the layer at a depth of 2 mm and 6 mm, as well as the temperature in the interelectrode space, show that without preliminary connection of the reduced potential, the temperature of the electrolyte in the interelectrode gap is equal to 30–50 °C, and the temperature of the heated surface, after 30 seconds heating, 200 °C lower than when heating with a preliminary connection of a potential of 20 V. This, apparently, is due to the instability of the process when connecting the technological potential. The preliminary switching on of the 20 V potential reduces the duration of the unstable mode from 10 to 1 second, which is practically sufficient for technological purposes. In this case, the temperature of the electrolyte in the interelectrode gap increased to 40 °C at a flow rate of 7.0 l/min.



○ **Fig. 1.13** Change in the heating temperature and current strength from time to time at various technological modes: *a* – at a voltage on the cell of 240 V (1), 220 V (2), 180 V (3) and at 300/180 V (4); *b* – graph of voltage changes 300/180 V

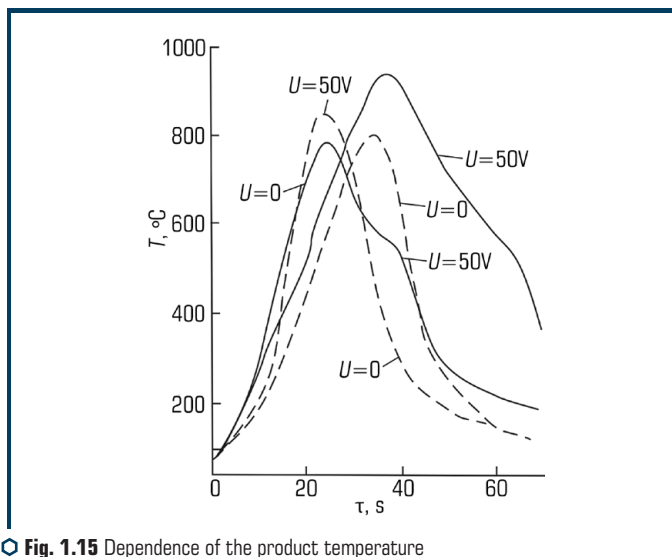
An increase in the pre-activation potential no longer affects the stability of the start of the heating technology, but the electrolyte temperature rises sharply and at 50 V it is 60 °C even at a flow rate of 16 l/min. It is known that the lowest electrolyte resistance is in the temperature range 45–50 °C. Experimental data make it possible to determine that switching on a voltage of 20–50 V for 2–3 seconds makes it possible to form a vapor-gas layer of increased resistance on the surface of the product and to increase the temperature in the interelectrode gap until its minimum resistance is reached.

This makes it possible to ensure the stability of the electrolyte-plasma heating technology without spending energy on heating the electrolyte in the tank. The study of the heating rate of the surface layers of the product, depending on the pre-switching voltage, showed (**Fig. 1.13**) that the most stable heating rate at a voltage of 20 V. temperature range of martensitic transformation. Connecting a reduced voltage to the electrolyte cell at the time of cooling the heated surface reduces its speed in the range of 300–400 °C. At the same time, with an increase in the voltage value up to 40–50 V, the cooling rate approaches the cooling rate in a special cooling medium (10–20 °C/s) (**Fig. 1.14**).



○ Fig. 1.14 Change in the rate of heating and cooling of the product: *a* – on the surface ($U_1=300$ V, $U_2=180$ V, $\Sigma\tau=20$ s); *b* – at a depth of 2 mm (1 – 50 V, 2 – 40 V, 3 – 30 V, 4 – 20 V, 5 – 0 V). Voltage for electrolyte cells – 300/180 V, heating time – 10–20 s

Technological modes (voltage value of the electrolyte cell) affect heating regardless of the depth of the heated layer (Fig. 1.15).



○ Fig. 1.15 Dependence of the product temperature at a depth of 6 mm on time during heating and cooling

Temperature measurements show that even after the end of the exposure time to the technological current, the bed temperature rises for another 5–10 seconds. Comparison of the rate of temperature change in the layer at a depth of 2 mm (**Fig. 1.14**) and at a depth of 6 mm (**Fig. 1.15**) shows that the effect of potential stress during cooling is more significant at a greater depth.

Depending on the magnitude of the electric potential between the surfaces of the electrode and the product, conditions are formed in the electrolyte cells for the formation of micro-arc discharges in the vapor-gas layer on the heated surface of the product. By changing the density and power of micro-arc discharges, by changing the voltage value, it is possible to control the cooling rate of the heated surface of the product (**Fig. 1.14, 1.15**).

The research experiments were carried out on samples of steel 45. Heating was carried out at a technological voltage of 280 V for 50 seconds.

After heating to the temperature of phase transformations, the voltage dropped in 4 s to 80 V. When the voltage was lowered, film boiling was observed on the surface of the product, accompanied by micro-arc discharges.

In this case, the heated surface is slowly cooled to 400 °C. After switching off the electric potential, the electrolyte nucleate boiling mode is realized on the surface, which is accompanied by a higher cooling rate. Analysis of the qualitative characteristics of the heat-strengthened surface showed that its hardness increased to 62–64 HRC, microcracks and defects on the surface were not observed.

1.4 STUDY OF HEAT FLOWS

As a result of measuring the temperature and subsequent calculations, the dependences of the change in the density of heat fluxes (**Fig. 1.16**) and temperature (**Fig. 1.17**) on the depth of the heated layer and the electrical conditions for the electrolyte cells were obtained.

Analysis of the results of the experiment shows that the power density of the heat flux greatly decreases in the depth of the product, which is due to heat dissipation and losses due to structural transformations. The power density of the heat flux through the surface during electrolytic-plasma heating changes almost 2 times with an increase in voltage by 40 V.

It is of practical interest to calculate the permissible rate of temperature change during heating without surface melting. An example of practical calculation of heating the surface of a product made of steel 40X with an EPP area of 16.3 cm² and a consumed power $q=0.33 \cdot 10^2$ W/cm² showed that the heating rate is 17–26 °C/s, while the surface temperature is 1172 °C, the heating time is 90 sec, energy efficiency more than 30 %.

Of practical interest is the estimation of the value of the maximum penetration Z_{\max} of the isotherm with a given value of the hardening temperature T_q . Experimental verification of the calculation formulas showed that for modes characteristic of hardening the tool holders of mining machines: $t=90$ sec; $l=800/1172=0.68$; $Z_{\max}=15$ mm.

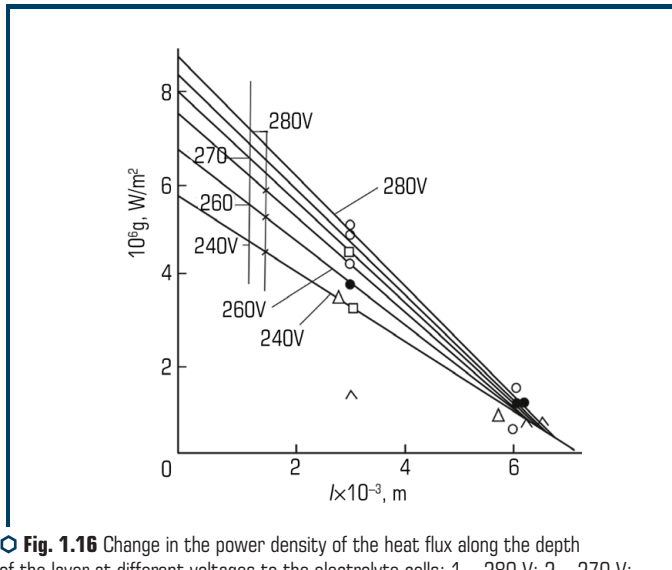


Fig. 1.16 Change in the power density of the heat flux along the depth of the layer at different voltages to the electrolyte cells: 1 – 280 V; 2 – 270 V; 3 – 260 V; 4 – 250 V; 5 – 240 V; 6 – 230 V

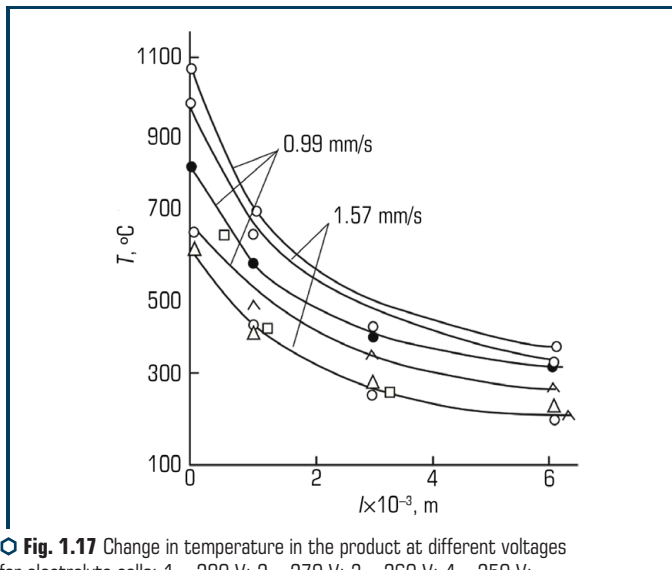


Fig. 1.17 Change in temperature in the product at different voltages for electrolyte cells: 1 – 280 V; 2 – 270 V; 3 – 260 V; 4 – 250 V; 5 – 240 V; 6 – 230 V

The critical energy flux densities for achieving the required heating depth depend not only on the thermophysical characteristics of the metal, but also on the product configuration, technological features of cooling, and heater efficiency. To warm up a local area of a product weighing 10 kg to a depth of 15 mm, the heating time should be 90 s. The permissible rate of temperature change, according to the calculation, is 40–50 °C.

For these conditions, the critical energy density (steel 40X at $T_{\text{max}}=870$ °C and heat treatment time 90 s) is $q_{\text{crit}}=1.8\cdot 10^6$ W/m².

The experimental work carried out confirmed the feasibility of electrolytic-plasma heating of a large class of products using combined power sources that ensured periodic switching on of high voltage 240–300 V, medium voltage 180–220 V and low voltage 20–50 V with switching periods of 2–10 s. In this case, it is possible to vary the heating and cooling rates of the hardened surfaces within a wide range.

ABSTRACT

The schemes of technological devices for the implementation of electrolytic-plasma processing of products of various configurations are presented. The industrial units for thermal cycling treatment of various tools and machine parts are described. The efficiency of the technology is shown in comparison with traditional methods of surface hardening.

KEYWORDS

Thermal cycling, structure refinement, hardening of the inner surface of the cylinder, drill pipes, saws, agricultural tools, machine parts, efficiency.

2.1 FEATURES OF HEATING TECHNOLOGY

The study of the plasma zone in the electrolyte heater at the cathode shows that a specific form of non-equilibrium electric discharge is formed in the gap between the electrolyte layer (liquid anode) and the surface of the product – the cathode. The discharge has the form of a distributed film with a low gas temperature and a high electron temperature. It consists of many streamers. A streamer is a weakly ionized thin channel that forms from a primary avalanche in a sufficiently strong field and grows in one or the other or in both directions to the electrodes; at the breakdown threshold of the flat gap – from the anode itself to the cathode. The streamer root is diffusively bound to the liquid anode electrode, which has a large surface area. The energy flux density to the anode is not high. The anode spots move and jets of superheated steam escape from them. Charges are transferred along these jets to the streamer root. In this discharge, there are no cathodic and anodic constrictions, and the discharge has the form of a diffuse one with distributed regions.

The following mechanism can be proposed for the formation of streamers directed to the cathode. Under the influence of variable gas pressure, the electrolyte surface acquires vibrations. As a result of these vibrations, the gas gap between the liquid electrode and the cathode surface changes greatly. The electric field strength in the electrolyte is low (up to 10 V/cm), but in the gas gap the strength is variable and can reach 1000–100000 V/cm.

This is the result of periodic changes in the cross section of the gas layer.

The current density in streamers and the frequency of their formation is limited by the ability of the liquid anode (electrolyte) to conduct electric current. Conductivity ions of the electrolyte are insufficient to maintain a high power density of energy at the cathode surface. The electrical

conductivity of the electrolyte is $c=20\text{--}40\text{ Ohm}^{-1}\cdot\text{m}^{-1}$. The electric field strength in the cathode (gas) region is 2–4 orders of magnitude higher than in the electrolyte.

The transport of the required amount of ions from the metal anode is also carried out by the hydrodynamic component. With a large volume charge and a high flow rate of the electrolyte, the component of the dynamic electrical conductivity is greater than the electrostatic one, which makes it possible to significantly (up to 10^4 W/cm^2) increase the energy power density on the surface of the product – the cathode.

Positive ions of carbon, nitrogen and metals create a layer adjacent to the heated surface of the product – the cathode. Electric discharges pass through this layer and intensify the processes of mass transfer. The introduction of an appropriate water-soluble salt into the electrolyte ensures the alloying of the product surface with elements that form positive ions.

In **Fig. 2.1**, the most typical schemes of electrolyte-plasma heaters are shown. Depending on the requirements for the product, heaters form different types of electrolyte cells (EC) in the interelectrode region [42, 44, 51–55].

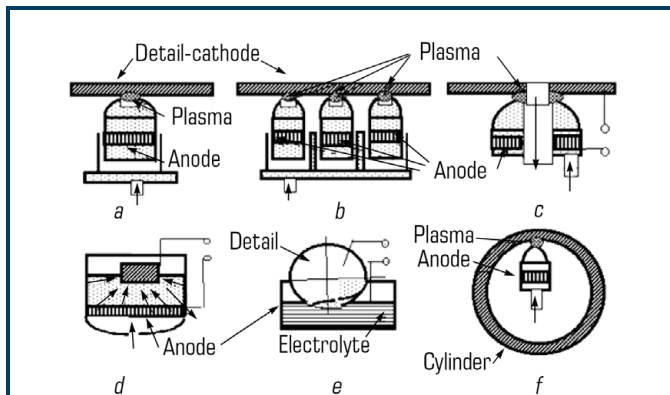


Fig. 2.1 Diagrams of technological devices intended for electrolytic-plasma hardening of products: *a, b, c* – flat surface; *d* – end face of the part; *e* – periphery of the saw blade; *f* – surfaces inside the cylinder

For example, to strengthen the outer surface of a drill rod or a flat surface of a sheet, the heater has the shape of a circular nozzle (**Fig. 2.1, a, b**), and the EC has the shape of a flat disk. To increase productivity, processing can be carried out simultaneously with 2–6 heaters (**Fig. 2.1, b**). The design parameters of the heater determine the efficiency of the process. To strengthen the hole, heaters have been developed, where the axial drain of the electrolyte is implemented (**Fig. 2.1, c**). EC has the shape of a flat ring. Heating of the end face of the part, for example, the end face of the sleeve, is carried out by immersing the surface into an anode cup filled with electrolyte (**Fig. 2.1, d**). EC has the form of a hardened surface, which is immersed in an electrolyte.

The periphery of a part such as a saw or a disc is hardened using a heater that is supplied from the bottom of the product (**Fig. 2.1, e**). Hardening of the inner surface of the cylinder is carried out by a small-sized heater, which is introduced into the product (**Fig. 2.1, e**).

By changing the heating mode, by controlling the electric field strength, it is possible to control the heating and cooling rate of the surface layer of the product, providing the thermal mode necessary for the formation of hardening structures [44].

Periodic disconnection of the electric potential provides a mode of thermal cycling treatment of the product surface. Surface cooling, in the pauses between the connection of the increased voltage, is carried out at a reduced voltage ($U_{cool}=20\text{--}36\text{ V}$) or without potential connection, $U_{cool}=0\text{ V}$ [42].

By periodically switching on and off the electric potential, the layer on the surface of the product is heated above the temperature of phase transformations. Then, by completely switching off or switching the electric potential strength by 36 V, the surface layer is cooled below the temperature of phase transformations. The subsequent repetition of the heating and cooling cycle makes it possible to implement the thermal cyclic hardening mode [42].

2.2 PRINCIPAL DIAGRAMS OF UNITS AND DESCRIPTION OF TECHNOLOGY

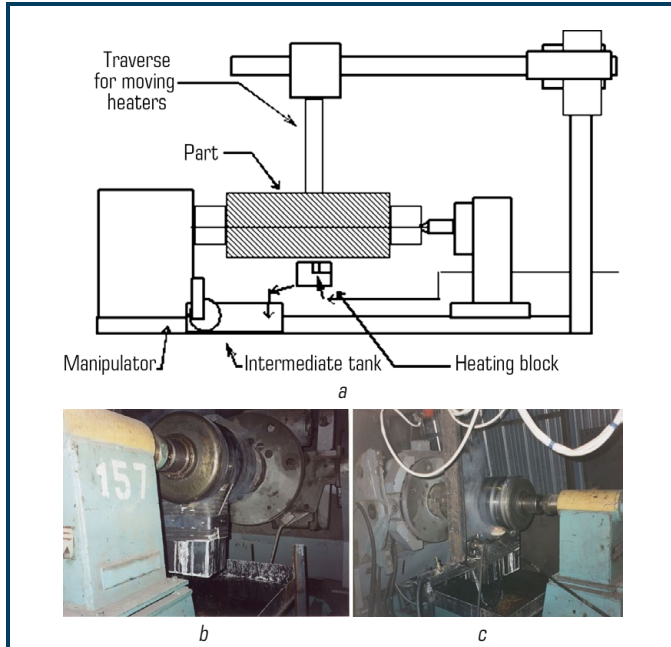
Electrolytic-plasma units are designed to harden the surface of products with various configurations (**Fig. 2.1**), for example: flat sheet, hole edge, shaft, roller, rod, saw teeth, inner surface of a long cylinder and other parts. The process of electrolyte-plasma hardening is carried out by heating the surface of the product with electric discharges in the plasma layer, which are formed between the layer of an aqueous solution of sodium carbonate (anode) and the metal surface of the product (cathode) [53, 54].

Heating is carried out by electric current, which flows through the plasma layer from the anode to the cathode. The power density of energy can be in the range of $0.5\text{--}1.5\cdot 10^3\text{ W/cm}^2$. The modified layer can be discrete and continuous. The thickness of the hardened parts of the layer reaches 2–10 mm. The spaces between the hardened areas have a low hardness, which increases the strength of the product.

The optimal range of speed of movement of the surface of the product relative to the heater or heater relative to the surface of the product is 300–1200 mm/min. It is possible to move the heater along the generatrix of the cylindrical product – 20–30 m per revolution.

The heater is brought to the surface from below so as to provide a 2–3 mm gap between the surface of the product and the edge of the heater. When moving the heater, the size of the gap is maintained by a ceramic stop or hydrostatically due to the special design of the heater mounting rod [53].

The unit can be made on the basis of a welding manipulator, which has the ability to fix and rotate a roll (roller). To move the heater, a traverse is selected, which is installed so that it is possible to move the heater along the generatrix of the working surface of the product. It is possible to use other mechanisms for fastening, rotation and linear movement of products [55, 56]. **Fig. 2.2** shows a diagram of a typical unit for the electrolytic-plasma hardening of cylinders and shafts.



○ **Fig. 2.2** View of unit for electrolytic-plasma treatment of the surface of the rolls: *a* – unit diagram; *b* – view from the side of the tailstock of the unit; *c* – view of the heater and shaft rotation drive

The unit is made on the basis of a standard manipulator (lathe or milling machine, welding manipulator) [56]. The product is fixed in the machine spindle. The spindle is equipped with a device for supplying electrical energy. The electrolyte heater is fixed on the machine support and is fed under the surface to be hardened or inserted into the cylinder bore. The tank with the pumping station can be installed under the machine support or at a distance from the machine. The electrolyte is fed into the heater at a constant rate. From the heater, electrolyte flows into the tank. The tank has a system of heat exchangers and sedimentation tanks. In **Fig. 2.2, b, c** shows a view of the unit for hardening shafts. The heaters are fixed in the process tank, which is installed on the cross arm bracket, under the surface to be hardened. The electrolyte is pumped to the heaters from the intermediate tank.

The electrolyte is fed into the intermediate tank by gravity due to the difference in electrolyte levels. Electrolyte supply is switched on by solenoid valves. From the process tank, the electrolyte flows by gravity into the intermediate tank where the pump is installed. The pump transfers the electrolyte to the main tank. In order to protect against electrolyte leakage, the solenoid valve and the pumps are switched on simultaneously.

A standard converter of electrical energy (it is possible to use the converter for air-plasma cutting) is additionally equipped with a control unit. This unit has a system for temperature control as well as a system for switching on the process voltage. The unit provides control of the heating and cooling rate. The periodic switching on of the electric potential allows to create a system of solid inclusions on the surface of the product. The product is attached to a standard manipulator. An electrolyte heater is brought under the product, which is included in the electrical circuit as an anode. The product is a cathode. The electrolyte from the tank is pumped into the heater and closes the electrical circuit between the anode electrode and the surface of the product. **Fig. 2.3** shows a diagram of the heater, which is mounted in the intermediate tank – 1. This tank is used to collect electrolyte and overflow it into the system for cooling and supply.

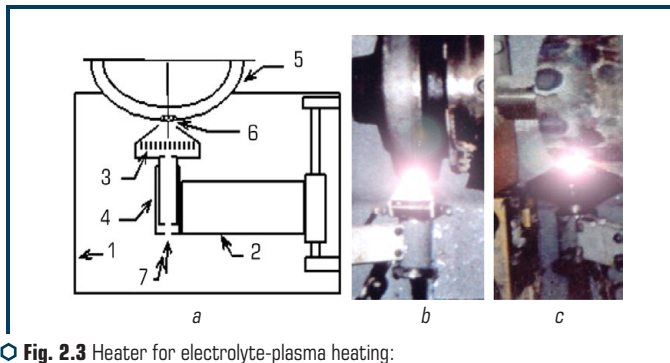


Fig. 2.3 Heater for electrolyte-plasma heating:
a – heater circuit; *b* – heater for rollers; *c* – heater for drill pipes

The heater is attached to the walls of the tank – 1 by means of a special bracket – 2, which provides electrical insulation and its movement along the height due to the electrolyte pressure. The electrolyte passes through electrode – 3, which has through holes and is included in the electrical circuit by the anode.

Under electrolyte pressure, the heater rod – 4 extends and provides a more accurate adjustment of the gap between the heated surface – 5 and the edge of the heater – 6. The electrolyte is fed into the heater from the system through holes – 7.

A universal unit for electrolytic-plasma treatment (**Fig. 2.4**) contains: a sealed tank for 2 m^3 – 1; non-conductive box with a transparent (sliding) cover – 2; an electrolyte heater is installed inside the tank – 3; which is fixed on the arm two portal manipulators – 4; the part/samples are fixed in a three-jaw chuck – 5, which rotates by an electromechanical drive – 6; the heater is connected by a flexible wire with an energy converter – 7; control panel of converter, portal and manipulator – 8.

On the top of the box there are technological holes for connecting the exhaust ventilation. Supply ventilation is provided through the slots in which the hand of the portal and manipulator moves, which excludes their contamination during electrolyte-plasma heating. A hydraulic system

is installed in the tank of the unit for supplying and controlling the flow of electrolyte, as well as for cleaning and cooling it. Electromechanical drives for the portal – 4 and manipulator – 6 are moved outside the active part of the unit.



Fig. 2.4 Universal unit for electrolytic-plasma treatment: *a* – general view; *b* – view of the manipulator

This design makes it possible to conduct electrolytic-plasma processing in the cathodic and anode modes, to observe the technology through transparent dielectric covers, to easily replace parts and adjust the technological mode. The removal of electromechanical drives outside the active area of the unit ensures their protection from splashes and electrolyte vapors and excludes failures.

The safety of the unit operation is ensured by interlocking contacts for closing transparent covers and the presence of a jet in the exhaust ventilation. A break in the interlocking contacts (switching off the ventilation or opening the cover) leads to a power cut-off of the electromagnetic relay of voltage input to the converter.

Fig. 2.5 shows a typical layout of the site for electrolytic-plasma hardening, which contains standard equipment: 1 – shaft rotator; 2 – tailstock of the rotator; 3 – traverse; 4 – traverse carriage; 5 – traverse fastening; 6 – tank; 7 – electric current converter; 8 – fence; 9 – door to the fence; 10 – control panel; and non-standard equipment; 11 – block of electrolyte-plasma heaters; 12 – intermediate tank with a pump for pumping waste electrolyte; 13 – hydraulic system: solenoid valve, intermediate tank, pump for electrolyte supply.

Transport pipelines for the electrolyte are made of a dielectric flexible hose $D_y=11$ mm for feeding and $D_y=20-24$ mm for draining the electrolyte by gravity.

The specialized unit is made on the basis of a welding manipulator, equipped with an electric current converter, a control panel and a tank with a pump. A heat exchanger is installed in the tank.

The EPP unit consists of a manipulator of bodies of revolution with a built-in regulator of rotation speed, electrolyte heaters, which are installed on a traverse having two degrees of freedom of movement (along the product and along the height). A heater is fixed under the surface of the

product to be hardened. Hardening is carried out by electric current, which is passed through an electrolyte electrode over a plasma layer adjacent to the surface of the product. The energy power density is $1-1.5 \cdot 10^3 \text{ W/cm}^2$.

Fig. 2.6 shows a unit for researching the technology of electrolytic-plasma treatment, which contains: a programmable complex for measuring the surface temperature and control of the technological mode of electrolyte-plasma heating – 1; three-coordinate manipulator control panel – 2; electric energy converter – 3; manipulator drive – 4; exhaust fan – 5; protective shields – 6; electrolyte tank – 7; hydraulic block for electrolyte supply control – 8.

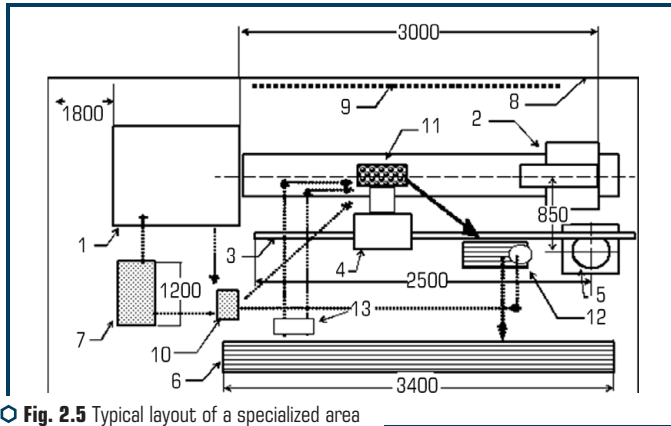


Fig. 2.5 Typical layout of a specialized area for electrolyte-plasma hardening

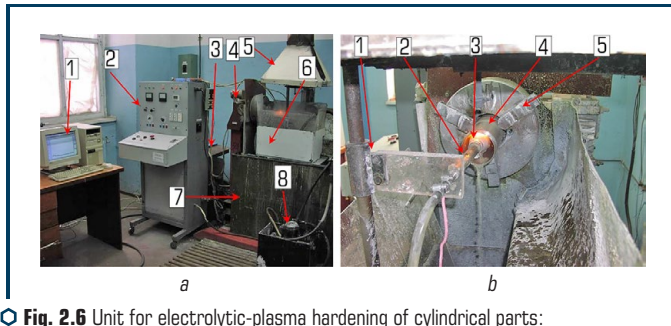


Fig. 2.6 Unit for electrolytic-plasma hardening of cylindrical parts: *a* – general view; *b* – view of the part processed by plasma

The unit (**Fig. 2.6, b**) contains: an electrical insulating bracket – 1 from a two-coordinate portal manipulator; rod – 2 for fixing the heater and electrolyte supply; ceramic heater – 3. The heater is pushed into the cylindrical hole of the product – 4, which is fixed with a three-jaw chuck – 5.

The electrolytic-plasma unit contains:

- system for electrolyte supply (tank, pump);
- electrolyte regeneration system;
- electrical energy converter (220, 300 V);
- remote control;
- electrolyte heater;
- product manipulator.

The operation of the unit for electrolytic-plasma hardening includes the following technological operations:

- the product is installed in a special mandrel of the unit spindle, above the open surface of electrolyte heaters;
- when lowering the protective cover of the tank for fixing electrolyte cells, the interlocking contacts are closed and the unit is ready for operation;
- switching on the electric potential and the pumping station is carried out by the «start» button and the automatic switch, respectively;
- electrolyte, filling the cells, closes the electrical circuit between the anode electrode and the workpiece to be treated. From this moment, the process of electrolyte-plasma treatment begins;
- the process is repeated until the entire surface of the product has been processed. After the end of the processing, the electric current converter and the valve for supplying the electrolyte are turned off;
- filling of electrolyte-plasma cells with electrolyte is carried out through an electromagnetic valve;
- the electrolyte is drained from the heaters into the intermediate tank. The electrolyte is pumped out of the tank by a pump;
- the entire processing cycle is monitored by instruments and signal lights;
- the ends of the current lead from the rectifier (+) are connected to the electrolyte cells; the ends from the rectifier (–) are connected to the product by means of a current collector;
- using a time relay, the operating time (switching on) of the rectifiers and the order of their switching on are set (see the operating instructions for the program time relays);
- effective voltage and actual current values are determined by the devices on the control cabinet panel;
- electrolyte cells are filled with electrolyte and complete the electrical circuit.

Technological parameters are shown in **Table 2.1**.

Switching of electrolytic-plasma units to the continuous hardening mode is carried out in the following order:

- switching on the electrolyte supply;
- switching on ventilation;
- turning on the shaft rotation;
- switching on the power electric circuit (300–340 V);
- turning on the feed, moving the heater along the generatrix of the shaft.

● **Table 2.1** Technological parameters of the electrolytic-plasma unit

Parameter name	Dimension	Value
1. The gap between the heated surface and the heater	mm	From 2 to 4
2. Voltage of rectifiers	V	34, 200, 320
3. Working current	A	50–200
4. Heating time	sec	From 1.0 to 9.0
5. Pause time	sec	From 0.5 to 2.0
6. Electrolyte consumption	m ³ /hour	1–5
7. Mass fraction of soda ash in the electrolyte	%	12–15

After hardening the surface of the product, the power circuit is turned off, the movement of the heater, the rotation of the product, the supply of electrolyte, and ventilation.

The implementation of the second stage of work involves heating the surface according to the cyclogram. For this, it is necessary to have a control panel for the cyclogram. The cyclogram assumes turning on simultaneously high (300–340 V) and low (200–220 V) voltage for 2–5 seconds, then turning off the high (300–340 V) voltage for 2–5 seconds, then connecting high voltage and so on. This makes it possible to increase the heating time of the local surface up to 30–50 sec and to warm it up to the temperature of phase transformations. The thickness of the heated layer is 5–10 mm.

Checking the operation of the rectifier switching modes is carried out at idle using a stopwatch and a voltmeter. Checking the efficiency of the unit in the mode of electrolytic-plasma hardening is carried out according to the readings of the ammeter and stopwatch, as well as the results of metallographic studies and industrial tests.

To ensure the stability of the technology, as well as the long-term and uninterrupted operation of the unit, it is necessary to carry out daily and periodic inspections of the unit in accordance with the operating instructions. To prepare the electrolyte, the consumption of soda ash (Na₂CO₃) with a mass fraction of Na₂CO₃ up to 15 % is required.

The heaters are fixed in the process tank, which is installed on the cross arm bracket, under the surface to be hardened. The electrolyte is supplied to the heaters by gravity, due to the difference in electrolyte levels in the main tank and in the heaters. Electrolyte supply is switched on by solenoid valves. From the process tank, the electrolyte flows by gravity into the intermediate tank, where the submersible pump is installed. The pump transfers the electrolyte to the main tank.

In order to protect against electrolyte leakage, the solenoid valve and the pump are switched on simultaneously. Soda ash consumption is up to 240 kg per year. Erosion of the anode mesh is up to 0.5 mm per week of work. The mesh is made of steel X18H9T. Changes after 2–3 months of work.

Water is consumed for the formation of plasma and evaporation in the process of cooling the heated surface. The concentration of soda in the electrolyte is periodically monitored, water is added to the tank and the consumption of soda is compensated.

2.3 HARDENING OF DRILL PIPES AND DRILLING RIG CONNECTORS

Drill pipes are the main connecting link of the rotor (rotator) with the rock destructive tool. In conditions of increasing depths, forced conditions and increasing power, high quality drill pipes, working rods, heavy bottoms and other elements of the drill string are required. At the same time, drill pipes are the most vulnerable part of drilling equipment. For example, in rotary drilling, statistics have established that 60 % of all accidents occur as a result of abrasive wear and breakage of drill pipes.

A string of drill pipes is an elastic system that, during drilling, perceives loads that vary in magnitude and direction. It is subjected to stretching, twisting and bending. The wear of drill pipes due to the friction of the string against the borehole wall weakens their strength and is often the cause of accidents.

Key elements of a drill string are main drill boring, drill pipes, tool joints, subs, and drill collars. In addition to the pipe-to-pipe connection, drill pipes are connected using the following elements, which also wear out:

- 1) nipples connecting the ends of the pipes along the internal thread and at the same time maintaining the outer diameter of the pipes;
- 2) couplings connecting the ends of the pipes along the external thread and while maintaining the inner diameter of the pipes;
- 3) locks, consisting of two elements, screwed onto the ends of pipes and connected to each other with a special thread; in this case, both the outer and inner diameters of the pipes are not preserved.

All technologies for hardening the surface of pipes and fittings using welding, heat treatment and electrode surfacing have been tested at different times and, despite the achieved increase in wear resistance of parts, have limited application. The reason for this is the softening of parts as a result of secondary heating after surfacing or chemical-thermal treatment, as well as a change in geometric dimensions (leashes). In addition, the high cost of surfacing materials and powders for spraying dramatically reduces the effectiveness of hardening drilling rig parts. Plasma hardening or HFC hardening on the untreated surface of the product is not effective.

To increase the wear resistance and strength of the pipe, it is proposed to create solid inclusions and compressive stresses on its outer surface and along the top of the thread. Solid inclusions should prevent abrasive wear, and compressive stresses should increase the fatigue strength of the product and increase the bending resistance [57].

We have developed a method, which consists in creating solid inclusions inside the surface layer of the product. These inclusions are formed by electrolytic-plasma thermal cyclic hardening (EPTCH), where the surface of the product is heated by electric energy, which is converted into heat at the border with the electrolyte – an electrically conductive renewable liquid layer. Cooling is carried out with the same electrolyte [57].

Experiments have shown that the creation of solid inclusions inside the surface layer of the product leads to the creation of an extremely high level of compressive stresses, which increases the fatigue strength and bending resistance. This allows to recommend this technology for

hardening products that operate under high bending loads, for example, drill pipes and fittings (adapters, nipples, etc.).

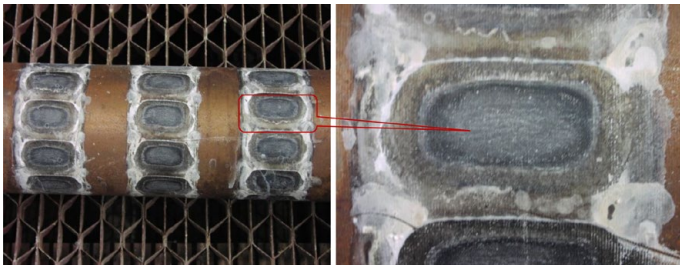
The EPTCH process is carried out on units with the following scheme: the product is installed on any standard manipulator; an electrolyte heater is brought under the product, which is included in the electrical circuit as an anode. The product is a cathode. The electrolyte from the tank is pumped into the heater and closes the electrical circuit between the electrode (mesh anode) and the surface of the product through the electrolyte (aqueous salt solution). **Fig. 2.3** shows a diagram of an electrolyte heater, which is mounted in the tank. This tank serves to collect and overflow electrolyte into the system for its supply.

Conversion of electrical energy into heat occurs mainly in a thin layer adjacent to the product. Analysis shows that the conductivity of this layer is two orders of magnitude lower than that of the electrolyte jet, which makes it possible to maintain a high electric field strength in it, up to $(0.5-1) \cdot 10^6$ V/m and provide a large voltage drop.

Micro-arcs are formed between the liquid anode, which is formed by the heater and the surface of the product (cathode). They are formed in the vapor-gas layer as a result of fluctuations in the surface of the liquid electrode and a local increase in the electric field strength. Since the discharge gap of micro-arcs is relatively small ($h=1-2$ mm at $d_c \gg h$), the energy losses in micro-arcs are insignificant, mainly, the energy is spent on heating the surface. The plasma-forming material is a water-based electrolyte, the same electrolyte is used to cool the heated surface. To increase productivity, processing can be carried out simultaneously with 2-6 electrolyte heaters.

Rapid heating and cooling of local sections of the pipe surface provides the formation of hard micro-structured areas with a smooth decrease in hardness to the base of the product (**Fig. 2.7**). The volume of these surface areas increases (due to martensitic transformations) and compressive stresses are formed between the inclusions, which multiply the strength of the product.

Relatively soft areas of the surface provide the possibility of bending the pipe without destroying it. The technology allows varying the rate of heating and cooling (50-400 °C/s) and, accordingly, the thickness of the hardened layer 1-10 mm.

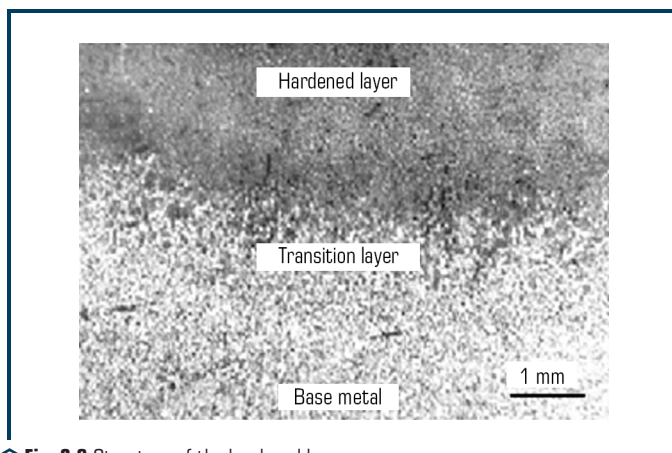


○ **Fig. 2.7** Exterior view of reinforced locations on the drill pipe

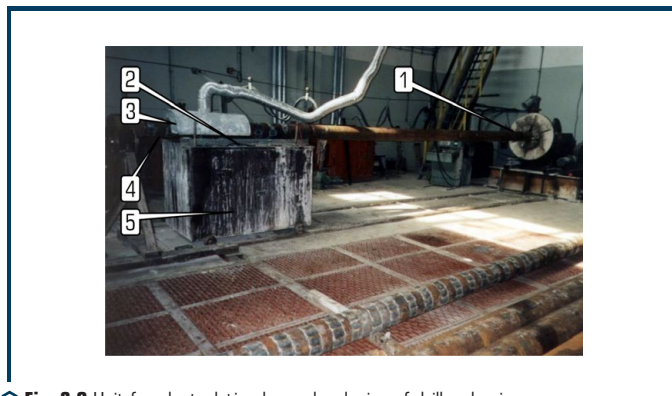
The hardness of the hardened layer is within 60 HRC. A high rate of heating and cooling ensures the formation of hardening structures with a smooth transition to the base metal of the product (**Fig. 2.8**). The thickness of the transition layer is 0.2–1 mm.

The configuration of the hardened layer depends on the design of the heater and can be round, square, annular or elliptical with a characteristic size of 10–45 mm. The hardness of the inclusions is: on steel 35XHSA – 50–55 HRC, on steel 40X – 55–60 HRC, on steel 65H – 60–68 HRC. The creation of a system of solid inclusions on the surface of products provides a multiple increase in wear resistance and compressive stresses in the surface layer of the product, which increase its strength.

The technological unit for EPTCH for hardening the surface of drill rods-pipes and fittings was developed on the basis of a welding manipulator (**Fig. 2.9**).

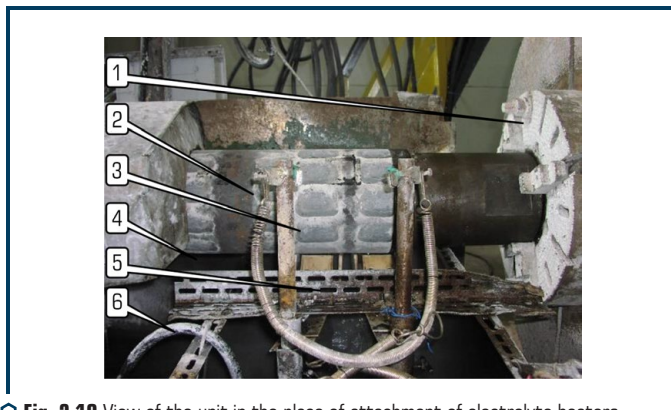


○ **Fig. 2.8** Structure of the hardened layer



○ **Fig. 2.9** Unit for electrolytic-plasma hardening of drill rods-pipes

Unit for electrolytic-plasma hardening of drill rods-pipes [57] contains manipulator – 1 (pipe rotator), electrolyte heater – 2, exhaust ventilation screen – 3, pipe support – 4, intermediate tank trolley – 5. View of heated the section in the pipe hardening plant is shown in **Fig. 2.10**. The unit contains: a cartridge for fastening a pipe – 1; drill pipe – 2; heated surface areas – 3; intermediate tank – 4; heater attachment point – 5; electrolyte supply pipeline – 6.

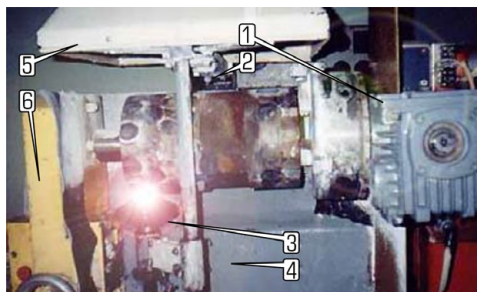


○ **Fig. 2.10** View of the unit in the place of attachment of electrolyte heaters

The operating mode of the unit is set by the power density of the plasma heating, the number and speed of movement of the heaters. The productivity of one heater is 60 sections/hour. The diameter of one hardened section is 35 mm. The consumption of electrical energy for the production of one hardened section with a diameter of 35 mm is 0.12 kW/h. The power density is $1\text{--}2 \cdot 10^3 \text{ W/cm}^2$.

To harden a single piece, such as a 250 mm drill pipe coupling, four strips of hardened sections must be created. The stripes are shifted relative to each other by half the distance between the sections. The distance between the sections is taken not less than the diameter of the section. Therefore, to harden one part, it is necessary to produce $11 \times 4 = 44$ (sections). Or spend $44 \times 0.12 = 5.28$ kWh. The machine time for the production of hardening of one part will be 44×30 (s) = 0.36 hours. Let's accept an auxiliary time equal to 0.14 hours. The total hardening time for one part is 0.5 hour (30 min). With an eight-hour working day, the hardening capacity on one unit will be 16 parts. Electricity consumption will be $5.28 \times 16 = 84.48$ kW/h. The capacity of the unit is proportional to the consumed power.

An electrolyte heater with a characteristic outlet size of 40 mm was used to strengthen the products for fixing the drill adapters. The heating and cooling cycle of one switch was 50 s. The power density during heating reached $2.4\text{--}10^3 \text{ W/cm}^2$. The unit (**Fig. 2.11**) was based on welding equipment, which had mechanisms – 1 for fixing products and rotation, as well as a mechanized ruler – 2 for moving electrodes – an electrolyte heater – 3. Under the hardened product there is an intermediate tank – 4 for collecting electrolyte.



○ Fig. 2.11 Type of unit for EPTCH drill rod adapters

Above the unit is fixed a screen – 5 for exhaust ventilation, and at the end of the unit there is an adjustable tailstock – 6, which is designed to support the products. A system of local solid inclusions with a diameter of 40 mm and a hardness of 60 HRC was created on the surface of various drill rod adapters using EPTCH (Fig. 2.12).

The creation of a system of solid inclusions that perceive wear loads and provide compressive stresses in the surface layer of the product increases their performance. Unhardened surface areas provide stress relaxation.



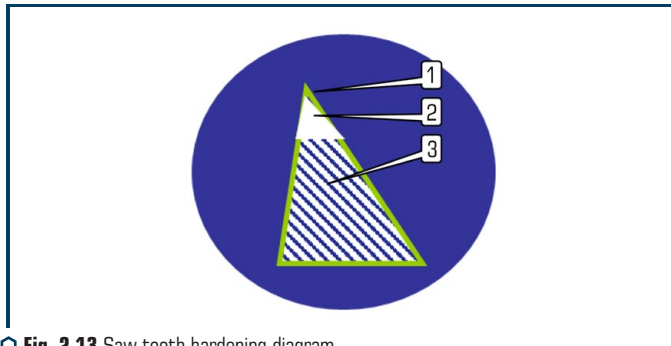
○ Fig. 2.12 Appearance of hardened adapters, various options

Tests have shown that local hardening of a product increases bending resistance by 30–40 %, which makes it possible to use this technique to strengthen products that operate under high bending loads, such as drill pipes. The serviceability of the drill pipe adapters after hardening has increased 2–3 times.

The technology of electrolyte-plasma thermal cyclic hardening (EPTCH) is effective for hardening such products as: adapters, pods, rods (pipes) of drilling rigs, pan bottoms, tool holders in the mining and ore industry.

2.4 SAW TOOTH HARDENING

The most common tool for cutting metal workpieces is saws. The saw tooth works in cramped conditions that limit heat dissipation, in the presence of abrasives and shock loads. The most heavily loaded saws are in metallurgy, for example, when cutting rolled products. Analysis of the existing technologies for hardening and operation of circular saws for cold cutting of bent shaped rolled products made it possible to assume that secondary hardening of the saw tooth tip may be the most acceptable, **Fig. 2.13**. The creation of a harder nano-structured layer – 2 at the top – 1 tooth is possible with the use of heating and cooling methods that provide speeds in excess of 500 °C/s. The high heating rate provides fast heating of a thin layer of the tip, without heating the base – 3 teeth, which will exclude its softening. To create a rapidly hardened layer on the tip of the saw tooth, a technology was developed and a special electrolyte-plasma hardening device was manufactured [58, 59].



○ **Fig. 2.13** Saw tooth hardening diagram

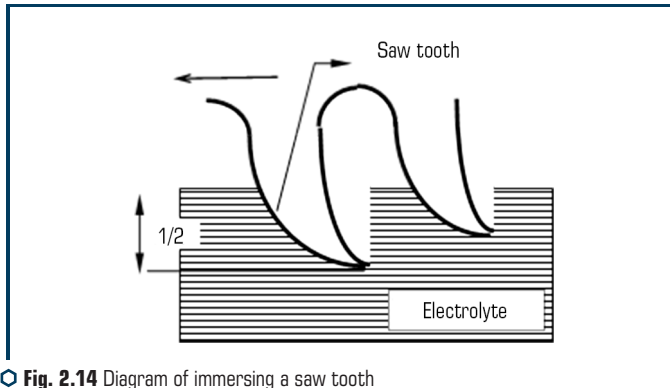
The basic principles of hardening technology include immersing the ends of the tooth by 1/2–3/4 of their height in a water-based electrolyte (15 % soda ash solution), **Fig. 2.14**. An electric current is passed through the electrolyte from the anode to the saw teeth (cathode). A plasma layer appears on the outer surface of the teeth touching the electrolyte conductive medium, which heats the surface to the temperature of phase transformations [59].

Hardening of all saw teeth is carried out by sequentially dipping the tops of the teeth into the electrolyte. In this case, the teeth are introduced into the electrolyte cell by the rear surface. Several teeth from 8 to 16 are heated at the same time, and 2 to 4 teeth are introduced into the electrolyte during the time before switching the electric potential. This allows for uniform heating and cooling of all saw teeth. For diffusion modification and deposition of alloying elements on the heated tooth surface, they are introduced into the electrolyte. An electric field with a strength of up to 10^6 V/m ensures the transport of elements to the heated surface and their diffusion into the surface. The deposition of alloying elements on the heated surface of the tooth and its friction

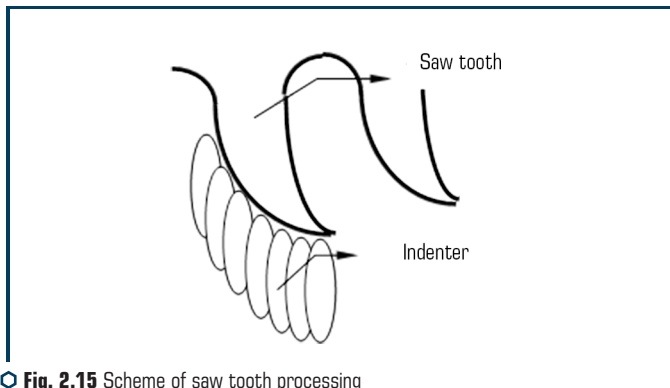
against the surface of the ceramic indenter, with the stimulating action of an electric current, provides a high diffusion rate. In **Fig. 2.14**, the layout of indenters accelerating diffusion processes is shown. Ions of alloying elements in the surface layer of the tooth form solid solutions and chemical compounds in the form of borides, carbides or nitrides.

Such processing provides directed movement of alloying elements into the surface and electrospark alloying with hard alloys, for example, tungsten carbides, which increases the redness and hardness of the posterior surface and apex of the tooth [60].

The saw teeth heated above the temperature of polymorphic transformations are sequentially removed from the electrolyte while smoothing them against a hard, cold indenter (**Fig. 2.15**), which stimulates diffusion. In addition, the combination of smoothing with cooling ensures the implementation of the mechanical heat treatment mode with the effects inherent in this treatment.

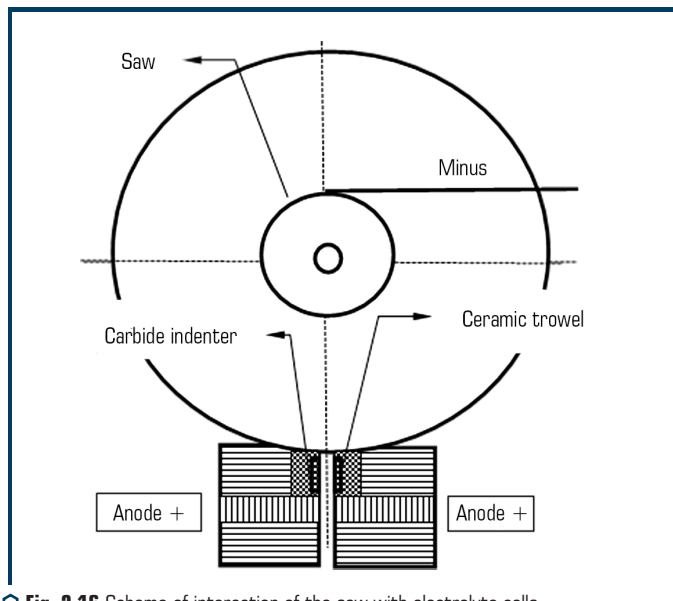


○ **Fig. 2.14** Diagram of immersing a saw tooth into the electrolyte cell of the heater



○ **Fig. 2.15** Scheme of saw tooth processing with an indenter (ceramic/carbide)

Fig. 2.16 shows a diagram of the interaction of the saw with electrolyte cells-heaters [58]. The immersion of the tooth in the electrolyte up to $3/4$ of its height provides heating up to half the height, but the heating temperature is uneven.



○ **Fig. 2.16** Scheme of interaction of the saw with electrolyte cells

The maximum heating temperature on the cutting edge of the tooth, which is $100\text{--}150\text{ }^{\circ}\text{C}$ higher than the temperature of polymorphic transformations of the alloy used for the manufacture of the saw. The saw teeth made of steel 9XC make it possible to overheat the cutting edge to $1200\text{ }^{\circ}\text{C}$, and when it is removed from the electrolyte, cool it in air to $400\text{--}450\text{ }^{\circ}\text{C}$ due to heat dissipation into the saw mass and electrolyte evaporation.

The following processing modes are optimal: the linear speed of movement of the teeth of the samples is 300 mm/min , which ensures the movement of one tooth per second or when turning on 280 V for 2 s , two teeth are inserted at increased voltage, and with simultaneous processing of 12 teeth, three increase cycles and three a cycle of lowering the voltage for each tooth [39].

Recommended modes of electrolytic-plasma hardening of the surface of the samples are shown in **Table 2.2**.

A specialized unit for hardening the teeth of a metallurgical saw is shown in **Fig. 2.17, 2.18**. A drain container is installed on the bed, inside of which there is a heater (**Fig. 2.17**). On the spindle – 1, the saw is attached – 2, the tops of the saw teeth are heated – 3 when they are immersed in the heater – 4, which is fixed in the drain tank – 5.

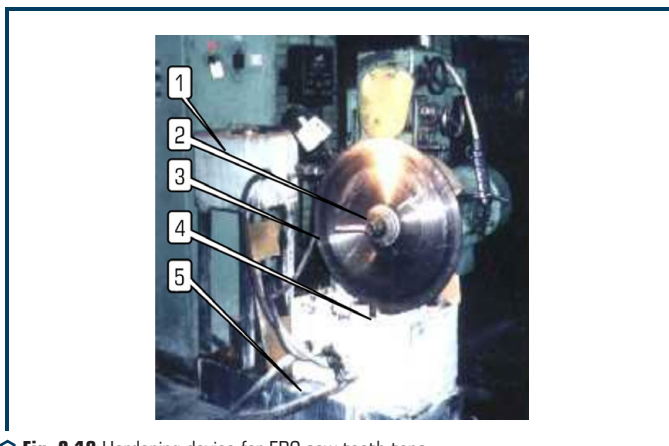
● **Table 2.2** Modes of electrolytic-plasma hardening of the sample surface

Steel grade	Immersion of the tooth (h) in the electrolyte mm	Current, A	Voltage, V Hardening Pause		Heating time, s Hardening Pause		Saw characteristic dimensions, $\delta \times d \times D$, mm
9KhFM	1/2h–3/4h	30–35	280	180	1.9–2	0.3–1	8×100×600

The unit contains (Fig. 2.18): a pressure tank – 1 with electrolyte, a rotator – 2 saws – 3 with a built-in speed controller and an electrolyte heater cell – 4. Saw – 4 is installed on the horizontal spindle of the unit so that its teeth are immersed in the electrolyte cells to a technologically determined depth [58].



○ **Fig. 2.17** View of the saw tooth electrolyte heater



○ **Fig. 2.18** Hardening device for EPC saw tooth tops

The unit contains a frame – 5, which contains the rotation mechanism of the circular saw. The rotation mechanism is equipped with a spindle fixed in bearing supports and connected to the drive motor by means of a gear reducer.

The processing of circular saws was carried out using electrolytic-plasma hardening. Circular saws were used at the AO Severstal plant. They were made of chromium/molybdenum/vanadium steels of the 90KhFM type (0.8–0.9 %; 0.3–0.6 % Mn; 0.15–0.35 % S; 0.15–0.30 % V; 0.4–0.7 % Cr; 0.3–0.7 % Mo) [39].

Heater anodes are made of corrosion-resistant steel 12X18H10T. The anode of the heater is connected to the positive pole of a variable voltage constant current source. A 15 % solution of soda ash in water was used as an electrolyte.

The electrolyte circulates in the hardening device forcibly in a closed loop: tank – pump – pressure tank – heater, drain tank – tank. The forced circulation system of the electrolyte promotes its homogenization and cooling, which additionally stabilizes the plasma heating condition.

The hardening device provides a rotational speed of the saw blade from 0.0003 to 0.01 s⁻¹. The immersion depth of the saw teeth in the electrolyte is adjusted by moving the spindle in the vertical direction. The teeth are immersed to a depth of 1–4 mm.

To carry out the hardening process, the circular saw – 2 is fixed on the spindle – 1. Then the circular saw is brought into rotation, the pump of the forced circulation of electrolyte system is turned on and the circular saw is lowered until its teeth are immersed in the electrolyte filling heater – 4 to the required depth. A constant voltage U_n is supplied to the anode – heater and cathode – circular saw. On the surfaces of the teeth immersed in the electrolyte of the heater – 4, a plasma arc is excited and burned. As each of the teeth of the rotating saw blade passes through the heater, they quickly heat up to the hardening temperature.

The study of various modes of hardening was carried out on circular saws with a diameter of 580 mm with the number of teeth $n=240$. It was found that at $U_n=260$ V, the rotational speed of the circular saw is 0.008 s⁻¹ and the voltage $U_0=26$ V, the hardness of the tops of the hardened teeth was 60–62 HRC. This satisfies the hardness requirements of the hardened saw blade teeth. The plasma arc burned evenly during heating, the saw blade remained cold.

To eliminate overheating of the sharp edges of the teeth, a pulsed heating mode was developed, according to which the voltage U_n abruptly changes during the heating process in accordance with the cyclogram. At a voltage of $U_n=U_{n1}=260$ V, the current density is 7–10 A/cm², a stably burning plasma arc intensely heats up the teeth of the circular saw. Since the duration of the pulse with voltage U_{n1} is limited by time t_1 , overheating of the sharp edges does not occur. After the time t_1 , the voltage U_n decreases to $U_{n2}=180$ V for a period of time t_2 , the plasma arc continues to burn, but the current density decreases to 4–6 A/cm² and the intensity of the heat release of the plasma arc. During this period, the teeth are warmed up to a certain depth without the danger of sharp edges melting, and the temperature of their surface decreases. At the next voltage pulse $U_{n1}=260$ V, the surface of the teeth again intensely heats up, but over a period of time τ_1 , the temperature of the sharp edges does not reach the temperature of overburning and melting, after

which the voltage again abruptly drops to $U_{n2}=160$ V, and during the time τ_2 , occurs equalization of temperature along the cross-section of the tooth apex. Consequently, during the residence of each of the teeth in the heater 5 sec their temperature rises continuously to the hardening temperature (820–870 °C), and overburning and melting of sharp edges can be avoided.

The use of impulse heating provided defect-free cold-cutting circular saws with hardened tooth tips having a hardness of 60–62 HRC. The microstructure of the hardened area is a «white» fine-lamellar martensite, which is poorly amenable to metallographic etching and has high wear resistance.

2.5 MODIFICATION OF THE HEAVY CRANKSHAFT TRUNNION SURFACE

2.5.1 THEORY AND EXPERIMENT TO OPTIMIZE THE RELIEF ON THE TRUNNION SURFACE

To increase the antifriction properties of the shaft surface, thermal and chemical-thermal processing methods are used. These methods, as a rule, are energy intensive and do not solve the problem of lubricating the friction surfaces at low speeds, for example, when starting the engine.

An electrolytic-plasma technology has been developed and equipment has been manufactured for the formation of local hard areas on the surface of the crankshaft trunnion of diesel engines with a thickness of up to 5 mm and a hardness of 55–62 HRC. After grinding, a special relief is formed on the surface, which provides hydrodynamic lubrication in the plain bearing. The technology for creating a relief provides multiple energy savings and is environmentally friendly.

Studies show [61] that it is possible to form an optimal relief on the trunnion surface in a plain bearing, which provides a liquid friction mode and, accordingly, reduces friction losses and the temperature of the wearing surfaces. The parameters of the peaks and valleys on the trunnion surface, which characterize the relief, are selected depending on the operating conditions.

To calculate the characteristics of the optimal relief on the working surface of the trunnion in a sliding bearing, the isothermal motion of a viscous incompressible fluid in a gap with a periodically changing cross section was considered [61, 62], **Fig. 2.19**. The change in the cross-section of the gap between the rubbing surfaces is due to the shape and frequency of placement of the tops and troughs of the relief.

The opposite surface, the inner surface of the plain bearing, is assumed to be smooth. In this case, the fluid motion in the gap was written by a system of second-order nonlinear partial differential equations [63].

Taking into account that the thickness of the lubricating layer is small (5–15 μm) at the top of the relief, then the calculation neglected the fluid flow across the layer, $V_z=0$.

The volumetric forces were excluded from the calculation, which is due to their smallness in comparison with the viscosity forces. The equations of fluid motion were written in partial derivatives taking into account the hydrodynamic pressure in the fluid layer p (Pa); dynamic coefficient of viscosity μ (Pa/s); the components of the speed of fluid movement along the X , Y , Z axis are V_x , V_y , V_z .

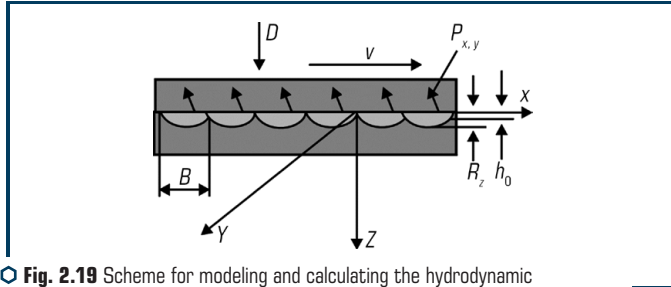


Fig. 2.19 Scheme for modeling and calculating the hydrodynamic lubrication of a sliding friction pair with a special relief on the trunnion surface

By integrating the equations and substituting into its solutions the values of the thickness of the lubricating film h_0 and the linear speed V , an expression was found for the hydrodynamic pressure on the surface of each top of the relief [63]:

$$P_{x,y} = \frac{\mu V B^2}{h_0^2 L} \left[\pi \beta^2 \sqrt{\frac{\alpha(1+2\alpha)}{1+\alpha}} - 4\alpha \right], \quad (2.1)$$

where $\alpha = h_0/R_z$ – relative thickness of the lubricating layer; R_z – height of the top of the relief, microns; $\beta = L/B$ – relative width of the hydrodynamic microcline; B , L – longitudinal and transverse distance between the tops of the relief, respectively, microns.

Analysis of equation (2.1) shows that if α can vary within 0.1–1, then β changes within 1–100. The parameter $\alpha = h_0/R_z$ is hydrodynamic, reflecting the complex interaction of the parameters of the relief, lubrication and friction conditions. Based on experimental data, this parameter is set within 0.5. The parameter $\beta = L/B$ characterizes the method of obtaining the relief. For the conditions for creating a relief using electrolyte-plasma technology, this parameter has a value of 1–10.

Total hydrodynamic force:

$$P = \sum_{1}^n P_{x,y}, \quad (2.2)$$

where n – the number of microroughnesses.

The area of the top of the relief, where the hydrodynamic pressure develops, is determined by the formula $S = BL/2$.

Equation (2.1) is solved for a specific sliding friction unit, where the contact pressure and the nominal contact area are known. It is assumed that the total hydrodynamic force P is equal to the load or the product of the contact pressure and the contact area. To solve the equation, let's take the values of the dynamic viscosity coefficient, the minimum permissible thickness of the lubricating film and the values of the sliding speed. The equation is solved with respect to the

following relief parameters: the height of the tops of irregularities, the longitudinal and transverse distances between them.

The theory was tested on models. The relief on the surface of the shaft was formed by rolling with balls. The main characteristic of the relief was its height – R_z was taken within 10. The sliding friction unit was lubricated with the Industrialnoe-45 mineral oil.

Studies on measuring the thickness of the lubricating layer have shown (**Fig. 2.19**, [63]) that depending on the sliding speed and the height R_z of the top of the relief, the lubricant layer changes at the top of the unevenness of the relief h_0 . The thickness of the oil layer reaches 16 microns. The lubricating layer increases with increasing sliding speed (**Fig. 2.20**).

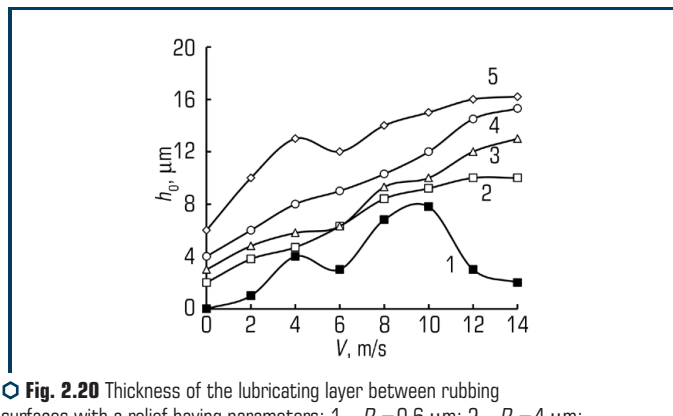


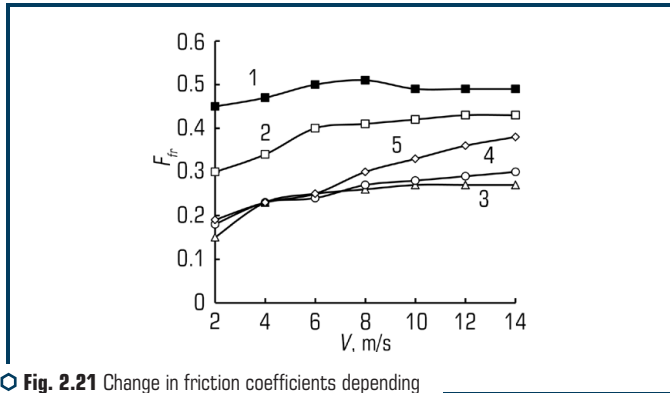
Fig. 2.20 Thickness of the lubricating layer between rubbing surfaces with a relief having parameters: 1 – $R_z=0.6 \mu\text{m}$; 2 – $R_z=4 \mu\text{m}$; 3 – $R_z=8 \mu\text{m}$; 4 – $R_z=12 \mu\text{m}$; 5 – $R_z=16 \mu\text{m}$

On the bearing surface, which had no relief ($R_z=0.6 \mu\text{m}$), no grease layer forms. Research shows that there is no lubricant layer on the shaft surface up to the friction speed $V=4 \text{ m/s}$. The formation of a lubricating layer in the speed range of 4–10 m/s can be explained by the hydrodynamic effects of shaft vibration. The greatest thickness of the lubricating layer is $8 \mu\text{m}$ at a sliding speed of 10 m/s. At higher speeds, the thickness of the lubricating layer decreases due to heating of the surface and a decrease in the viscosity of the lubricating fluid.

On the surface of the trunnion, which has a relief (**Fig. 2.20**, $R_z=6\text{--}20 \mu\text{m}$), a lubricating layer is formed in the entire range of the studied speeds (**Fig. 2.21**). Accordingly, friction losses are 2–3 times lower than with friction in the bearing, where the trunnion has a smooth surface (**Fig. 2.21**).

The relative thickness of the lubricating layer, which was measured at the tops of the trunnion surface relief, depends on the sliding speed. It varies within 0.5–2. Studies show that the shape of the relief peaks, which is characterized by the value of ρ , has a decisive influence on the tribotechnical characteristics. For a ground surface ($R_z=0.6 \mu\text{m}$) the value of ρ has a value in the

range of 0.01–0.001. Such a relief on the trunnion surface does not provide an opportunity for the formation of a hydrodynamic lubricating layer.

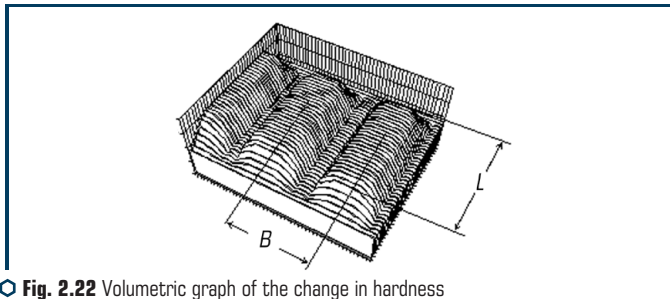


○ Fig. 2.21 Change in friction coefficients depending on the relief and sliding speed

When the specimen slides over the surface, which has a relief $\beta > 1$ (Fig. 2.20, graph 2–4), a lubricating layer is formed in the entire range of the studied speeds (0–14 m/s). Accordingly, friction losses are reduced (by 2–3 times), Fig. 2.21.

2.5.2 TECHNOLOGY OF FORMING A RELIEF ON THE TRUNNION SURFACE

An electrolyte-plasma technology has been developed for the formation of solid projections of the relief on the surface of the crankshaft trunnions for diesel engines [64, 65]. Using this technology, hard areas 25 mm wide are created on the working surface of the shaft trunnion, which periodically alternate with soft areas of the surface, Fig. 2.22.



○ Fig. 2.22 Volumetric graph of the change in hardness on the surface of the crankshaft trunnion

With $B=25$ mm, the longitudinal distance between the top of the relief, respectively, and $L=50$ mm, the transverse distance between the top of the relief, the relative width of the hydrodynamic microline will be equal to $\beta=2$ (Fig. 2.22).

Hard surface areas have a microcrystalline structure with a smooth transition to the structure of the base metal (Fig. 2.23).

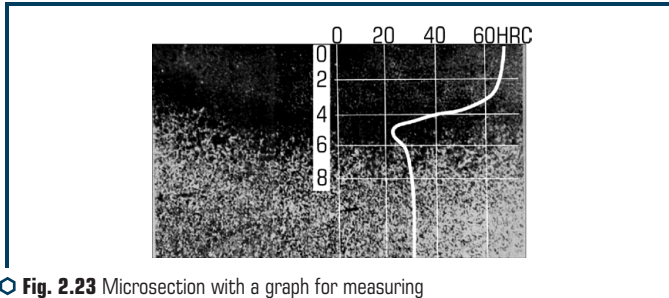


Fig. 2.23 Microsection with a graph for measuring the hardness of the hardened layer of the shaft trunnion

Hard areas have a lower machinability than soft ones, which, after abrasive processing, ensures the formation of a relief (Fig. 2.24).

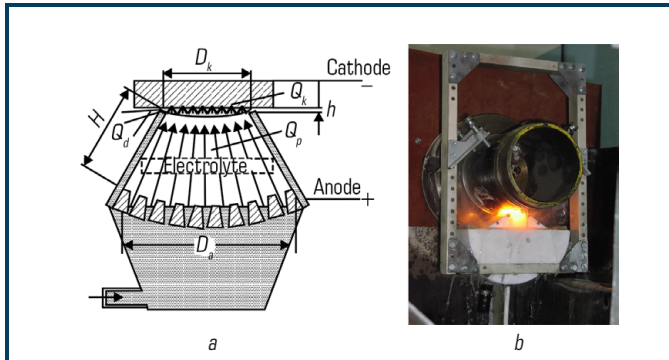


Fig. 2.24 Electrolyte-plasma heater for the formation of solid areas on the surface of the crankshaft trunnion: a – diagram; b – type of working heater

The relief consists of hard, wear-resistant protrusions and depressions, which have a depth of up to $R_z=15$ μm with a width of $B=25$ mm. The minimum allowable thickness of the lubricating layer at the top of the relief can be 5 microns and, therefore, the relative thickness of the lubricating layer $\alpha=0.3$. An analysis of formula 1 shows that at minimum speeds, at the moment of the start of movement, a lubricating layer of 5 μm is formed at the top of the unevenness, even

at a contact pressure of hundreds of MPa. With an increase in speed, the load capacity of the bearing increases and, accordingly, the minimum thickness of the lubricant layer at the top of the unevenness increases. Formula 1 is simplified; more detailed theoretical calculations, methodology, and experimental results are given in [64].

When the diesel engine is running, the gap in the crankshaft bearing is filled with grease. The depressions on the axle surface contain micro-volumes of oil. When the surfaces move on the side walls of the cavities, hydrodynamic wedges are formed, the carrying capacity of which depends mainly on the viscosity of the lubricating fluid, the sliding speed and the angle of rise of the hydrodynamic wedge.

Calculations using the formula show that the thickness of the lubricating layer above the top of the relief can be from 10 to 20 μm and depends mainly on the parameters of the relief (**Fig. 2.21–2.23**). The special relief provides a fluid friction mode even at low shaft rotation speeds. In this case, the oil is captured by the depressions of the relief and moves to the loaded bearing area, which excludes frictionless modes without lubrication, reduces friction losses, surface temperature and wear.

The formation of a special relief is provided by heating to the hardening temperature of the surface sections of the shaft trunnion. Heating is carried out by electric discharges in the plasma layer, which is formed between the surface of the product and the liquid electrode (electrolyte) [64–67]. An aqueous solution based on an alkali metal salt is used as the electrolyte. The heated surface is cooled with the same electrolyte. The heating device contains a housing made of a dielectric material and a metal anode with characteristic dimensions D_a (**Fig. 2.24**). The anode has holes through which the electrolyte flows to the cathode (heated surface).

Energy is mainly spent on heating the cathode Q_s – the surface of the product. The dissipation of energy Q_e is small, which is due to the small thickness of the layer h (2–3 mm), compared with the active heating area limited by the diameter of the outlet nozzle of the heater D_k (perimeter $S=300$ mm). Changing the geometric ratios of the heater D_a/D_c , h/H and electric modes provides control over the heating and cooling rate of the product surface in the range of 20–500 $^{\circ}\text{C/s}$, with a specific surface heating power of 10^3 – 10^4 W/cm^2 [66, 67].

Electrolytic-plasma technology provides a hardened layer thickness from 1 to 10 mm on the surface of a product made of steel 0.5 % C.

When the heating time changes during the electrolytic-plasma treatment, the depth of the hardened layer changes, for example, at 40 s treatment, the surface layer is hardened to a depth of 10 mm, at 7 S – up to 1 mm.

The maximum hardness of the hardened layer (900 MPa) does not depend on its thickness and gradually decreases from the maximum hardness to the hardness of the base and, as a rule, does not depend on the heating time [66]. The crankshaft trunnions were hardened on a special unit (**Fig. 2.25**). The crankshaft is fixed and periodically rotated by an amount equal to the distance between the hardened sections.

Processing is carried out by a hinged heater, which is installed on the crankshaft trunnions. The unit is completed with an electrolyte tank, pump, power supply, temperature control system.

The electrolyte is supplied to a heater, which is housed inside a dielectric material housing. The heater has a built-in sensor that detects the radiation of the heated surface and sends a control signal to the electric power control system of the heater.

The technology is carried out in the following order. On command from the control panel, voltage is applied, which provides heating of the surface area above the temperature of phase transformations. Then the voltage is turned off, the surface is cooled with an electrolyte. After cooling, the tempering mode is carried out, cyclic heating of surface areas to a temperature of 150–200 °C and cooling.

In the process of periodic repetition of the heating/cooling/turning technology, a system of hard areas is formed on the surface of the shaft trunnion. Heating for 25–35 seconds and cooling with an electrolyte creates hard rectangular areas 20×50 mm on the trunnion surface, a hardened layer up to 5 mm deep, and a hardness of up to 60 HRC (**Fig. 2.26**).

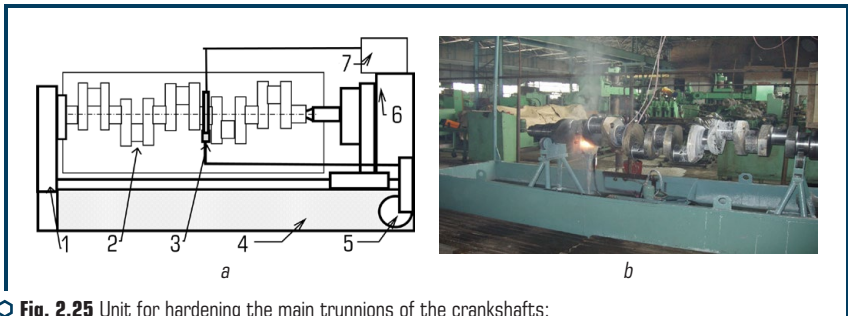


Fig. 2.25 Unit for hardening the main trunnions of the crankshafts:
a – unit diagram; *b* – type of operating unit

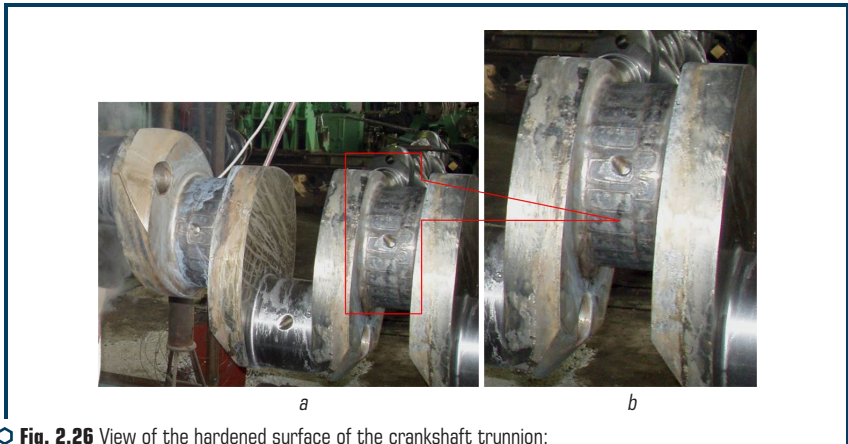


Fig. 2.26 View of the hardened surface of the crankshaft trunnion:
a – view of the shaft; *b* – view of solid rectangular areas

The analysis of the work performed showed that the proposed technology is environmentally friendly and energy-saving. According to the technology adopted earlier in production, a large-sized crankshaft ($\approx 1500\text{--}2000$ kg) was nitrided in a chamber electric furnace of the CHA 13.45.16/6 m type (furnace load – 3 shafts, nitriding time – 72 hours).

The consumption of electrical energy for processing one shaft is 6075 kWh. The thickness of the hardened layer reaches 0.5 mm. Electrolytic-plasma treatment is carried out at significantly lower energy consumption – 30 kW·hour. The thickness of the hardened layer reaches 5 mm.

A comparative analysis of the efficiency of shaft hardening when using electrolytic-plasma technology and nitriding in a shaft furnace is shown in **Table 2.3**.

● **Table 2.3** Comparative analysis of the efficiency of shaft hardening by electrolytic-plasma technology and nitriding

Shaft hardening technology	Steel grade	Energy consumption, kW/h	Processing time, h	Hardened layer	
				Hardness, HRC	Layer thickness, mm
Electrolytic-plasma	40	30	5	60	5
In a chamber electric furnace of the CHA 13.45.16/6 m type	34XH1M	6 075*	72	60	0.5

**the given data are calculated on one shaft*

With the same hardness –60 HRC, the electrolytic-plasma technology provides a 10 times thicker layer, which is important for damping the load in a heavily loaded bearing. The analysis showed (**Table 2.3**) that the electrolyte-plasma technology consumes 200 times less electric energy and 13 times more efficiently than the replaced nitriding technology.

2.6 THERMAL CYCLIC TREATMENT OF INTERNAL CYLINDER SURFACES

2.6.1 PROBLEM STATEMENT

The industry uses long cylinders. These are cylinders of hydraulic jacks, pumps, cannon barrels, engine and compressor cylinders, etc. High requirements for the strength of products limit the use of volumetric methods of thermal and chemical-thermal treatment.

Two types of electrolytic-plasma technology are proposed: thermal cycling (EPTCT) of the inner surface of the product and modification of surface properties (EPM) by means of its electrolyte-plasma chemical-thermal treatment.

Electrolyte-plasma technologies are carried out by introducing an electrolyte heater inside the cylinder and heating by electric arcs between the surfaces of the product and the liquid electrode. Electric arcs are formed in a plasma layer containing alloying elements. A solution of metal salts

in water is used as a liquid electrode. Cooling is carried out with the same electrolyte. Electrolyte heaters can be made with geometric dimensions that provide processing of the inner surface of a cylinder with a diameter of up to 60 mm to a depth of 10 m.

It is possible to create local hardened areas located on the surface according to a certain law. For example, in **Fig. 2.27** shows a diagram of the arrangement of round sections in a checkerboard pattern, in a line or in a solid surface layer.

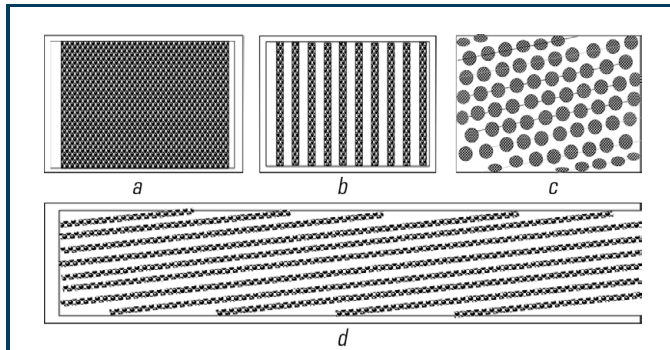


Fig. 2.27 Variants of hardening the inner surface of the cylinders: *a* – hardening of the entire surface; *b* – hardening with stripes, width 10–35 mm, which are perpendicular to the generatrix; *c* – variant of the distribution of solid inclusions on the inner surface of the cylinder; *d* – hardening with stripes 10–35 mm wide, which are performed at an acute angle to the generating surface

This arrangement ensures the creation of compressive stresses in the surface layer and the formation of plastic, uniformly distributed surface areas, which, as they wear, form cavities for lubrication and ensuring the transition to a liquid friction mode. The area of these areas is 100–300 mm². The depth of the heated layer can be 0.1–10 mm. Hard surface areas serve as treads for abrasive wear.

Electrolytic-plasma treatment of the inner surface of the cylinders is also possible in sections in the form of continuous strips.

2.6.2 ELECTROLYTIC-PLASMA THERMAL CYCLING TREATMENT (EPTCT)

Surface areas are heated with an electric current, which is passed through an electrolyte electrode over a plasma layer adjacent to the surface of the product. The surface of the product is cooled with the same electrolyte at a reduced power density of electrical energy. A periodic change in the strength of the electric current changes the power density and, accordingly, the surface temperature. The power density of electrical energy during heating is $1\text{--}3 \times 10^4$ W/cm², and upon cooling up to 100 W/cm². The thermal cycling mode is carried out by periodically heating

the surface of the product above the phase transformation temperature and cooling it below the transformation temperature.

Electrolytic-plasma technology provides on the surface of the product the creation of a system of solid inclusions (**Fig. 2.27**), which can have a round, square, annular or oval shape.

These inclusions have a higher wear resistance (hardness) and create compressive stresses in the surface layer. Untreated, soft surface areas provide relaxation of stresses generated during operation.

2.6.3 PRINCIPLE OF CHEMICAL-THERMAL TREATMENT OF THE CYLINDER SURFACE

The essence of the process of electrolyte-plasma heating consists in the formation of a part-cathode of a water-based electrolyte composition on the surface to be hardened and maintaining the plasma layer for the time required for heating.

When hardening, an electrolyte is used based on water-soluble salts containing such alloying elements as carbon, nitrogen, molybdenum, tungsten, chromium, etc. This makes it possible to obtain these elements in a plasma layer that is adjacent to the heated surface. The electrostatic field forms a layer with positively charged elements on the heated surface of the product. Combined cyclic heating of alloying elements and the surface of the product ensures diffusion and chemical-thermal treatment. Abnormally high hardness during hardening by this method is explained by diffusion processes, non-oxidative heating, and rapid cooling of the surface, cleaned of dirt and oxides.

Processing can be carried out in local areas without heating the entire product. The cyclic change in the temperature of the surface layer of the product intensifies the diffusion process. The change in temperature is controlled by a change in the strength of the electric field in the gap between the surfaces of the product and the liquid electrode.

Electrolytic-plasma technology also provides on the surface of the product hardened areas in the form of a solid surface (**Fig. 2.27, a**), strips without overlap (**Fig. 2.27, b**), as well as strips located at an acute angle to the generating surface (**Fig. 2.27, c**).

For hardening processing of the inner surface of long cylinders and the formation of microrelief, new technological methods and unit design are used: processing modes, electrolyte composition, as well as designs of electrolyte heaters and technology automation systems. For processing long cylinders, it is possible to simultaneously form an optimal microrelief of the surface and harden the surface layer by creating compressive stresses; the use of local chemical-thermal treatment of surface areas; combination of technologies for thermal cycling and chemical-thermal treatment of local areas of the inner surface.

From traditional technologies, laser technology can be used to harden the inner cylindrical surface. Compared to laser technology, electrolyte-plasma technology has the following advantages:

1. The technology allows heating with a large spot ($d=20-60$ mm), which has a uniform distribution of power density over the spot, which allows heating the surface layer to a depth of 10 mm.
 2. The coefficient of efficient use of electrical energy in the proposed technology is many times higher than in laser technology.
-

3. Cooling is carried out with the same liquid, which provides effective cooling of thick layers and, accordingly, simplifies the technology.

4. The presence of a transparency window in the electrolyte allows introducing temperature control sensors, automating the heating and cooling process and ensuring high quality.

5. Controlling the power density within 10^3 – 10^5 W/cm² allows to control the heating rate and heat up to the transformation temperature, both thick layers (up to 10 mm) and thin (up to 100 microns).

6. Cooling with an electrolyte while inducing an electric current intensity makes it possible to control over a wide range the rate of cooling of the product surface.

7. The use of electrolytes containing alloying elements makes it possible to carry out chemical-thermal treatment simultaneously with thermal cycling.

8. The transmission of power through the copper conductor makes it possible to machine small-diameter cylinders of large lengths without power loss depending on the length.

9. Costs for the purchase and operation of electrolytic-plasma equipment are lower than those for equipment of traditional methods of heat treatment.

10. The productivity of electrolytic-plasma processing by local areas to a depth of 5 mm is 1 m²/hour with a consumption of electrical energy of 15 kW/hour. Power density is 1×10^3 W/cm².

11. The productivity of modifying the entire surface without breaks to a depth of 0.1 mm is 1 m²/hour at an electrical energy consumption of 5 kW/hour. Power density is 3×10^3 W/cm².

12. Processing performance is proportional to the power expended.

13. EPTCT increases bending resistance by 30–40 %. The formation of the surface relief reduces friction losses by 2–3 times.

2.6.4 EQUIPMENT

The unit for electrolytic-plasma treatment of the heater of the inner surface of pipes includes the following main components (assembly units) of the equipment: manipulator by product (standard); tank and electrolyte supply system; electrolyte heaters; electric current converter; non-contact temperature control system; automated control system for heating and manipulator.

The electrolyte heater is fixed on a special long traverse and has the ability to linearly move along the axis of the product – pipe – 1 or cylinder (**Fig. 2.28**). There is a supply of electrolyte and electric current along the axis of the heater. The ends of the wire from the rectifier (+) are connected to the solid electrode-anode – 2; the ends from the rectifier (–) are connected to the product (through the current collector).

The heater (**Fig. 2.28**) moves inside the cylindrical surface and has corresponding supports – 3. The spent electrolyte flows down the lower surface of the pipe into the tank. This ensures the cooling of the pipe.

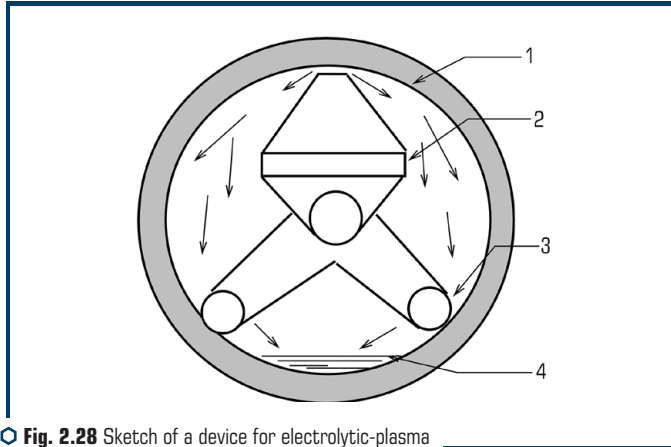


Fig. 2.28 Sketch of a device for electrolytic-plasma treatment of the inner surface of pipes

Units for electrolytic-plasma treatment of the inner surface of pipes/cylinders can be made on the basis of a welding manipulator (Fig. 2.29). The unit is equipped with an electric current converter, systems for contactless control of the surface temperature of the product, a digital signal converter, a numerically programmable device and a computer.

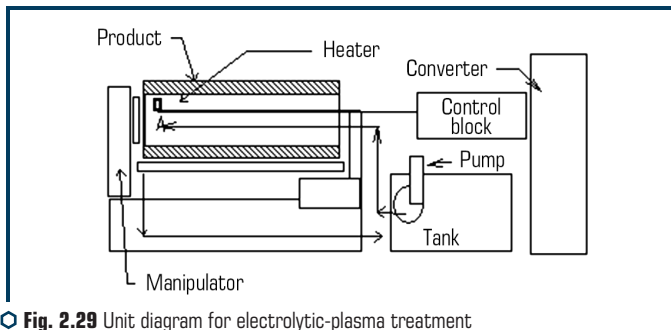


Fig. 2.29 Unit diagram for electrolytic-plasma treatment of the inner surface of pipes/cylinders

The power supply of the heater is a transformer/rectifier. It consists of three separate devices with a rated operating voltage (V) of power supplies, power supplies 340, 320, 300, 280, 260; supporting 220, 200, 180, 160 and preparation 60, 40, 20.

The transformer control unit (CU) can consist of a time relay or be made on the basis of a numerically programmable device with surface temperature correction from non-contact sensors. The control unit, by means of thyristor switches, sets the operating time (switching on) of the

rectifiers and the order of their switching on and off. The control cabinet is equipped with thyristor switches or power relays and serves to turn on and off the operating voltages. The electrolyte temperature in the system is stabilized by means of a heat exchanger located in the tank.

To supply electrolyte, a tank with a pump with a capacity of up to 10 l/min is built into the unit. The electrolyte heater is equipped with a temperature control system, which is connected to the control circuit by means of an optoelectronic digital converter.

The mode of operation of the technology is set by changing the density of electric power in the plasma layer and the speed of movement of the heater. The mechanism of electrolytic-plasma heating provided the development of methods for controlling the rate of heating and cooling of the surface of the product in the range of 20–500 °C/s, at a power density of 10^3 – 10^5 W/cm².

As a result, the technology of thermal cyclic surface hardening of the surface of products and chemical-thermal treatment has been developed. The use of the principle of periodic lowering and increasing the electric voltage in the interelectrode layer made it possible to harden the surface of the product to a depth of 10 mm.

Fig. 2.30 shows the external view of the device for hardening the cylinders, view of the heater.



Fig. 2.30 View of the cylinder heater: *a* – the moment the heater is inserted into the cylinder; *b* – the moment of heating-switching on the operating voltage

The cylinder is mounted in a three-jaw manipulator chuck. The heater, mounted on a cylindrical rod, is introduced along the axis of the cylinder. Channels for electrolyte supply, as well as fastening and insulation of the cord from the temperature sensor and the wire for supplying the electric potential are made inside the rod.

Periodic movement of the heater inside the cylinder of the slurry pump and holding in heating mode for 45 seconds provide heating of the pipe layer to the transformation temperature to a depth of 3 mm. The hardened pipe sections have a hardness of 45–50 HRC. As a result,

hardened cylinders were obtained (**Fig. 2.31**), which have a higher rigidity and provide an increase in performance by 3 or more times.



○ **Fig. 2.31** View of the slurry pump cylinders:
a – external view of the cylinder; *b* – view of the hardened surface

For hardening, ceramic heaters were used, assembled on a rod – a metal tube (**Fig. 2.32**). To supply the electric potential, a metal rod is used, which also provides the introduction of the electrolyte into the heater. In the upper part of the heater there is a window for the heater outlet and provision of conditions for electrolyte-plasma heating.



○ **Fig. 2.32** View of an electrolytic-plasma heater for hardening the inner surface of cylinders

Experimental work has shown that, depending on the technological conditions, it is possible to obtain secondary hardened structures on the surface of the product with a thickness of 0.3 to 10 mm and a hardness of up to 68 HRC. The results of hardening, depending on the type of alloy being hardened, are shown in **Table 2.4**.

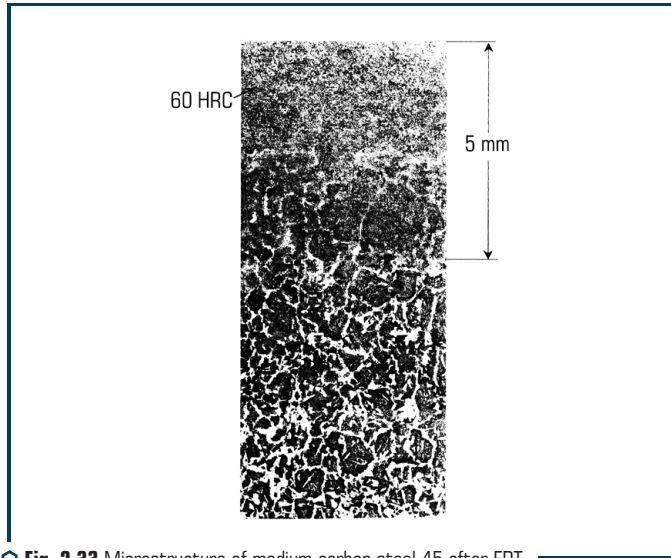
● **Table 2.4** Characteristics of the hardened layer depending on the material of the product and technological processing parameters

Alloy composition	Heating time, s	Hardness, HRC	Layer thickness, mm
0.4 % C; 2 % Cr	$(2+4) \times 5 = 30$	62...64	3
0.4 % C; 2 % Cr	$(2+4) \times 7 = 42$	64...65	4
0.4 % C; 2 % Cr	$(2+4) \times 9 = 54$	64...65	5
0.4 % C; 2 % Cr	$(2+4) \times 10 = 60$	63...65	7
0.4 % C; 2 % Cr	$(2+4) \times 12 = 72$	62...63	10
0.2 % C; 2 % Cr; 0.25 % Mn	$(3+6) \times 4 = 36$	47...48	4
0.2 % C; 2 % Cr; 0.25 % Mn	$(3+6) \times 6 = 54$	47...50	6
0.2 % C; 2 % Cr; 0.25 % Mn	$(3+6) \times 7 = 63$	47...48	8
0.25 % C; 11 % Cr; 1 % Ni	$(2+2) \times 7 = 28$	55...56	4
0.25 % C; 11 % Cr; 1 % Ni	$(2+2) \times 10 = 40$	51...52	7
Cast	$(2+6) \times 5 = 40$	55...56	5
Cast	$(2+10) \times 5 = 60$	56...58	8
0.35 % C	$(2+2) \times 5 = 20$	52...55	2
0.35 % C	$(2+2) \times 10 = 40$	52...55	6
0.35 % C	$(2+2) \times 15 = 60$	50...53	10
0.4 % C; 1 % Cr	$(2+2) \times 10 = 40$	62...64	6
0.4 % C; 1 % Cr	$(2+2) \times 15 = 60$	62...63	10
0.65 % C; 1 % Mn	$(2+2) \times 10 = 40$	64	5
0.9 % C; 1 % Cr; 1 % V; 1 % Mo	$(2+2) \times 4 = 16$	67	1
0.9 % C; 1 % Cr; 1 % V; 1 % Mo	4	68	0.300

2.7 SURFACE STUDY

2.7.1 PROPERTIES OF THE HARDENED LAYER

The study of the surface of products after electrolytic-plasma hardening shows, **Fig. 2.33**, that a finely dispersed structure is formed in the layer of the material of the product, which has been directly heated, consisting of structureless martensite with a hardness of 4000–6000 MPa and bainite with a hardness of 2200–2800 MPa. The depth of the hardened layer, depending on the processing modes and requirements for the product, can be from 0.5 to 10 mm.



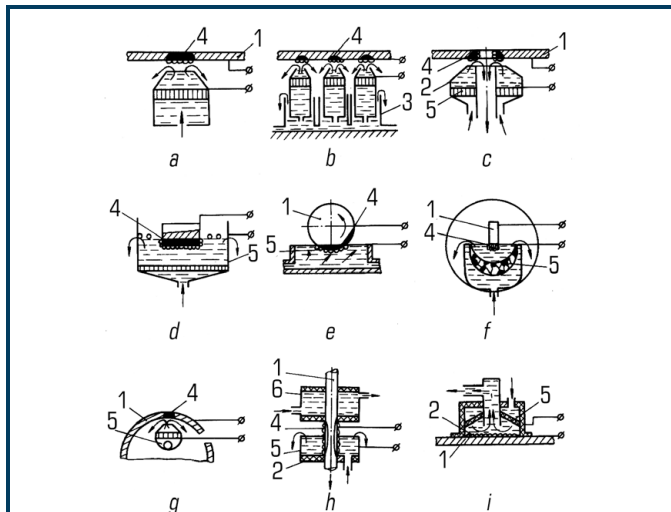
○ Fig. 2.33 Microstructure of medium carbon steel 45 after EPT

As the distance from the layer of electrolyte-plasma hardening to the heat-affected zone increases, the structure of the material of the article acquires a slightly different character. As a result, of the slow removal of heat, hypoeutectoid ferrite is released in the form of a grid along the grain boundaries. Judging by the ferrite mesh, there is a decrease in the austenitic grain, in addition, the uneven grain is clearly expressed. Near the heat-strengthened area, ferrite precipitates in the form of a discontinuous grid. Inside the grains, a finely dispersed structure is preserved, consisting of a sorbitol component and structureless martensite, the microhardness of which varies in the range of 2300–3900 MPa. In the base metal, the amount of the ferrite component with a hardness of 1200–1800 MPa noticeably increases, both along the grain boundary and in the grain.

2.7.2 FUNDAMENTAL CAPABILITIES OF EPT TECHNOLOGY

The research results (see Chapters 4 and 5) were used in the development of specific technologies for hardening products operated in an abrasive environment and having a permissible wear of 3–10 mm [42, 52, 68, 69]. These technologies are designed to create thick hardened layers by means of electrolytic-plasma hardening. Let's consider options for typical technologies and devices [70–78] for electrolytic-plasma hardening treatment. For example, for hardening sheet products-pans of scraper conveyors or screens of coal preparation machines (Fig. 2.34, a–c) [72, 73]. Heating of products for hardening is carried out by telescopic heaters 2 [64, 74, 75], which are

installed in blocks 3 and heat local sections of the sheet product in the form of small cylindrical inclusions. The heated area is cooled with the same electrolyte.



○ **Fig. 2.34** Diagram of devices for electrolytic-plasma hardening: *a, b, c* – devices for hardening sheet products; *d, e, f* – devices for hardening by dipping; *g, h, i* – devices for hardening surfaces of complex shapes. Internal, cylindrical, flat products – 1; electrolyte cell body – 2; telescopic device – 3; heated surface – 4; anode – 5

To warm up a sufficiently thick layer (up to 10 mm), the technological voltage of the electric current is reduced to 180–220 V.

In this case, the heating rate depends on the duration of parallel connection of sources with low and high voltage. Mode selection studies are provided in Chapter 5.

The end heating of products with simultaneous chemical-thermal treatment is carried out according to the scheme (**Fig. 2.34, d–f**), where the electrolyte flows through the anode grid located at the bottom of the electrolyte cell. A ferroalloy can be laid on the mesh, which dissolves in the electrolyte and refines it with alloying elements.

The use of devices with soluble electrodes allows surface diffusion alloying with carbon, nitrogen, molybdenum, chromium, etc. [42, 69, 54, 77]. It is even possible to completely melt the surface of the article [78] and form it in a liquid state under the pressure of an electrolyte. With the same pressure, it is possible to carry out hot deformation of the heated surface [79] and, at the same time, its hardening.

Heat hardening of products of the «tool holder» type of a roadheader is carried out by a heater in the form of a cylindrical can-anode 5 (**Fig. 2.34, d**) [76, 80]. Technological equipment for

hardening tool holders is made in the form of a rotor line [71] with six cylindrical anodes having different modes of inclusion in the electrical circuit [81]. To reduce the cooling rate of the heated surface, an additional electrical potential of 20–40 V is connected to the electrolyte cell.

In this case, the speed is reduced by 30–40 %. On a similar device, it is possible to harden the ends of the [82] has a capacity of up to 800,000 parts per year. The thickness of the hardened layer is 1–2 mm.

The device for hardening the end faces of tool holders has a capacity of up to 300,000 parts per year and hardens the end face to a depth of 10–15 mm.

Telescopic heaters [64, 74, 75] can be used to harden the inner cylindrical surfaces (**Fig. 2.34, g**). In this case, the hardened areas of the surface can be in the form of round areas, spiral and longitudinal stripes.

The heating quality is controlled by a special electrical circuit [54]. The principle of operation of this device is based on the measurement and analysis of the electrical conductivity of the vapor-gas layer along the surface of the heated product and the change in its electrical conductivity when the temperature changes.

Special heaters (**Fig. 2.34, i**) [79, 80] allow heating the surface of the product together with the powder material up to melting, which provides conditions for alloying the surface in the melt, for example, with the components of a mixture of surfacing powder such as FBKh and boron carbide. Long cylindrical products can be cleaned and heated in a special device (**Fig. 2.34, h**) [55], which heats in an electrolyte-plasma cell with a vertical cylindrical anode 5, and cooling in a special cooler with a flowing electrolyte.

An original technology of liquid vanadium surface vanadium in an electrolyte has been developed [83], which ensures the formation of a vanadium carbide coating on a specific surface without heating the entire product.

An analysis of the technologies and devices for electrolytic-plasma hardening developed by us shows that it is possible to harden the surfaces of almost any product used in difficult conditions of abrasive wear of agricultural, road machines, mining and mining equipment and other machines.

2.8 DEVICE FOR HARDENING THE TOOL HOLDERS (CAMS) OF THE CUTTING UNITS OF THE ROADHEADERS AND SHEARERS

It has been established that the service life of the cutting bodies of roadheaders and shearers in the coal industry is due to the wear resistance of the protruding parts of the cam and the strength of the socket-hole fixing the cutter. In addition, wear of the working surfaces of the cam increases the consumption of cutters and sharply reduces the productivity of coal machines.

Based on the analysis of the configuration of the worn surface of the products, it was decided to electrolyte-plasma hardening of the front part of the cam even before welding. The technology made it possible to obtain a layer with a thickness of 10–15 mm and a hardness of up to 60 HRC on the product.

Experimental batches of hardened cams (**Fig. 2.35**) (tool holders) in the conditions of the manufacturer's enterprise were assembled on the screws of the cutting body and tested in the conditions of coal mines (at «Chelyabinskugol», «Donetskugol», «Pavlogradugol»). Industrial tests have shown that the performance of cutting bodies assembled from hardened cams increased 1.53 times. From an economic point of view, this is tantamount to a corresponding decrease in the production of cutting bodies, which in their cost are up to 10 % of the cost of the entire combine.

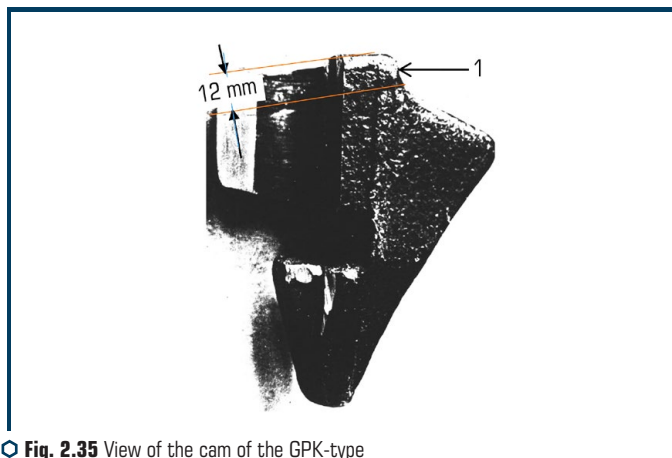
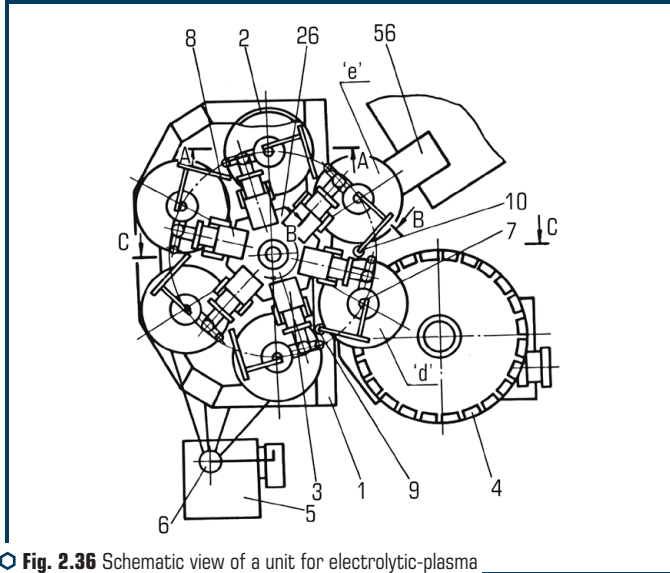


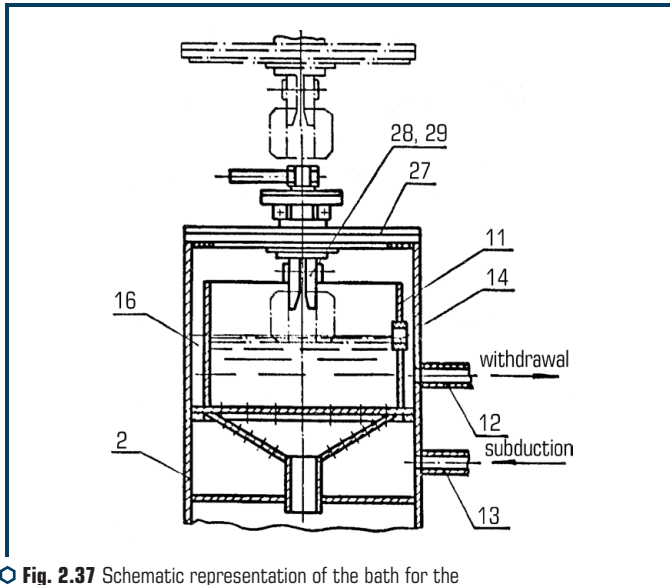
Fig. 2.35 View of the cam of the GPK-type roadheader (1 hardened layer, 10–15 mm thick)

After the tests, it was decided to introduce the technology for hardening the cams at the factories of mining machines (machine-building plants in Kopeysk KMZ and Gorlovka GMZ), for which technological, semi-automatic units with a capacity of up to 300,000 cams per year were developed and manufactured. A description of units for hardening cams is given in Chapter 8. (A list of documents on testing and implementation of technology for hardening cams is given in Appendix 11). In accordance with the terms of reference TZTO 09287 «Unit of electrolyte-plasma thermal cyclic hardening of shearer auger cams», a technological semi-automatic unit was developed and manufactured [54, 71, 82].

The unit (**Fig. 2.36**) consists of the following mechanisms: frame 1, a number of electrolyte baths 2, lifting and turning device 3, swivel table 4, system 5 for electrolyte circulation, jet pump (ejector) 6, grips (cathodes) for part 7, consoles 8 with grips, movable stop 9, hard stop 10. Electrolytic-plasma bath 2 (**Fig. 2.37**) contains an anode 11, made in the form of a cylindrical bowl with a perforated bottom, a drain hole 12 and an electrolyte supply channel 13. In the cylindrical bowl 11 there are drain holes 14 with an adjustable washer 15. Between the inner wall of the bath 2 and the anode bowl 11 there is an annular cavity 16.



○ Fig. 2.36 Schematic view of a unit for electrolytic-plasma hardening of cams



○ Fig. 2.37 Schematic representation of the bath for the implementation of electrolyte-plasma heating and cooling of the cam

The electrolyte circulation system (**Fig. 2.38**) contains a 17 tank for cooling, a pump 18 for pumping electrolyte, a supply pipe system 19, a pressure tank 20, a pressure head system 21 and a 22 outlet pipe system. The tank has a system 23 for cooling the electrolyte. At the end of the lifting-and-rotating device, a bath lid 27 and grippers 28 for the product 29 are fixed.

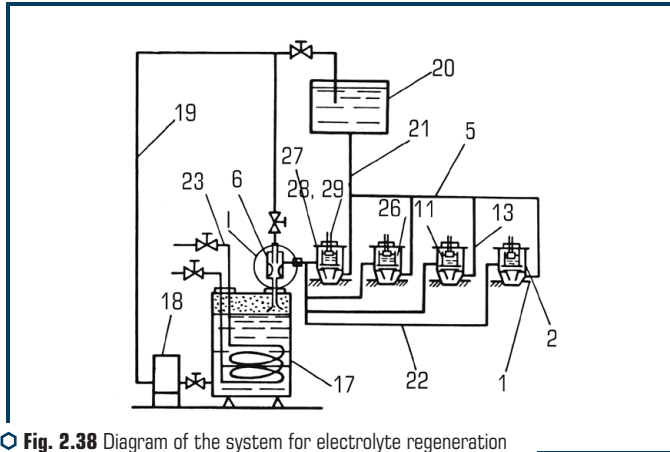


Fig. 2.38 Diagram of the system for electrolyte regeneration and its distribution into the heating cells of the unit

The device works as follows. The products are installed on the table of the rotary device 4, which rotates synchronously with the consoles 8, which have grips 7. Fixing the cams, the consoles transfer them to the baths 2 and immerse them in the electrolyte, where is the heating carried out. For cooling, the cams are transferred to the next bath. The device has 6 baths, which provides a mode of repeated heating in 1, 2, 3 and 4 baths, and then a mode of pre-cooling to the temperature of martensitic transformation in the 5th bath and a mode of cooling to room temperature in bath 6. The unit contains elements for sealing baths – cover 27 and elements for condensation of electrolyte vapor – jet pump 6. The electrolyte supply system (**Fig. 2.38**) provides cooling and uniformity of its flow in the electrolyte bath.

The electrical diagram of the device (**Fig. 2.39**) provides for the presence of a software device for connecting high (350 V) and lower (110–190 V) voltages to electrolyte cells, as well as 110 V voltage on the last cells, which provide cooling of the heated layer of the part.

The device has wide technological capabilities and, with appropriate restructuring, it is possible to harden the ends of conveyor bushings, couplings and other products.

In order to increase the efficiency of end heating and cooling of products, a number of electrolyte baths and telescopic heaters have been developed [70, 54, 74, 76, 81, 82], which make it possible to strengthen almost all known products. These heaters, for example, can be installed in various units.

The device has an electrolyte supply system similar to that described (**Fig. 2.38**).

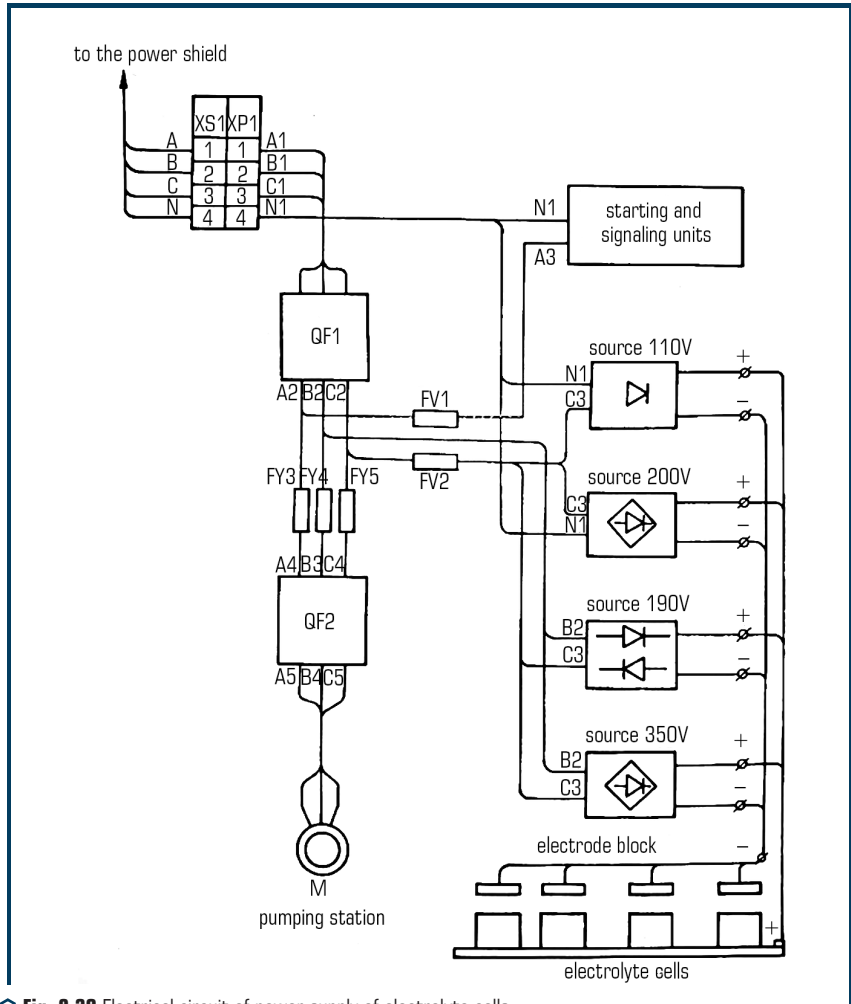


Fig. 2.39 Electrical circuit of power supply of electrolyte cells

This design of the device provides uniform end heating of products of various lengths and diameters, as well as local heating of a part of the part, which has a significant mass and size. The heating mode is selected by the flow rate of the electrolyte and the taper of the electrode.

The considered device (Fig. 2.40) has a more complex design due to the need for automatic control of the temperature of the electrolyte in the interelectrode gap. This device consists of a housing 1, inside of which a mesh anode 2 and a mesh equalizer of electrolyte flow 3 are installed.

In the lower part of the housing, a chamber 4 is made for collecting contaminants and a hatch 5 for draining them. The chamber 4 and the anode cavity are connected by a pipeline 6 so that an annular slot 7 is formed along its periphery. In the lower part of the chamber (in the hatch), a conical plug 8 is made, which, by means of a lever 9, allows the electrolyte to be drained. The top of the chamber is closed with a lid 10, through which it is possible to enter the part 11 for heating and hardening. The system of holes 12 determines the electrolyte level. Below these holes, directly in the area of its discharge, there is a sealed cylinder 13 filled with freon 14. This cylinder is connected by a pipeline 15 with the gas cavity 16 of the pneumohydraulic regulator and equipment 17, 18 for external input of the control pressure.

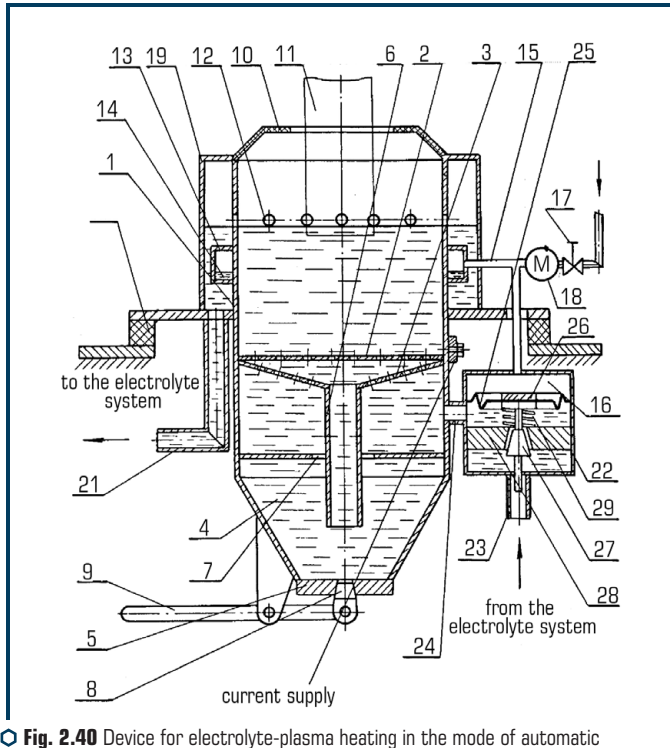


Fig. 2.40 Device for electrolyte-plasma heating in the mode of automatic control of the electrolyte temperature by means of a pneumo-hydraulic valve

In the lower part of the chamber (in the hatch), a conical plug 8 is made, which, by means of a lever 9, allows the electrolyte to be drained. The top of the chamber is closed with a lid 10, through which it is possible to enter the part 11 for heating and hardening. The system of holes 12 determines the electrolyte level. Below these holes, directly in the area of its discharge, there is a sealed cylinder 13 filled with freon 14. This cylinder is connected by a pipeline 15 with the gas cavity 16 of the pneumohydraulic regulator and equipment 17, 18 for external input of the control pressure.

The pneumohydraulic regulator is included in the electrolyte supply system 19, 20, 21, 22, 23, 24 and has the ability to change the cross-section of the passage slot by moving the diaphragm 25, stem 26 and lowering the valve 27 in the seat 28.

The essence of the device is to adjust the flow rate of the electrolyte, depending on its heating and to ensure a stable temperature, and, consequently, electrical conductivity and cooling capacity.

This design ensures the stability of heating products during their automatic feeding, as well as the same cooling mode by controlling the temperature of the electrolyte.

2.9 HARDENING OF SHEET STEEL PARTS

2.9.1 METHOD OF HARDENING SHEET PRODUCTS

The problem lies in the fact that there are a number of products that operate in difficult conditions, for example, in the development of rock mass in underground mines, where abrasive wear of working surfaces is accompanied by bending alternating loads. To strengthen such products, a method has been developed, which consists in creating solid inclusions on the wearing surface.

On an article made of a sheet, local small areas of the surface are heated with an electrolytic-plasma heater on one side until the austenitizing temperature is reached on the opposite side of the sheet from the place of heating application while simultaneously cooling the sheet along the periphery of the heated area, and the heated areas are cooled simultaneously from both sides. In this case, the largest linear dimension of the hardened area should not exceed 4–5 sheet thicknesses.

The combination of the above technological methods ensures the production of local hardened areas with the same hardness throughout the volume and from different sides. The formation of areas with the same martensitic transformation on both sides causes a uniform increase in its volume and the creation of compressive stresses in the sheet, the same on both sides, which ensures the straightness of the sheet even with a hardening volume reaching 50 %.

A specially introduced technological method of cooling the heated section along its periphery provides localization of heating in the size of a small section, which causes a transition zone of no more than 1–1.5 mm, and, accordingly, the possibility of frequent placement of the sections to be hardened.

The method has been tested on medium-carbon steel sheets (steel 35) used for the manufacture of scraper conveyor chutes. Sheet thickness is 8 mm.

Heating was carried out until the austenitization temperature was reached on the opposite side from the place where heating was applied by an electrolyte-plasma heater. The electrolyte flow rate through the sprayer for cooling the heated surface area was set at 0.01–0.03 m³/s. Cooling of heated sections is carried out immediately after disconnecting the technological potential to the electrolyte cells of the heater. The cooling time was 10–35 s.

Along the periphery of the electrolyte heater, a device was installed for supplying air with electrolyte (air consumption 2–3 m³/h, and electrolyte 0.0001 m³/s).

When testing the method, the deflection of the sheet was measured on the basis of 100 mm, the size of the spot of solid inclusions on both sides of the sheet and the hardness were determined. Hardness characterized the completeness of martensitic transformations, the ratio of the sizes of

solid inclusions from the side of the heater and from the opposite side characterized the uniformity of heating of the sheet section through.

Reinforced steel 35 sheets were subjected to a bend test prior to welding. In this case, the bending force and deflection of the sheet were recorded. The bending force was increased until the sheet reached plastic deformation stresses. Tests have shown that 20 % of the nominal surface occupied by hardened sections increases its bending resistance by 30 % (**Fig. 2.41**).

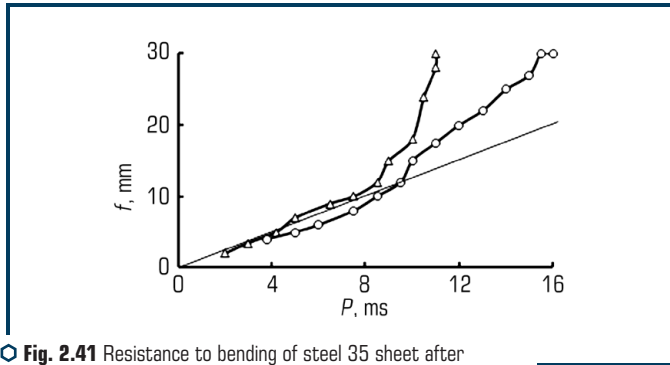


Fig. 2.41 Resistance to bending of steel 35 sheet after hardening by local areas, 20 % of the nominal surface

The structure of hardened sections of steel sheet (steel 35) is finely acicular and coarsely acicular martensite up to 50–60 % by volume, the rest is trostomartensite. The transition zone of reed martensite has a hardness of 40–45 HRC.

The considered method of hardening sheet products has the following technical advantages: it is possible to harden sheet products practically without a leash, ensuring the volume of hard areas in the sheet up to 60 %, which increases the wear resistance of parts, allows them to be operated in harsh conditions, with alternating loads and vibrations. In this case, the hardened areas work as solid macroinclusions, and plastic deformation of the sheet occurs in the soft non-hardened metal surrounding these inclusions.

2.9.2 SHEET STEEL PARTS (PAN BOTTOM, MESH)

In the mining and coal processing industries, welded structures made of sheet steel are widely used. These are pans of scraper conveyors (**Fig. 2.42**), chutes for lowering rock mass, overlap, mesh for coal preparation machines and other products.

One of the factors restraining the increase in the wear resistance and strength of welded structures made of steels of mass use is their softening in the heat-affected zone. An increase in strength due to an increase in the content of alloying elements leads to an increase in the likelihood

of the formation of hardened structures in the vicinity of the seam zone and, as a consequence, to the formation of cold cracks in welded joints.

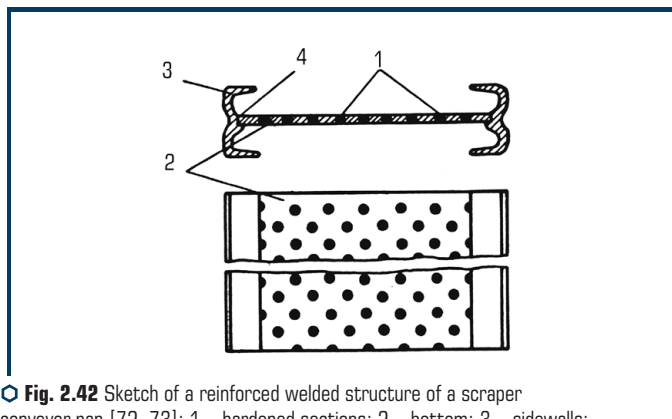


Fig. 2.42 Sketch of a reinforced welded structure of a scraper conveyor pan [72, 73]: 1 – hardened sections; 2 – bottom; 3 – sidewalls; 4 – welded seam

One of the most economical methods of increasing the strength and wear resistance of such products is the local hardening of the wearing surfaces from electrolytic-plasma heating.

Parts on the pan bottoms were hardened in local staggered sections, in the most wear-out areas of the product. Section diameter was 30 mm. Then the parts were welded into a product. The resulting product-pan of the scraper conveyor (Fig. 2.43) [72, 73], was widely tested in the conditions of the Kuzbas mines. At the same time, no damage to the welds was noted.

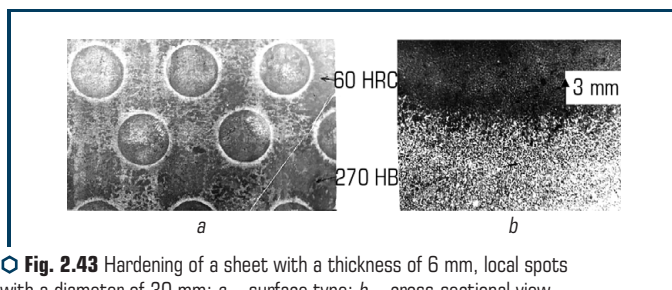


Fig. 2.43 Hardening of a sheet with a thickness of 6 mm, local spots with a diameter of 30 mm: *a* – surface type; *b* – cross-sectional view of the spot with hardening to a depth of 3 mm

The test results showed that the pan's efficiency increased 2 times.

This technology and equipment was introduced at the machine-building plant in the production of scraper conveyors. Using the experience of hardening pans, sieves from coal preparation

machines were hardened according to a similar scheme (**Fig. 2.44**). The sieves were made of sheet steel 35, 8 mm thick. The holes were 8 mm in diameter. The operating conditions of sieves and pans are practically the same.

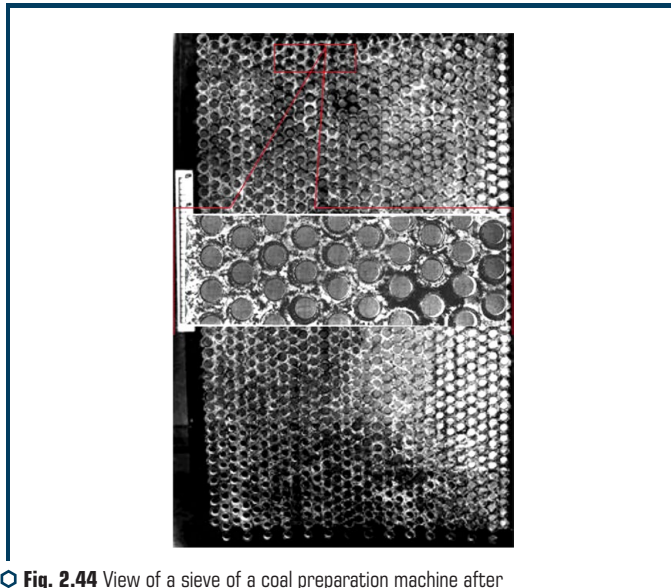


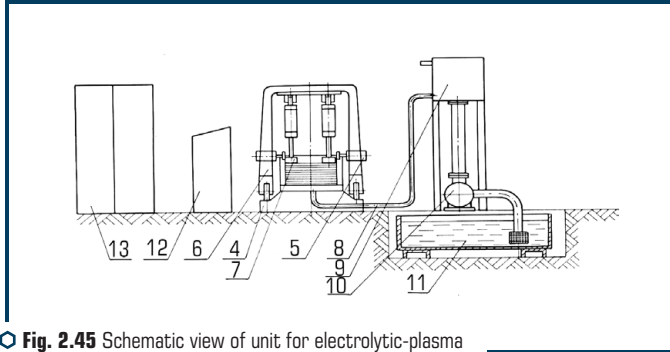
Fig. 2.44 View of a sieve of a coal preparation machine after electrolytic-plasma hardening

The electrolytic-plasma hardening of the sieves, like those of the pans, was carried out with telescopic heaters, but for the sieves it was necessary to orient the heaters along the hole in order to provide hardening of the hole surface. This complicates the technology.

Industrial tests of sieves have shown that the hardened sections of the sieves wear less and, as it were, shield the unhardened ones. This conclusion made it possible to make a decision to create a unified design of the technological unit for both sieves and pans, regardless of the location of the holes. According to the test data at the Donetskugol Production Association, the sieve efficiency has doubled.

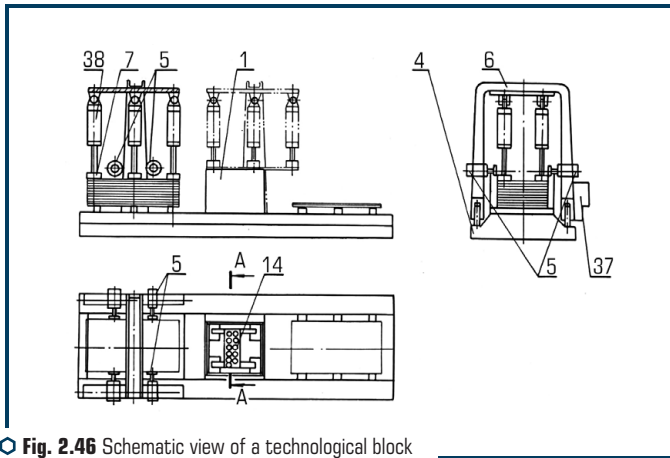
2.9.3 UNITS FOR ELECTROLYTIC-PLASMA HARDENING OF PRODUCTS FROM SHEET MATERIAL

The technology of strengthening sheet products is carried out on a special technological unit (**Fig. 2.45**). The unit consists of a technological unit 4.7, a tank 11 with electrolyte, a pump 9 and a pressure head tank 10.



○ Fig. 2.45 Schematic view of unit for electrolytic-plasma hardening of sheet products

The unit is controlled and supplied from separate units 12. The technological unit (**Fig. 2.46**) consists of a movable portal 6, which contains pneumatic cylinders 5 with electromagnetic suction cups 7.



○ Fig. 2.46 Schematic view of a technological block for strengthening sheets

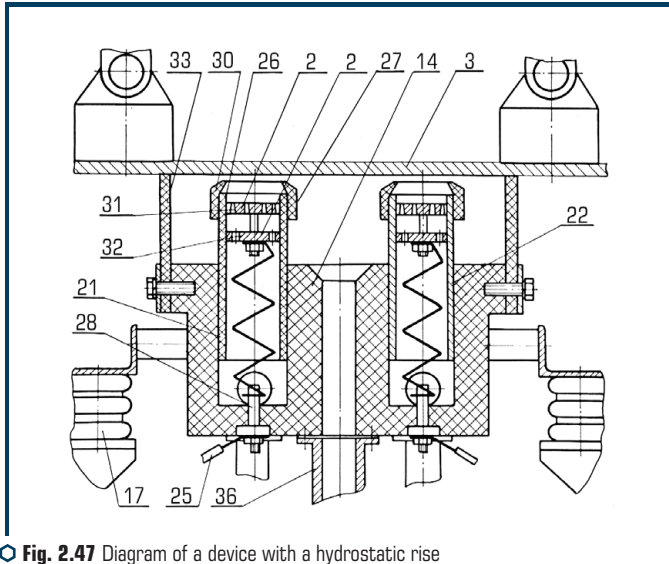
In the middle of the technological block there is a device 14 with electrolyte-plasma heaters, which are fixed in the housing with the possibility of vertical movement under the action of the electrolyte pressure [75–77].

This device (**Fig. 2.47**) consists of a dielectric body 1, installed on the fit of movement in the cylindrical holes 2 of the body of the heaters 3, which contain anodes 4 in the form of a grid and flexible current conductors 5. The body of the device 1 is fixed on insulators 6, which are mounted in the technological block providing electrical safety. The sheet is hung over the heaters in a horizontal

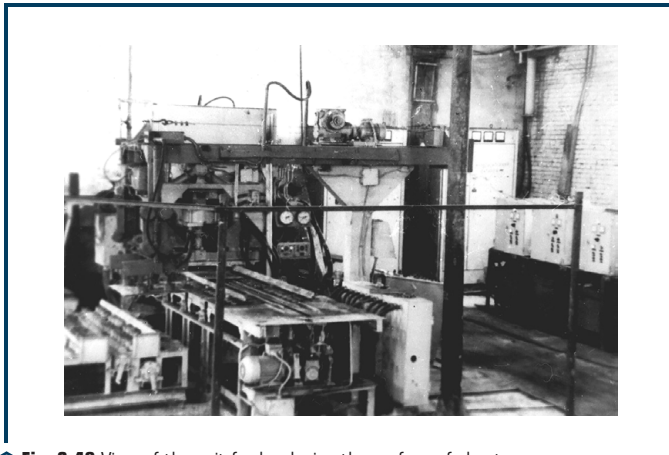
position, then the electrolyte supply is turned on, the electrolyte pressure raises the heaters to the surface of the sheet, and thus the electrical circuit is closed and the heating process is in progress.

After turning off the electric potential, the heated section is cooled by the same electrolyte.

Fig. 2.48 shows a view of the unit for strengthening products 1 from sheets.



○ **Fig. 2.47** Diagram of a device with a hydrostatic rise of electrolyte-plasma heaters



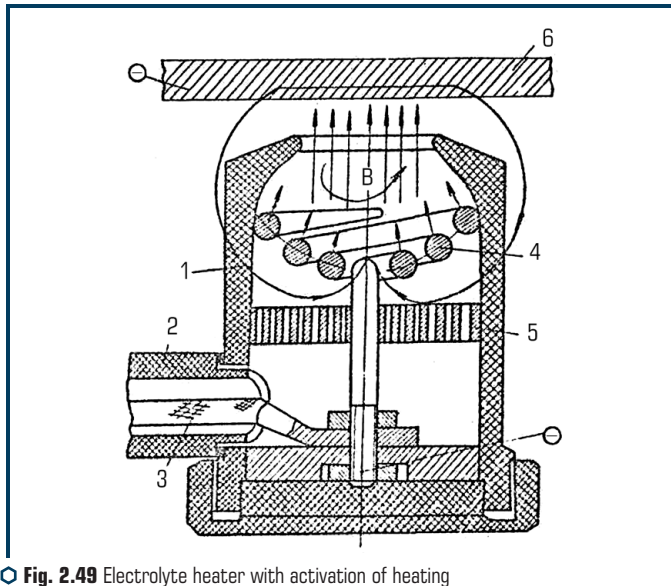
○ **Fig. 2.48** View of the unit for hardening the surface of sheets

Sheet products were stacked under the portal and then, as the technology was implemented, they were moved by the portal onto the technological block and into a stack with reinforced sheets.

2.10 HEATER CONSTRUCTIONS AND THEIR APPLICATION

2.10.1 ELECTROLYTIC-PLASMA HEATERS

A device for heating products in an electrolyte (**Fig. 2.49**) contains a bath 1, a fitting 2 for supplying an electrolyte, a bus for supplying an electric potential 3, an anode 4, a liquid-electrolyte damper 5, a workpiece (cathode) 6. Anode 4 is made in the form of an open spiral, the diameter of the turns of which increases towards the outlet of the bath, and its axis coincides with the axis of the outlet. Anode 4 is made in the form of a spiral made of stainless wire. The electrical potential is connected to the central circuit of the open spiral. The diameter of the spiral turns increases towards the outlet of the bath, and the axis of the spiral coincides with the axis of the outlet.



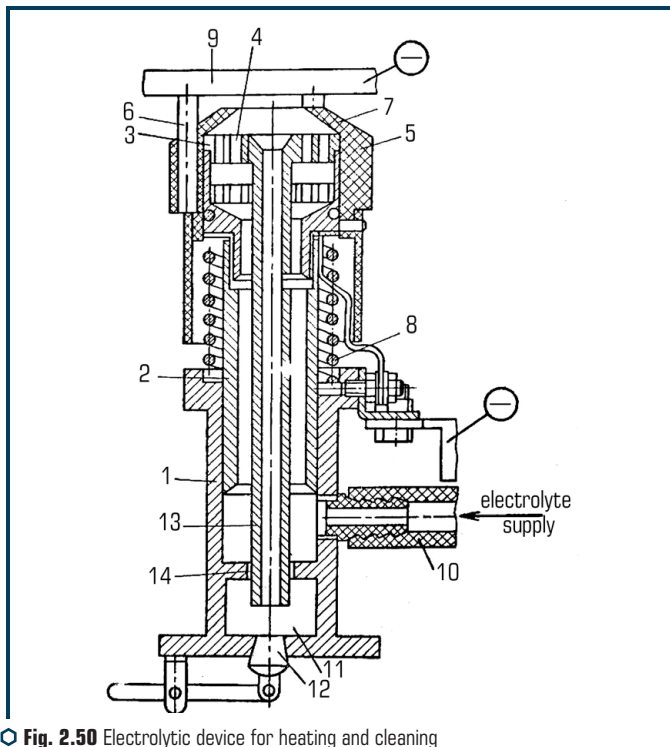
○ **Fig. 2.49** Electrolyte heater with activation of heating by a magnetic field, according to USSR Patent 1375659 A1

The device works as follows. The electrolyte is fed through the nozzle 2 into the bath 1 and through the electrolyte outflow damper 5 passes between the turns of the spiral anode 4 to the surface of the heated part 6. When the electrical target is closed, an electric current flows from

the anode 4 to the part 6 through the electrolyte. The removal of electric current from the sections of the spiral causes it to pass through the previous sections and, accordingly, the formation of a magnetic field, the density of which depends on the magnitude of the current and the curvature of the sections of the spiral. The magnetic field is closed through the part and the environment. The imposition of a magnetic field in the case of heating the product in the electrolyte accelerates the circulation of the electrolyte in the area of the part 6 while pushing it away from the center of the cathode under the action of centrifugal forces. The interaction of the magnetic field of the spiral electrode and the intrinsic magnetic field of the electric current lines makes it possible to create a zone of overvoltage, overheating of the electrolyte and the formation of a plasma layer, bypassing the stages of unstable operation.

Device for local heating and cleaning of product surfaces.

For local heating and cleaning of the surface of products, a heater with a telescopic lifting of the heating head with an electrolyte has been developed (Fig. 2.50).



○ Fig. 2.50 Electrolytic device for heating and cleaning local surface areas according to USSR Patent SU 1331074 A

The device consists of a housing 1, inside of which a prefabricated telescopic anode is installed, having a glass 2 with meshes 3 with holes 4 installed in it. The conical dielectric nozzle 5 moves freely along the anode and contains stops 6 and a limiter in the form of an inner housing 7. The spring 8 elastically presses the anode with the nozzle 5 against the workpiece 9. To supply the electrolyte is a fitting 10. In the lower part of the housing 1 there is a chamber 11 with a hatch 12 for collection. The chamber 11 is connected to the anode along its axis by a pipeline 13. In the bottom of the housing 1 around the pipeline 13 there is an annular slot 14. The holes 4 are made tangential. The negative electrical potential is supplied to the workpiece 9, and the positive electrical potential is supplied to the anode.

The device is brought under the part-cathode, the electrolyte supply and current are switched on. The electrolyte is turbulized by making tangential holes in the anode. When the electrolyte rotates, loose particles of contaminants, due to the pressure difference in the center and along the periphery, move to the center – to the pipeline, are deposited through the pipeline into the chamber for collecting particles and contaminants. Particles are deposited through a slot made in the bottom of the housing coaxially with the pipeline, which pass through the anode holes at the moment the electrolyte supply is stopped. This facilitates the collection of impurities and equalization of the electric current in the electrolyte, which leads to stability and uniformity of heating. The device works as follows. The device is brought under part 9, for example, a sheet of steel for the pan of a scraper conveyor, supported by stops 6. Then, the electrolyte supply is switched on through the nozzle 10 and the electric current is connected through the current lead. Due to the dissipation of electrical energy, a plasma heating zone is formed at the electrolyte-workpiece interface. Electrolytic-plasma heating is characterized by the ability to clean the heated surfaces from scale, dirt and to disperse sharp protruding burrs. All these contaminants under the action of centripetal forces from the electrolyte flow swirling in the cavity between the conical nozzle and the cathode are collected through a pipeline into the lower chamber of the housing. The electrolyte is twisted due to the special design of the holes, the axes of which intersect with the axis of the cavity. Inclined holes in the anode of the plasmatron ensure the rotation of the electrolyte flow. Solid particles suspended in it or placed on the bottom rotate together with the electrolyte. During rotation, the particles move to the center due to the pressure difference in the center of the plasmatron and along the periphery. The pressure difference is due to the difference in electrolyte speeds. In addition, the particles are decelerated by friction against the bottom, thereby increasing the centripetal force.

Solid particles, moving towards the center under the action of the difference in electrolyte pressures, are deposited through the central hole and are excluded from the «anode-electrolyte-detail» electrical circuit. The angle of inclination of the holes in the anode, the flow rate of the electrolyte, its density affect the plasmatron process, but are not decisive factors. The process of concentration of solid particles to the axis of the plasmatron will proceed under any parameters in the presence of liquid circulation.

The slot made in the bottom of the housing around the pipeline is designed to precipitate through it those solid particles that pass through the anode holes at the moment the electrolyte

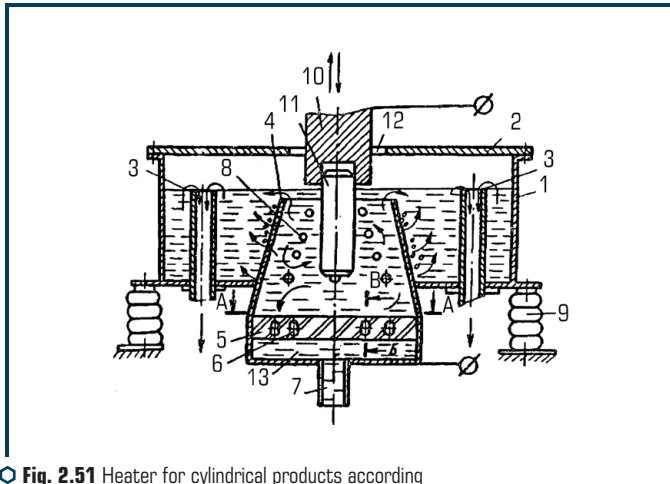
supply is stopped. If these particles are not isolated, then they can accumulate, be carried away by the electrolyte flow and, ultimately, disrupt the stability of the electrolyte-plasma heating.

As a result, it is easier to collect contaminants to the center of the bath and the lines of electric current in the electrolyte are leveled. As dirt accumulates from the lower chamber, it is removed by opening the hatch. Thus, pollution and scale are excluded from participation in the heating process, increasing the stability and uniformity of heating, and, consequently, the efficiency of the device and the quality of the processing process.

The use of a device for zone heating of parts in an electrolyte has the following technical advantages: it is possible to conduct a continuous process of cleaning and heating the surface of products, ensuring high quality and stability, which will exclude the possibility of an emergency, closing the anode-part electrical circuit through contamination.

Device for end heating of products.

For the end heating of products, a device has been developed (Fig. 2.51), which contains a bath 1 with drain pipes 3, an electrode made in the form of a hollow truncated cone (K) 4 with holes on the side surfaces and located with a smaller base up and below the level of the upper ends of the pipes 3, and a shield 5 with tangential holes 6. The axes of the holes 6 intersect with the axis of the conical chamber 4. The use of this device allows the formation of a plasma layer at low voltage and equalization of the temperature along the immersion depth of the part.



○ Fig. 2.51 Heater for cylindrical products according to USSR Patent SU 1537695 A1

The device contains a bath 1 with a lid 2 and with drain pipes: 3, electrodes, one of which is made in the form of a hollow truncated cone 4 with an open smaller base, installed in the bath 1,

facing the lid with a smaller base 2 below the upper ends of the electrolyte drain pipes 3, screen 5 with tangential holes 6, placed in a cone at the larger base. The axes of the holes 6 intersect with the axis of the cone 4. A fitting 7 is made under the screen 5 in the bottom of the cone, holes 8 are made in the upper part on the lateral surface of the cone 8. The bath 1 is installed on ceramic insulators 9. The device has a holder 10 of the product 11, which has the ability to return translational movement. The device has a pressure tank with electrolyte (not shown) and a power source connected to the cone 4 and the holder 10. The electrolyte is drained through a heat exchanger into the tank, from where it is fed to the pressure tank.

The device works as follows. The product 11 is fixed in the holder 10 and lowered through the hole 12 in the cover 2 and the cone 4. Then the electric potential is connected and the electrolyte is fed through the fitting 7 into the cavity 13. From this cavity through the holes 6 in the screen 5, the electrolyte is fed into the cone 4. The electrolyte level in the electrode (cone) quickly rises and reaches the surface of the item 11, then the rate of raising the electrolyte level sharply decreases. A decrease in the rate of raising the electrolyte level is due to the outflow of electrolyte from the conical electrode through the holes 8. With a small contact surface of the article with the electrolyte surface, a plasma layer is immediately formed. The area of the plasma layer smoothly increases as the electrolyte level rises and the product is immersed.

The electrolyte flow in the interelectrode gap is twisted and a uniform «flooded» jet washes the heated surface and the electrode. After the upper electrolyte layer reaches the level of the drain pipes, a stagnant zone forms in the lower part of the bath, which resists the electrolyte escaping through holes 8. The bulk of the electrolyte comes out through the upper part of the cone, providing the required temperature regime in the heating zone.

As the tapered electrode narrows, the electrode gap decreases and the electrolyte flow rate increases, which ensures an increase in the heating temperature of the part of the part 10 immersed in the surface layer of the electrolyte, and, consequently, a decrease in the heating temperature gradient along the immersion depth.

The direction of the electrolyte flow in the interelectrode gap and its helical movement help to maintain a uniform plasma layer and ensure uniform heating.

The volumes of the cone and the bath are selected from a ratio of 1:5–1:10. The volume of the bath is taken at a height equal to the distance from the bottom of the bath to the upper end of the cone. With a volume ratio of 1:3, the speed of immersion of the part in the electrolyte, and in some cases, there is a sharp increase in the current and the breakdown of the vapor-gas envelope. With a ratio of 1:5 and higher, a smooth, stable start of the heating process is ensured. The ratio between volumes above 1:10 is impractical due to an unjustified decrease in productivity.

The proposed device provides a slow immersion of the product under the electrolyte layer with simultaneous smooth formation of the plasma layer at the minimum allowable voltage of the electric potential, then, as the bath and the cone are filled with electrolyte and the formation of a stable plasma layer, the electrolyte speed in the interelectrode gap increases, as well as the provision of a spiral flow electrolyte.

The proposed device, by changing the taper of the electrode and the flow rate of the electrolyte, provides end heating of products of various diameters and lengths, as well as local heating of parts having a significant mass and heat capacity of the part that is not to be processed.

Of interest is a non-contact method for monitoring the heat treatment of steel parts. The essence of the method lies in the fact that the thickness of the vapor-gas layer around the part directly depends on the temperature, and the conductivity of this layer depends on the thickness. Measurement of time from the beginning of cooling of the part, i.e. when the conductivity of the vapor-gas layer is low, until the period of a sharp increase in conductivity, i.e. reducing the temperature to 200–300 °C, completely allows to characterize the initial temperature of the part and regulate the quality of heating.

Method for quality control of surface hardening of steel part.

Fig. 2.52 depicts a device for implementing a method for quality control of surface hardening of a steel part when heated in a bath with an electrolyte.

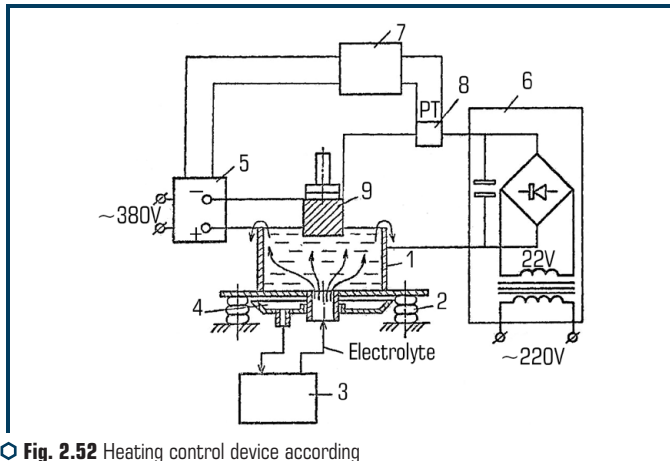


Fig. 2.52 Heating control device according to the USSR Patent SU 1481260 A1

The device consists of a bath 1 installed on insulators 2, an electrolyte supply system 3, a pan 4 for collecting electrolyte, a source 5 of a process electric current, a source 6 of a measuring electric current (measuring system), a control system 7 with a source 5 of a process current and a current relay 8. Part 9 is fixed with a holder, which is the output link of the automated loading device (not shown).

The device works as follows. Part 9 is immersed in bath 1 under a layer of electrolyte supplied from system 3. Excess electrolyte flows into pan 4 and then into system 3. Process electric current source 5 is turned on and part heating begins. When heated, the measuring system 6

is turned off due to the blocking of the diode by reverse current. After disconnecting the process current, the measuring system 6 is connected, which is configured by means of a current relay 8 and a time relay to turn on the control circuit (not shown). The discrete control range, if: the time from the start of cooling to the decrease in the resistance of the electrical measuring system is not enough, in this case the process voltage is increased by 10–15 V, and the next cycle of heating and measurement is carried out. Thus, the control system not only controls the heating quality, but also controls the heating mode,

As a result of the periodic connection of the bath and the part at the moment of its cooling to a source of electric direct current, as well as measuring the time from the beginning of cooling to a decrease in the electrical resistance of the boundary layer to the part to the electrical resistance of the electrolyte, a new technical effect arises – control of the existence of a vapor-gas layer around the cooled surface of the part, which entails control of the surface temperature of the part, since the thickness of the vapor-gas layer directly depends on the temperature, and the conductivity of this layer depends on the thickness. In turn, measuring the time from the beginning of the cooling of the part, i.e. when the conductivity of the vapor-gas layer is low, until the period of a sharp increase in conductivity, i.e. reducing the temperature to 200–300 °C, fully allows to characterize the initial temperature of the part and regulate the quality of heating.

PTT with a mechanized drive of control circuits is used as a source of electrical power with technological current. The measuring power system is assembled from a 22 V transformer, a rectifier and a 20 μ F capacitor; a diode is connected in series to the circuit, which acts as a key. Current relays and time relays are included in the same circuit. The time relay disconnects the current relay after a specified time interval. If the relay manages to operate, i.e. if the heating temperature is insufficient, the mechanized PTT control circuit turns on and the process voltage increases.

The test of the method for controlling the quality of heating a part in a bath with electrolyte is carried out at a power of the measuring system $N=2.5$ kW, voltage, $U_m=22$ V. Parts are heated from 300 to 1100 °C. The time from the start of cooling of the part to the decrease in the resistance of the circuit and the appearance of a measuring current of 20 A in it is measured. Analysis of the results of testing the method shows that at a product temperature of 300 °C, the measuring current flows in the circuit without time delays. At a temperature of 600 °C, the delay is 3–4 s, at 800 °C – 5–10 s, at 900 °C – 15–18 s, at 950 °C – 18–21 s, etc.

Thus, for a part with a certain heating area and temperature, there is a stable time from the start of cooling to the appearance of conductivity or the disappearance of the gas-vapor layer. This time, through a special measuring system, is converted into a signal that controls the process current, which ensures the automation of quality control. Thus, a simple system makes it possible to automate the control of the heating quality of the part for controlling its temperature.

Method and device for electrolytic-plasma cleaning of the surface of metal products.

The method and device for thermochemical cleaning of the surface of metal products (Fig. 2.53) is used to remove scale, burrs and dirt from products such as round-link chains, augers, and cables.

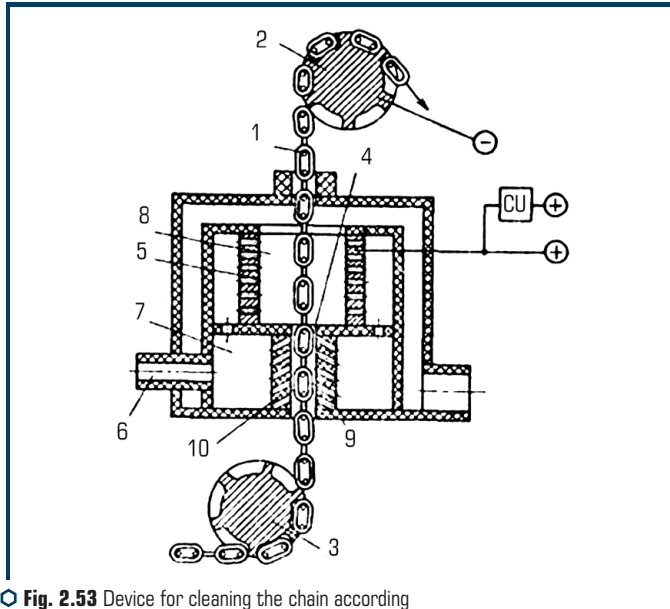


Fig. 2.53 Device for cleaning the chain according to USSR Patent SU 1611625 A1

The product 1 is moved by means of the drive 2 and tension 3 rollers in the channel 4 of the stripping device. Anode 5 is constantly connected to an electric current source of reduced voltage of 20–50 V. When electrolyte is supplied through a branch pipe 6, it enters the ring distributor 7, from it – into the electrolytic cell 8 and flows out into the axial channel 4 through the nozzles 9 of the dielectric sprayer 10, designed for seals. In the electrolytic cell 8, the anode – electrolyte – cathode (product) electric circuit is closed, and a gas-vapor layer is formed along the surface of the product. This layer consists of water vapor, oxygen and hydrogen. Connection to the anode 5 of an electric potential, increased voltage is accompanied by heating of the surface to melt and oxidize the tops of burrs and sharp corners. After the burrs have melted, the high voltage is cut off. The speed of the product is limited so that the time it takes for the product to pass through the electrolyte jets is not less than the time of the pass-through period. The method is carried out as follows. The product – round link chain 1 is moved by means of drive 2 and tension 3 rollers in channel 4 of the protective device. Anode 5 is constantly connected to a low-voltage electric current source of 20–50 V. When electrolyte is supplied through a branch pipe 6, it enters the ring distributor 7, from it – into the electrolytic cell 8 and flows out into the axial channel 4 through the nozzles 9 of the dielectric sprayer 10 and through the anode, interacting with the product, and the electrolyte from the electrolytic cell flows down into the axial channel 4 of the dielectric sprayer 10, and its excess enters the ring current distributor 7. The dielectric sprayer 10 acts as a seal in

the device. In the electrolytic cell 8, the anode – electrolyte – cathode (product) electric circuit is closed, and a gas-vapor layer is formed along the surface of the product. The gas-vapor layer is formed as a result of electrolysis of the electrolyte during the passage of electric current from the anode to the cathode. This layer consists of water vapor, oxygen and hydrogen. The connection to the anode 5 of the electric potential of increased voltage is accompanied by an intense release of Joule heat in this vapor-gas layer, this layer is heated to 2000–4000 K and the surface of the product is rapidly heated. The tops of burrs and sharp corners are heated to melt. Burr tops are intensely oxidized. After the burrs have melted, the high voltage is cut off. The heating process stops and goes into the electrolysis process, the surface cools down quickly. All ceramic and oxide layers crack and peel off from the product due to thermal expansion. If necessary, the process is repeated on the same segment of the product. The method was carried out when cleaning the round link chain 16X84 from contamination (scale and burrs) remaining after cutting off the flash. The voltage of the electric potential was set low (10, 20, 30, 40, 50 and 60 V) and increased (180, 200, 220, 250, 280, 300 and 320 V). The circuit was cleaned for a single turn on of the increased potential for a time of 1, 2, 4, 5, and 7 s, while the time for turning on the low potential was not limited.

Example 1. The influence of the on-time of the increased potential was determined at a fixed reduced potential of 30 V and an increased potential of 250 V. Experiments have shown that for this circuit 1–2 s is not enough to melt the tops of the burrs. Heating for 4–5 s rounded the top of the burrs, and heating for 7 s was accompanied by melting of the protruding surfaces of the chain. The contaminants were cleaned in the electrolysis mode, and the scale exfoliated after 2 high-potential inclusions.

Example 2. The influence of the increased voltage on the cleaning mode was determined at a fixed reduced voltage of 30 V and a heating time of 4 s. Experience has shown that at low voltage (130 V), the heating process is low-energy and the surface of the product was not cleaned. The increase in voltage was accompanied by a high-quality cleaning of the surface. When the voltage was increased to 300 V, the surface of the product melted.

Example 3. At a fixed overvoltage of 300 V and a time of 4 s, the undervoltage value was changed. At a potential of 10 V, the vapor-gas layer along the surface of the product is unstable and thin, which led to the instability of the process of heating the surface of the product, and the surface was not cleaned in 4 s. The change in voltage from 20 to 50 V practically did not affect the stripping process. A further increase in voltage was accompanied by a transition to a micro-arc process and a sharp slowdown in the cooling of the product. At this voltage, the surface heating was intense.

Device for electrolytic-plasma coating.

The device for electrolytic-plasma coating (**Fig. 2.54**) contains a container 1 made of insulating material with double walls: inner 2 and outer 3, between which there are annular grooves for electrolyte drain 4, for electrolyte injection 5, for gas supply 6. Bottom part 7 of the container 1 is made tapering and open downward, and along the perimeter of the bottom part 7 there is an annular slot 8 for gas supply.

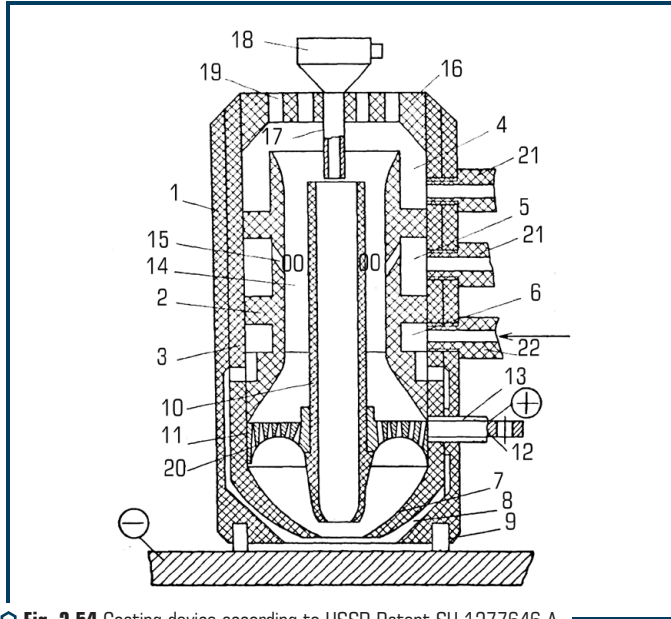


Fig. 2.54 Coating device according to USSR Patent SU 1277646 A

To seal the gas, a seal 9 is provided. A pipe 10 is fixed along the axis of the container, which passes through the anode 11 from the bottom part 7 of the container 1 to the top. To the anode 11 is connected an electrical input 12, insulated with a sleeve 13. To the annular gap 14 between the pipe 10 and the walls of the container are channels 15, the axes of which intersect with the axis of the container at an acute angle. Channels 15 are directed downstream of the electrolyte. The device is closed by a lid 16, on which a branch pipe 17 from the powder feeder 18 is fixed. The lid 16 has holes 19 for the outlet of vapors and gases. Holes 20 are made in the anode 11 to pick up electricity and direct polarity to the powder. The branch pipes 21 are intended for supplying and draining the electrolyte. Gas is supplied through pipe 22.

The device is installed on the seals 9 and pressed by additional force from the manipulation mechanism (not shown in the drawing) to the surface to be treated. Then the electrolyte is fed through the nozzles 21 into the groove 5, from where it rushes under pressure down the channels 15 and the annular gap 14. The electrolyte passes down through the anode 11 and through the holes 20 to the bottom part 7 of the container 1, where the anode 11 and the cathode closes the electrical circuit-detail. Due to the overheating of the electrolyte, a plasma layer forms near the surface of the part, which cleans the part from dirt and oxides, and also heats it up. Depending on the electrical parameters of the anode-cathode electrolyte cell, various modes of surface heating are possible. An annular slot 8 serves to localize the heating surface, through which gas is supplied

by means of a branch pipe 22 and an annular groove 6. It is also possible to change the heating mode of the product surface with the gas consumption. The powder material is fed from the feeder 18 through the nozzle 17 directly into the pipe 10, where it passes through the gas-liquid layer under the action of gravity and settles on the surface of the product. Part of the powder under the action of a gas-liquid jet passes the edge of the pipe 10 and enters the annular gap 14, where it is carried away by the flow of electrolyte to the anode 11 through the holes 20, respectively, acquires a positive charge and is deposited on the surface of the product. Thus, all the powder material that has entered the device is deposited on the surface of the product. The layer of powder material on the surface of the product is thin, electrically conductive and has a developed surface. Due to these circumstances, the electrolyte-plasma layer passes from the product surface – electrolyte interface to the powder layer – electrolyte interface. Since the heat removal from material particles – powders having point contact with the surface of the product is limited, and they are heated from almost all sides by plasma having a temperature of 3000–4000 °C, the powders melt and, under the action of surface tension forces, spread over the clean surface of the product with a temperature of 800–900 °C. Thus, local fusion and spreading of the powder particles form a coating. Since the formation process is carried out at a high temperature of the product on a clean surface in a reducing atmosphere of an electrolyte plasma, therefore, a high quality of the coating, 100 % continuity, and diffusion adhesion is determined. The use of a multicomponent suspension makes it possible to form complex multicomponent coatings on the surface of an article with a predictable quality in advance. The device makes it possible to apply coatings on both flat and bulky products, for example, bodies of revolution, with a corresponding change in the configuration of the bottom part, which expands the technological capabilities of the device. So, on a flat sheet with a thickness of 10 mm without preliminary cleaning, the device allows for 15–20 s to apply a layer of chromium-nickel alloy, dense with a glossy surface, 0.2–0.3 mm thick, and the hydraulic cylinder rod 80 mm in diameter and 450 mm long can be coated with a layer of chromium-nickel hard alloy 40 μm in 6 min.

2.10.2 TOOLS FOR AGRICULTURAL MACHINERY AND PROCESSING INDUSTRY

Electrolytic-plasma hardening of tools for agricultural machinery and the processing industry has been tested on some of the most wearing products.

These are hammers, feed crushers, which are used in the KDM unit, manufactured by the Novgorod-Volynsk machine-building plant and knives, as well as the lining of the drum of the forage harvester «Ros», produced by the machine-building plant in Bila Tserkva. The standard technology used in factories for hardening the surfaces of products by means of high-frequency currents does not provide sufficient hardness of products and, in addition, hardening with high frequency current is not economical (energy utilization rate is 20–30 %).

Electrolytic-plasma technology provides high hardness (60–64 HRC) of hardened local areas. The spaces between the sections have a low hardness, which provides stress relaxation and allows these products to be used in difficult, stressful conditions.

In addition, the power of the electrolytic-plasma unit for hardening these products was only 5 kW (for comparison, the power of the factory unit of HFC for hammer hardening is 500 kW). A feature of the technology is that it is possible to locally harden the part of the product that is possibly wearing out to the required depth.

Universal unit for hardening products of agricultural machinery.

The unit is designed for local hardening of wear surfaces of products operated in an abrasive environment during cutting (destruction) of soil and rocks of various strengths (**Fig. 2.55**). The unit has wide technological capabilities and, with appropriate restructuring, it is possible to harden the ends of conveyor bushings, couplings and other products where hardening of ends and edges is necessary.

The developed unit has three modifications for hardening disc harrows and seeder discs; for hardening the tooth of an excavator; for microplasma oxidation of the piston bottom of a diesel engine.

Despite a wide variety of hardened products, both in size and configuration, the basis of the unit did not change by 85 %. Only the places of unit of products and the design of the heaters were changed.

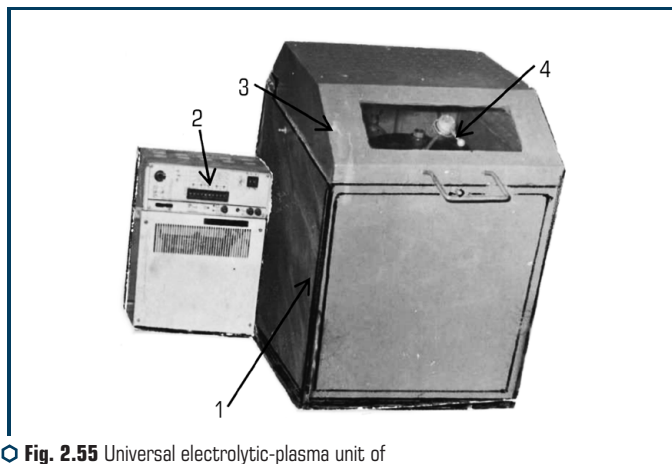
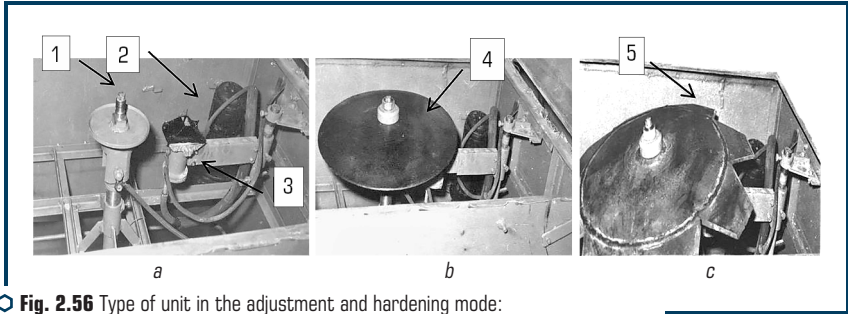


Fig. 2.55 Universal electrolytic-plasma unit of low power (up to 5 kW) for local hardening of wear surfaces of products

The unit (**Fig. 2.55**) consists of: tank 1, which simultaneously serves as the power body of the unit; converter of electrical energy 2 combined with a control panel; a movable cover 3, which serves to protect against electrolyte splashes and at the same time provides electrical safety; the cover has a viewing window with a handle 4 for manual manipulation of the product; the suction of vapors and products of water electrolysis is carried out through the pipeline. The unit has a spindle – 1 for fastening products and an electrolyte heater – 2 with electrolyte and electricity supplies – 3 (**Fig. 2.56**).



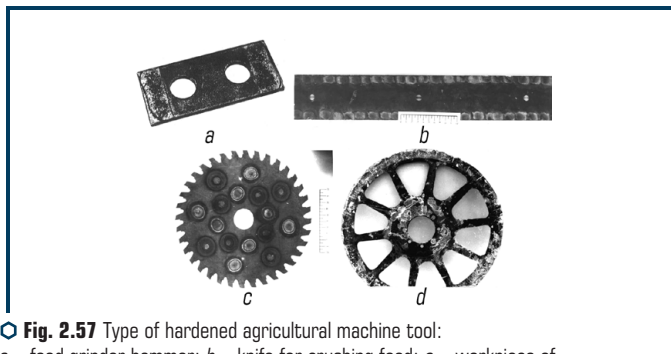
⊙ **Fig. 2.56** Type of unit in the adjustment and hardening mode:
a – adjustment mode; *b* – hardening of the seeder disks; *c* – harrow disk hardening

It is possible to strengthen disc products with a diameter of up to 600 mm and extended parts with a length of up to 400 mm. Strengthening is carried out by local hardened sections, which allows not to waste energy on heating the entire product and, moreover, not to have large installed capacities.

The advantage of this unit is that it is always ready for work and the energy for heating is spent only when the electrical circuit is closed: the surface of the product-electrolyte-electrode.

It is possible to install various heaters inside the unit, for example: with a round outlet; with a rectangular hole; telescopic with a spring; telescopic without spring; for strengthening the holes. This technological unit has been tested on a number of products (**Fig. 2.58**), for example, for hardening disks of seeders – 4, disc harrows – 5, knives, hammers, whips, beet harvester disks, saws, etc. Depending on the task at hand, the heater is replaced in the unit and its capabilities can be expanded. The study of the sales market for the technology and unit for electrolytic-plasma hardening shows that in terms of efficiency and readiness for operation, this unit, due to the increase in the cost of energy resources, is out of competition and can be used in almost any repair facility.

Fig. 2.57, 2.58 show photographs of typical products hardened in the unit (**Fig. 2.55**).



⊙ **Fig. 2.57** Type of hardened agricultural machine tool:
a – feed grinder hammer; *b* – knife for crushing feed; *c* – workpiece of a carbide saw; *d* – beet harvester disc



○ **Fig. 2.58** Reinforced tool for agricultural machines: *a* – plow blade; *b* – forage drum lining

Application area.

Electrolytic-plasma thermal cyclic hardening provides a system of solid inclusions of a certain shape with a thickness of up to 10 mm on the surface of products. The shape of this area depends on the configuration of the outlet nozzle of the heater, and the thickness of the solid layer is determined by the processing time. The hardened areas of the surface create compressive stresses in the surface layer of the part and, after abrasive processing, form depressions and protrusions of the relief, for the implementation of hydrodynamic lubrication of the sliding bearing.

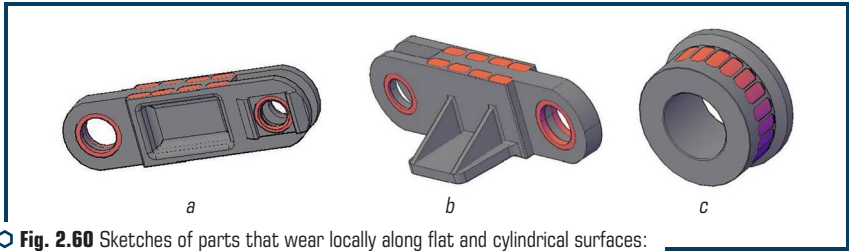
EPP has a wide ability to control the rate of heating and cooling of the surface. As a result, it is possible to obtain solid layers with a thickness of 0.3 to 10 mm on the surface of the product. The hardness of areas on the surface of a product made of 35XGSA steel is 52–58 HRC, 40X steel is 55–64 HRC, and 65G steel is 62–68 HRC.

The technology of electrolytic-plasma hardening is effective for hardening such items as: internal cylindrical surfaces (**Fig. 2.59**).

Heavy conveyor supports and supporting wheels (**Fig. 2.60**); wheels of a heavy portal crane (**Fig. 2.61**); the teeth of the gear wheels (**Fig. 2.62**).



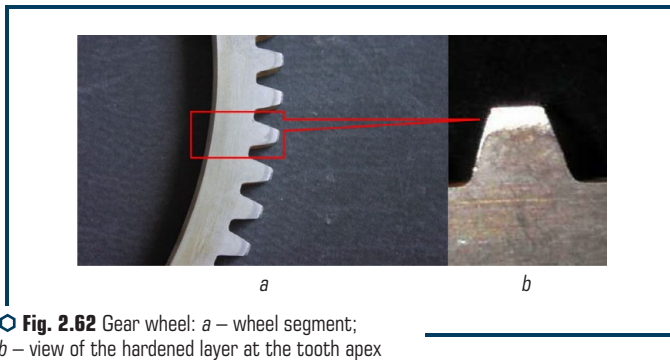
○ **Fig. 2.59** Long cylindrical parts, after hardening of the inner surface, cast iron compressor cylinder



○ **Fig. 2.60** Sketches of parts that wear locally along flat and cylindrical surfaces: *a, b* – shackle of a heavy chain conveyor; *c* – gantry crane wheel



○ **Fig. 2.61** Wheel of a heavy gantry crane: *a* – view after hardening; *b* – view of strengthened local places



○ **Fig. 2.62** Gear wheel: *a* – wheel segment; *b* – view of the hardened layer at the tooth apex

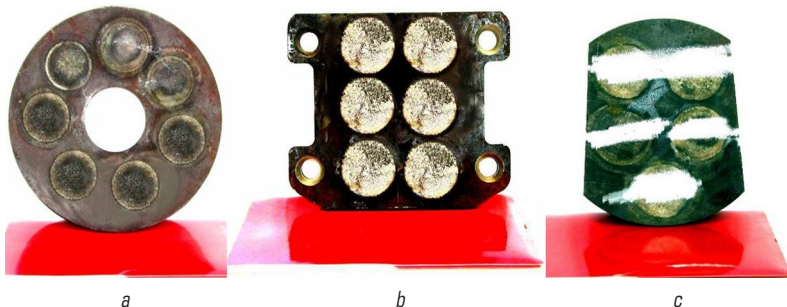
The surface of the lining of a heavy ball mill (**Fig. 2.63**); steel parts with local solid inclusions 60 mm in diameter, used in the repair of railway transport (**Fig. 2.64**).

Knife tools for bending sheets and cutting rolled products (**Fig. 2.65**).

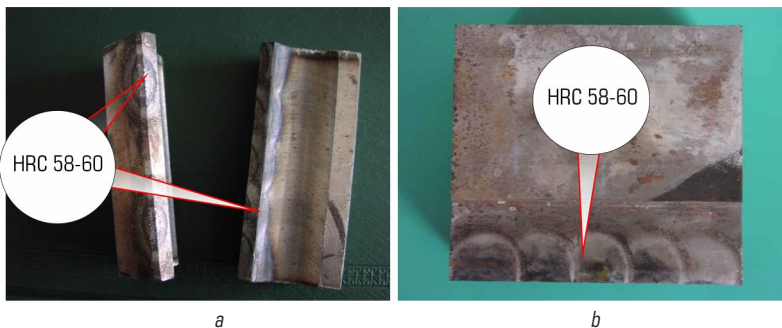
Electrolytic-plasma hardening is effective in hardening: knives and saws for cutting rolled steel; adapters, pods, rods (pipes) of drilling rigs, pans, tool holders, etc. in the mining and ore industry; discs, plows, openers, knives in agricultural machines and much more.



○ Fig. 2.63 Lining of a heavy ball mill after hardening: *a* – top view; *b* – view from the lining end



○ Fig. 2.64 Steel parts after hardening with local inclusions of 60 mm diameter, used in the repair of railway transport; *a*, *b* – parts fixed by electric arc welding; *c* – parts fixed with bolts



○ Fig. 2.65 Type of hardened tool: *a* – knives for sheet bending; *b* – knives for cutting rolled products

The creation of a system of solid inclusions on the surface of products provides a multiple increase in wear resistance (2–5 times), bending resistance (by 30–40 %) and prevents brittle fracture of the part under extremely high loads (**Fig. 2.66**).



○ **Fig. 2.66** Ball joint

This allows the technology to be used to strengthen products that operate in an abrasive environment with high bending loads, for example, ball joints in the steering mechanism of a car.

ABSTRACT

The possibility of using the electrolyte-plasma process not only as a tool for heating and surface hardening, but also for refining the surface of products (rolled products) is shown. Technological schemes and results of laboratory tests are presented.

KEYWORDS

Sheet metal, heater design, cleaning modes.

3.1 ABOUT DEVICES FOR CLEANING AND HEATING SHEETS

In the metallurgical industry, up to 60 % of energy costs are spent on heating blanks and cleaning them from contamination and an oxidized metal layer. Heating is carried out mainly by gas-air methods, which have a low efficiency of energy use (30–40 %) and oxidize the metal surface. As a result, a layer of scale forms on the surface. Its removal from the surface of the workpiece is energy intensive and difficult. For surface cleaning, acid etching methods are usually used, which require a lot of energy to neutralize them. The presence of traces of scale on the surface of the workpiece causes increased wear of the deforming tool and destruction of the workpiece.

Developed in recent years, electrical contact heating does not provide uniform heating and creates defects at the point where the electric current is supplied. These defects are the reason for the destruction of the workpiece during further processing.

The implementation of non-oxidative heating, the creation of protective films and the control of heating over a wide temperature range is a major problem in metallurgical processes. To prepare the structure and increase the plasticity of the workpiece, thermal cyclic heating is important, which can be done only with the use of electrical heating methods. Solving these problems will ensure the receipt of quality products. The most important problem for the industry is also reducing the energy intensity of products, which is possible with the use of new heating methods that significantly increase the efficiency of energy use.

Electrolyte-plasma technology makes it possible to carry out non-oxidizing, thermal cyclic heating of long metal workpieces, carried out simultaneously with cleaning the surface from scale, dirt and creating a protective film. Energy-saving technology for heating and cleaning metal blanks in ferrous metallurgy, based on the conversion of electric current into heat, switched by a plasma from an electrolyte.

Electrolyte-flame heating is accompanied by the reduction of metal oxides and the removal of various kinds of loose contaminants, organic films and the creation of a protective film on the metal surface.

New in energy-saving electrolyte-plasma heating and cleaning technology is that they carry out contactless switching of electric current through the plasma layer, which serves as a medium for generating electrical discharges. The discharges heat and clean the workpiece, and the active elements of the plasma reduce oxides and create a protective film. At the same time, the coefficient of useful use of electrical energy when heating the metal reaches 80 %.

The electrolyte is transparent to the radiation of the heated metal, which makes it possible to introduce temperature control sensors, automate the process and ensure high quality heating.

The contactless transmission of energy makes it possible to heat a long workpiece without losing energy and destroying the switching devices and the metal surface. This ensures reliable and long-term operation of technological devices.

The development of energy-saving electrolyte-plasma methods for heating metal blanks is carried out using the principles of synergy, concentration selectivity and discreteness. The intensification of heating will occur due to nonlinear physicochemical effects with a synergistic multifactorial effect, and the supply of energy portions to the workpiece material will be carried out with a certain frequency that affects the processes of transformation of its structure.

The workpiece is heated by electric discharges in the plasma layer, which is adjacent to its surface. Discharges are initiated by switching the electric current with layers of plasma with increased conductivity. A periodic change in the power density of electrical discharges accordingly changes the surface temperature, which creates conditions for thermal cycling.

The thermal cycling mode is carried out in the environment of electrolysis products of the electrolyte, by periodically heating the surface of the article above the phase transformation temperature and cooling it below the transformation temperature. This ensures surface cleaning, oxidation reduction, creation of a protective film and increases the ductility of the workpiece.

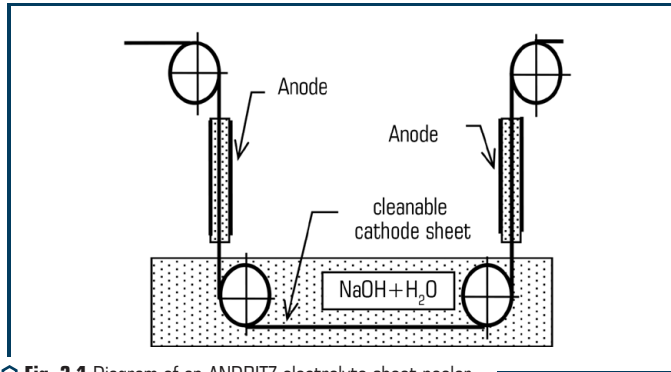
The device for heating the workpiece uses an electrolyte based on soluble salts containing alloying elements. The electrolyte passes through the cells of the electrode, where the recombination of ion charges takes place, which are moved by a hydrodynamic current to the surface of the workpiece. Thus, the transport of alloying elements to the surface of the workpiece and the creation of a protective film, which protects the surface from oxidation and reduces wear of the working surfaces of the tool, is carried out. Thermal cyclic heating intensifies the processes of diffusion of alloying elements into the surface of the workpiece and increases the plasticity of the metal.

Part of the energy consumption (10–15 %) is spent on heating and evaporation of the electrolyte – the formation of a vapor-gas layer.

Fig. 3.1 shows a typical diagram of an electrolyte-plasma unit for anodic polarization for cleaning the surface of a sheet, operating at a reduced voltage – up to 150 V [40].

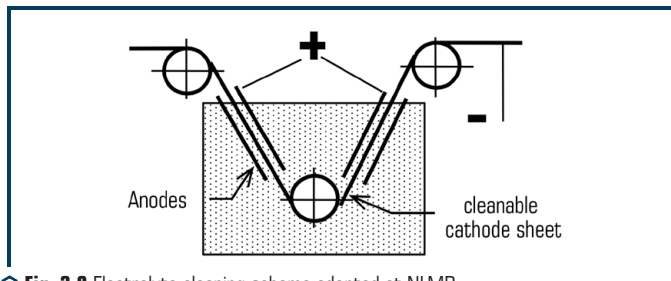
To improve the quality of the surface of critical parts of the repair removal of various coatings, a method of plasma electrolyte treatment with anodic polarization with high (100–360 V) voltage

in electrolytes based on salts of inorganic carboxylic acids of low (2–7 %) concentration is proposed [84]. At voltages below optimal values, the vapor-gas shell can break off and a transition to active electrochemical dissolution of the alloy is possible. If the vapor-gas shell is stable, then the processes of oxidation of the surface and dissolution of the surface of the anode-article occur simultaneously [84].



○ Fig. 3.1 Diagram of an ANDRITZ electrolyte sheet peeler

For example, NLMP uses electrolytic cleaning prior to coating in conjunction with brushing and pickling. Cleaning device, **Fig. 3.2**, contains anodes parallel to the surface of the sheet. An alkaline electrolyte is fed into the interelectrode gap.



○ Fig. 3.2 Electrolyte cleaning scheme adopted at NLMP

The sheet serves as a cathode. Cleaning according to this scheme provides no more than 20 mg of contamination per 1 m² of leaf surface. The main disadvantages of this cleaning method are: poor quality; high energy intensity; the need for washing and drying the sheet; impossibility to combine heating and cleaning of the sheet in a cycle [40].

For electrolyte-plasma heating by an electric current, a switched electrolyte electrode and a plasma layer adjacent to the workpiece surface, a higher voltage is required – up to 300 V.

A periodic change in the electric current intensity changes the power density of electric discharges in the plasma layer and, accordingly, the workpiece surface temperature. The thermal cycling mode is carried out by periodically heating the surface of the product above and cooling it below the transformation temperature. The introduction of active elements into the plasma provides, simultaneously with thermal cyclic heating, surface cleaning and, to protect against oxidation, the deposition of a dense and thin coating. Dozens of firms and institutes work in the field of electrolytic-plasma cleaning and heating, technologies and devices have been developed that mainly use the anode mode of switching on the workpiece, patents have been obtained, for example, [85–89].

Fig. 3.3 shows a diagram of unit for thermal cyclic heating, cleaning and chemical-thermal treatment of the surface of a sheet product. The active element of the vapor-gas layer is hydrogen, which is a powerful reducing agent of oxides, and the introduction of such elements as sodium, aluminum, chromium provides chemical-thermal treatment and protection of the cleaned surface from oxidation. The great advantage of the proposed heating method is the high efficiency of electrical energy, which, in combination with the combined action of cleaning and diffusion of alloying elements, provides high efficiency.

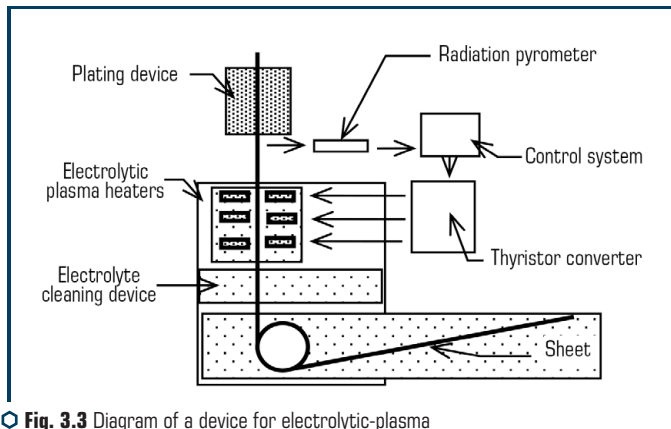


Fig. 3.3 Diagram of a device for electrolytic-plasma cleaning of a sheet, heating and heating control

Automated control provides controlled heating, cleaning and formation of a protective film on the surface of the workpiece. The presence of a transparency window in the electrolyte makes it possible to introduce temperature control sensors, automate the heating and cooling process, and ensure high quality of metal thermal cycling in a given temperature range. Contactless transmission of energy makes it possible to heat workpieces of great length without loss of energy and destruction of switching devices. This ensures reliable and long-term operation of technological devices.

The development of energy-saving electrolyte-plasma methods for heating billets will be carried out using the principles of synergy, concentration selectivity and discreteness. The intensification

of heating and cleaning will occur due to nonlinear physicochemical effects with a synergistic multifactorial effect, and the supply of energy portions to the workpiece material will be carried out with a certain frequency, which affects the processes of transformation of its structure.

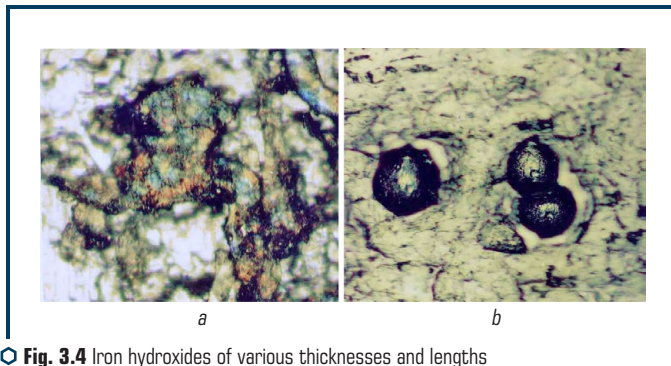
3.2 EFFICIENCY OF ELECTROLYTIC-PLASMA CLEANING

The sheet on its surface has a layer of corrosion (iron hydroxides) of varying thickness and length. Corrosion can take the form of a local spot or occupy an extended area. The surface relief of the sheet is not visible under the corrosion layer (**Fig. 3.4**). On the surface of the sheet, there are point defects in the form of depressions and non-metallic inclusions (**Fig. 3.4, a**) and local inclusions of scale (**Fig. 3.4, b**).

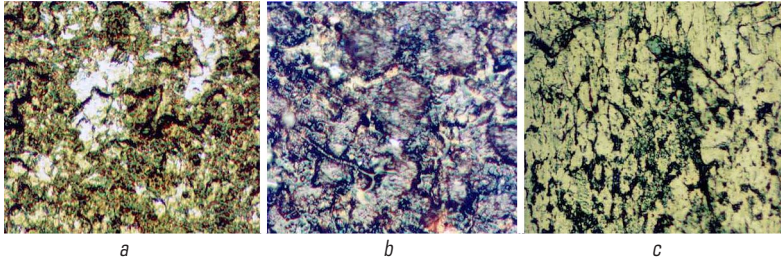
Loose contaminants that contain metal and non-metal particles, organic films, a thin layer of liquid that cover the entire surface of the sheet, including areas with layers of corrosion. Through these contaminants, the surface relief of the sheet, characteristic for each type of steel, is visible (**Fig. 3.5**). Contamination is also located in microcavities, under the surface of the sheet. The most common loose contaminants and corrosion traces usually do not hide the surface relief. But under this layer there are open pockets with non-metallic inclusions, which are clearly visible after washing the surface with alcohol (**Fig. 3.5, b**).

The scale layer can be dense. Sometimes scale inclusions have the correct shape (**Fig. 3.4, b**). It can be seen in the photograph that even with an increase of $\times 500$, sharpness is directed both to the surface of the inclusion and to the characteristic features of the relief, which confirms our assumption that it is the inclusion on the surface, and not the surface particle (dust grain).

When removing loose contaminants from the surface (washing with alcohol), it can be observed that it consists of characteristic «plateaus», depressions in the surface and depressions (inclusions) of various sizes (**Fig. 3.5, b**).



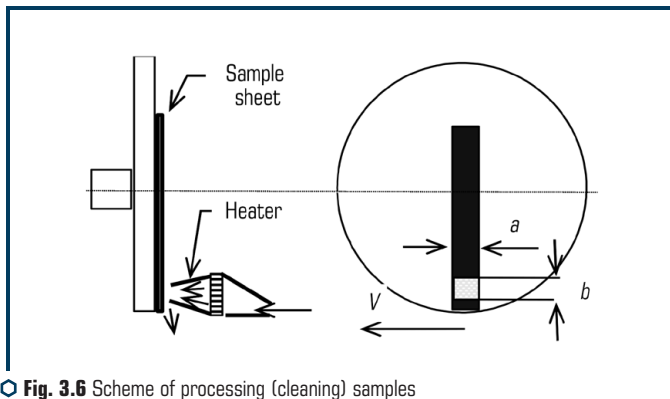
○ **Fig. 3.4** Iron hydroxides of various thicknesses and lengths on the surface of the sheet: *a* – local layers of corrosion; *b* – scale



○ **Fig. 3.5** Layers of corrosion, scale and loose contamination of various thicknesses and lengths on the sheet surface

Experimental work on cleaning samples from sheet steel was carried out on a special stand (**Fig. 3.6**). This stand had a faceplate for holding samples and an electrolyte-plasma device for heating/cleaning. The technology was controlled by means of a controlled electric energy converter – a rectifier.

Samples of sheet steel are fixed on a faceplate (**Fig. 3.6**) with the ability to move at a speed of 10 m/s. The active area of the electrolyte-plasma device for heating/cleaning is $a \cdot b$ 7.5 cm² (3-2.5). The sample surface was cleaned at a speed of 10 m/s. Carried out 1, 2, 3-fold processing of the surface area.



○ **Fig. 3.6** Scheme of processing (cleaning) samples in laboratory conditions

The quality of cleaning is assessed visually, by the number of visible stains and dirt particles, as well as by the color of the surface. The heating temperature of the leaf surface was assessed by the presence of traces of melting and tarnishing colors. Samples of sheet steel O30/CRS and Full Hard/O27 were used.

The results of experimental work showed that after one pass of the electrolyte-plasma heater, there are no loose contaminants on the cleaned surface of the sheet (**Fig. 3.7**). In places of the surface where there was corrosion, defects occur in the form of a typical etching pattern.

On the surface of the sample after cleaning, a clear relief with traces of etching corrosion is visible. Inclusions that were not destroyed at a given energy density are also seen. The surface cleaning results on Full Hard/O27 steel samples showed that the surface acquired a light gray metallic color. All tops of irregularities and protruding boundaries of the «plateau» and depressions have a characteristic melting. The photograph of the surface (**Fig. 3.7**) shows that all the depressions and cavities are not in sharpness, which confirms the assumption about the destruction of the non-metallic inclusions located there. Round «craters» and inclusions remain on the surface.

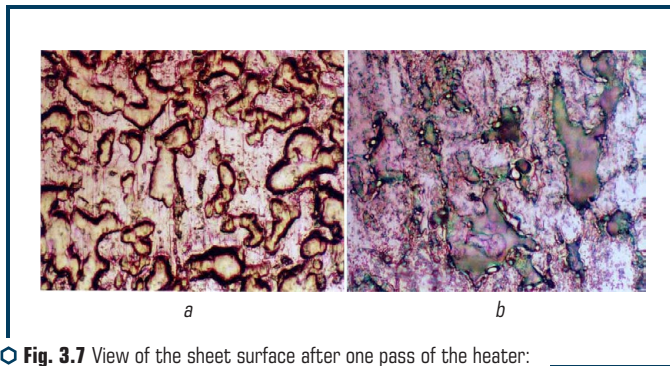


Fig. 3.7 View of the sheet surface after one pass of the heater: *a* – steel O30/CRS; *b* – steel Full Hard/O27

The cleaning effect is clearly visible on steel O30/CRS after three passes. In the photograph of an uncleaned surface (**Fig. 3.4, 3.5**), the surface relief is hardly visible and a layer of corrosion is visible (highlighted in yellow by light filters).

A characteristic lowering of the «plateau» relief can be seen on the cleaned surface (**Fig. 3.7, a**). The sharp edges of the «plateau» boundaries have traces of melting (**Fig. 3.7, b**).

The thermal mechanism of destruction of non-metallic inclusions can be traced by comparing the characteristic relief of the depression (pocket) in **Fig. 3.8** and the type of melted trough boundaries. Despite the increase of $\times 500$ in **Fig. 3.8, a, b**, the surface of the inclusion in the depression is visible, which is not shown in **Fig. 3.7**. Apparently, the rapid heating of the boundaries of the depression before melting destroys the nonmetallic inclusion. An empty cavity is formed at the point of inclusion.

This mechanism is clearly shown in the photograph (**Fig. 3.8, b**). Here it is possible to observe strong fusion of the boundaries and traces of thermal influence, which accompany the heating of the periphery of the non-metallic inclusion. Inside the crater cavity, apparently, there are oxides, scale residues and melted metal particles.



○ **Fig. 3.8** View of the surface of a Full Hard/027 steel sheet after electrolytic-plasma cleaning

It is characteristic that the cleaning of the Full Hard/027 and 030/CRS steel samples was carried out under the same conditions, at the same energy density, but all protruding boundaries and tops of irregularities on the surface of the Full Hard/027 steel samples were uniformly melted (**Fig. 3.7, b** and **Fig. 3.8**).

After cleaning steel 030/CRS samples, no flashing was observed (**Fig. 3.7, a**). Only the melting of the boundaries of cavities (pockets) containing non-metallic inclusions was observed.

With a 2.0 cm wide active sprayer slot and a sheet width of 30.5 cm, the total heating area is 61 cm² on one side and 122 cm² on both sides. Productivity is 10 m/min.

The required current is $122 \cdot 5 = 610$ A. The power expended for processing the surface of the sheet with one row of sprayers will be $610 \cdot 280 = 170$ kVA.

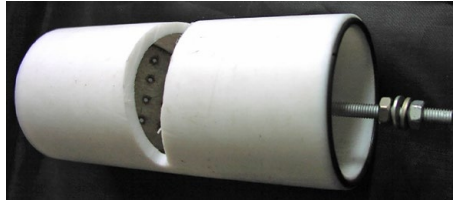
For thermal cycling and heating, it is necessary to have at least 3 rows of sprayers. In this case, their electrical power will be $170 \cdot 3 = 510$ kVA.

The calculated coefficient of efficient use of electrical energy spent on heating the sheet is taken as 70 %, or $510 \cdot 0.7 = 357$ kVA.

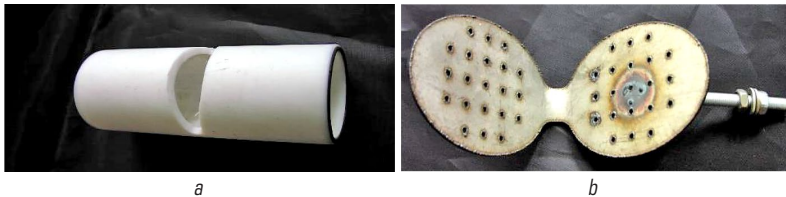
Effectively combine cleaning and heating of the sheet before metallization (coating) technology. It is proposed (**Fig. 3.4**), directly under the crucible for metallizing the sheet, to install a block of three slot-type sprayers. Install temperature control systems under the crucible. The readings of this system, in the form of a proportional electrical signal, are introduced through an automated adapter into the power thyristor circuit for controlling the electric field strength. This will allow not only to clean the surface, but also to melt its defects, to control the heating temperature of the sheet.

3.3 DEVICE FOR CLEANING AND HEATING ROLLED PRODUCTS

The device for heating rolled products includes chambers (**Fig. 3.9**). Structurally, the chambers are made of a dielectric cylindrical body (**Fig. 3.10, a**) and an anode (**Fig. 3.10, b**), with through holes for supplying an electrically conductive medium-electrolyte to the processed rolled surface.



○ **Fig. 3.9** Chambers for cleaning and heating rolled products



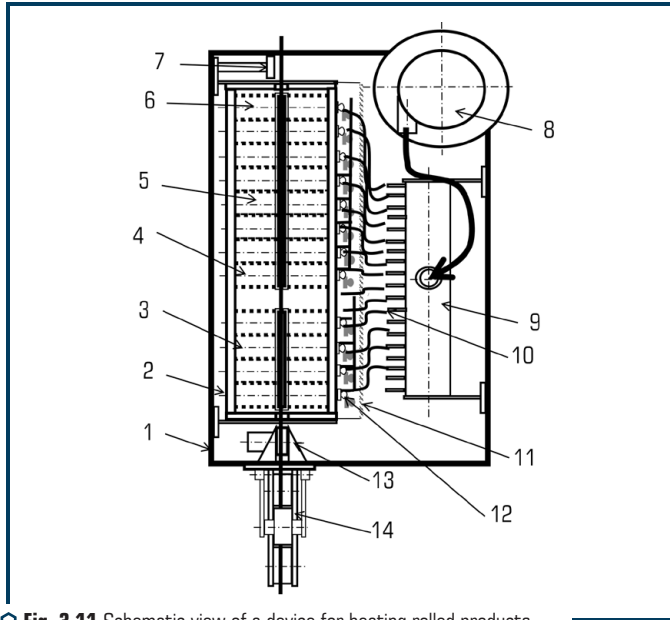
○ **Fig. 3.10** Details of the chamber for cleaning and heating rolled products: *a* – dielectric body; *b* – anode

To maintain a uniform and trouble-free technological mode of surface treatment, the device has a system for fixing the anode and the object being processed relative to each other. This device makes it possible to form a layer of plasma with reducing properties that is stable in time in the near-surface zone. Energy transfer is carried out by supplying an electrically conductive medium – electrolyte – to the surface to be treated through the anode with through holes (**Fig. 3.10, b**). The electrolyte is an aqueous solution of a metal salt.

This design of the device (**Fig. 3.11**) provides non-oxidative heating of long products or chemical-thermal treatment of the surface of products. The problem of uniform heating of the product over the section is solved by choosing the technological modes of heating and temperature control.

The Rolled product moves through the chamber by means of specialized devices for coiling and winding Rolled product into rolls.

The device (**Fig. 3.11**) contains several discrete chambers isolated from each other (3, 4, 5, 6) – reactors with anodes that have through holes and are connected to electrical circuits with different voltages. There is also a sensor – 13 for measuring the speed of the rolling and sensor – 7 for measuring the temperature of the rolling. The first sensor ensures trouble-free operation when changing the speed of rolling. It blocks voltage activation at low speeds. And the second sensor is included in the electrical voltage control circuit at the output chamber, which provides an increase-decrease in the heating power of the Rolled product, depending on its temperature.



○ Fig. 3.11 Schematic view of a device for heating rolled products

In the device for heating rolled products, discrete chambers (Fig. 3.9) are made of non-conductive material (fluoroplastic or ceramics) and contain a volume of flowing electrolyte limited by conductive anodes, the surfaces of which are equidistant from the processed rolled surface. In the anodes (Fig. 3.10, *b*), holes are made, the axes of which are oriented to the surface to be treated, and windows are made in the upper part of the chambers for removing vapors and electrolyte drain. The anodes in the chambers located at the inlet of the rolled metal are connected to an electric circuit with a maximum electric current of 280–340 V. In the subsequent chambers, the anodes are connected to a reduced voltage of 200–240 V.

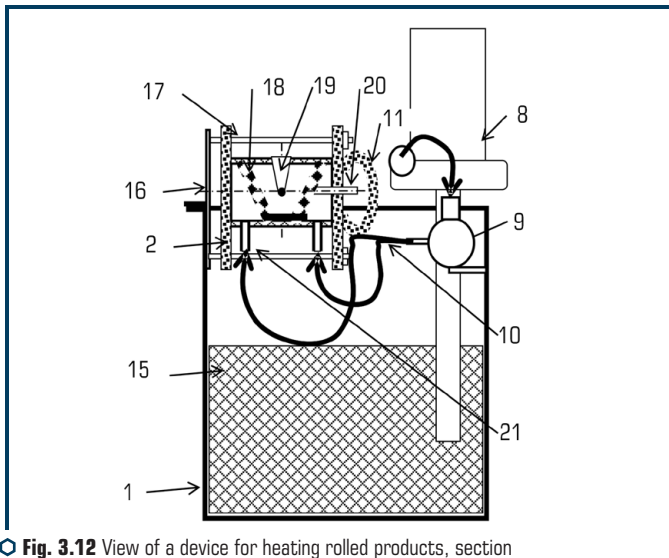
Placement at the exit of the chambers of the sensor – 7 measurements of the intensity and wavelength of the radiation of heated rolled products and the inclusion of the output signal from this sensor, as a control one, into an electric circuit with an electric power control regulator, provides the ability to control the intensity of the electric current at the anode of the chambers-reactors located on exit rolling. This ensures monitoring and control of the temperature of the rolled product by means of electrical feedback from the sensor to the control circuits of the electric power regulator of the output chamber.

Ultimately, an optimal heating mode is set in each of the chambers, which ensures uniform heating of the Rolled product over the section. The sensor provides control and management of the temperature of the rolled product at the exit from the last chamber.

During the operation of the device, in the first chamber, an intensive heating mode of cold rolled products is carried out, which comes from the unwinding device, in the second and subsequent chambers, intensive heating alternates with moderate heating, which allows the temperature to be equalized over the cross section of the rolled product, and a controlled heating mode is set in the last chamber. The heating mode in the last chamber is controlled by a temperature sensor and a program for controlling the power of the electrical circuit.

The device for heating rolled products (**Fig. 3.11**) has symmetry about the longitudinal axis of the heated rolled products. This device contains a tank-bed – 1, a body – 2 made of non-conductive material, discrete chamber-reactors 3, 4, 5, 6 for heating rolled products, a proximity sensor – 7 for rolled temperatures, a pump – 8 for electrolyte supply, a hydraulic system – 9 for electrolyte consumption control, electrolyte distributor – 10 in discrete chambers, protective case – 11, electrical contacts – 12 for switching electrical energy, rolling speed sensor – 13, dry current collector – 14 for grounding and damping rolling vibrations.

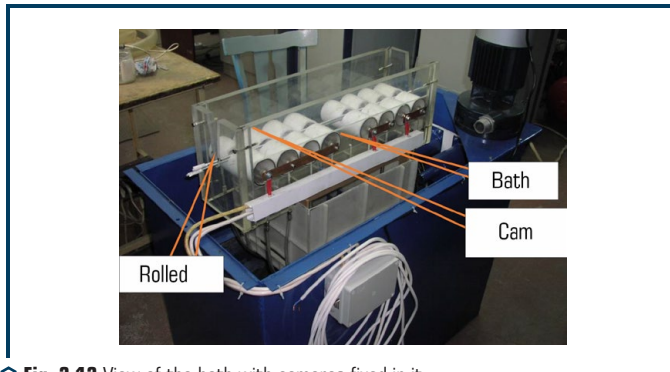
Fig. 3.12 shows a view of a device for heating rolled products, a section through the heater. The tank-bed – 1 contains electrolyte – 15, the chambers are fixed by means of a case – 2 made of non-conductive material, as well as brackets – 16 and studs – 17. Chambers have metal anodes 18. Windows 19 are made in the center of the chambers. The anodes are connected to the power supply by means of terminals – 20, which are covered with a case – 11. The pump – 8 supplies electrolyte through the hydraulic system – 9 to control the flow of electrolyte and the distributor – 10. The electrolyte is supplied to the discrete chambers through the choke – 21.



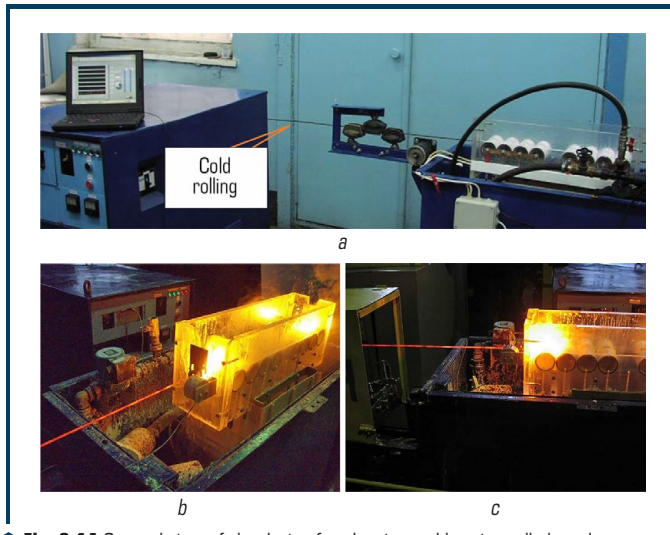
○ **Fig. 3.12** View of a device for heating rolled products, section through the heater

As a result, the open windows of the chambers form an extended bath filled with a flowing electrolyte, **Fig. 3.13**. Rolled product is immersed in this bath, which has a longitudinal displacement, and each section of the rolling sequentially passes through the windows of all chambers. The rolled metal is stretched into a line and moved from one roll to another by means of standard coiling and winding devices.

Rolled steel stretched in a line is placed along the axis of the electrolyte bath, which is formed from the open windows of the chambers (**Fig. 3.14**). The supply of electrolyte to each of the chambers ensures that the bath is filled with electrolyte.



◉ **Fig. 3.13** View of the bath with cameras fixed in it



◉ **Fig. 3.14** General view of the device for cleaning and heating rolled products

The anodes in the chambers are individually connected to regulated sources of electric current. The anode in the first reactor chamber is connected to a high voltage of 280–340 V. This voltage ensures the formation of a plasma layer even on the cold and oxide-contaminated rolled surface and heats the rolled stock at a rate of 200–500 °C/s. The anodes in the subsequent chambers are connected to a reduced voltage of 180–220 V, which ensures the maintenance of the plasma layer and heating of the rolled stock at a rate of 50–150 °C/s. The low heating rate ensures uniform heating of the entire rolled section without overheating the surface. The anode in the last chamber is connected by means of a controlled electric current source. The control is carried out by means of a signal from the temperature sensor at the outlet of the device for heating the rolled stock. The sensor measures the surface temperature, which allows to control the heating power in the last reactor chamber. The presence of three or more, isolated from each other, discrete chamber-reactors provides the ability to connect each chamber to an individual source of electric current. This ensures uniform heating of rolled products without overheating the surface. Gauges for measuring the speed of rolling, rolling temperature and an automated heating power control system, using a special program, provide the ability to automate heating control and exclude a violation of the heating technology (**Fig. 3.14**).

In the device for heating rolled products discrete chambers are made of non-conductive material and electrically conductive anodes. The inclusion of anodes in an individual electrical circuit ensures the transfer of energy to the rolling stock with minimal losses for heating the electrolyte. Reducing losses for heating the electrolyte is also ensured by such essential features as the execution of through holes in the anodes, the axes of which are directed to the center of the reactor chamber, where the heated rolling moves.

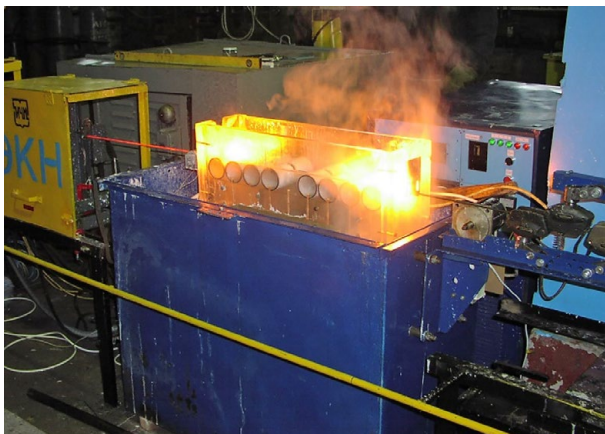
To improve the quality of heating and ensure the safety of work, the device contains a sensor for measuring the speed of the product, which is included in the electrical circuit for controlling the process current.

The sensor provides the ability to turn on the process current only at a certain speed of the rolled products, which excludes overheating at low speeds or when the rolling stock is stationary. Testing a device with a different number of chambers for heating rolled products showed that an increase in the number of chambers to 3 or more ensured uniform heating of rolled products at a speed of 30 m/s.

An increase in the number of cameras is necessary to ensure processing performance. At high speeds of rolling stock, more than 60 m/s, a device with 8 chambers is required (**Fig. 3.15**).

Tests have shown that when the anode is connected in the first chamber to a low voltage of 180–220 V, the device does not work and does not provide high-quality heating. The connection of the anode in the first chamber for 320 V ensures cleaning and heating of the rolled stock already in the first chamber and the continuation of the heating technology in the subsequent chambers, where the anodes are connected to a reduced voltage.

The most optimal options are processing modes No. 6, 10, 12 (**Table 3.1**).



○ Fig. 3.15 Type of unit with 8 chambers for cleaning and heating rolled products

● Table 3.1 Modes of electrolytic-plasma technology for cleaning and heating rolled products

No.	Number of chambers	Voltage at the anode of the first chamber, V	Voltage at the anodes of subsequent chambers, V	Heating power control on the last chamber	Rolled product movement speed, m/s	Heating temperature of the rolled product surface, °C
1	2	180	300	no	30	400
2	2	340	340	no	30	600
3	3	340	220	no	30	900
4	3	340	220	no	30	1000
5	4	180	300	no	30	1200
6	4	340	200	Yes	30	1000
7	5	200	200	No	60	400
8	5	340	200	Yes	60	900
9	6	340	180	No	60	800
10	6	340	180	Yes	60	1000
11	7	340	180	No	60	900
12	8	340	180	yes	60	1000

The device for cleaning and heating rolled products can be used in various industries.

CONCLUSIONS

Electrolyte-plasma technology and equipment for cleaning rolled products in the metallurgical industry in the cathodic mode are proposed. The technology and equipment can be used for heating long-length workpieces before deformation and for surface preparation of long-length workpieces before coating with zinc. For example, JSC Cherepovets Steel Rolling Plant has 37 galvanized wire production lines. According to the plant, up to 30 % of the cost of this wire is the cost of cleaning the wire with acids and their neutralization. Up to 10 % of the cost is energy consumption for heating the wire. The technologies of electrolytic-plasma heating, cleaning, thermal cycling and deposition of a protective coating are carried out simultaneously, on the same unit, which expands the scope of their application. The above advantages of the developed readjustable unit will make it possible to widely use the technology and equipment in the metallurgical and machine-building industries.

ABSTRACT

Technological methods of surface chemical-thermal treatment (CTT) using the electrolyte-plasma processing method are described. The used technological equipment is described. The results of studies of processes of surface alloying of metal alloys are presented.

KEYWORDS

Soluble anode, suspension, micropowder, nitrogen-containing electrolyte, electrolysis, deposition of alloying elements, concentration.

4.1 INTRODUCTION

There are various methods of thermal and chemical-thermal treatment of the surface of steel parts, including methods of heating the surface with concentrated energy sources. Electrolyte-plasma technology also makes it possible to implement chemical-thermal treatment of products [39, 42, 53, 90, 91]. The essence of the technology lies in the fact that in a dielectric bath with a flowing liquid-electrolyte, an electrode connected to a voltage source is placed, which is an anode. The workpiece to be processed is connected to the second pole of the same voltage source and is the cathode. The surface of the part is brought in until it touches the surface of the electrolyte. Electric arcs are excited at the interface between the metal product and the electrolyte, which causes the surface to heat up to a temperature that is optimal for chemical-thermal treatment. The subsequent disconnection of the voltage ensures rapid cooling of the surface with the electrolyte. Contact of the surface of the part with the electrolyte causes the formation of many electrical discharges, which form a plasma layer separating the surface of the part – the cathode and the surface of the electrolyte – an aqueous solution of salt. Depending on the activity of the elements that make up the plasma layer, reactions of metal reduction from oxides and (or) plasma-chemical reactions of the formation of carbides, nitrides and complex compounds take place on the surface of the part. A high heating rate causes large temperature gradients and elastoplastic deformation of the surface layer of the product, which significantly accelerates diffusion processes [92], creates conditions for phase hardening and refinement of the crystal structure. Cyclic heating of the surface layer of the product will provide thermal diffusion transfer of elements.

An unit for local thermal diffusion deposition of coatings on the surface of cylindrical products should be able to control the temperatures of the plasma and the workpiece surface being

processed, which determines the flexibility and efficiency of the electrolyte-plasma technology. The electrolyte used in the unit must ensure: environmental safety, availability of materials, technological flexibility. Two directions of experimental work are presented. The first is obtaining alloying elements from a solid anode electrode using electrochemical dissolution. The second is the introduction of a powdery material into the plasma layer, which is formed on the treated surface of the part. The main constituent of the electrolyte is water. Water molecules are highly resistant to heat. At temperatures above 1000 °C, water vapor begins to decompose into hydrogen and oxygen: $2\text{H}_2\text{O} \leftrightarrow 2\text{H}_2 + \text{O}_2$. Superheated hydrogen, due to its lightness and positive charge, forms a layer on the heated surface of the product, which is connected by the cathode. In this layer, hydrogen is a reducing agent. To intensify the reduction of oxides, carbon is introduced into the plasma layer, which is also a good reducing agent. Let's use micropowders of oxides of copper, zinc, aluminum, chromium, as well as micropowders of carbon (graphite) and others. Glycerin was used to plasticize the electrolyte – powder suspension.

The materials selected for experiments have the following distinctive features: insolubility in alkaline media, the ability to adsorb fatty acids, low specific gravity and microdispersity. These materials are evenly distributed in the electrolyte and transported using a pump through the hydraulic system of the unit with an alkaline solution to the plasma layer, where the processes of reduction and plasma-chemical synthesis of products are carried out, which condense on the surface of the product.

4.2 EXAMPLES OF EQUIPMENT FOR SURFACE CTT

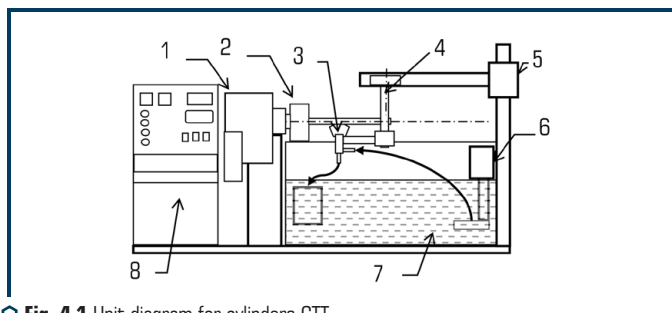
The industry uses long cylinders. These are hydraulic drives, pumps, engine and compressor cylinders, etc. The performance of these products depends on the wear of the inner cylindrical surfaces. High requirements for the strength of products limit the use of volumetric methods of thermal and chemical-thermal treatment.

Electrolyte-plasma technologies for chemical-thermal treatment of cylindrical surfaces were carried out on the unit (**Fig. 4.1**), by introducing an electrolyte heater inside the cylinder. Surface heating is carried out by electric arcs between the surfaces of the product and the liquid electrolyte electrode. A solution of metal salts in water is used as a liquid electrode. Electric arcs develop in a plasma layer containing alloying elements. Cooling is carried out with the same electrolyte. A periodic change in the strength of the electric current changes the power density and, accordingly, the surface temperature. The power density of electrical energy when heated is up to 10^4 W/cm^2 , and when cooled up to 100 W/cm^2 . Periodic heating of the surface of the article above the phase transformation temperature and cooling it below the transformation temperature carry out the thermal cycling mode. The unit includes the following components (assembly units) (**Fig. 4.1**): product manipulator (rotator) – 1; device for fastening products – 2; electrolyte heater – 3; holder for heater – 4; traverse for moving the heater – 5; pump – 6; tank – 7 and electrolyte supply system; electric current converter – 8. The unit is also completed with a non-contact temperature control

system and an automated heating control system. Heater – 3 is fixed on a special traverse – 4 by means of insulators in the inner cavity of the upper part of the tank. The heater has a fitting for electrolyte inlet. The ends of the wire from the rectifier (+) are connected to the anode in the electrolyte heater. The ends from the rectifier (–) are connected to the product via a current collector.

The experiments were carried out on a modernized unit for electrolytic-plasma treatment (Fig. 2.6). The unit includes the following main components (Fig. 4.2): a non-contact temperature control system and an automated control system – 1 heating the surface of the product; an electric current converter and a manipulator control system – 2; manipulator device for fastening the product – 3; electrolyte heater – 4; large tank with electrolyte – 5; small tank with a pump – 6.

Heater – 4 is fixed on a special traverse by means of insulators in the inner cavity of the upper part of the tank.



⊙ Fig. 4.1 Unit diagram for cylinders CTT



⊙ Fig. 4.2 Unit of chemical-thermal surface treatment of cylindrical surfaces

The use of electrolytes based on water-soluble alkaline salts and carbon micropowders, aluminum oxides, chromium oxides, etc. allows to restore alloying elements directly in the plasma layer,

which is adjacent to the heated surface. The electric field forms a layer with positively charged alloying elements on the heated surface of the product. Combined cyclic heating of alloying elements and the surface of the product provides plasma-chemical synthesis, diffusion and chemical-thermal treatment of the surface of the product.

CTT can be carried out on local areas of the surface without heating the entire product. The cyclic change in the temperature of the surface layer of the product intensifies the diffusion process. A change in the temperature of local areas of the surface is controlled by a change in the electric field strength in the gap between the surfaces of the product and the liquid electrode using a specialized heater, as well as a measuring and control complex (**Fig. 4.3**).

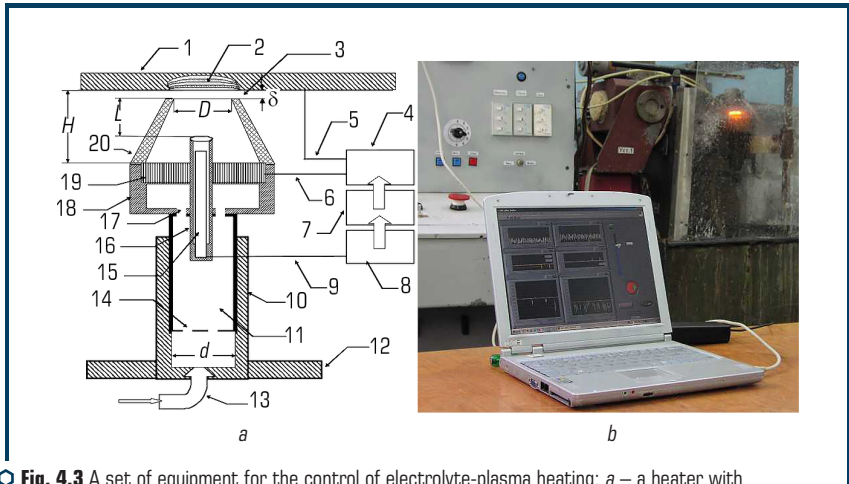


Fig. 4.3 A set of equipment for the control of electrolyte-plasma heating: *a* – a heater with a temperature measurement sensor; *b* – type of measuring complex and electrolytic-plasma equipment

The heater is designed for controlled heating of the product – sheet – 1, by local exposure to electrolyte plasma – 2, in through the gap – 3, the heated product is included in the electrical circuit – 5, by means of a controlled converter – 4, the other pole 6 from the converter is connected to the anode of the heater. The converter receives a control signal from the unit – 7, which is included in the electrical circuit with an analog converter – 8 of the control signal received through the conductor – 9. The heater is installed in the housing – 10, by means of a sliding rod – 11. The housing is fixed on the arm – 12 manipulators and is connected to the pipeline – 13, through which the electrolyte is introduced, which through the jets – 14 provides the lifting force and optimization of the gap – 3. The sensor for measuring the temperature – thermistor – 15 is installed in the case – 16 and through the holes 17 in the anode case – 18, is fixed in anode – 19 so as to provide an optimal distance in the hydrodynamic concentrator – 20. The sensor provides an actual reading of the surface temperature. These results are analyzed and a control signal is generated,

which is converted in the converter 4 into an overvoltage and/or undervoltage of an electric current. The system in **Fig. 4.3** provides temperature stabilization of heating, which makes it possible to carry out a long-term chemical heat treatment process without overheating the surface.

The temperature and heating time were controlled using a special device with a feedback on the product temperature through an infrared sensor. The sensor is built-in along the axis of the heater, perpendicular to the heated surface, which makes it possible to capture radiation from the heated surface. The electrical signal from the sensor, after amplification, is fed to the input of the analog-to-digital converter (ADC) ADA-1406. The signal is analyzed using analog software and by means of an ADC it gives the necessary signal to the control relay. The device has the ability to preset the signal corresponding to the characteristic heating temperatures T1 and T2. The analog device analyzes and compares the signal strength from the infrared sensor and the preset signal values.

The analysis shows that the temperature T1 has been reached and then the program turns off the increased voltage (250–320 V) at which accelerated heating of the surface occurs. The electrolytic-plasma process continues at a reduced voltage (120–220 V), which is characterized by cooling of the heated surface. Analysis of the next signal level shows that the surface temperature has dropped and reached T2 – the software issues an ADC command to connect an overvoltage (250–320 V).

Plasma-chemical synthesis is carried out in a plasma layer on the surface of the product. An increase in the electric field strength up to 300 kV/m leads to the formation of electric discharges, which heat the layer on the surface of the product and intensify the processes of oxide reduction and plasma chemical synthesis. The strength of the electric field ensures the transportation of the products of reduction and plasma-chemical synthesis to the surface of the product.

The kinematic scheme of the unit provides the CTT possibility on the outer and inner surfaces of the cylinders. The unit has three coordinates for the movement of the plasma device and one coordinate – the rotation of the product (sample). The unit is completed with an electric current converter and a control system, which includes a photoresistor sensor and an analog control system – Logic type.

The unit provides for two systems for supplying electrolyte. The electrolyte is used for switching electrical energy and for transporting the powdery material into the plasma layer. During operation, the heater is filled with electrolyte and closes the electrical circuit (between the surface of the sample (cathode) and the anode).

The optimal placement of the product relative to the heater is so that the hardened surface hangs over the heater from above. When hardening the inner surface of the cylinders, the heater is introduced into the product, **Fig. 4.4**. In this case, the product-cylinder – 1 is fixed horizontally, the cathode – 2 in the heater is parallel to the surface of the cylinder, and the heater is fixed by rollers – 3 on the lower surface of the cylinder. Spent electrolyte flows down the bottom of the cylinder surface – 4.

The process electric voltage is supplied to the heater from a rectifier, which consists of three separate devices with a rated operating voltage (V) of power sources: power 340, 320, 300, 280, 260; supporting 220, 200, 180, 160 and preparation 60, 40, 20. The rectifier control unit contains a time relay and is made on the basis of a programmable device with surface temperature

correction from non-contact sensors. The time relay, by means of thyristor switches, sets the operating time (switching on) of the rectifiers and the order of their switching on and off. The actual values of the process current are determined by the instruments on the panel of the control cabinet. To supply electrolyte, a tank with a pump with a capacity of up to 10 l/min is built into the unit. The electrolyte temperature in the system is stabilized by means of a heat exchanger located in the tank.

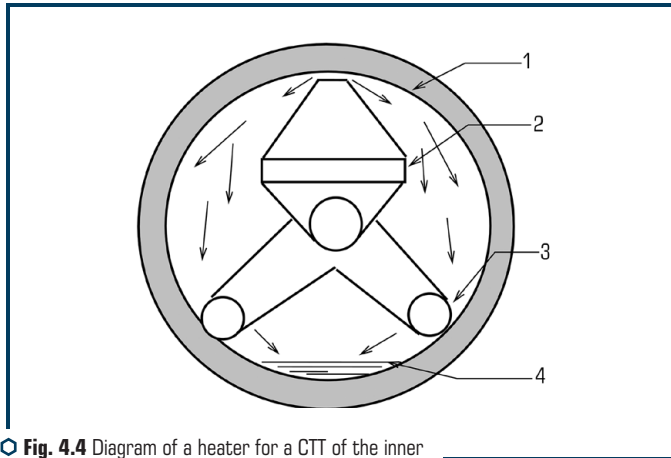


Fig. 4.4 Diagram of a heater for a CTT of the inner surface of a cylinder

Methods for controlling the rate of heating and cooling of local sections of the surface of the product in the range of 20–500 °C/s, at a power density of up to 10^4 W/cm², were used for CTT. The use of the principle of periodic decrease and increase of the electric voltage in the interelectrode layer made it possible to heat the surface layer to a depth of 10 mm and, accordingly, to harden this layer on the surface of the product [44, 90–92].

The movement of the heater relative to the inner surface of the cylinder allows the formation of a hardened layer, which can have various configurations. The outlet nozzle of the heater can be of any geometry that will suitably form the appearance of a hardened surface area. For example, an elliptical nozzle has formed staggered or helical portions of the corresponding shape with respect to the generatrix of the product. Continuous movement of the heater provides the formation of helical lines with different angles of rise on the surface to be hardened. A characteristic feature of the shape of the hardened sections is the large size of the sections or the width of the helical lines (from 15 to 50 mm), which causes the formation of a layer with compressive stresses.

The electrolyte heater is equipped with a temperature control system, which is connected to the control circuit by means of an optoelectronic digital converter-sensor. The mode of operation of the technology is set by changing the density of electric power in the plasma layer and the speed of movement. The sensor axis is perpendicular to the cell cross-sectional plane, and the electrolyte

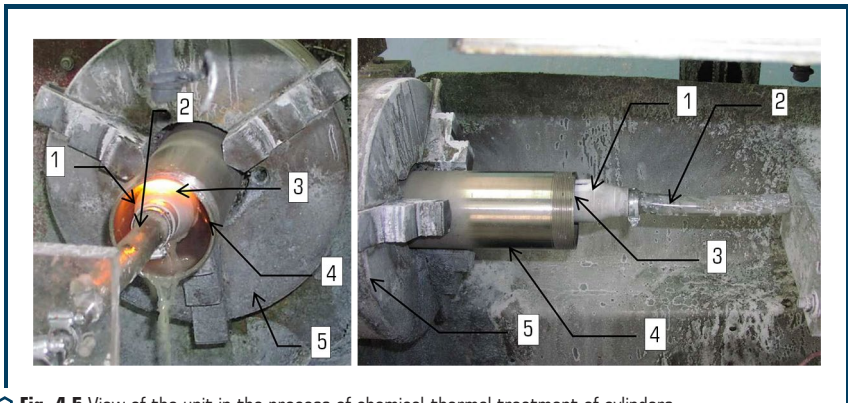
is supplied through the channels of the metal electrode so that the sensor is placed under an electrolyte layer 10–20 mm thick.

A sensor for non-contact measurement of the amount of radiation from the heated surface of the product can be made in the form of a photoresistor and is included in the arm of the bridge circuit so that with an increase in the amount of radiation, the magnitude of the measurement signal increases and decreases with decreasing to certain values, which serve as a signal for the electrical potential switching circuit. The use of sensors in the device for non-contact measurement of the amount of radiation from the surface of the product, ensures the automation of the technology and the implementation of the technology of thermal cycling of the surface in a given temperature range.

To analyze the signal from the sensor, an analog system for analyzing and controlling the voltage of the process current between the electrode gap is selected. This ensures high quality CTT and the formation of hardened structures with a low level of stress. The use of the above features causes the layer-by-layer formation of hardened layers, where hard structures alternate with soft ones, which serve for stress relaxation, as well as an increase in toughness at high hardness.

To test the method of chemical-thermal treatment, a specialized unit was made, equipped with a device for thermal cycling of products (**Fig. 4.2, 4.3**).

Fig. 4.5 shows the adjustment of the device for the CTT of the inner surfaces of the cylinders. Heating is carried out by electric current, which is switched between a special anode electrode and the surface of the product through an electrically conductive liquid – electrolyte. The heater for cylinders CTT has the shape of a ceramic conoid, the anode is built-in along the conoid axis – 1, and the electrolyte is fed through a metal tube – 2, which performs the functions of fixing and supplying electric current. Nozzle – 3 serves to form an electrolyte jet and is located in the upper part of the cylindrical part of the ceramic body. The processed samples – cylinders – 4 are fixed in a three-jaw self-centering chuck – 5.



○ **Fig. 4.5** View of the unit in the process of chemical-thermal treatment of cylinders

Specialized electrolyte-plasma heaters were designed and manufactured for CTT of external cylindrical and flat surfaces, **Fig. 4.6** with replaceable metal anodes – 1, dielectric bodies – 2, ceramic nozzles – 3.

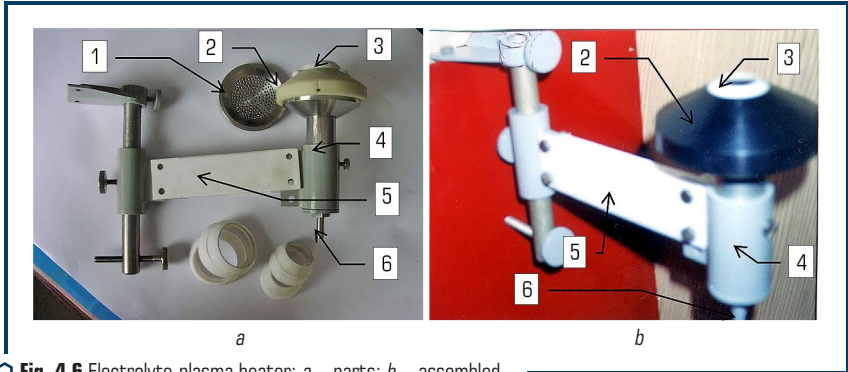


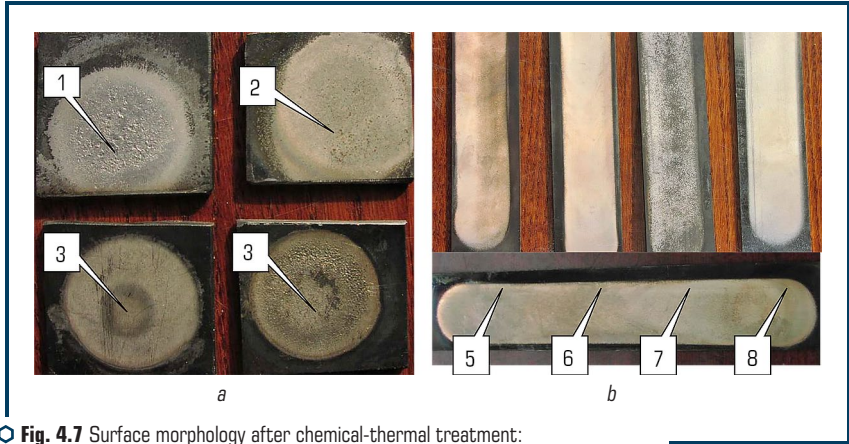
Fig. 4.6 Electrolyte-plasma heater: *a* – parts; *b* – assembled

The heaters were fixed on the support of the device by means of a bracket – 4 and insulating plates – 5. The electrolyte was supplied to the heater through a fitting – 6. The heater (**Fig. 4.6, b**) is installed under the part with a gap between the ceramic nozzle – 3 and the processed surface of 2–3 mm. The electrolyte is fed through the nozzle 6 and enters the hydrodynamic concentrator – 2 through the metal anode – 1 (**Fig. 4.6, a**).

4.3 CTT USING SOLUBLE NET ANODES

The study was carried out on samples that were annealed; the defect layer from the surface of the samples was removed by an abrasive method. The roughness of the samples corresponded to Rz-3.6 μm used flat samples made of steel 3. The elemental composition of the surface of the samples was determined using a SEM-515 scanning electron microscope (Philips, Holland) equipped with a Link microanalyzer. Micro X-ray spectral analysis of the distribution of elements was carried out on a Comebax SX 50 device (France) with a probe diameter of 1 μm .

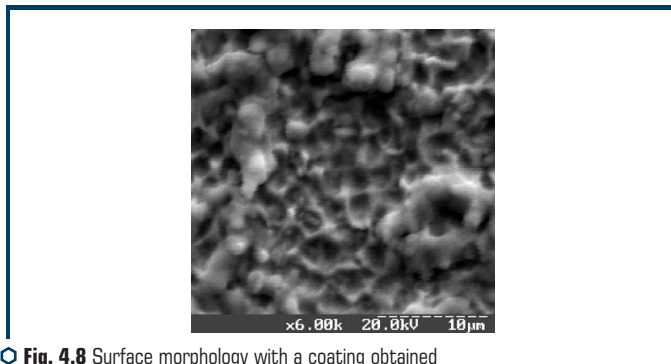
Work on CTT was carried out with a heater for flat surfaces (**Fig. 4.5**) on the unit (**Fig. 4.2**) with local sections (**Fig. 4.7, a**) having a diameter of 30 mm and stripes per passage (**Fig. 4.7, b**) having a width of 30 mm and a length 200 mm. The efficiency of the introduction of alloying elements during the dissolution of the grid – anode was tested. The mesh – the anode was made of sheet brass, which contained 90 % copper, zinc (up to 9 %). The resulting coating is characterized by a characteristic reddish color (**Fig. 4.7, a** – sample 2 and **Fig. 4.7, b** – samples 5, 6). The integral analysis of the coating on the sample surface was averaged over an area of $80 \times 80 \mu\text{m}$ from a layer about 2.5 μm thick.



○ **Fig. 4.7** Surface morphology after chemical-thermal treatment:
a – local areas – diameter 30 mm; *b* – in stripes – width 30 mm, length 200 mm

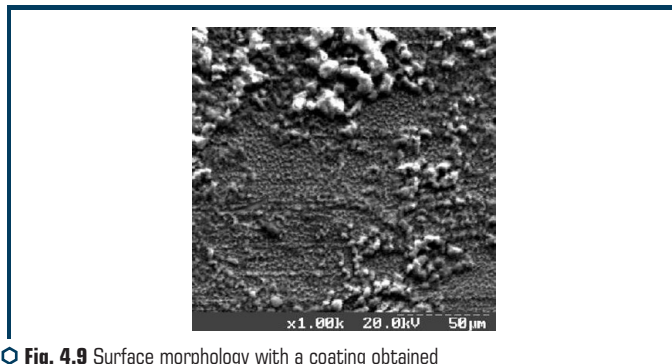
The surface temperature was varied in the range 800–1500 °C. **Fig. 4.7, a** shows the morphology of the local surface at 1500 °C. In **Fig. 4.7, a** (samples 1 and 4), it can be seen that the surface is melted and has a developed relief. The roughness of the surface when heated to 1000 °C practically did not change (**Fig. 4.7, a** (samples 2 and 3)). When processing the strip (per pass), the surface temperature varied from 800 to 1500 °C. At temperatures up to 1000 °C, the surface roughness has not changed, **Fig. 4.7, b** (samples 5, 6, 8, and 9). At high temperatures, traces of metal melting appear on the surface, **Fig. 4.7, b** (sample 7).

Fig. 4.8, 4.9 show the surface morphology. Overheating of the coating practically did not affect its chemical composition, but the relief is characterized by local areas of melting of the coating material.



○ **Fig. 4.8** Surface morphology with a coating obtained in a mode with heating up to 1000 °C

At a temperature of 800 °C, a less rough coating is obtained (**Fig. 4.9**), with small local areas of melting. The chemical composition of the coating is practically the same.



○ **Fig. 4.9** Surface morphology with a coating obtained in a mode with heating up to 800 °C

The analysis results show that the coating contains elements that make up the composition of the soluble anode material. The surface layer contains up to 15 % alloying elements.

The next stage of the work was to check the possibility of dissolving the anode, which is made of chromium-containing materials and the formation of a surface layer with an increased chromium content.

The mesh anode was made of stainless steel 12X18N9T, containing: 17–19 % chromium, 8–9 % nickel, 0.6–0.8 % titanium, no more than 0.8 % silicon (Si), no more than 2.0 % manganese (Mn), no more than 0.30 % copper (Cu), no more than 0.12 % carbon (C), no more than 0.03 % phosphorus (P) and sulfur (S). A layer of ferrochrome granules was laid on the mesh surface, which contained up to 70 % chromium, up to 9 % silicon, and the rest iron. The processing was carried out with heating of the sample surface in the temperature range of 500–1150 °C.

Analysis of the results of the experiment shows (**Table 4.1**) that the amount of alloying elements in the surface layers depends on the heating temperature and processing time.

At a surface temperature below 900 °C, the content of alloying elements in the surface layer is significantly reduced (**Table 4.1**).

● **Table 4.1** Content of Cr and Si after electrolytic-plasma heating of the surface in different modes

No.	Electrode material	Time	Temperature	Si content, %	Cr content, %
1	X18H9T + FeCr	100	950–1150	0.95	1.74–1.91
2		30	1150	0.7	1.31–1.44
3		180	500	0,5	0.13–0.33
4		180	800	0,6	0.8–0.93

The results of the study showed that it is possible to use soluble mesh anodes for the introduction of alloying elements into the electrolyte. To dissolve a sufficiently large volume of the anode material and enrich the electrolyte with the required amount of alloying elements, it is necessary to increase the CTT time.

4.4 CTT USING MICROPOWDERS IN ELECTROLYTE SOLUTION

CTT with the use of various micropowders in an electrolyte solution has also been shown to be effective. For example, copper oxide micropowders with a fineness of 3–6 μm were introduced into the electrolyte.

The results of the study, **Table 4.2**, showed that a layer is formed on the surface, which contains copper up to 9 %. Alloying elements are evenly distributed in the surface layer. The processing was carried out with heating the sample surface to a temperature of 950–1100 °C. The roughness of the surface has not changed (**Fig. 4.10**). **Fig. 4.11** shows the surface morphology and the point where the distribution of alloying elements was measured. Alloying elements silicon, manganese, titanium and aluminum were obtained from the electrolyte and by enriching it with the products of the grid dissolution.

● **Table 4.2** Content of chemical elements of a sample doped from an electrolyte containing copper oxide powder

No. of point	Object of research	Content of chemical elements, mass %					
		Fe	Si	Mn	Ti	Al	Cu
1	Frame analysis	89.53	0.48	0.68	0.11	0.56	8.63
2	Frame analysis	89.36	0.26	0.59	0.1	0.45	9.24
3	Frame analysis	89.46	0.6	0.43	0.21	0.3	9.0
4	Point analysis	89.86	0.29	0.52	0.28	0.38	8.68
5	Point analysis	89.36	0.22	0.29	–	0.75	9.38
6	Point analysis	96.89	–	0.68	0.47	–	1.96

The analysis of the research results shows that in the plasma layer there is a reaction of copper reduction from oxides and a chemical-thermal reaction of the deposition of copper ions on a heated steel substrate. To activate this reaction, it is advisable to use nanosized powders of oxide and carbon powders in the form of a reducing agent.

Dispersion of powders plays an important role in electrolytic-plasma chemical-thermal treatment. For example, titanium oxide powders (dispersion 1.3 μm), powders of aluminum oxide and carbon (dispersion up to 15 μm) were introduced into an electrolyte based on an aqueous solution of sodium carbonate Na_2CO_3 . The treatment was carried out in local areas with a diameter of 30 mm and on

a pass with heating the surface to a temperature of 900 °C. The analysis of the processing results showed (**Table 4.3**) that a layer is formed on the surface with up to 2 % titanium and aluminum. In some areas of the surface, local areas with a titanium content of up to 21 % are observed. In **Fig. 4.10** the numbers show the locations of the analysis. An increase in the surface heating temperature to 1100 °C increased the processing efficiency (**Table 4.4**). The titanium content also increased when analyzing over the area of the frames up to 3–4 %. The distribution of titanium over the area is more uniform (**Fig. 4.11**) than when heated to a temperature of 900 °C. There are local areas with a Ti content of 20–21 %. It can be noted that the aluminum content in the surface layer of the coating increased to 0.5–1.3 %. The high temperature treatment also increased the surface roughness.

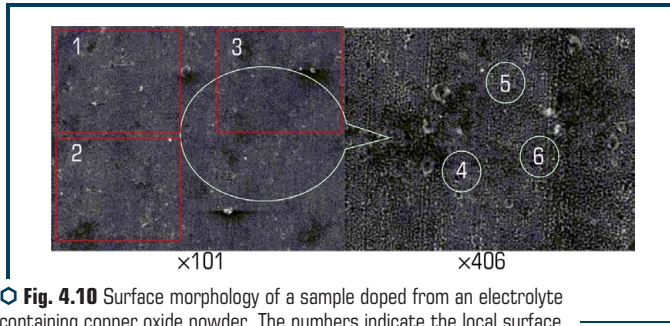


Fig. 4.10 Surface morphology of a sample doped from an electrolyte containing copper oxide powder. The numbers indicate the local surface where the elemental analysis was carried out

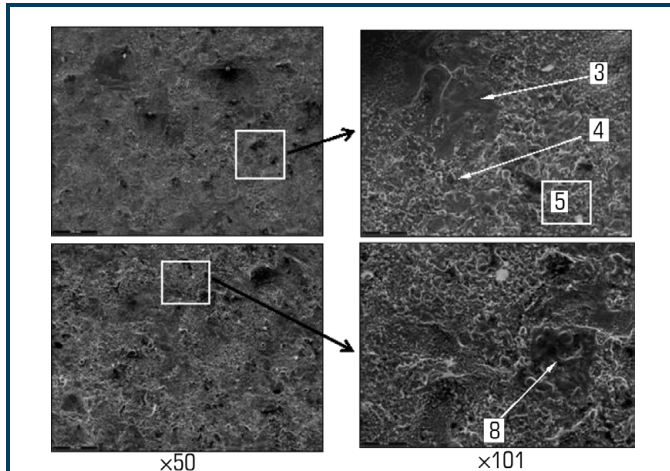


Fig. 4.11 Surface morphology of a sample doped from an electrolyte containing powders of titanium oxide, aluminum oxide and carbon (graphite). Surface temperature is 900 °C

The technology used micropowders of metal oxides with different dispersion. The titanium oxide powder had a lower dispersion and, therefore, the possibility of its heating and reduction with carbon was higher than that of aluminum oxides.

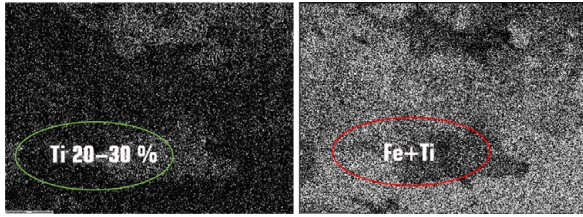
● **Table 4.3** Content of chemical elements on the sample surface (heating temperature is 900 °C) doped from an electrolyte containing powders of titanium oxide, aluminum oxide and carbon

No. of point	Object of research	Content of chemical elements, mass %				
		Fe	Si	Mn	Ti	Al
1	Frame analysis (×50)	97.37	0.47	0.66	0.42	1.08
2	Frame analysis (×50)	97.72	0.33	0.74	0.38	0.83
3	Point analysis (on dark)	98.43	0.33	0.42	–	0.82
4	Point analysis (on dark)	98.02	0.48	0.47	–	1.0
5	Fragment analysis (on light)	98.98	–	0.6	0.18	0.22
6	Frame analysis (×101)	97.05	0.8	0.47	0.8	0.9
7	Frame analysis (×101)	95.46	0.73	0.7	1.67	1.46
8	Point analysis (on dark)	76.36	0.36	0.6	21.73	0.97

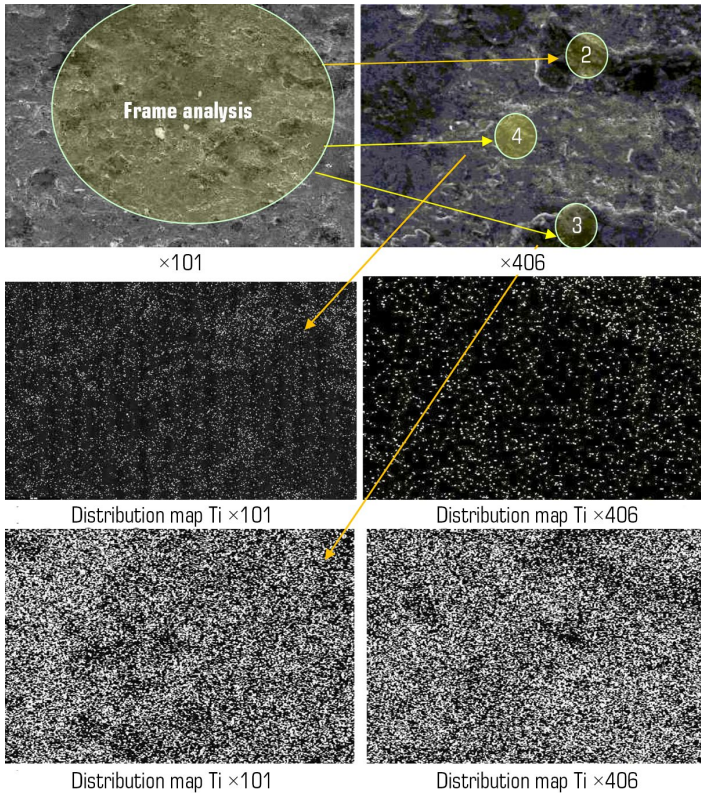
Analysis of the surface of the samples showed, **Table 4.4**, that the number of surface areas with titanium content is significantly higher, **Fig. 4.12, 4.13** than aluminum, the maximum aluminum content in the formed layer is 1.3 %.

● **Table 4.4** Content of chemical elements on the sample surface (heating temperature 1100 °C), doped from an electrolyte containing powders of titanium oxide, aluminum oxide and carbon

No. of point	Object of research	Content of chemical elements, mass %				
		Fe	Si	Mn	Ti	Al
1	Frame analysis	95.12	0.57	0.58	3.24	0.5
2	Point analysis	75.37	1.09	0.47	21.74	1.33
3	Point analysis	77.94	0.46	0.67	20.07	0.86
4	Point analysis	95.22	0.52	0.92	3.0	0.34
5	Frame analysis (×101)	96.5	0.55	0.68	1.86	0.41
6	Frame analysis (×101)	93.63	0.56	0.32	4.24	1.26
7	Frame analysis (×50)	93.72	1.24	0.5	3.22	1.33



○ Fig. 4.12 Titanium concentration in the surface layer of the sample



○ Fig. 4.13 Surface morphology of a sample doped from an electrolyte containing powders of titanium oxide, aluminum oxide and carbon (graphite). Surface temperature is 1100 °C

The results of this work have confirmed the possibility of reduction of metal oxides with carbon and the deposition of metals on the surface of a heated product. This technology can be combined with heating for hardening. To increase the efficiency of the technology, it is necessary to use nanopowders of metal and carbon oxides, which will accelerate the chemical reduction reactions.

4.5 CTT IN ELECTROLYTES BASED ON AQUEOUS NITROGEN FERTILIZER

The analysis of possible electrolytes, which do not cause difficulties in utilization and are active in the implementation of plasma-chemical synthesis, has also been carried out. It is known that metals such as titanium, aluminum and iron are active towards nitrogen. The additional introduction of carbon into the plasma makes it possible for the plasma-chemical synthesis and deposition of the carbon nitrides of the above metals.

Nitrogen-containing electrolytes include aqueous solutions of nitrogen fertilizers, primarily ammonium sulfate and nitrate and carbamide (urea). Ammonium salts, the anions of which exhibit more pronounced oxidizing properties, decompose irreversibly: a redox reaction proceeds, during which the ammonium ion is oxidized and the anion is reduced.

Ammonium nitrate (NH_4NO_3) is a highly effective mineral fertilizer, containing at least 34.4 % nitrogen. Molecular weight – 80.0. Important, in practical terms, compound – urea (NH_2)₂CO is obtained by the interaction of carbon dioxide with ammonia under pressure: $\text{CO}_2 + 2\text{NH}_3 = (\text{NH}_2)_2\text{CO} + \text{H}_2\text{O}$. Urea is a white crystal, readily soluble in water. It is used in agriculture as a highly concentrated nitrogen fertilizer and as an additive to feed for ruminants. Urea is obtained from cheap plastics, and also serves as a starting material for the production of many organic substances and pharmaceuticals.

Experiments on the deposition of a hard coating were carried out on the basis of nitrogen-containing electrolytes and powders of titanium oxide and graphite. A hard coating with a thickness of up to 30 microns was obtained, which was submitted for research.

Considering that titanium-based alloys are the main material for the manufacture of cylinders, a series of experiments was carried out to form a coating using a nitrogen-containing electrolyte without powders. The experiments were carried out on VT1-0 titanium samples (Ti – 98.61–99.7 %; Fe – up to 0.18 %; C – up to 0.07 %; Si – up to 0.1 %; N – up to 0.04 %; O – up to 0.12 %; H – up to 0.01 %).

It is known that anodic heating of the VT1-0 alloy in a solution containing 5 % ammonia and 10 % ammonium chloride ensures the formation of diffusion coatings on the surface [93–99]. In this electrolyte, heating is unstable due to the formation of insoluble compounds on the sample surface.

An X-ray study of nitrated surface layers (DRON-2, cobalt radiation) revealed titanium nitride TiN with a certain amount of TiO_2 oxides, which was formed during the first two minutes of treatment, but it was not detected with a longer saturation. Also, no continuous layer of titanium nitrides was found.

The oxide coating formed during the anodic nitriding process has increased the corrosion resistance of commercial titanium. The test for resistance to continuous corrosion and stress corrosion

cracking of the samples was carried out in an aqueous solution containing 6 % hydrochloric acid and 20 % protein-vitamin concentrate (PVC). The fluoroplastic beakers with the solution and samples were placed in steel sealed autoclaves at 133 ± 2 °C and a pressure of 0.3 MPa and held for 400 h (continuous tests). Cyclic tests were carried out during the same time in the following modes: pouring 6 % hydrochloric acid solution, loading 20 % PVC, sealing and heating to 133 °C, holding for 2 h followed by cooling to room temperature, etc. The corrosion rate of untreated commercial titanium in this environment is 0.138 mm/year under continuous testing. Anodic nitriding in an electrolyte with concomitant oxidation leads to a decrease in corrosion rates by two orders of magnitude during continuous testing.

Saturation of titanium specimens with nitrogen according to the above modes led to an increase in their strength indicators after corrosion tests with a slight decrease in plasticity. Tensile tests were carried out on cylindrical specimens with a working part diameter of 3 mm and a height of 30 mm.

Low-alloy titanium alloys (VT1-0, OT-4, PT-3V, PT-7M) were subjected to corrosion tests. Samples $50 \times 20 \times (1.5-3)$ mm in size were nitrided in an aqueous solution containing 7.5 % ammonia and 10 % ammonium chloride for 5 min at a voltage of 220 V (the heating temperature was not measured). Resistance to continuous corrosion was determined by the method in two aqueous media, the duration of exposure of the samples in each medium was 1176 h and at a test temperature of 25 °C or 700 at 50 °C.

It follows from the results obtained that anodic nitriding with oxidation reduces the corrosion rate of titanium alloys by two orders of magnitude. Anodic nitriding of titanium alloys according to the indicated modes leads to some increase in microhardness in the surface layer up to 1 mm thick. The increased microhardness indicates the presence of a diffusion surface layer. An increase in microhardness is also facilitated by accelerated cooling in solution for both alloys.

The results obtained suggest the possibility of using short-term anodic nitriding combined with oxidation to increase the corrosion resistance and wear resistance of titanium alloys.

Taking into account the above experience, the titanium samples were processed in the cathodic mode at a heating temperature of 900 °C. Electrolyte composition: 2.5 % – ammonium chloride; 10 % – carbamide (urea) and 2.5 % – glycerin. Samples of titanium with a hard coating having a thickness of up to 60 microns have been obtained.

Chemical thermal treatment of titanium-based alloys is problematic due to gas impurities. The main impurities of titanium are hydrogen, oxygen, nitrogen and carbon. These elements form interstitial solid solutions with titanium and a number of compounds with different types of chemical bonds [99, 100].

It is seen from the titanium – oxygen phase diagram [100] that oxygen increases the temperature of the $\alpha \rightarrow \beta$ transformation and expands the temperature range of the α phase; is an α -stabilizer. With prolonged heating, titanium is oxidized and scale forms on its surface. The color of the scale layer on titanium obtained up to 820 °C is yellow, from 820 to 950 °C – from orange to brown. The scale contains rutile [100, 101]. The formation of a solid solution of oxygen in titanium distorts the crystal lattice and significantly changes the mechanical properties of titanium. An increase in the oxygen content leads to a sharp increase in the strength, hardness and decrease in the ductility of titanium.

Nitrogen, like oxygen, is an element that stabilizes the α -phase – it expands the region of this phase. During the high-temperature reaction of titanium with nitrogen, titanium nitrides are formed, which readily dissolve in the metal. The content in titanium even in small amounts of nitrogen, like oxygen, promotes the formation of the acicular α' -phase and, to an even greater extent than oxygen, reduces the ductility and increases the strength and hardness of titanium.

The solubility of hydrogen in β -Ti reaches 2 % and exceeds the solubility of hydrogen in iron by a factor of thousands. As the temperature rises, the ability of titanium to form hydrides decreases, while the solubility of hydrogen decreases. Hydrogen diffuses in β -Ti much more slowly than in α -Ti. A noticeable absorption of hydrogen by titanium starts from a temperature of 300 °C.

When titanium, which has absorbed hydrogen in quantities greater than 0.002–0.003 %, is cooled, not all of the hydrogen is retained in solid solution at room temperature. Some of the hydrogen in titanium forms a hydride. Upon slow cooling, hydrides precipitate in the form of thin plates, and upon hardening, in the form of dispersed particles [100, 101]. An increase in the hydrogen content to 0.01 % has no noticeable effect on the hardness, strength, and ductility of titanium [102, 103]. The ductility of titanium decreases with a further increase in the hydrogen concentration.

Carbon dissolves in titanium in insignificant amounts. The maximum solubility of carbon in α -Ti is 0.28 % at a temperature close to the point of $\alpha \rightarrow \beta$ transformation. With decreasing temperature, the solubility of carbon in α -Ti sharply decreases. About 0.06% carbon dissolves in β -Ti, i.e. almost 5 times less than in α -Ti. A decrease in the ductility and an increase in the strength and hardness of the metal take place at a content of more than 0.1–0.2 % C [102–104].

The grain size significantly affects the hydrogen brittleness of titanium and its alloys. For fine-grained titanium (after annealing at 700 °C for 6 h), the impact toughness remains practically unchanged in the case of a hydrogen content of 0.01 % [100, 103, 104]. For the same titanium with coarse grains (after annealing at 1100 °C, 10 h) at a hydrogen content of 0.01 %, the impact strength sharply decreases from 70 to 20 J/cm².

Titan CTT (VTO-1). The study of chemical thermal treatment (CTT) treatment was carried out on flat and cylindrical specimens made of VTO-1 titanium.

Several types of heaters for flat and internal cylindrical surfaces have been developed and manufactured for processing samples.

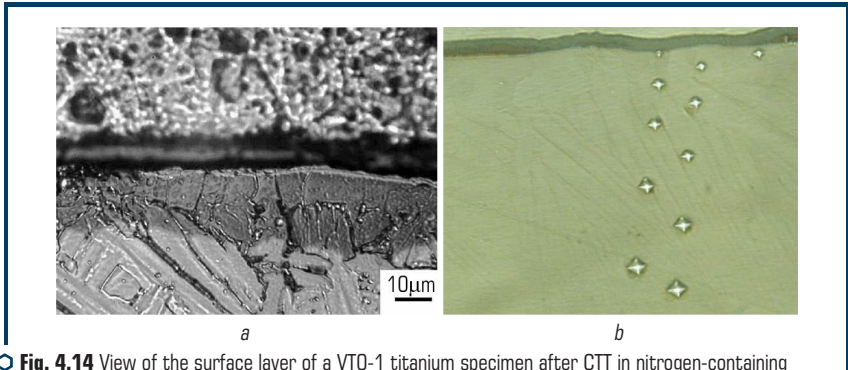
Chemical-thermal treatment of the samples was carried out in the cathodic mode at a surface heating temperature of 850–900 °C. Pulse processing mode: pulse-voltage – 260 V, current – 20–25 A; pause-voltage – 180 V, current – 10–18 A. Pulse and pause time – 1 sec. The total processing time – 1 minute.

An electrolyte of the following composition was used: 15 l – distilled water, 2 kg – carbamide, 250 ml – ammonium chloride, 1 l – glycerin, 600 ml – soda ash, 2600 ml – ammonium nitrate.

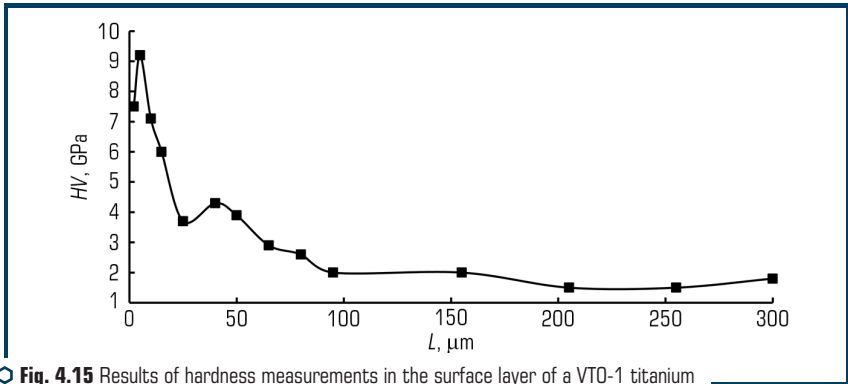
The study of the samples was carried out on transverse thin sections, which were etched in a solution: 1 part of hydrofluoric acid + 2 parts of nitric acid + 1 part of glycerol. The sample section was immersed in the etching solution 4 times for 4 seconds. Photographs of thin sections

were taken on a Neophot-32 optical microscope. The hardness was measured on a Leco M-400 microhardness tester, the load was 10 grams.

Studies have shown that a multilayer coating is obtained on the surface of a VT0-1 titanium specimen (**Fig. 4.14**). The first layer – nitride ceramics, has a thickness of 10–15 μm and a hardness of up to 8–9 GPa (**Fig. 4.14, b**). The second layer has a thickness of up to 100 microns with a hardness of 9 to 2 GPa (**Fig. 4.15**).



○ **Fig. 4.14** View of the surface layer of a VT0-1 titanium specimen after CTT in nitrogen-containing plasma: *a* – etched in a solution of hydrofluoric acid, 20 sec; *b* – without etching



○ **Fig. 4.15** Results of hardness measurements in the surface layer of a VT0-1 titanium specimen after HTT in nitrogen-containing plasma

It can be noted that the hardness in the second layer gradually decreases from the maximum to the hardness of the base metal (**Fig. 4.15**). A ceramic layer 10–15 μm thick has a hardness of 7.5–9 GPa.

The maximum hardness is obtained at the interface between the ceramic and the modified layer >9 GPa. The hardness of the modified layer gradually decreases to the hardness of the base to a depth of 150 microns.

An increase in the immersion time of the sample section in the etching solution up to 6 times 4 seconds each showed that the modified layer is inhomogeneous and at a depth of 25 microns there is a layer that is practically not etched (**Fig. 4.16**).

Below and above this border, the modified layer is etched along the borders. The thickness of the non-etched layer is up to 10 microns. The ceramic layer on the sample surface is partially dissolved (**Fig. 4.16**).

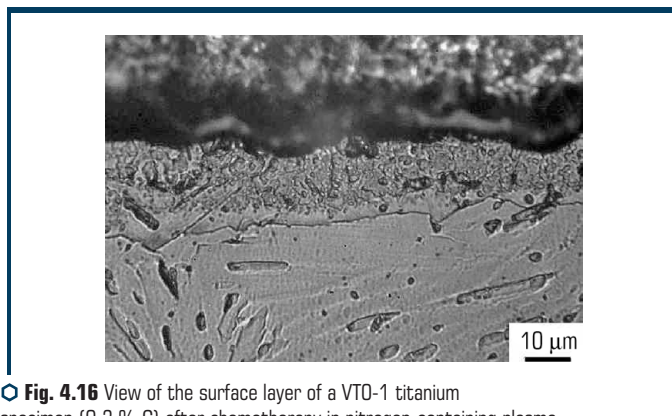


Fig. 4.16 View of the surface layer of a VTO-1 titanium specimen (0.3 % C) after chemotherapy in nitrogen-containing plasma. Etched in hydrofluoric acid solution – 1 min

Steel surface CTT. Chemical-thermal treatment of steel was studied on samples of steel-3 (0.3 % C). The samples were processed in the cathodic mode at a surface heating temperature of 900–1000 °C. The electrolyte used was water-soluble nitrogen-containing salts: ammonium chloride, carbamide, and glycerin. Processing mode: pulse-voltage – 300 V, current – 30–35 A; pause-voltage – 220 V, current – 15–20 A. Pulse time – 1 sec and pause time – 2 sec. The total processing time – 2 minutes.

A transverse microsection was made from the samples, which was etched in an alcohol solution: 4 % – concentrated nitric acid + 96 % – ethyl alcohol. The total etching time is 18–20 seconds with re-polishing. Studies have shown that a modified layer up to 40 microns thick is obtained on the surface. This layer has a microcrystalline structure and increased hardness (**Fig. 4.17**).

A layer modified with nitrogen (**Fig. 4.17**) was obtained on the surface of steel-3 in 2 minutes of heating in a nitrogen-containing plasma.

The high productivity of modification is explained by the fact that the technology is intensified by electric discharges that are generated between the surfaces of the electrolyte and the sample.

The maximum hardness of the modified layer from the surface of the samples is 3.8 GPa at a depth of 10 μm (**Fig. 4.18**).

Further, the hardness gradually decreases to the hardness of the base at a depth of 35 microns.

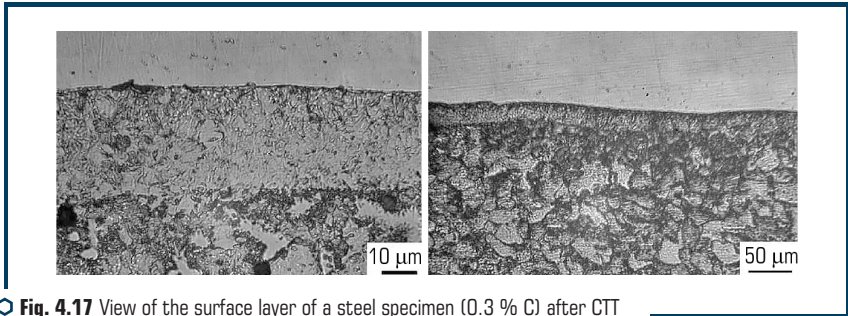


Fig. 4.17 View of the surface layer of a steel specimen (0.3 % C) after CTT in nitrogen-containing plasma

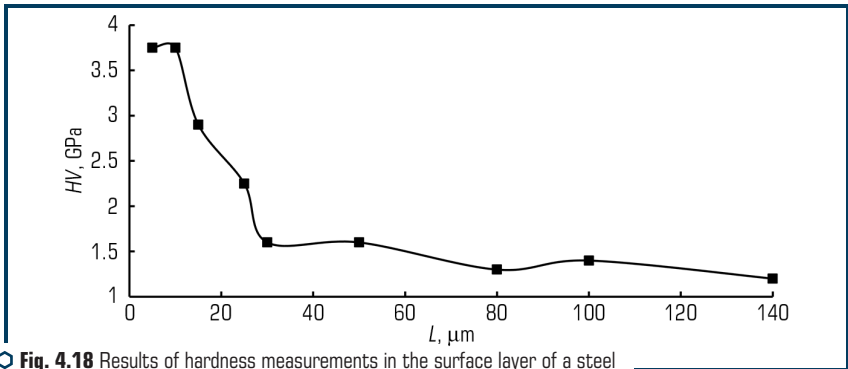


Fig. 4.18 Results of hardness measurements in the surface layer of a steel specimen (0.3 % C) after CTT in nitrogen-containing plasma

CONCLUSIONS

Electrolytic-plasma treatment with local heaters using a suspension (electrolyte + micropowders) makes it possible to combine the processes of coating deposition, CTT and thermal cyclic hardening.

Chemical-heat treatment of the surface due to alloying with elements of erosion of the mesh-anode is ineffective and can only serve as an addition to alloying with elements, products of destruction of micropowders introduced into the electrolyte.

CTT in a suspension of a mixture of micropowders of metal and carbon oxides is sufficiently effective for surface alloying with metals and deposition of a metal coating. The main disadvantage of this technology is the difficulty in controlling the surface heating temperature and maintaining a plasma layer that is stable in thickness.

Nitrogen-containing electrolytes (based on fertilizers) are effective for chemical treatment and the formation of hard coatings on articles made of titanium and steel-based alloys.

5 ELECTROLYTIC PLASMA OXIDATION (EPO)

ABSTRACT

The chapter touches upon some aspects of one of the broad areas of electrolyte-plasma processes – micro-arc oxidation. The schemes of devices, technological modes and results of studies of the obtained coatings on various materials are described. Examples of using the MAO technology are given.

KEYWORDS

Micro-arcs, anode mode, direct/alternating current, aluminum alloys, electrolyte composition.

5.1 EQUIPMENT AND TECHNOLOGY

5.1.1 TECHNOLOGY FEATURES

A feature of electrolyte-plasma oxidation, as it is also called micro-arc oxidation (MAO), is that during processing, energy is transferred to the surface of the product through the plasma layer in the form of a specific form of non-equilibrium electric micro-discharges. The discharges are diffusively bound to the electrolyte surface of the «liquid electrode». Under the influence of changing pressure at the point of discharge binding, the surface of the electrolyte acquires an oscillatory motion. As a result, the size of the gap between the surfaces of the liquid electrode and the solid body changes periodically. The electric field strength in the electrolyte itself is low (up to 80–200 V/m), but in the layer adjacent to the surface of the product (boundary) the strength has a variable value and can reach 10,000–1,000,000 V/m. The tension depends primarily on the voltage and the distance between the boundaries of the media.

In the process of electrolysis, oxygen is released on the anode product, which is activated by electrical discharges and oxidizes the metal of the product. As the oxide layer grows, in order to maintain the electric oxidation mode, it is necessary to increase the electric field strength until stabilization of micro-arc discharges occurs. The oxidation process has a damping character and for its renewal it is necessary to increase the electric field strength to a value that ensures the breakdown of the oxide layer and the formation of arc discharges. The lifetime of the discharges varies within 0.1–1 ms. The onset of breakdown of the oxide layer is massive, which is accompanied by a sharp surge of electric current, up to 10 A/cm². The extinction of the discharges proceeds gradually over time and with an increase in the thickness and dielectric strength of the oxide coating.

The thickness of the resulting oxide coatings on the surface depends on the electric field strength and can be in the range of 5–1000 microns.

Oxidation of local areas of the surface is carried out by a special electrolyte cell. The cell has a housing made of a dielectric material and a metal electrode with characteristic dimensions. Openings are made in the electrode through which electrolyte is supplied under pressure to the surface of the product.

The developed devices make it possible to carry out oxidation at interelectrode gaps of 20–30 mm, which reduces the loss of electrical energy. The technology provides for the formation of an oxide layer up to 250 μm at an electric current voltage of ≈ 500 V. The optimum electrolyte temperature for the implementation of the technology is 50–60 $^{\circ}\text{C}$, which is ensured through the use of electrical energy losses in the interelectrode gap of the electrolyte cell.

The coating consists mainly of a refractory alumina phase ($\alpha\text{-Al}_2\text{O}_3$). The introduction of fine powders, for example, chromium oxide, into the electrolyte ensures the movement of the powder particles to the coating and their fusion into the aluminum oxide layer.

It is known that the addition of metal salts or dispersed mineral powders to the electrolyte makes it possible to alloy the coating. A large reserve in the technology of changing the chemical and phase composition of the coating has a circuit and mode of connecting the surface to an electrical converter. Anode mode is used classically. The process can be intensified by briefly switching to the cathodic mode or by impulsely increasing the voltage in the anodic mode. In the process of oxidation, the formation of mixed oxides of aluminum and metals occurs, which are included in the complex anion of the electrolyte. The introduction of metal anions into the electrolyte can be carried out by dissolving the electrode-cathode of the corresponding alloy. In the steady-state mode of oxidation, the current density is 0.1–0.5 A/cm^2 . The main parameters allowing to control the process of micro-arc oxidation and coating properties are electrolyte concentration, voltage and current density, temperature, duration of the process, alloy composition and its heat treatment.

5.1.2 DESIGN OF THE MAO UNIT

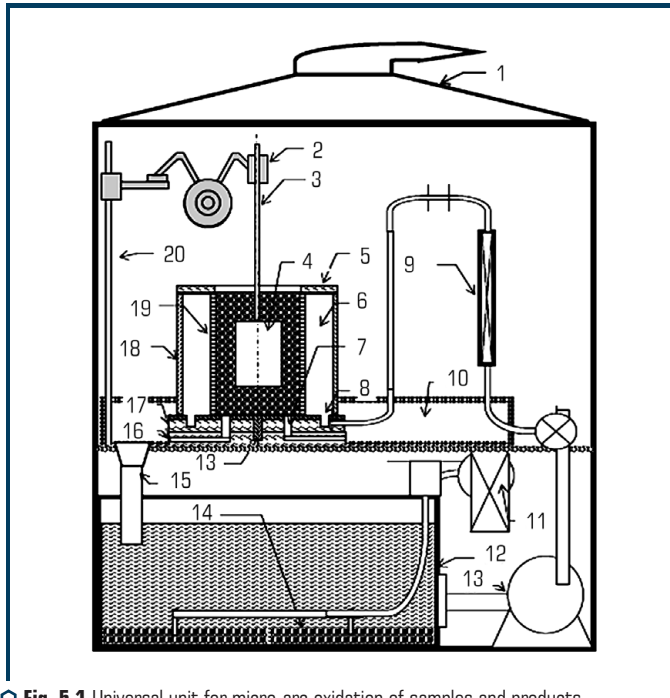
The configuration of the product and the need to ensure high productivity of processing of various products impose special requirements on the design of units for micro-arc oxidation (MAO).

Currently, devices have become widespread, where the technology is carried out by immersing a product in a specialized vessel – a reaction chamber. This is a versatile device that provides processing of the entire surface of the product.

A universal unit for micro-arc oxidation of samples and products is proposed (**Fig. 5.1**). On this unit it is possible to simulate the production processes of oxidation of various types of products and the processing of products during serial production.

The reaction chamber for MAO is fixed in a special room or cabinet equipped with ventilation systems. The metal electrode in the reaction chamber has a supply of electric current and electrolyte.

The ends of the supply current from the rectifier (\pm) are connected to the electrode and the product by means of current collectors.



○ Fig. 5.1 Universal unit for micro-arc oxidation of samples and products

When the electric potential is turned on, a vapor-plasma layer is formed on the surface of the product immersed in the electrolyte. Electric discharges pass through this layer, which are diffusion-bound on the electrolyte surface. The number of cycles of high and low electric field strength, as well as the total processing time, is changed by means of a time relay.

The electrolyte, filling the reaction chamber, closes the electrical circuit between the electrode and the treated surface of the sample. The process of oxidation of the sample surface is in progress. After the end of the technology, the source of electric current is turned off and the surface is cooled with electrolyte.

The drain of the electrolyte from a specialized vessel – the electrode is carried out into the technological bath made of non-conductive material and then into the tank through the nozzle.

Unit for micro-arc oxidation of samples and single items contains: a fume hood – 1; electrode holder – 2; electrode for fixing the sample – 3; sample or workpiece – 4; the lid of the reaction chamber – 5; cavity in the chamber for electrolyte distribution – 6; channels for electrolyte drain – 7;

channels for electrolyte supply – 8; electrolyte supply control system – 9; technological bath – 10; compressor for air supply – 11; electrolyte tank – 12; pump – 13; electrolyte aeration system – 14; pipeline for drainage of electrolyte from the technological bath – 15; device for regulating the drain of electrolyte from the chamber – 16; base for a specialized camera – electrode – 17; the outer wall of the reaction chamber – 18; electrode in the reaction chamber – 19; manipulator – sample holder – 20.

Preparation for operation of the unit is carried out in the following order: the fixing of the sample – product – 4 is regulated, the axis of which should be vertical, the gap between the surface of electrode – 19 in the reaction chamber and the surface of the product is regulated. Adjustment is carried out by moving in the electrode holder – 2.

The gap between the electrode surface and the product is set at least 20 mm. The deviation of the heater axis from the vertical is allowed no more than ± 3 deg. It is necessary to control: the presence of a ground connection to the fume cupboard; the presence and operation of the locking closure by the hood of the fume cupboard.

Fig. 5.2 shows the MAO units for processing large-sized parts and samples.

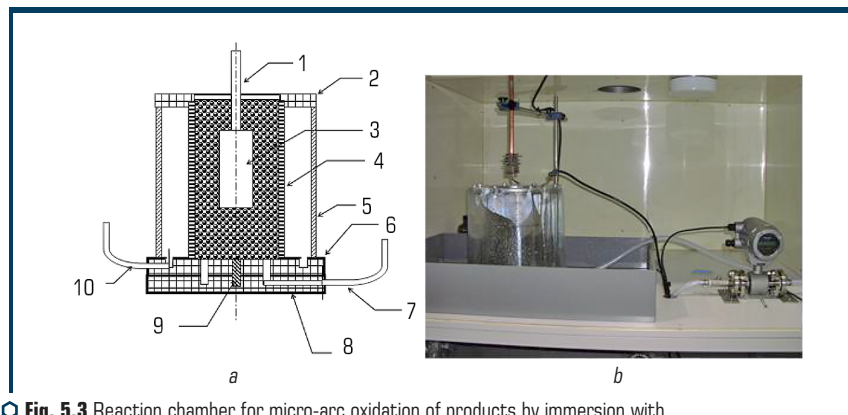


Fig. 5.2 Type of universal units for MAO samples and products: *a* – unit for large-sized parts; *b* – laboratory (bench-top) unit for MAO surface of samples and small parts

5.2 CONSTRUCTIONS OF REACTION CHAMBERS FOR MAO OF SURFACE OF PRODUCTS

A specialized vessel-electrode (reaction chamber) is designed for oxidizing the surface of products with a complex shape (**Fig. 5.3**).

The reaction chamber contains a cylindrical electrode – 4, which is made of stainless steel and has a large number of evenly spaced holes. These holes connect the cavity bounded by the wall – 5. The electrolyte is supplied through the nozzle – 10 from the tank by a pump. The drain of electrolyte from chamber – 4 is controlled by changing the cross-section of the holes in the disc – 8, which is carried out by turning this disc around the stud – 9.



◆ **Fig. 5.3** Reaction chamber for micro-arc oxidation of products by immersion with an electrolyte flow sensor: *a* – diagram; *b* – general view

Part 3 is located along the axis of the reaction chamber electrode. By turning the disc, the cross-section of the drain holes is limited, then the electric potential is connected and the electrolyte supply is turned on. The electrolyte level in the chamber rises smoothly, as a result of which the oxidized area smoothly increases. A smooth increase in the oxidized area allows to control the amount of consumed electric current and, accordingly, reduce the power of the electric power source.

The technical data of the reaction chamber are given in **Table 5.1**.

The electrolyte-plasma reaction chamber switches the electric current between the metal electrode-cathode and the surface of the product – the anode, the formation and maintenance of the vapor-plasma layer on the surface of the product.

The process of electrolytic-plasma micro-arc oxidation of heating begins with filling the internal volume of the reaction chamber and smoothly closing the electrical circuit between the electrode and the treated surface of the product.

The process includes surface preparation by wetting and forming a vapor-gas layer, forming a plasma layer, by simultaneously switching on the power voltage and supporting voltage, and heating.

◆ **Table 5.1** Technical data of the reaction chamber

No.	Parameter name	Unit of measurement	Value
1	Reaction chamber diameter and length	m	0.2-0.3
2	Electrolyte level increase rate	mm/s	0–10
3	Electrolyte consumption through the reaction chamber	l/min	1–10
4	Rated working current	A	0.01–50
5	Noise level	Db	before 60
6	Effective size of the oxidized surface	mm×mm×mm	100-100-100

After the end of heating, the electric current converter is turned off. The surface is cooled with electrolyte supplied through the heater. This does not disconnect the preparation voltage.

The electrolyte is drained into the tank through openings in the bottom and the upper open part of the reaction chamber.

Another version of the device for oxidation is shown in **Fig. 5.4**. The device contains: a housing 7, a reaction chamber 3 is fixed inside the housing, having a system of through channels for the formation of submerged jets. The electrolyte is fed through the fitting 4 and the holes 6 into the cavity 2 and then supplied to the surface of the article 8 and then the electrolyte is removed through the holes 5 and the open part of the reaction chamber 1.

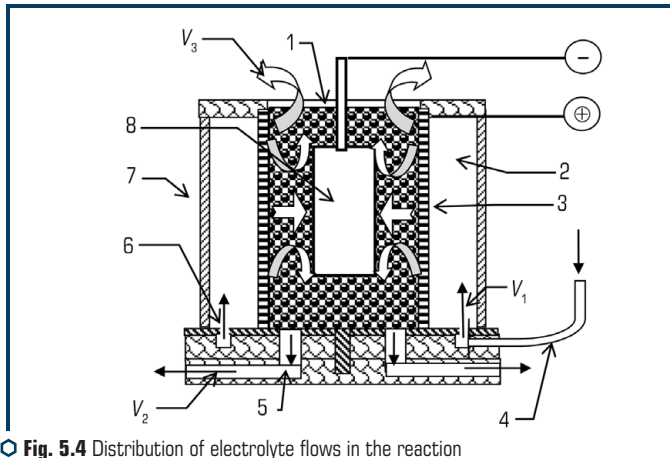


Fig. 5.4 Distribution of electrolyte flows in the reaction chamber of a typical micro-arc oxidation plant

In oxidation devices, the total electrolyte consumption is $V_1 = V_2 + V_3$. The electrolyte consumption should ensure a smooth increase in the electrolyte level in the reaction chamber, provided that it is heated no higher than 60 °C.

Oxidation is carried out in the area of micro-arc discharges, which are formed on the surface of the product. The onset of breakdown of the oxide layer is massive, which is accompanied by a sharp surge of electric current, up to 10 A/cm². The decrease in the intensity of electrical discharges proceeds gradually with an increase in the thickness and dielectric strength of the coating. Adding rare-earth salts or dispersed mineral powders to the electrolyte makes it possible to alloy the coating.

For micro-arc oxidation of the bottom and walls of the combustion chamber of the engine piston, special devices have been developed (**Fig. 5.5**). In this unit, the electrolyte cell includes, in the form of an integral structural element, a wall – 1 and a bottom – 2 of a piston combustion chamber. Cell body – 3 is made of non-conductive material and is fixed to the bottom of the piston by means of a rubber cuff – 4.

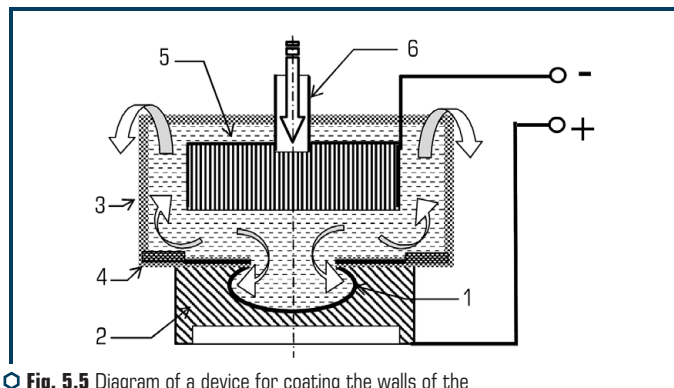


Fig. 5.5 Diagram of a device for coating the walls of the combustion chamber of a piston of an internal combustion engine

The device has an individual system of forced supply of electrolyte from a hydraulic electrolyte supply system. The electrolyte is supplied through a pipeline – 6 from the top of the cell through a metal, porous electrode – 5.

In the electrode – 5 channels are made in which the recombination of positive ions and the formation of negative ones take place. In the process of implementing the technology, the electrolyte closes the electrical circuit between the surface of the product and the surfaces of the channels in the electrode. The amount of negative ions that moves from the cathode to the walls of the combustion chamber – the anode, depends on the strength of the electric field and on the speed (volume) of the flowing electrolyte. In **Fig. 5.5**, the flow of electrolyte from the cathode to the surface of the product is shown by arrows.

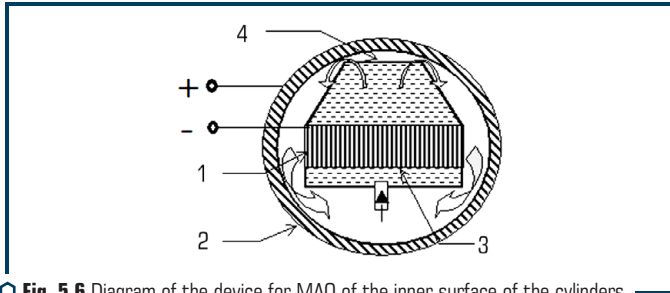
The proposed technological scheme provides for the introduction of dispersed non-metallic particles into the electrolyte, movement and fixation on the surface of the product, in the layer of aluminum oxide. It is possible to use powders of diamond, metal oxides, carbides, nitrides, spinels and other materials.

Electrolyte anions are deposited on the surface of dispersed particles, which gives them a negative charge and ensures movement to the surface of the product under the action of electrophoretic forces. With an increase in the concentration of anions and a decrease in the electrolyte temperature, the effect of introducing dispersed particles into the coating, together with anions, increases.

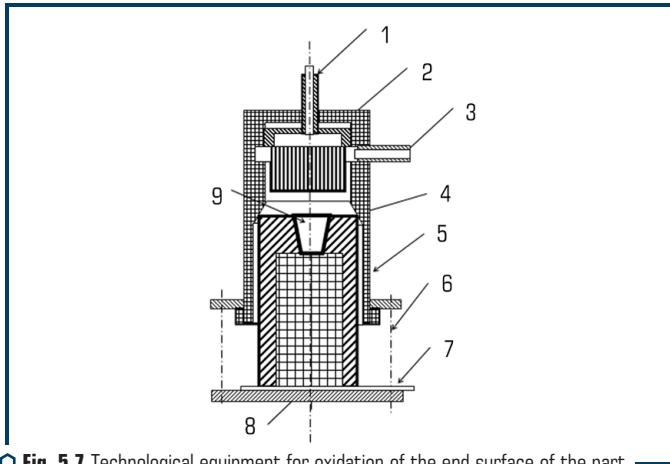
To form a coating of oxides on the inner surface of the cylinder, a device is used (**Fig. 5.6**), where the electrolyte cell 1 is introduced into the cylinder 2. The cell contains a porous electrode 3 through which the electrolyte is passed. The electrolyte closes the electrical circuit between the electrode and the surface of the cylinder in the gap 4, then, after use, flows down the bottom surface of the cylinder and is removed outside the hardened product.

The electrolyte in the hydraulic system is aerated with air, cooled, the amount of dispersed particles is renewed, and then fed back into the electrolyte cell. Technological equipment for

oxidizing the end part of the part surface is shown in **Fig. 5.7**: fitting for supplying electrolyte to the electrode assembly – 1; electrode assembly – 2; electrolyte drain fitting – 3; sealing cone – 4; body made of non-conductive material – 5; studs – 6; copper plate – 7; base made of non-conductive material – 8; hole in the surface of the part – 9. For MAO of the surface of the part – 9, an interelectrode gap is formed between the surface and the metal electrode – cathode – 2.



○ **Fig. 5.6** Diagram of the device for MAO of the inner surface of the cylinders



○ **Fig. 5.7** Technological equipment for oxidation of the end surface of the part

A reaction chamber – 4 is formed, which is bounded by the walls of the case – 5 and is sealed by pressing the end of the part against the cone – 4, cases – 5. Compression is carried out with studs – 6. Electric current is supplied to the part through a copper plate – 7. Waste electrolyte, steam and electrolysis products are removed through the nozzle – 3. This equipment provides the possibility of MAO of the surfaces of the part and holes at its end.

Due to their simplicity, MAO processes successfully compete in terms of cost with vacuum deposition of coatings and electrochemical methods. Preliminary surface preparation

consists only in cleaning and degreasing. No additional measures like annealing or surface activation are required.

For coating, the samples are usually immersed in a reservoir to a depth of 30–50 mm directly below the surface of the electrolyte, which is cooled and activated by stirring. A metal rod in a fluoroplastic sheath is usually used as a sample holder. The working pressure of the electrolyte in the hydraulic system is selected in accordance with the selected MAO mode and is adjusted to ensure the required flow rate. The device, as a rule, has the function of recording the main parameters of MAO – the average value of the current, the amplitude of the cathode and anode voltages, and the temperature of the electrolyte. It should be noted that there are a number of features in the choice of parameters of the MAO process, which are characteristic either for the formation of a dense layer of oxides, or a porous layer, or for the formation of a composite layer from micropowders.

Current density is one of the main parameters in MAO. Usually, to achieve the necessary conditions for plasma electrolysis, the current density is set in the range of 0.01 to 0.3 A/cm². As the coating grows, the voltage increases rapidly at first, then slowly, until constant plasma conditions are established. The critical rate of voltage change corresponds to the establishment of a spark discharge on the electrode surface. This value is very dependent on the characteristics of the metal-electrolyte combination and is usually in the range 120–350 V. In the first stage of the process, sparking is observed in the form of uniform white light surrounding the electrode. As the coating grows, it changes and appears as individual yellow sparks that move rapidly across the surface. Gradually the density of sparks decreases, but their power increases. Finally, a few red spots appear, moving slowly across the surface. From time to time, these powerful arcs will cause current fluctuations and damage to the coating. Therefore, as soon as such arcs are detected, the process ends immediately.

MAO processing can be carried out using both anodic and cathodic polarization of the product, as well as at an alternating, high-frequency voltage. When choosing the polarity of the product, it should be borne in mind that anodic treatment is preferable when there is a thin oxide layer on the surface.

In MAO technology, voltage is the main characteristic that must be controlled. Control over the process consists in the fact that with a rapidly growing stress in the first stage and maintaining statistical conditions in the second stage, the temperature of the treated surface is stably low.

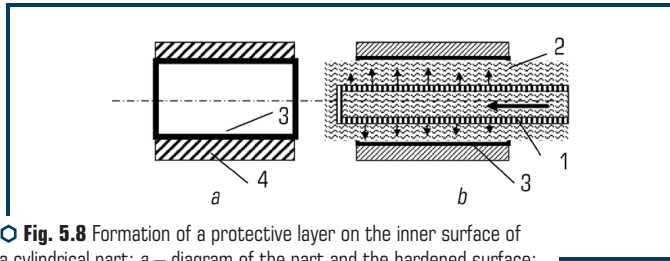
At the initial stage of the first stage, a rapid increase in voltage causes the formation of numerous bubbles on the surface of the electrode due to electrolysis of the solution and the release of Joule heat. When the voltage reaches approximately 75 V, a spark occurs. An increase in the applied voltage causes an increase in the intensity of the sparking. When the characteristic voltage reaches 175 V, this sparking of bubbles around the electrode transforms into a uniform glow. The complete separation of the electrode from the electrolyte, the formation of a continuous vapor cloud, is evidenced by a sharp drop in the current on the electrode surface. During MAO, the sample temperature is a linear function of voltage and, if possible, is reduced to the electrolyte temperature. In this case, the current density is 0.5 to 1 A/cm².

To reduce losses in the electrolyte, it is advisable to perform two technological methods: reducing the gap between the surfaces of the electrode and the workpiece, as well as organizing the flow of electrolyte in the gap from the electrode to the workpiece.

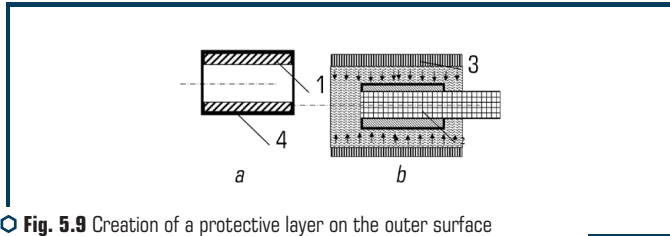
The implementation of these techniques provides a decrease in losses for heating the electrolyte and, accordingly, a decrease in the temperature of the workpiece/sample.

The use of these technological methods makes it possible to create coatings differentiated in thickness on the surface of parts and/or to implement MAO on local surfaces of parts.

For this purpose, it is necessary to develop specialized tooling, which has various modifications, depending on the configuration of the parts. **Fig. 5.8** shows the layout of the electrode – 1 and electrolyte flows – 2 for the MAO of the inner surfaces – 3 cylinders – 4, the MAO of the outer surface of the cylindrical part – the shaft is carried out according to the one shown in **Fig. 5.9**, diagram.



○ **Fig. 5.8** Formation of a protective layer on the inner surface of a cylindrical part: *a* – diagram of the part and the hardened surface; *b* – technological scheme of MAO



○ **Fig. 5.9** Creation of a protective layer on the outer surface of a cylindrical part: *a* – part diagram; *b* – technological scheme of MAO

It is proposed to fix the part – 1 on the insulator – 2 and insert it into the cavity of the cylindrical electrode – 3 with a minimum gap of 20 mm between the electrode.

To reduce energy losses, it is necessary to organize the flow of electrolyte between the electrode gap from the electrode surface to the shaft surface. Such a scheme of technological equipment ensures the formation of coating – 4 on the surface of the shaft with minimum energy losses and maximum productivity.

Fig. 5.10 shows a diagram of the formation of the MAO coating on the end surfaces – 1 of the part-sleeve – 2.

The part is fixed with non-conductive strips – 3 and is placed between the electrodes – 4 with a minimum gap. In this gap, the flow of electrolyte is organized from the electrode to the surface of the part.

MAO of large-sized products with internal surfaces – cavities of various depths, is carried out by introducing an electrode inside the cavity with a centralized supply of electrolyte (**Fig. 5.11**).

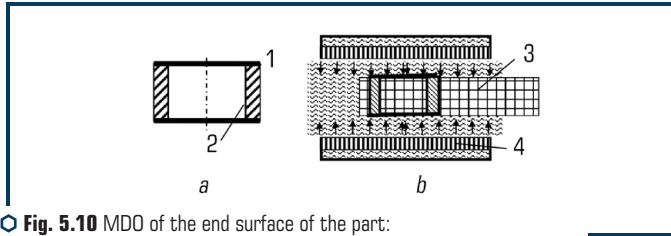


Fig. 5.10 MDO of the end surface of the part:
a – sketch of the part; *b* – technological scheme of hardening treatment

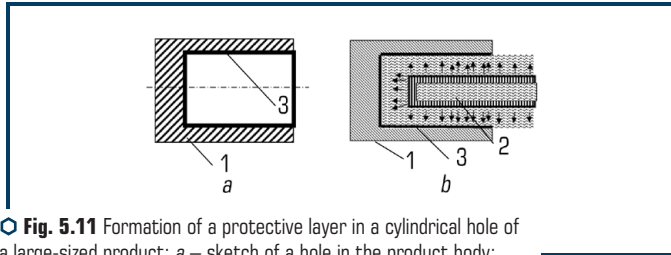


Fig. 5.11 Formation of a protective layer in a cylindrical hole of a large-sized product: *a* – sketch of a hole in the product body; *b* – diagram of the hole walls MAO

Product – 1 can be installed on a technological pallet and not immersed in an electrolyte tank. The electrolyte is supplied through electrode – 2 and commutes the electric current to the inner surface of the cavity – 3 products.

The directed movement of carriers of electric charge in the electrolyte and the minimum path of their movement ensure the efficiency of the MAO process of the inner surfaces of the product.

Of interest is the MAO of several parts at the same time on alternating current. This MAO method is shown schematically in **Fig. 5.12**. Parts 1 and 4 must be protected with a coating from the side of the working surface, which has a complex shape in the form of various pockets – 3. The parts are included in the electrical circuit of a regulated alternating current source – 2 and fixed by means of insulators – 5. On the opposite side from the side surface to be hardened, electrodes – 7 and 11 are fixed on the electrically conductive platform 6, which, by means of pipelines 8 and 12, create an electrolyte flow in the gaps 9 and 13 between the surfaces of the electrode and parts. The electrolyte drain into the hydraulic system is carried out through pipelines 10 and 14. The electrodes – 15, as a rule, are grounded. This connection scheme allows for MAO of two, and with a multiphase source, and more part.

It is advisable to apply the same technological scheme for MAO of extended products, for example, pipes (Fig. 5.13).

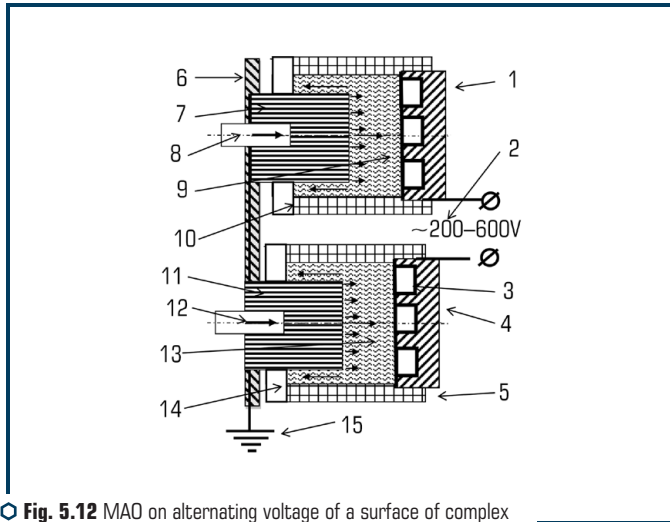


Fig. 5.12 MAO on alternating voltage of a surface of complex geometric shape on two parts

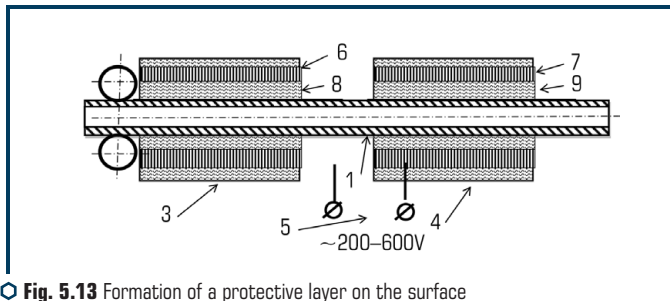


Fig. 5.13 Formation of a protective layer on the surface of an extended product (pipe)

Product – 1 is fed by rollers – 2 and, accordingly, is grounded. Along the way of the product, electrode devices – 3, 4 are installed, where the electrodes are connected to the phases of sources – 5, having different electric current strength. At the beginning of the product, a low voltage is connected, for example, 200 V. To the next electrode along the path of the product, 300 V is connected, etc. to a voltage that will correspond to the thickness of the planned protective layer. The electrodes – 6, 7 cover the product around the periphery and create an optimal gap – 8, 9 between the electrodes, which ensures the MAO effectiveness.

5.3 EXAMPLES OF MAO OF PARTS WITH DIFFERENT CONFIGURATION OF WORKING SURFACES

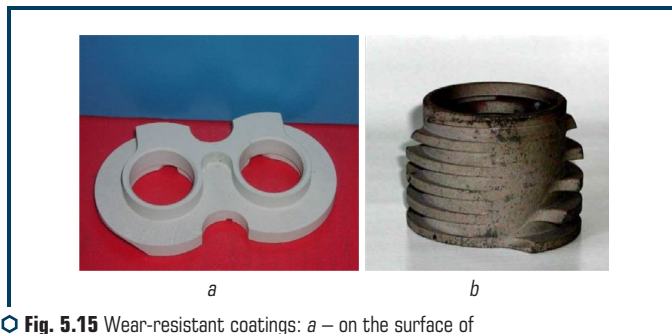
Using the previously given MAO technological schemes, protective coatings were obtained for a number of products with a complex configuration.

For example, heat-shielding coatings with a thickness of 150–200 μm on the bottom of the piston (**Fig. 5.14**) ensure that the engine can operate in forced modes and increase its performance.

A wear-resistant coating, up to 250 microns thick, was created on the surface of the front sliding bearing in the pump of high-pressure hydraulic systems and the rotor for crushing and forming feed pellets from an agricultural product (**Fig. 5.15**).



○ **Fig. 5.14** Type of heat-protective coating on the bottom of the pistons: *a* – diesel engine; *b* – ICE



○ **Fig. 5.15** Wear-resistant coatings: *a* – on the surface of the end bearing; *b* – on the rotor of the feed crusher

Fig. 5.16 shows covers for high-voltage devices with protective electrical insulating coatings, 100–150 μm thick. The coatings were applied on both sides.

A special feature of MAO is the ability to form protective coatings on thin edges/walls, on threads and in deep internal cavities.

Fig. 5.17 shows housings made of high-strength, ceramic-coated aluminum alloy.



○ Fig. 5.16 Instrument covers



○ Fig. 5.17 Enclosures of geodetic instruments with electrical insulating and wear-resistant coating

On alternating current, using a two-phase voltage, MAO was carried out on the parts of the die equipment (Fig. 5.18). MAO of parts was carried out with a smooth increase in voltage from 150 to 500 V.



○ Fig. 5.18 Parts of die tooling with ceramic coating

The distance between the electrode gap was set to 15 mm. As a result, a ceramic layer with a thickness of up to 200 μm was formed.

5.4 ELECTROLYTE COMPOSITION

In practice, MAO treatment requires careful selection of the metal – electrolyte combination. This can be achieved on the basis of polarization tests, which are usually used for studies of metal passivation [104–109].

There are 6 main groups:

1. Salt solutions that provide rapid dissolution of aluminum, for example, NaCl, NaClO₃, NaOH, HCl, NaNO₃.
2. Electrolytes that provide slow dissolution of the metal, for example, NaCl, NaClO₃, NaOH, HCl, NaNO₃.
3. Electrolytes providing passivation of metal in a narrow voltage range, for example, sodium acetate or phosphoric acid.
4. Fluoride electrolytes with complex behavior, e.g. KP, NaF.
5. Electrolytes providing weak metal passivation.
6. Electrolytes that provide strong metal passivation, for example, boric acids and salts of carbon and phosphoric acids, inorganic polymers (for example, silicates, aluminates, wolframites, molybdenites) and alkali metal phosphates, which can form polymer anions.

Electrolytes of group 4–6 make it easy to achieve spark discharge voltage and are most successfully used to obtain coatings using MAO technology.

These electrolytes are classified into 4 groups in terms of their contribution to the coating composition:

- a) solutions that only introduce oxygen into the coating;
- b) electrolytes containing anionic components that contribute other elements;
- c) electrolytes containing cationic components that contribute other elements;
- d) suspensions providing cataphoresis-transport of solid particles that contribute to the composition of the coating.

In electrolytes of groups (b) and (c), the coating is formed both by oxidizing the substrate and by applying other electrolyte components to the substrate surface. This makes it possible to obtain a wide range of modifications in the composition of coatings and their properties, and therefore these groups are considered the most promising.

Also, with MAO, colloidal solutions of sodium or potassium silicate are widely used, as well as multicomponent electrolytes based on silicates. In addition to silicates, the solution may contain substances that increase the conductivity of the electrolyte, for example, Na (0.5 to 20 g/l), NaOH or KOH (1 to 50 g/l) and/or provide an oxide layer with stabilizing elements, for example, Na₂B₄O₇·10H₂O (40 g/l), glycerin (10 g/l), Na₂CO₃ or K₂CO₃ (≤500 g/l) and modifying components, for example, NaAlO₂ (2 to 20 g/l), Na₆P₆O₁₈ (≤150 g/l). For special purposes, in order to integrate the effects of cataphoresis in the oxidation process, fine powders of solid materials with a high melting point and/or dry lubrication (to improve resistance to friction and wear) are introduced into the electrolytes.

5.5 COMPOSITION AND STRUCTURE OF COATING

5.5.1 MAO OF ALUMINUM-MAGNESIUM ALLOYS IN DIRECT CURRENT

Alloys of the Al-Mg system are characterized by a combination of satisfactory strength, good ductility, very good weldability and corrosion resistance. In addition, these alloys are characterized by high fatigue strength. The creation of an oxide coating on the working surfaces of products significantly increases their efficiency and increases the scope of application of alloys. For example, hulls of high-speed ships are made of aluminum-magnesium alloys, shaped castings (casting magnesium), sheets, wire, rivets, and so on (deformable magnesium) are made. Alloy properties depend on the percentage of metals. AMG sheet, in addition to aluminum and magnesium, contains iron, copper, manganese, zinc and other metals, depending on the grade of the alloy. Any AMG sheet is resistant to corrosion, high weldability by argon-arc, roller and resistance spot welding. Deformation of the AMG sheet depends on the percentage of magnesium, the more magnesium, the lower the deformability. Conversely, the lower the percentage of magnesium content, the higher the deformation properties, both in the cold and in the hot state.

MAO of high-strength aluminum alloy 7075 (Al-Zn-Cu-Mg) was carried out on a micro-arc oxidation unit (a) in the arc oxidation mode (b) (**Fig. 5.3**).

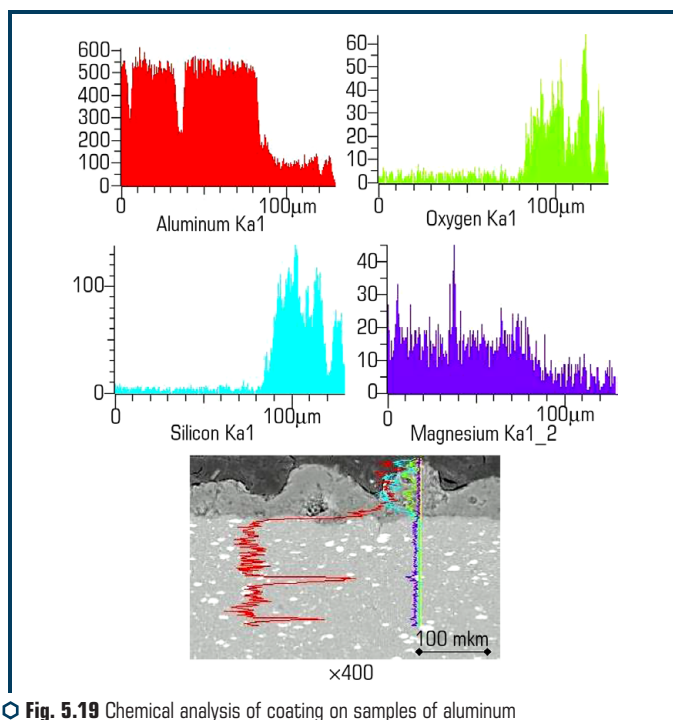
Oxidation is carried out in the area of micro-arc discharges, which are formed on the surface of the sample. A smooth increase in the voltage of the electric current leads to a decrease in the intensity of electrical discharges and a gradual increase in the thickness of the coating, an increase in its electrical strength. The onset of breakdown of the oxide layer is massive, accompanied by sharp surges of electric current, up to 10 A/cm². A large reserve in the technology of changing the chemical and phase composition of the coating has the circuit and mode of connecting the surface to an electrical converter. In the MAO process, mixed oxides of aluminum and metals are formed, which are included in the complex anion of the electrolyte. For example, the introduction of iron and copper anions into the electrolyte provides the formation of composite oxide coatings with high performance properties. In the steady-state mode of oxidation, the current density is 0.1–0.5 A/cm². For micro-arc oxidation, specialized power supplies have been developed that provide regulation of the amplitude values of current (0–170 A) and voltage (0–1 kV) in both anodic and cathodic processing modes. The main parameters that make it possible to control the MAO process and the properties of the coatings are the electrolyte concentration, voltage and current density, temperature, duration of the process, alloy composition and its heat treatment.

Specimens were made of high-strength aluminum alloy 7075 (Al-Zn-Cu-Mg), analogous to B95, ultimate strength 560 MPa, yield strength 490 MPa, and relative elongation 6 %. MAO of the samples was carried out for 30 minutes with an increase in the electric anode voltage up to 400 Volts, with a short-term (for 1 sec) switching to the cathodic mode up to 500 Volts. Processing modes:

- impulse asymmetric current;
- aeration of the electrolyte with air;

- voltage during the formation of the initial coating 110–250 V;
- current density 15–45 A/dm²;
- processing time up to 30 minutes; electrolyte temperature 30–60 °C;
- electrolyte consumption 4–8 l/min.

An aqueous solution was used as an electrolyte: NaOH – 5 g/l; Na₂SiO₃ – 30 g/l; Na₄P₂O₇ – 6 g/l; Al₂O₃ – 70 g/l. The processing was carried out by connecting the sample with the anode for 120 seconds to a voltage of 200 V. The current varied from 50 A to 2 A in 30 seconds. Subsequent switching to 250 V was accompanied by a change in current from 10 A to 2 A, within 200 seconds. When the current reading dropped to 2 A, the electrical voltage was switched at 300 Volts and this voltage was maintained for 600 s. The next voltage of 350 volts was connected for 900 s. Turn-on current – 10 A changed to 1 A in 900 s. In 30 minutes, an oxide coating was formed, up to 100 μm thick (**Fig. 5.19**).



○ **Fig. 5.19** Chemical analysis of coating on samples of aluminum alloy 7075 (Al-Zn-Cu-Mg) after MAO

Coating studies (**Fig. 5.19**) show three distinct areas obtained by the MAO method. It was found that the use of alkaline and silicate-alkaline solutions (for example, Na₂SiO₃ and NaOH) leads

to broadening of the inner dense layer, which mainly consists of γ - and α - Al_2O_3 phases, and in this case complex phases Al-Si-O are present, mullite ($\text{Al}_6\text{Si}_2\text{O}_{13}$, Al_4SiO_8). Switching to a higher voltage creates conductive defects and accelerates the oxidation process. The coating has high roughness and surface defects. Coating thickness is 100 microns.

The next batch of samples was made from alloy A6062 (Al-Mg-Si). The tensile strength is 205 MPa, the yield point is 170 MPa, and the elongation is 10 %. The research results are shown in **Fig. 5.20**.

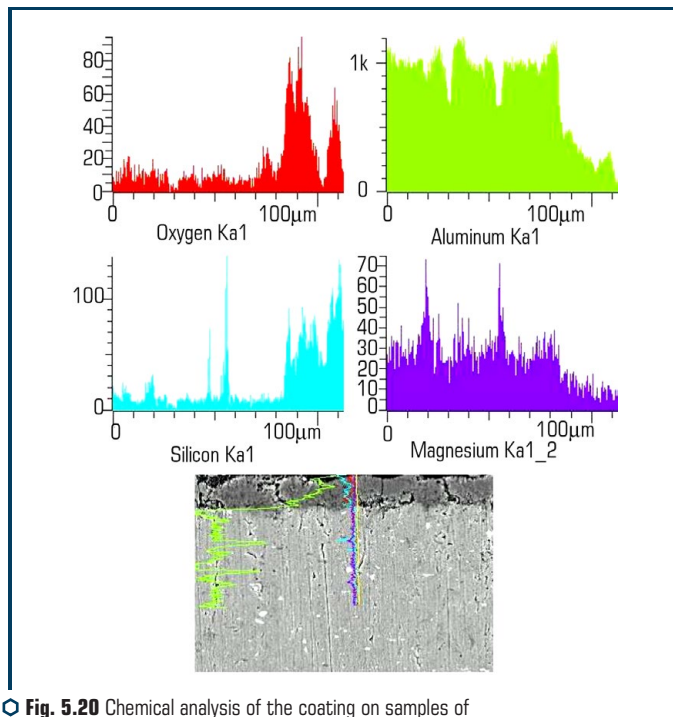


Fig. 5.20 Chemical analysis of the coating on samples of the aluminum alloy A6062 (Al-Mg-Si) after MAO

MAO of samples from A6062 was carried out in modes similar to those for the previous samples. Research shows three distinct areas in coatings (**Fig. 5.20**). This is a border area with a large excess of oxygen and a gradual decrease in the aluminum content. The second region is with a high content of silicon and oxygen, and the third is mullite ($\text{Al}_6\text{Si}_2\text{O}_{13}$, Al_4SiO_8). A high density of electric current pulses when an increased voltage is turned on leads to the creation of through defects in the form of breakdown channels and cracks, which increased the conductivity of the oxide layer and ensured the formation of a coating within 100 microns in 30 minutes.

Alloy A6062 is used for the manufacture of welded containers, oil pipelines, gas pipelines, stamped products, dishes and many household items.

It was found that the use of alkaline and silicate-alkaline solutions (for example, Na_2SiO_3 and NaOH) leads to broadening of the inner dense layer, which mainly consists of γ - and α - Al_2O_3 phases; complex phases Al-Si-O are present. The relative content of the harder phase increases with increasing current density. The content of α -aluminum can reach 60 % for coatings formed on copper-containing aluminum substrates, while the γ - Al_2O_3 phase is predominantly formed on magnesium-containing aluminum alloys.

The work on the formation of oxide coatings on the surface of samples from the AMG-3 alloy (Mg 2.3–3.8 %, Mn 0.3–0.6 %) in an aqueous solution of KOH was carried out using a different circuit for connecting the source voltage. MAO was carried out according to the anode connection scheme with periodic connection to the anode of a voltage increased by 20–30 %.

Metallographic analysis shows that the resulting layer on the samples ($> 120 \mu\text{m}$) has a higher density near the substrate (**Fig. 5.21**). There is a loose, porous layer on the surface, the thickness of this layer is 30–50 μm . Oxidation was carried out in a flowing electrolyte flow, with a minimum gap between the electrodes of 25 mm and a maximum voltage of 340 V. It is known that oxidation of aluminum alloys without alloying additions on the surface forms an oxide film with a thickness of $< 250 \mu\text{m}$ with a microhardness of 7–8 GPa [9].

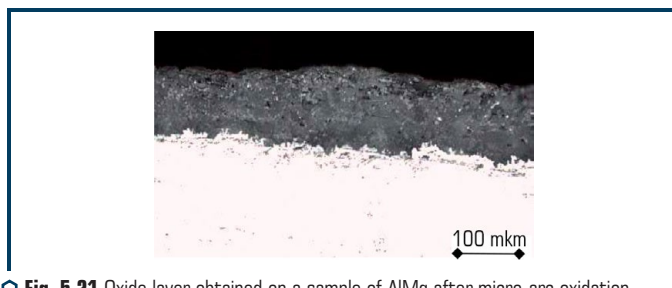


Fig. 5.21 Oxide layer obtained on a sample of AlMg after micro-arc oxidation

The developed unit (**Fig. 5.3**) allows for oxidation at interelectrode gaps of 20–30 mm, which reduces electrical energy losses and ensures the formation of an oxide layer up to 150 microns, at an electric current voltage of $\approx 340 \text{ V}$, it is known that the optimum electrolyte temperature for implementing the technology is 50–60 $^{\circ}\text{C}$.

To ensure this temperature, the electrolyte is heated by using losses in the electrolyte cell by reducing the flow in the gap.

The mass spectrum of secondary ions (**Fig. 5.22**), obtained by bombarding the coating with an argon ion beam, showed that the coating has a complex composition.

It includes the constituents of the electrolyte (Na , H_2O , CO , CO_2 , COH , Ca), the products of plasma-chemical synthesis from the constituents of the sample material and plasma (Al , Mg ,

AlN, AlO, MgO), as well as from the elements that make up the electrode-cathode and products of plasma chemical synthesis between these elements and plasma (Fe, Mn, Cr, V, VO, MnO).

By changing the composition of the electrode-cathode, it is possible to microalloy the oxide coating with elements that make up the electrode and products of plasma-chemical synthesis.

X-ray phase analysis of the coating (**Fig. 5.23**) showed that the coating consists mainly of a refractory phase of aluminum oxide ($\alpha\text{-Al}_2\text{O}_3$) and aluminum. The introduction of fine powders, for example, chromium oxide, into the electrolyte ensures the movement of the powder particles to the coating and their fusion into the aluminum oxide layer. **Fig. 5.24** shows a view of the surface of the sample. The high-temperature form is mainly concentrated at the oxide-metal interface. Electrolyte anions are deposited on the surface of dispersed particles, which gives them a negative charge and ensures movement to the surface of the product under the action of electrophoretic forces.

With an increase in the concentration of anions and a decrease in the electrolyte temperature, the effect of introducing dispersed particles into the coating is enhanced. Studies of the phase composition of ceramic coatings obtained by introducing stimulating additives of various composition and concentration into the electrolyte showed that the introduction of dispersed solid particles creates conditions for an increase in their percentage at the oxidized surface, ensuring the production of composite coatings, for example, introducing chromium oxide into the hydraulic system. (fineness up to 10 microns, content in the electrolyte 2–3 %) led to an increase in the content of chromium oxide at the surface of the product up to 15 %.

The MAO of the combustion chamber of a diesel piston was carried out using an electrolyte based on an aqueous solution of $\text{KOH} + \text{Na}_2\text{SiO}_3 + \text{SiO}_2$. The technological scheme (**Fig. 5.5**) provides circulation of the electrolyte with a minimum interelectrode gap of 25 mm.

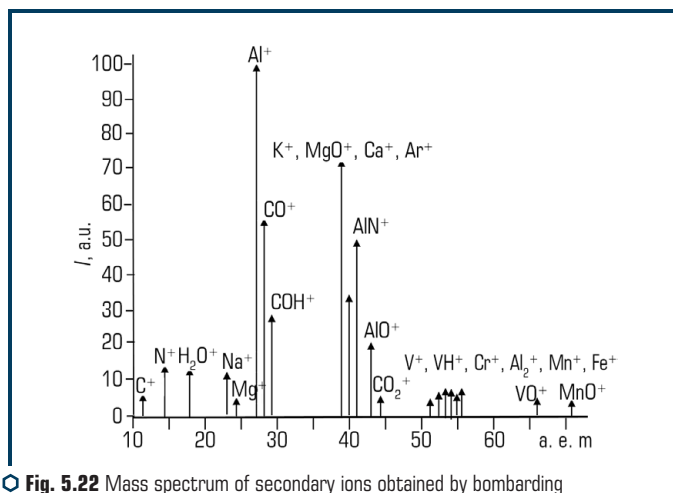
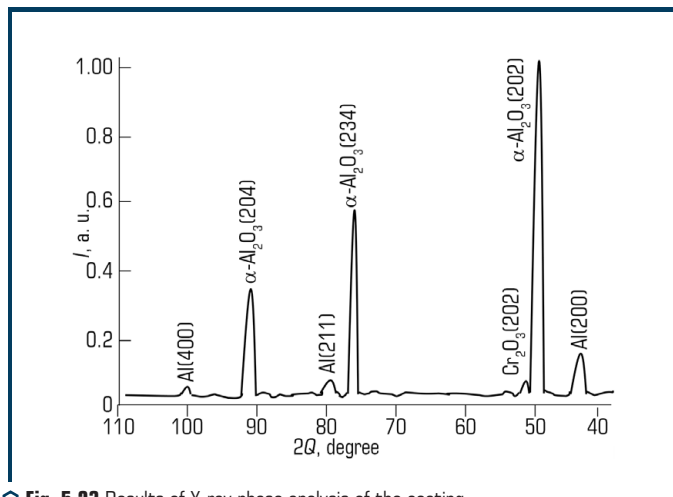
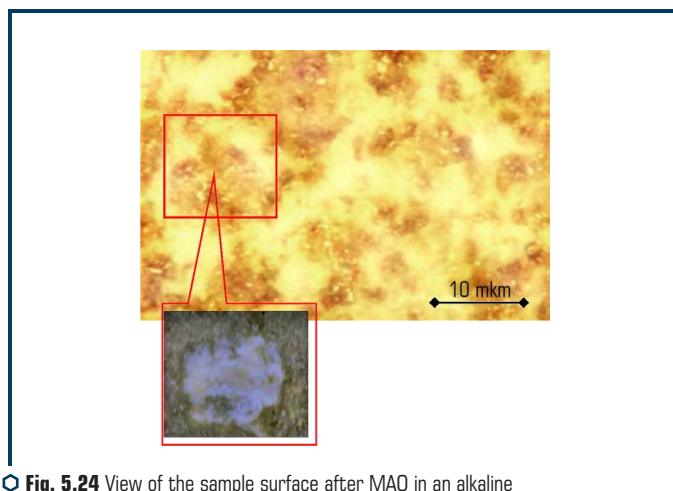


Fig. 5.22 Mass spectrum of secondary ions obtained by bombarding an aluminum alloy with an argon ion beam after micro-arc oxidation



○ Fig. 5.23 Results of X-ray phase analysis of the coating



○ Fig. 5.24 View of the sample surface after MAO in an alkaline electrolyte with the addition of Cr_2O_3 micropowder

X-ray diffraction analysis of the ceramic coating created in the combustion chamber showed that its composition largely depends on the oxidation regime and the composition of the electrolyte (Table 5.2). The basis of the ceramic coating is a mixture of aluminum oxides: low-temperature $\gamma\text{-Al}_2\text{O}_3$ and high-temperature forms δ -, $\alpha\text{-Al}_2\text{O}_3$. The high-temperature form is mainly concentrated at the oxide-metal interface.

● **Table 5.2** Phase composition of the ceramic layer

Chemical compound or element	Content, %
Al	11.3
MgAl ₂ O ₄	0.0001
Mullite	44.7
NaAlSiO	33.3
CaAlSiO	1.3
SiO ₂	16.8
Si	0.7
Al ₂ O ₃	0

The density of the upper layer of the coating with the phase composition (Al₂O₃; Al; CrO₃) is 3.74 g/cm³, which is close in value to the density of α -Al₂O₃ ($\rho=3.98$ g/cm³). The adhesion of the coating of the oxidized layer of aluminum (determined by scribing with a diamond pyramid) ranges from 42 to 67 MPa in different areas. And the hardness of some areas of the coating ranges from $1.36 \cdot 10^4$ N/mm² to $1.72 \cdot 10^4$ N/mm² in dark points where there are inclusions of the CrO₃ phase.

Anions of the electrolyte are included in the structure of the anodic oxide, and the introduction of anions increases with an increase in the concentration of various stimulating additives in the electrolyte and with a decrease in the operating temperature of the electrolyte. The content of the brittle, not adhering to the substrate, mullite phase in the specified ceramic coating is given in **Table 5.2**.

The developed principles of constructing the technology are universal and make it possible to develop devices for applying high-quality oxide coatings to hard-to-reach surfaces of products, for example, the inner surfaces of a cylinder or the bottom of a piston.

Work was carried out to apply a heat-shielding layer to the walls of the combustion chamber of the piston. The piston was made of an alloy (Al+6 % Si). Metallographic analysis shows that the resulting layer (over 120 μ m) is denser near the substrate. There is a loose, porous layer on the surface, the thickness of this layer is 30–50 μ m. The hardness of the oxidized layer depends on the substrate material and is 4.5–7 GPa. Oxidation was carried out in KOH electrolyte at a maximum voltage of 340 V. For micro-arc oxidation of the bottom and walls of the piston combustion chamber, a special unit was developed using the technological scheme (**Fig. 5.5**).

The product was oxidized in the following order. At the initial moment of time, an electric current voltage of ≈ 110 V was connected to the interelectrode gap. As a result, in 60 s, an oxide film is formed, which reduces the current density 50 times (from 10 mA/cm²). Then the voltage was increased to 200 V (current density 2 mA/cm²). After holding for 5 min, the electric voltage was increased to 270 V. A further increase in the voltage to 340 V provided the formation of a coating with a thickness of up to 150 μ m. Dispersed particles of chromium oxide were fused into the coating. **Fig. 5.27** shows a dispersed particle in an alumina layer obtained by micro-arc oxidation.

This technology was used to process a batch of diesel engine pistons that have passed bench tests for thermal cycling. Tests have shown that the coating withstood up to $1.5 \cdot 10^6$ cycles without destruction. A four-position semi-automatic unit was developed and manufactured, which, with a single-shift load, provided oxidation of 150,000 pistons per year.

The design of the developed device can be built into automated lines, and a centralized hydraulic electrolyte dispensing system provides control of its composition and regeneration. The design of the unit allows the introduction of rare-earth salts into the electrolyte, which ensures alloying of the coating and increases its physical and mechanical properties.

5.5.2 MAO OF ALUMINUM-MAGNESIUM ALLOYS IN ALTERNATING CURRENT

As mentioned above, a large reserve in the technology of changing the chemical and phase composition of the coating has the circuit and mode of connecting the surface to an electrical converter. The anode mode with a periodic increase in potential or the anode mode with pulse switching to the cathodic mode makes it possible to intensify the technology and obtain dense coatings melted from the surface, **Fig. 5.25**.

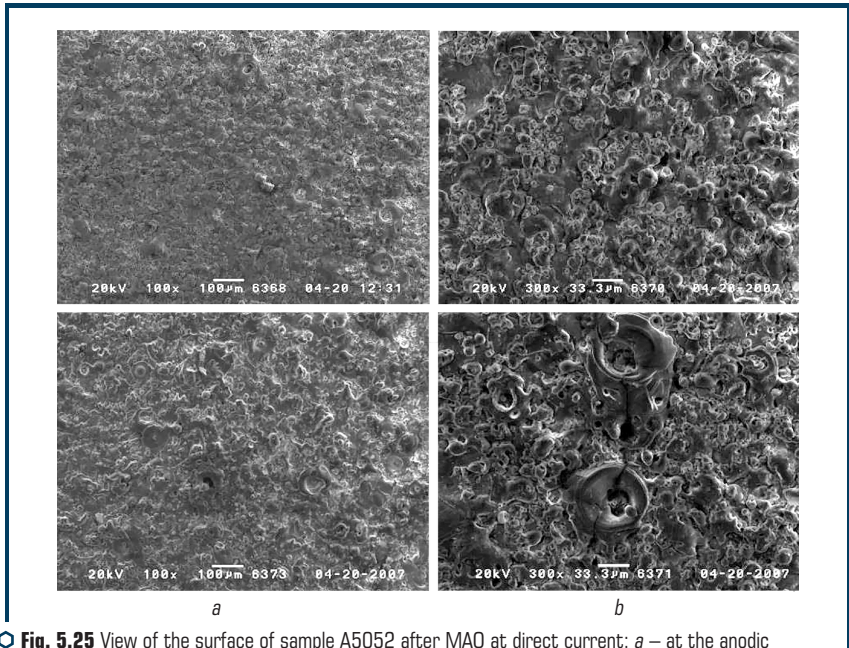
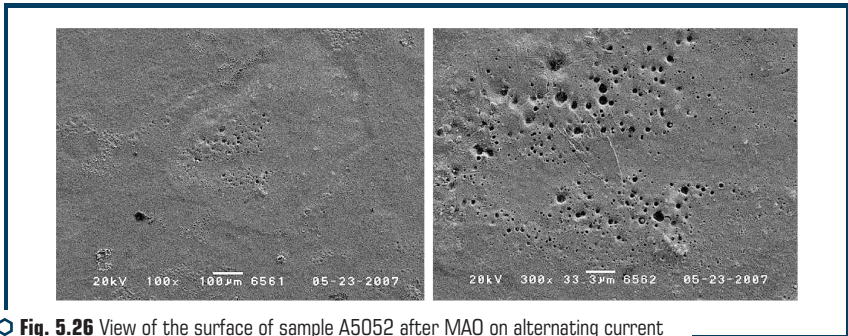


Fig. 5.25 View of the surface of sample A5052 after MAO at direct current: *a* – at the anodic mode with a periodic increase in voltage; *b* – periodic switching to the cathodic mode

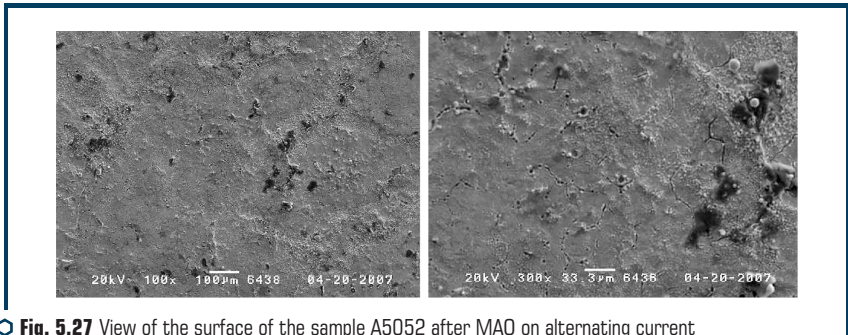
MAO of aluminum samples with periodic switching to the cathodic mode is distinguished by a higher surface roughness and fusion of the oxide layer (**Fig. 5.25, b**).

In the steady-state mode of oxidation, the current density is 0.1–0.5 A/cm². The main parameters that make it possible to control the process of micro-arc oxidation and the properties of coatings are electrolyte concentration, voltage and current density, electrolyte temperature, process duration, alloy composition and heat treatment.

Of interest is the MAO technology with the connection of samples/products to an alternating current electric circuit. The technological connection diagram is shown in **Fig. 5.12, 5.13**. One of the advantages of this scheme is a multiple increase in the productivity of oxide coating formation. The surface of the sample A5052 after MAO on alternating current with a smooth increase in the electric potential from 150 to 400 V is characterized by low roughness (**Fig. 5.26**). Micropores are visible on the surface, which ensure the electrical conductivity of the layer and the possibility of its formation. **Fig. 5.27** shows a view of the surface of sample A5052 after MAO on alternating current with a pulsed voltage of 500 V and a smooth increase in the main electric potential from 150 to 400 V. The surface is characterized by low roughness and the presence of microdefects in the form of cracks and pores.



○ **Fig. 5.26** View of the surface of sample A5052 after MAO on alternating current with a smooth increase in electric potential from 150 to 400 V



○ **Fig. 5.27** View of the surface of the sample A5052 after MAO on alternating current with a pulsed voltage of 500 V and a smooth increase in the main electric potential up to 400 V

It should be noted that in the initial state, the A5052 alloy consists at least of such components as Al-Mg with the presence of such impurities as Cu, Fe, Mn, Zn and other elements.

MAO of the surface of samples from alloy A5052 was carried out on alternating current with a pulsed voltage of 500 V and a smooth increase in the main electric potential to 400 V. This technology was carried out using an aqueous solution of $\text{KOH} + \text{Na}_2\text{SiO}_3 + \text{SiO}_2$. The adopted oxidation scheme is distinguished by high productivity and quality of the oxidized layer.

Metallographic analysis of samples from alloy A5052 shows that the resulting oxide layer (more than 150 microns) is denser near the aluminum substrate (**Fig. 5.28**). On the surface, the oxide layer has a high porosity and consists of many melted areas in the form of microcraters and drop-like traces of the oxide layer melting (**Fig. 5.27**). Analysis of the research results shows that the micro-arc process propagates inside the pores of the coating. Traces of localization of micro-arcs in the form of melted craters are also noticeable in the pores of the coating. It can be noted that the oxide layer is formed not only from the coating surface, but also from the pore surface into the coating, which provides an oxide layer with a developed surface inside the sample.

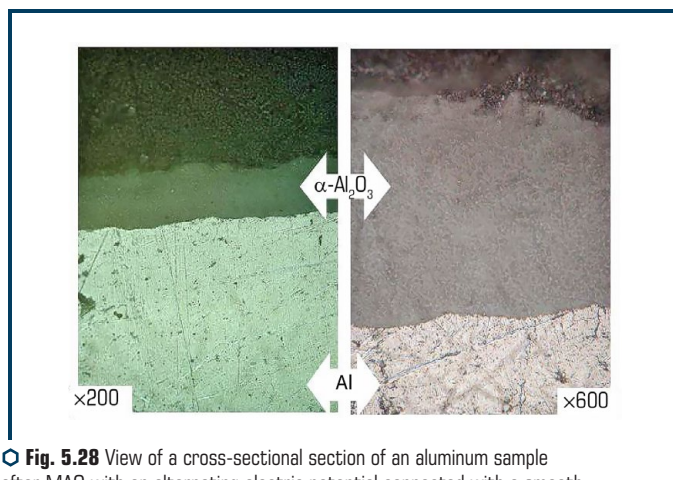


Fig. 5.28 View of a cross-sectional section of an aluminum sample after MAO with an alternating electric potential connected with a smooth increase in voltage from 150 to 400 V

The developed technological unit allows simultaneous oxidation of two samples/parts with interelectrode gaps of 20–30 mm, which reduces electrical energy losses and ensures the formation of a dense oxide layer up to 150 microns, at an alternating voltage of up to 400 V (**Fig. 5.29**).

For example, the formation of an oxide layer on the surface of the stamping dies (**Fig. 5.18**) took 30 minutes. The roughness of the coating on the surface of the matrices was rather low and the matrices were used without further mechanical processing. The hardness of the oxide layer is tens of times higher than the base metal.

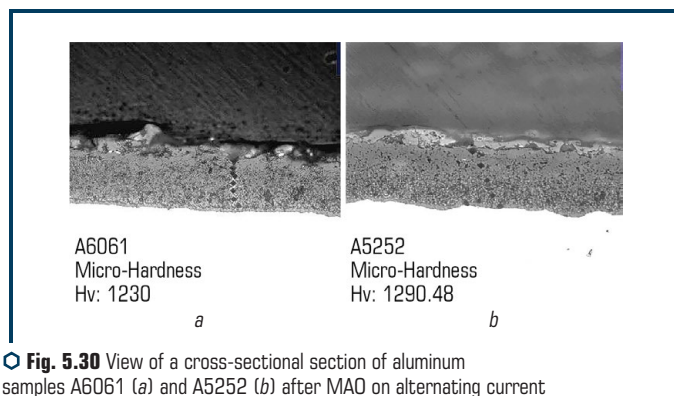


○ **Fig. 5.29** View of a thin section of a coating with imprints obtained by measuring hardness

Depending on the composition of the electrolyte and the polarity of the electrode, many schemes for connecting samples to the electrical circuit of the power supply can be used. The basis of the process is the connection of a potential that is higher than the breakdown voltage that occurs in the oxide film growing on the surface of the passaged anode, and is characterized by the presence of numerous arcs moving rapidly along the surface to be treated. Complex compounds can be synthesized within the high-voltage breakdown channels formed throughout the growing oxide layer. These compounds consist of oxides of both the substrate material (usually aluminum) and of the generated elements (for example, silicon). Plasma-chemical interactions of plasma in multiple surface discharges lead to the growth of the coating in both directions from the substrate surface. Although the local temperatures are extremely high, the temperature in the bulk of the coating is below 100 °C. With some particular combination of electrolyte composition and current mode, the discharge modifies the microstructure and phase composition of the substrate from a metal alloy to a complex ceramic oxide. As a result, a thick wear-resistant layer (up to 500 μm) with a hardness of up to 18 GPa can be obtained at an alternating potential.

Samples of alloys A6061 (a) and A5252 (b) were connected to an alternating current electric circuit with a smooth increase in the electric potential from 150 to 400 V and a periodic switching on of a pulse voltage of 500 V for 1–2 seconds. The MAO technology of samples (2 pcs) was carried out 20 min.

Fig. 5.30 shows thin sections of the oxide layer for samples from alloys A6061 (a) and A5252 (b). The ceramic layer differs from the one obtained earlier (**Fig. 5.28, 5.29**). It has a microporous structure that is evenly distributed throughout the layer.



○ **Fig. 5.30** View of a cross-sectional section of aluminum samples A6061 (a) and A5252 (b) after MAO on alternating current with a pulsed connection of a voltage of 500 V and a smooth increase in the main electric potential from 150 to 400

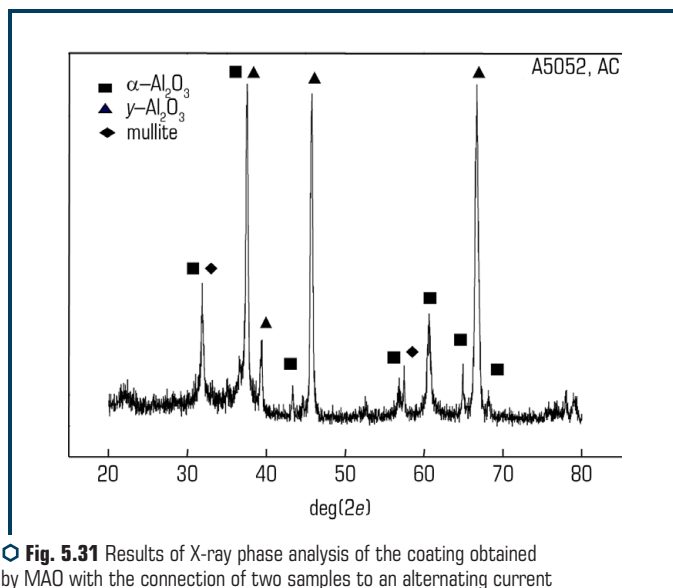
A layer of fused ceramic is visible on the surface, which has defects in the form of cracks and pores. The hardness of the main oxide layer is Hv – 1230–1240.

The results of X-ray phase analysis of the coating (**Fig. 5.31**) obtained by MAO with the connection of two samples to an alternating current electric circuit with a pulsed voltage of 500 V and a gradual increase in the main electric potential from 150 to 400, show that the ceramic layer consists mainly of α - Al_2O_3 (202), α - Al_2O_3 (234), α - Al_2O_3 (204) having a rhombohedral structure with parameters, $a=0.3253\text{-}0.0022$ nm and angle $\beta=56.65\text{-}0.8$. The intensity of the peaks Al (200), Al (311), Al (400) having a cubic FCC lattice with lattice parameters $a=0.4032\text{-}0.0303$ nm decreased significantly. In addition, peaks of the Al-Si-O complex phases were found.

The prospect of new plasma electrolyte processing schemes is significant. They can be expected to prove useful in ever-expanding applications, in particular in view of the increasing desire to use alloys based on aluminum, magnesium, which have an optimal strength-to-weight ratio.

Studies show that an increasing concentration of silicate in the electrolyte leads to accelerated growth of the coating due to the inclusion of Si in the structure of the coating and the formation of complex phases Al-Si-O, **Table 5.3**. The elemental distribution over the thickness of the coating, when silicon is present in the alkaline electrolyte, varies depending on the type of particles containing silicon.

The addition of 15 g/l sodium silicate to the electrolyte leads to the fact that from 3 % to 5 at. % silicon penetrates into the coating and the concentration of Cu and Mg significantly decreases, which, in turn, increases in the interfacial region. The position of the maxima of the Cu and Mg content also shifts towards the substrate. When silicon is introduced in the form of a fine powder, the Si content in the coating increases (up to 40–60 % on the surface), but it is non-uniformly distributed over the thickness. Accordingly, the profiles of Al and other alloy composites also change. When alkaline solutions with dissolved silicon are used, the uniformity of the coating thickness depends on the composition of the electrolyte.



○ Fig. 5.31 Results of X-ray phase analysis of the coating obtained by MAO with the connection of two samples to an alternating current electric circuit with a pulsed voltage of 500 V and a gradual increase in the main electric potential from 150 to 400

◆ Table 5.3 Modes and some characteristics of oxide films [106–109]

Na_2SiO_3 (g/l)	Processing time (min)	Current density (A/dm^2)	Coating thickness (μm)	Al-Si-O stoichiometry	Al_2O_3 to Al-Si-O ratio
2	120	12	85	$\text{Al}_{0.26}\text{Si}_{0.08}\text{O}_{0.06}$	1.0
4	80	25	75	$\text{Al}_{0.23}\text{Si}_{0.10}\text{O}_{0.67}$	0.6
6	60	25	110	$\text{Al}_{0.22}\text{Si}_{0.12}\text{O}_{0.65}$	0.4
20	25	25	120	$\text{Al}_{0.13}\text{Si}_{0.19}\text{O}_{0.68}$	0.1

Homogeneous coatings can be obtained only in the presence of some balanced combinations of silicon and alkali; an increase in the concentration of silicate leads to an increase in the growth of the coating at the ends of the sample, where the processes of silicon polycondensation are facilitated due to more intense sparking.

On the contrary, an increase in the alkaline concentration causes local dissolution of the oxide layer and the formation of pits along the surface of the sample. Oxide coatings obtained in concentrated silicate solutions (50–300 g/l) are thicker and more homogeneous. They have, however, an increased outer layer that can reach 90 % of the total coating thickness. Mostly such layers are amorphous to X-radiation and usually consist of 40–43 % Si, 1–4 % Al, 1–4 % Na,

and 49–58 % O. As a rule, these silicate coatings have a foam structure with high volumetric porosity and relatively low mechanical properties. The composition of these coatings can only be changed by introducing additional substances into the electrolyte. Electrolytes containing fine powders of Al_2O_3 , Fe_3O_4 , TiO_2 , MgO , Cr_2O are often used for these purposes. However, due to the high volumetric porosity, the distribution of elements in such coatings is extremely non-uniform.

5.6 OXIDE COATING CHARACTERISTICS AND APPLICATION

Oxide coatings can impart significant hardening to aluminum substrates. This effect is most pronounced on flat sheet substrates, when a 100–200 % increase in the effective Young's modulus is observed. This increase depends on the thickness of the sheet and the relative depth of the oxide layer.

The effective adhesion of the oxide layer, as estimated by the micro-indenter, tends to increase with the thickness of the coating. In coatings 200–250 μm thick, the adhesion force is comparable to the tensile limit of the substrate in the case of aluminum. One of the explanations for the increase in adhesion is a structural change in the inner region of the coating due to diffusion processes. It is also likely that thicker coatings give better support to the load and that the interface is therefore less susceptible to stress when the load is applied.

Structural variations tend to create a non-uniform distribution of hardness throughout the oxide coating. Usually, the hardest – 30 microns from the coating – substrate interface, is due to the maximum content of high-temperature oxide phases in the zone of the dense inner layer. The maximum hardness values are up to 17 GPa for α -aluminum based coatings, 12 GPa for α -phase coatings and 4–9 GPa for mullite based coatings. In each case, the porous outer regions of the coating are of low hardness.

The oxide coating layer on aluminum samples reaches 100–350 μm , depending on the time and MAO modes. Films obtained on aluminum alloys by MAO methods demonstrate abrasion resistance comparable to that of WC-based composites and coatings. The wear resistance of oxide coatings in corrosive environments can be improved due to the composition of the electrolyte and the MAO regime.

The friction characteristics of oxide coatings under conditions of friction with a lubricant depend on the porosity and quality of the liquid introduced into the pores. The friction coefficient for a pair of oxide layer and steel from the usual friction coefficients for steel of 0.4 decreases to $\mu \approx 0.015$ – this result was obtained in the case when the oxide film was impregnated with oil. A study of the friction coefficients of aluminum alloy samples against each other in industrial water and seawater showed that after MAO a combined pair of coatings based on $\alpha\text{-Al}_2\text{O}_3$ had $\mu = 0.023\text{--}0.025$ at pressures up to 16 MPa. A pair of coatings based on $\gamma\text{-Al}_2\text{O}_3$ showed $\mu = 0.005\text{--}0.008$ up to a critical pressure of 8 MPa. Friction pairs based on mullite coatings can withstand critical pressures up to 4 MPa.

Coatings obtained, for example, in a concentrated silicate electrolyte, quite successfully withstand significant external heat fluxes without affecting adhesion – partly due to high porosity.

The high electrical resistance and breakdown strength of silicon and aluminum ensure good dielectric properties of MAO coatings. The intrinsic resistance values are obtained as $2.7 \cdot 10^{14}$ before $3.5 \cdot 10^{13}$ Ohm. In this respect, coatings obtained in a solution with a dissolved silicate content of 1 to 5 % have the best properties. Electrical resistivity is also a factor in plasma electrolysis. It decreases when the process transforms into arc discharge mode, then remains constant, regardless of the oxidation time.

The experience of using (or applying) MAO methods shows that the coating can successfully compete with anodizing and thermal oxidation, as well as provide an alternative to other «composite materials» in various industries. The remarkable properties of wear, friction, corrosion and heat resistance of these coatings attract manufacturers of equipment (products) for the use of this technology in the textile industry, aviation, space and oil and gas production, and cleaning. The simplicity of equipment, high processing efficiency and the possibility of continuous processing of products by MAO methods are also of practical interest for its use in industry. Moreover, MAO methods can be used as a pretreatment for duplex processing involving electroplating, PVD or other coating methods. For example, thin, hard PVD coatings can be applied to thick MAO diffusion layers to obtain good adhesion and toughness under heavy loads.

REFERENCES

1. Sluginov, N. (1880). On luminous phenomen, observed in liquids during electrolysis. J. Russ. Phys. Chem. Soc., 12, 193–203.
2. Schulze, G., Betz, H. (1937). Elektrolytkondensatoren. Berlin: Kraysn, 178.
3. McNiell, W., Nordbloom, G. F. (1958). Pat. No. 2854390 US. Metod of making cadmium niobate. U.S. Class: 205/477; 204/164; 205/322. CPC Class: C01G 33/00 (20130101); C01P 2006/40 (20130101). published: 30.09.1958.
4. McNiell, W., Gross, L. L. (1966). Pat. No. 3293158 US. Anodik spark reaktion processes and articles. U.S. Class: 205/316; 205/321; 205/320; 205/322; 205/323. CPC Class: C25D 11/026 (20130101); C25D 9/06 (20130101). published: 20.12.1966.
5. Markov, G. A., Markova, G. V. (1976). Pat. No. 526961 USSR. Sposob formovki anodov elektroliticheskikh kondensatorov. MPK: H01G 9/04. No. 1751524. declared: 24.02.1972; published: 30.08.1976, Bul. No. 32.
6. Nikolaev, A. V., Markov, G. A., Peshchevitskij, B. I. (1977). Novoe iavlenie v elektrrolize. Izvestiia Sibirskogo otdeleniia Akademii nauk SSSR. Seriiia khimicheskikh nauk, 5 (12), 32–33.
7. Markov, G. A., Tatarchuk, V. V., Mironova, M. K. (1983). Mikrodugovoe oksidirovanie aliuminiii v kontsentrirovannoi sernoi kislote. Izvestiia Sibirskogo otdeleniia Akademii nauk SSSR. Seriiia khimicheskikh nauk, 3 (7), 34–37.
8. Snezhko, L. A., Beskrovnyi, Iu. M., Nevkrytyi, V. I., Chernenko, V. I. (1980). Impulsnyi rezhim dlia polucheniiia silikatnykh pokrytii v iskrovom razriade. Zashchita metallov, 16 (3), 365–367.
9. Snezhko, L. A., Rozenboym, G. V., Chernenko, V. I. (1981). Issledovanie korrozionnoi stoikosti splavov aliuminiii s silikatnymi pokrytiiami. Zashchita metallov, 17 (5), 618–621.
10. Snezhko, L. A., Chernenko, V. I. (1983). Energeticheskie parametry protsessa polucheniiia silikatnykh pokrytii na aliuminii v rezhime iskrovogo razriada. Elektronnaia obrabotka materialov, 2 (110), 25–28.
11. Snezhko, L. A., Chernenko, V. I. (1983). Mekhanizm dielektricheskogo proboiia pri formovke anodnykh keramicheskikh plenok na AMg 5. Elektronnaia obrabotka materialov, 4, 38–40.
12. Tchernenko, V. I., Snezhko, L. A., Chernova, C. B. (1984). Elektrilmshe dlia formovki keramicheskikh pokrytii na aliuminii v rezhime iskrovogo razriada. Zashchita metallov, 20 (3), 454–458.
13. Snezhko, L. A., Pavlus, S. G., Chernenko, V. I. (1984). Anodnyi protsess pri formovke silikatnykh pokrytii. Zashchita metallov, 20 (4), 292–296.
14. Markov, G. A., Mironova, M. K., Potapova, O. G. et. al. (1983). Struktura anodnykh plenok pri mikrodugovom oksidirovanii aliuminiii. Izvestiia AN SSSR. Neorganicheskie materialy, 19 (7), 1110–1113.

REFERENCES

15. Petrosiants, A. A., Malyshev, V. N., Fedorov, V. A., Markov, G. A. (1984). Kinetika iznashivaniia pokrytii, nanosenykh metodom mikrodrugovogo oksidirovaniia. *Trenie i iznos*, 5 (2), 353–357.
16. Malyshev, N., Bulychev, S. I., Markov, G. A., Fyodorov, V. A., Petro-Syants, A. A., Kudinov, V. V., Shorshorov, M. H. (1980). Fiziko-mekhanicheskie kharakteristiki i iznosostoičnost pokrytii, nanosenykh metodom mikrodrugovogo oksidirovaniia. *Fizika i khimiia obrabotki material*, 1, 82–87.
17. Fyodorov, V. A., Belozherov, V. V., Velikosel'skaya, N. D., Bulychev, S. I. (1988). Sostav i struktura uprochnennogo poverkhnostnogo sloia na splavakh aliuminiia, poluchaemogo pri mikrodrugovom oksidirovaniia-142 ni. *Fizika i khimiia obrabotki material*, 4, 92–97.
18. Rudnev, V. S., Gordienko, P. S. (1987). Nekotorye dannye o iskrovom rezhime formirovaniia anodnykh elektroliticheskikh pokrytii na aliuminii i ego splavakh. *Vladivostok*, 55–e. Dep. v VINITI, 3384–B87.
19. Khrisanfova, O. A., Gordienko, P. S. (1989). Vliianie ionnogo sostava elektrolita i rezhimov oksidirovaniia na fazovyi sostav pokrytii, poluchaemykh na metallakh. *Vladivostok*, 71–e. Dep. v VINITI, 2986–B89.
20. Gordienko, P. S., Nedozorov, P. M., Volkova, L. M., Yaroyava, T. P., Khrisanfova, O. A. (1989). Fazovyi sostav anodnykh plenok na splave NTSu-1, poluchennykh pri potentsialakh iskreniia v vodnykh elektrolitakh. *Zaschita metallov*, 25 (1), 125–128.
21. Kurze, P., Krysmann, W., Marx, G. (1982). Zur anodischen Oxidation von Aluminium unter Funkenentladung (ANOF) in Wassrigen Electrolyten. *Wiss. Tech. Hochsch. Karl-Marx-Stadt.*, 24 (6), 665–670.
22. Dittrich, K.-H., Krysmann, W., Kurze, P., Schneider, H. G. (1984). Structure and properties of ANOF Layers. *Crystal Research and Technology*, 19 (1), 93–99. doi: <http://doi.org/10.1002/crat.2170190117>
23. Krysmann, W., Kurze, P., Dittrich, K.-H., Schneider, H. G. (1984). Process characteristics and parameters of Anodic Oxidation by spark discharge (ANOF). *Crystal Research and Technology*, 19 (7), 973–979. doi: <http://doi.org/10.1002/crat.2170190721>
24. Kurze, P., Schreckenbach, J., Schwarz, T., Krysmann, W. (1986). Coating by anodic oxidation with spark discharge. *Metalloberflaeche*, 40 (12), 539–540.
25. Saakin, L. S., Yefremov, A. P., Ropyak, L. Y., Apelfeld, A. V. (1986). Corrosion Control and Environment Protection. Informative Survey. Moscow: VNII-OENG, 6.
26. Fyedorov, V. A., Kan, A. G., Maksutov, R. P. (1989). Surface Strengthening of Oil & Gas Trade Facilities by Micro Arc Oxidation. Moscow: VNII-OENG, 6.
27. Markov, G. A., Gizatullin B. S., Rychazhkova I. E. (1982). Pat. No. 926083 USSR. Sposob elektroliticheskogo nanesenii silikatnykh pokrytii. MPK: C25D 9/06 (2006.01). No. 2864936. declared: 04.01.1980; published: 07.05.1982, Bul. No. 17.
28. Hradkovsky, R. J., Bayles, Jr. S. H. (1974). Pat. No. 3956080 US. Coated valve metal article formed by spark anodizing. U.S. Class: 205/316; 205/321; 427/344; 106/600; 205/322;

- 205/323; 428/450. CPC Class: B41N 3/03 (20130101); C25D 9/04 (20130101); C25D 11/06 (20130101); C25D 11/26 (20130101); C25D 11/30 (20130101); C25D 11/32 (20130101); C25D 11/34 (20130101); H01G 9/0032 (20130101); C25D 11/026 (20130101). published: 11.05.1976.
29. Brown, S. D., Kuna, K. J., Van, T. B. (1971). Anodic Spark Deposition from Aqueous Solutions of NaAlO_2 and Na_2SiO_3 . *Journal of the American Ceramic Society*, 54 (8), 384–390. doi: <http://doi.org/10.1111/j.1151-2916.1971.tb12328.x>
30. Van, T. B., Brown, S. D., Wirtz, G. P. (1977). Mechanism of anodic spark deposition. *American Ceramic Society Bulletin*, 56 (6), 563–566.
31. Ostroumov, G. A. (1979). *Vzaimodeistvie elektricheskikh i gidrodinamicheskikh polei*. Moscow: Nauka, 310.
32. Plank M. (1890). Ueber die potential differenz zwischen zwei verdunnten losungen binarer electrolyte. *Annalen der Physik und Chemie*, 276 (8), 561–576. doi: <http://doi.org/10.1002/andp.18902760802>
33. Iasnogorodskii, Ia. Z. (1949). *Nagrev metallov i splavov v elektrolite*. Moscow: Mashgiz, 128.
34. Yerokhin, A. L., Nie, X., Leyland, A., Matthews, A., Dowe, S. J. (1999). Plasma electrolysis for surface engineering. *Surface and Coatings Technology*, 122 (2-3), 73–93. doi: [http://doi.org/10.1016/s0257-8972\(99\)00441-7](http://doi.org/10.1016/s0257-8972(99)00441-7)
35. Nikitin, V. N., Eretnov, K. I., Artemev, A. V. (1983). Issledovanie prikatodnoi zoni nesatsionarnogo rezhima elektrolitnoi obrabotki. *Elektronnaia obrabotka materialov*, 2, 35–37.
36. Slovetzkii, D. I., Terentev, S. D., Plekhanov, V. G. (1986). Mekhanizm plazmenno-elektrolitnogo nagreva metallov. *Teplofizika vysokikh temperatur*, 2 (24), 353–363.
37. Chernenko, V. I., Snezhko, L. A., Papanova, I. I., Litovchenko, K. I. (1995). *Teoriia i tekhnologii anodnykh protsessov pri vysokikh napriazheniiakh*. Kyiv: Naukova dumka, 197.
38. Raizer, Iu. P. (1992). *Fizika gazovogo razriada*. Moscow: Red. fiz.-mat. lit., 536.
39. Tyurin, Yu. N., Tiuliapin, A. N., Traino, A. I., Iusupov, V. S. (1998). *Elektrolitno-plazmennaiia zakalka diskovykh pil*. MITOM, 1, 9–11.
40. Eretnov, K. I., Lebedev, S. V. (1997). *Protsessy nagreva i ochistki poverkhnosti metallov v elektrolite i ikh prakticheskoe ispolzovanie*. Lipetsk, 152.
41. Fediukin, V. K. (1977). *Termotsiklicheskaia obrabotka stali i chugunov*. Leningrad: LGU, 144.
42. Tyurin, Yu. N. (1986). A.S. No. 1312974 SSSR. Sposob termicheskoi obrabotki izdelii. MPK: C21D 1/78. declared: 11.04.1984; published: 22.01.1986.
43. Pogrebnjak, A. D., Kul'ment'eva, O. P., Kobzev, A. P., Tyurin, Y. N., Golovenko, S. I., Boiko, A. G. (2003). Mass transfer and doping during electrolyte-plasma treatment of cast iron. *Technical Physics Letters*, 29 (4), 312–315. doi: <http://doi.org/10.1134/1.1573301>

-
44. Tyurin, Y. N., Pogrebnjak, A. D. (2001). Electric heating using a liquid electrode. *Surface and Coatings Technology*, 142-144, 293–299. doi: [http://doi.org/10.1016/s0257-8972\(01\)01207-5](http://doi.org/10.1016/s0257-8972(01)01207-5)
 45. Gorelik, S. S., Rastorguev, L. N., Skakov, Iu. A. (1970). *Rentgenograficheskii i elektronnoopticheskii analiz. Prilozheniia*. Moscow: Metallurgii, 366.
 46. Bariakhtar, V. G. (Ed.) (1996). *Fizika tverdogo tela: Entsiklopedicheskii slovar*. Kyiv: Naukova dumka, 1295.
 47. Bariakhtar, V. G., Buravlev, Iu. M., Shevchenko, V. P. (2000). *Trudy OTTOM 2000*. Kharkiv: NNTS KHFTI, 155.
 48. Landau, L. D., Lifshits, E. M. (1959). *Elektrodinamika sploshnykh sred*. Moscow: Fizmatgiz, 632.
 49. Kochin, N. V., Kibel, I. A., Roze, N. V. (1963). *Teoreticheskaia gidromekhanika. Part. 1*. Moscow: Fizmatgiz, 583.
 50. Landau, L. D., Lifshits, E. M. (1953). *Mekhanika sploshnykh sred*. Moscow: Gostekhizdat, 788.
 51. Pogrebniak, A. D., Tyurin, Yu. N., Ivchenko, A. P., Ponariadov, V. V., Ruzimov, Sh. M., Kulmenteva, O. P., Kshniakin, V. S. (2003). Osobennosti i preimushchestva elektrolitno-plazmennoi zakalki. *Metallofizika i noveishie tekhnologii*, 25 (10), 1329–1353.
 52. Tyurin, Yu. N. (1984). Pat. No. 1375659 SSSR. Ustroistvo dlia nagreva izdelii v elektrolyte. MPK: C21D 1/44. No. 3715006. declared: 27.03.1984; published: 23.02.1988, Bul. No. 7.
 53. Tyurin, Yu. N., Golovenko, S. I. (2001). Elektrolitno-plazmennaiia obrabotka izdelii iz stali. *Sb. Trudov OTTOM-2. Tekhnologiiia termicheskoi i termomekhanicheskoi obrabotki*. Kharkiv, 160–167.
 54. Oleinikov, M. A., Zuev, I. V., Kazimirov, N. G. (1989). Pat. No. 1481260 SSSR. Sposob kontroliia termicheskoi obrabotki stalnykh detalei pri nagreve v vanne s elektrolitom. MPK: C21D 1/46(2006.01), C21D 11/00(2006.01). No. 4308349. declared: 22.09.87; published: 23.05.1989.
 55. Tyurin, Yu. N., Gnibeda, V. P. (1990). A.s. No. 1611625. SSSR. Sposob termokhimicheskoi zachistki poverkhnosti metallicheskiikh izdelii. MPK: B23K 7/06 (2006.01). No. 4473489. declared: 15.08.1988. published: 07.12.1990, Bul. No. 45.
 56. Tyurin, Yu. N. (1990). Elektrolitno-plazmennaiia uprochniiaushaia obrabotka detalei svarnykh konstruksii. *Avtomaticheskaiia svarka (Dep.)*. Kyiv, 10.
 57. Tiurny, Yu. N., Smyrnov, S. P., Subbotyn, V. P. (2007). Pat. No. 79234 UA. Prystrnii dlia obrobky poverkhnii dovhomirnykh vyrobiv. MPK: C25D 5/00, C21D 1/42 (2006.01), C21D 9/08 (2006.01), C25F 1/00. No. 2003054871. declared: 28.05.2003; published: 11.06.2007, Bul. No. 8.
 58. Barabantsev, G. E., Tiuliapin, A. N., Lukanin, Iu. V., Tyurin, Yu. N., Riabinkova, V. K., Traino, A. I. (1998). Pat. No. 2123535 RU. Ustroistvo dlia zakalki diskovykh pil. MPK: C21D 9/24 (2006.01), C21D 1/44 (2006.01). No. 97112338/02. declared: 15.07.1997; published: 20.12.1998.
-

59. Barabantsev, G. E., Tiuliapin, A. N., Lukanin, Iu. V., Tyurin, Yu. N., Rosliakova, N. E., Traino, A. I. (1998). Pat. No. 2119538 RU. Sposob zakalki diskovykh pil. MPK: C21D 1/44 (2006.01). No. 97112299/02. declared: 15.07.1997; published: 27.09.1998.
60. Barabantsev, G. E., Lukanin, Iu. V., Tiuliapin, A. N., Rosliakova, N. E., Tyurin, Yu. N. (1999). Pat. No. 2138564 RU. Sposob uprochneniia pily. MPK: C21D 9/24 (2006.01). No. 98106746/02. declared: 30.03.1998; published: 27.09.1999.
61. Snegovskii, F. P., Tyurin, Yu. N. (1975). Vliianie mikrorelefa vala na rabotosposobnost manzhetnykh uplotnitelnykh uzlov. Problemy treniia i iznashivaniia. Tekhnika, 7, 64–69.
62. Snegovskii, F. P., Tyurin, Yu. N. (1976). Hidrodinamicheskaia smazka manzhetnogo uplotnitelnogo uzla s vibronakatannym valom. Vestnik mashinostroeniia, 1, 31–36.
63. Tyurin, Yu. N. (1977). Teoreticheskoe i eksperimentalnye issledovanie, razrabotka i vnedrenie uzlov valov s gidrodinamicheskoi smazkoi Dissertatsii na soiskanie uchenoi stepeni kandidata tekhnicheskikh nauk. Rostov-na-Donu, 256.
64. Tyurin, Yu. N. (1987). A.S. No. 1340165 SSSR. Ustroistvo dlia termicheskoi obrabotki detalei. MPK: C21D 9/48. declared: 26.06.1985; published: 02.11.1987.
65. Tyurin, Yu. N. (1987). A.S. No. 1311263 SSSR. Sposob uprochneniia stalnykh detalei. MPK: C25D 11/02. declared: 22.05.1985; published: 15.01.1987.
66. Tyurin, Yu. N., Garkavyi, N. I., Golovenko, S. I., Duda, I. M. (2009). Uprochnenie sheek krupnogabaritnykh kolenchatykh valov. Zhurnal Uprochniiauschie Tekhnologii, 9, 39–42.
67. Tyurin, Yu. N., Golovenko, S. I., Duda, I. M. (2010). Pat. No. 90378 UA. Method for heat treatment of articles. MPK: C21D 1/00. No. a 2008 09410. declared: 18.07.2008; published: 26.04.2010, Bul. No. 8.
68. Tyurin, Yu. N., Garbuzov, A. P. (1989). Pat. No. 1470781 SSSR. Sposob i ustroistvo zakalki listovogo prokata. MPK: C21D 1/40. declared: 26.08.1986; published: 07.04.1989.
69. Tyurin, Yu. N. (1989). Pat. No. 1488321 SSSR. Sposob nagreva detalei. MPK: C21D 1/44. declared: 10.04.1987; published: 22.02.1989.
70. Pogrebniak, A. D., Tyurin, Yu. N., Boiko, A. G., Zhadkevich, M. L., Kalyshkanov, M. K., Ruzimov, Sh. M. (2005). Elektrolitno-plazmennaiia obrabotka i nanesenie pokrytii na metally i splavy. Uspekhe fiziki metalov, 6, 273–344.
71. Tyurin, Yu. N., Shleenko, V. I., Semenova, L. V., Anufriev, A. V. (1990). Pat. No. 1537695 SSSR. Ustroistvo dlia zonnogo nagreva detalei v elektrolite. No. 4336032. declared: 01.12.1987; published: 23.01.1990.
72. Tyurin, Yu. N., Kiselev, E. I., Gnibeda, V. P., Semenov, V. V., Gavrilov, B. P., Girshovich, G. A. (1988). Pat. No. 1399231 SSSR. MPK: B65G 19/28 (2006.01). Skrebkovyi konveier. No. 3980642. declared: 27.11.1985; published: 30.05.1988.
73. Tyurin, Yu. N., Kalafatov, A. P., Zuev, I. V. (1990). Pat. No. 1546362 SSSR. Reshtak skrebkovogo konveera. MPK: B65G 19/28 (2006.01). No. 4428164. declared: 23.05.1988; published: 28.08.1990.

REFERENCES

74. Tyurin, Yu. N. (1986). Pat. No. 1277646 SSSR. Ustroistvo dlia elektrolitnogo plazmennogo naneseniiia pokrytii. MPK: C25D 11/02. declared: 11.12.1984; published: 15.08.1986.
 75. Tyurin, Yu. N. (1987). Pat. No. 1331074 SSSR. Ustroistvo dlia zonnogo nagreva detalei v elektrolite. MPK: C21D 1/44. declared: 18.07.1985; published: 02.11.1987.
 76. Tyurin, Yu. N. (1989). Pat. No. 1441168 SSSR. Ustanovka dlia termicheskoi obrabotki detalei. MPK: C21D 1/44. declared: 27.07.1987; published: 09.10.1989.
 77. Tyurin, Yu. N. (1990). Pat. No. 1605527 SSSR. Ustanovka dlia nagreva i okhlazhdeniia izdelii v elektrolite. MPK: C21D 1/44. declared: 10.02.1988; published: 19.05.1990.
 78. Tyurin, Yu. N. (1998). Pat. No. 1439835 SSSR. Sposob litia s kristalizatsiei pod davleniem. MPK: V22 F9/10. declared: 15.02.1987; published: 10.08.1998.
 79. Tyurin, Yu. N. (1988). Pat. No. 1396362 SSSR. Sposob goriachego deformirovaniia zagotovok. MPK: B23K 11/06. declared: 06.06.1986; published: 25.01.1988.
 80. Tyurin, Yu. N. (1987). Pat. No. 1381851 SSSR. Ustanovka dlia naplavki. MPK: B23K 11/06. declared: 01.09.1986; published: 15.10.1987.
 81. Tyurin, Yu. N. (1989). Pat. No. 1464481 SSSR. Ustroistvo dlia zonnogo nagreva detalei v elektrolite. MPK: C21D 1/44. declared: 09.03.1987; published: 29.08.1989.
 82. Tyurin, Yu. N. (1986). Pat. No. 1150956 SSSR. Ustroistvo dlia elektrolitno-plazmennogo uprochneniia detalei. MPK: C21D 1/44. declared: 04.01.1984; published: 19.11.1986.
 83. Tyurin, Yu. N. (1991). Pat. No. 1602071 SSSR. Sposob zhidkostnogo vanadirovaniia splavov na osnove zheleza. MPK: C23C 8/00. declared: 16.02.1989; published: 13.08.1991.
 84. Belonogov, V. A., Belonogova, G. U. (1996). Elektrolitno-plazmennaiia obrabotka zharo-prochnykh splavov. Probl. Energo. mashinostr. Ufa, 117.
 85. Kashin, Iu. A. (1982). A.s. No. 933742 SSSR. Ustroistvo dlia nagreva zagotovok. MPK: S21D1/40, C21D9/62. No. 2933773. declared: 03.06.1980; published: 07.06.1982.
 86. Fominov, A. Ia. (1977). A.s. No. 579324 SSSR. Ustroistvo dlia posledovatel'nogo nagreva zagotovok v elektrolite. MPK: S21D 1/44. No. 2149083. declared: 23.06.1975; published: 05.11.1977.
 87. Anagorskii, L. A., Brinza, V. N., Dolgov, M. V., Malysheko, N. F., Fominov, A. Ia., Frantseniuk, I. V. (1974). A.s. 411136 SSSR. Ustanovka dlia nagreva metalla v elektrolite. MPK: C21D 1/44, C21D 9/46. No. 1407548/22-1. declared: 23.02.1970; published: 15.01.1974.
 88. Stanishevskii, V. K., Kosobutskii, A. A., Parshuto, A. E., Khlebtsevich, V. A., Matushevskii, I. I., Levin, B. G. (1990). A.s. No. 1615241 SSSR. Sposob elektrolitno-plazmennoi obrabotki i ustroistvo dlia ego osuschestvleniia. MPK: S25F7/00. C25D 7/06. No. 4611410. declared: 01.12.1988; published: 23.12.1990.
 89. Riabkov, D. V. (1998). Pat. No. 97100692. Sposob mnogofunktsionalnoi obrabotki po-verkhnostei i ustroistvo dlia ego osuschestvleniia. MPK: C23C16/44. No. 97100692/02. declared: 24.01.1997; published: 20.05.1998.
-

-
90. Pogrebnyak, A. D., Kaverina, A. S., Kylyshkanov, M. K. (2014). Electrolytic plasma processing for plating coatings and treating metals and alloys. *Protection of Metals and Physical Chemistry of Surfaces*, 50 (1), 72–87. doi: <http://doi.org/10.1134/s2070205114010092>
 91. Pogrebniak, A. D., Tyurin, Yu. N. (2002). Osobennosti elektrolitno-plazmennoi zakalki (EPZ). *Zhurnal tekhnicheskoi fiziki*, 72 (11), 119–120.
 92. Larinov, L. N., Mazanko, V. F., Falchenko, V. M. (1981). Massoperenos v metallakh pri impulsnom nagruzhении. *FizKOM*, 4, 56–58.
 93. Bodiатko, M. N., Vurzel, F. B., Kremko, E. V. et. al. (1988). *Gazotermicheskаia obrabotka keramicheskikh oksidov*. Minsk: Nauka i tekhnika, 223.
 94. Emlin, B. I., Gasik, M. I. (1978). *Spravochnik po elektrotermicheskim protsessam*. Moscow: Metallurgiya, 288.
 95. Glinka, N. L. (1984). *Obschaya khimiya*. Leningrad: Khimiya, 704.
 96. Belkin, P. N. (2005). *Elektrokhimiko-termicheskаia obrabotka metallov i splavov*. Moscow: Mir, 336.
 97. Blaschuk, V. E., Kareta, N. M., Onoprienko, L. M., Pasinkovskii, E. A. (1986). Vlianie elektrolitnogo azotirovaniia korrozionnuu stoikost tekhnicheskogo titana VT1-0. *Elektronnaia obrabotka metallov*, 3, 20–22.
 98. Duradzi, V. N., Morar, N. N., Polotebnova, N.A., Kiseeva, L. V. (1986). O fazovom sostave poverkhnosti metallov. obrabotannykh v elektrolitnoi plazme. *Elektronnaia obrabotka materialov*, 1, 49–52.
 99. Gurevich, S. M., Zamkov, V. N., Blaschuk, V. E. et. al. (1986). Povyshenie korrozionnoi stoikosti nizkolegirovannykh titanovykh splavov azotirovaniem v elektrolite. *Metallurgiya i tekhnologiya svarki titana i ego splavov*. Kyiv: Naukova Dumka, 240.
 100. Kornilov, I. I., Zabrodskaia, M. N., Boriskina, N. G., Brynza, A. P. (1977). Kinetika dlitelnogo okisleniia titana. *Metallovedenie i termicheskаia obrabotka metallov*, 5, 49–51.
 101. Kolachev, B. A., Livanov, V. A., Bukhanova, A. A. (1974). *Mekhanicheskie svoystva titana i ego splavov*. Moscow: Metallurgiya, 544.
 102. Kolachev, B. A., Livanov, V. A., Elagin, V. I. (1981). *Metallovedenie i termicheskаia obrabotka tsvetnykh metallov*. Moscow: Metallurgiya, 415.
 103. Tsvikker, U. (1979). *Titan i ego splavy*. Moscow: Metallurgiya, 512.
 104. Malkov, A. V., Gorshkov, Iu. V. (1980). Kompleksnaia metodika opredeleniia kriticheskikh kontsentratsii vodoroda v titanovykh polufabrikatakh i konstruktsiiakh. *Voprosy metallovedeniia i tekhnologii legkikh i zharoprochnykh splavov*. Moscow: VILS, 160–162.
 105. Blaschuk, V. E. (1989). Povyshenie korrozionnoi stoikosti nizkolegirovannykh titanovykh splavov azotirovaniem v elektrolite. *Elektronnaia obrabotka materialov*, 5, 18–20.
 106. Chernenko, V. I., Snezhko, L. A., Papanova, I. I. (1991). *Poluchenie pokrytii anodno-iskrovym elektrolizom*. Leningrad: Khimiya, 128.
-

REFERENCES

107. Boiko, A. G., Pogrebniak, A. D., Tyurin, Yu. N., Veidzhang, Zh., Golovenko, S. I. (2005). Struktura i svoistva obraztsov iz konstruktsionnoi stali 35 posle elektrolitno-plazmennoi obrabotki. Vestnik SumGU, 4 (76), 101–108.
108. Gordienko, P. S. (1996). Obrazovanie pokrytii na anodno poliarizovannykh elektrodakh v vodnykh elektrolitakh pri potentsialakh iskreniia i proboia. Vladivostok: Dalnauka, 215.
109. Atroschenko, E. S., Kazantsev, I. A., Rozen, A. E. (1996). Tekhnologiiia polucheniia pokrytii mikrodugovym oksidirovaniem. Novye promyshlennye tekhnologii. Tekhnicheskii progress v atomnoi promyshlennosti. Seriiia – Tekhnologiiia montazhnykh rabot. Moscow, 28–33.

Edited by
Volodymyr Korzhyk

SURFACE MODIFICATION OF METAL PRODUCTS BY ELECTROLYTE PLASMA

Volodymyr Korzhyk, Yuriy Tyurin, Oleg Kolisnichenko

Monograph

Technical editor I. Prudius
Desktop publishing T. Serhiienko
Cover photo Copyright © 2021 V. Korzhyk

PC TECHNOLOGY CENTER
Published in December 2021
Enlisting the subject of publishing No. 4452 – 10.12.2012
Address: Shatylova dacha str., 4, Kharkiv, Ukraine, 61165
